Submitted, accepted and published by:
Progress in Energy and Combustion Science 38 (2012) 215-282

Progress in Chemical-Looping Combustion and Reforming Technologies. A review.

Juan Adánez*, Alberto Abad, Francisco García-Labiano, Pilar Gayán, Luis F. de Diego

Dept. of Energy & Environment, Instituto de Carboquímica (ICB-CSIC).

Miguel Luesma Castán, 4, Zaragoza, 50018, Spain.

Abstract

This work is a comprehensive review of the Chemical-Looping Combustion (CLC) and Chemical-Looping Reforming (CLR) processes reporting the main advances in these technologies up to 2010. These processes are based on the transfer of the oxygen from air to the fuel by means of a solid oxygen-carrier avoiding direct contact between fuel and air for different final purposes. CLC has arisen during last years as a very promising combustion technology for power plants and industrial applications with inherent CO_2 capture which avoids the energetic penalty present in other competing technologies. CLR uses the chemical looping cycles for H_2 production with additional advantages if CO_2 capture is also considered.

The review compiles the main milestones reached during last years in the development of these technologies regarding the use of gaseous or solid fuels, the oxygen-carrier development, the continuous operation experience, and modelling at several scales. Up to 2010, more than 700 different materials based on Ni, Cu, Fe, Mn, Co, as well as other mixed oxides and low cost materials, have been compiled. Especial emphasis has been done in those oxygen-carriers tested under continuous operation in Chemical-Looping

prototypes. The total time of operational experience (≈ 3500 h) in different CLC units in the size range 0.3-120 kW_{th}, has allowed to demonstrate the technology and to gain in maturity. To help in the design, optimization, and scale-up of the CLC process, modelling work is also reviewed. Different levels of modelling have been accomplished, including fundamentals of the gas-solid reactions in the oxygen-carriers, modelling of the air- and fuel-reactors, and integration of the CLC systems in the power plant. Considering the great advances reached up to date in a very short period of time, it can be said that CLC and CLR are very promising technologies within the framework of the CO_2 capture options.

Keywords

Combustion, Reforming, CO_2 capture, Chemical-Looping Combustion (CLC), Chemical-Looping Reforming (CLR), oxygen-carrier

* Corresponding author: Tel: (+34) 976 733 977. Fax: (+34) 976 733 318. E-mail address: jadanez@icb.csic.es (Juan Adánez)

Contents

1. Introduction

According to the IPCC [1], "warming of the climate system is unequivocal", considering that eleven of the recent years (1995-2006) rank among the twelve warmest years in the instrumental record of global surface temperature since 1850. It is also clear that climate change can strongly modify the biodiversity on the earth [2]. Among the possible causes, it seems that most of the warming observed over the past 50 years is attributable to human activities, as a consequence of the gases emitted to the atmosphere [3], the so-called greenhouse gases (GHG).

There are several greenhouse gases proceeding from human activities, each of one presenting different global warming potential (GWP) [4]. The concept of GWP takes account of the gradual decrease in concentration of a trace gas with time, its greenhouse effect whilst in the atmosphere and the time period over which climatic changes are of concern. The main gases affecting the greenhouse effect are H_2O, CO_2, CH_4, N_2O, CFC´s and SF_6 [1]. The contribution to the global greenhouse effect of the different gases is related to their GWP and to the concentration in the atmosphere at a given time. In this sense, CO_2 is considered the gas making the largest contribution to the GHG effect as a consequence of two factors. The first one is that CO_2 represent the largest emissions of all the global anthropogenic GHG emissions, with percentage values as high as 75%. The second one is their high residence time in the atmosphere: the lifetime of CO_2 from fossil fuel uses might be 300 years, plus 25% that lasts forever [5].

The carbon dioxide concentration in the atmosphere has increased strongly over the few past decades as a result of the dependency on fossil fuels for energy production. The global atmospheric concentration of CO_2 increased from a pre-industrial value of about 280 ppm to 390 ppm in 2010 [6]. To assure the increase in average temperature was lower than 2 ºC –which it is considered as the limit to prevent the most catastrophic

changes in earth– the CO_2 concentrations must not exceed 450 ppm. This means that the CO_2 atmospheric concentration must raise no more than 15% over today's concentrations.

Therefore, it is generally accepted that a reduction in emissions of greenhouse gases is necessary as soon as possible. In 1997, the nations participating in the United Nations Framework Convention on Climate Change (UNFCCC) drafted the historic agreement known as the Kyoto Protocol [7]. After ratification in 2005, its provisions include a mean reduction in the GHG emissions of the 39 developed countries of 5.2% over the period 2008-2012 compared to 1990 levels.

Up to now, the technological options for reducing net CO_2 emissions to the atmosphere have been focused on [8]: a) reducing energy consumption, by increasing the efficiency of energy conversion and/or utilization; b) switching to less carbon intensive fuels; c) increasing the use of renewable energy sources (biofuel, wind power, etc.) or nuclear energy, and d) sequestering CO_2 by enhancing biological absorption capacity in forest and soils. It is clear that no single technology option will provide all of the emissions reductions needed. Even, the added efforts of all the above solutions will probably not allow reaching the desired low levels of CO_2 emissions.

Under this context, CO_2 Capture and Storage (CCS) appears as an additional option necessary to reach the above objectives. It must be considered that energies from fossil sources (gas, oil and coal), those giving off CO_2, will still satisfy over 80% of the energy demand during the first part of the 21st century, and unfortunately they will not yet be ready to be substituted by renewable sources massively in the near future [9]. According to the analysis made by the IPCC and IEA [8,10], the CCS could account for 19% of the total CO_2 emission reductions needed this century to stabilize climate change at a reasonable cost. Therefore, the development of CCS technologies to market

maturity is essential for the production of clean energy from fossil fuels both to ensure a continued role of these fuels, in particular coal, as well as to reduce CO_2 global emissions [11].

The purpose of CCS technology is to produce a concentrated stream of CO_2 from industrial and energy-related sources, transport it to a suitable storage location, and then store it away from the atmosphere for a long period of time. The IPCC Special Report on Carbon Dioxide Capture and Storage [8] gives an overview of the different options available for the capture, transport and storage processes.

Regarding CO_2 capture, three main approaches were considered for industrial and power plants applications: post-combustion systems, oxy-fuel combustion, and pre-combustion systems. All these technologies have undergone a great development during the last years and some of them are available at commercial scale. A brief overview of the current situation of these technologies can be found in the work of Toftegaard et al. [12]. However, although most of the technologies can reduce CO_2 emissions, they also have a high energy penalty, which results in a reduction of energy efficiency of the processes and an increase in the price of the energy.

Thus, great efforts have been carried out during last years to develop new low-cost CCS technologies. The CO_2 Capture Project (CCP) –Phase I– decided at the beginning of 2000 to collaborate with governments, industry, academic institutions and environmental interest groups to develop technologies that greatly reduce the cost of CO_2 capture [13]. The objective was to identify the most promising technologies that had the potential to deliver performance and efficiency improvements resulting in close to a 50% reduction in the cost of CO_2 capture. Among them, the Chemical-Looping Combustion (CLC) process was suggested among the best alternatives to reduce the economic cost of CO_2 capture [14]. Moreover, the IPCC in their special report on

Carbon Dioxide Capture and Storage identified CLC as one of the cheapest technologies for CO_2 capture. Later, the EU project "Enhanced Capture of CO_2" (ENCAP) focused the research in the development of cost efficient pre-combustion and oxy-fuel processes for CO_2 capture, including CLC [15]. Taken as a reference a pulverised fuel fired power plant without CO_2 capture using bituminous coal as fuel, the increase in the electricity generation cost for a CLC plant was about 12-22%. The incremental in the electricity cost was lower than the calculated for other technologies of CO_2 capture. The estimated cost of the capture per tonne of CO_2 avoided was 6-13 € for CLC. Similar evaluations concluded that the cost was 18-37 € for a pre-combustion technology using IGCC, and 13-30 € for an oxy-fuel process. Additionally, if the environmental impact is also considered, CLC is even more preferred to other CO_2 capture options [16,17].

The main drawback attributed to CLC was a very low confidence level as a consequence of the lack of maturity of the technology. It must be considered that this is an emerging technology. However, during the last 10 years it has experienced a great development as it will be shown in this review.

1.1. Process overview of chemical looping cycles for CO_2 capture

Different Chemical-Looping cycles have been proposed for CO_2 capture including both the transference of CO_2 or oxygen [18]. Commonly, the term Chemical-Looping is referred to those processes transporting oxygen. Thus, the term "Chemical-Looping" has been used for cycling processes that use a solid material as oxygen-carrier containing the oxygen required for the conversion of the fuel. To close the loop, the oxygen depleted solid material must be re-oxidized before to star a new cycle. The final purpose of the conversion of the fuel can be the combustion or the hydrogen production.

Table 1 shows a summary of different Chemical-Looping processes proposed in the literature.

For combustion purposes, the oxygen depleted solid material must be regenerated by oxygen in air. In general, these processes are known with the general term "Chemical-Looping Combustion" (CLC). CLC processes can address gaseous or solid materials as primary fuels. In CLC of gaseous fuels, the oxygen carrier reacts directly with the fuel e.g. natural gas, refinery gas, etc. Different possibilities arise for processing solid fuels as coal, biomass, etc. In the Syngas-CLC process, the oxygen-carrier comes into contact with the gasification products (syngas) obtained in a gasifier. In this process, the fuel fed into the CLC system is gaseous although the primary fuel is solid. To avoid the gasifier, solid fuel and oxygen-carrier can be mixed in a uniquely reactor. In the in-situ Gasification CLC (iG-CLC) process, the oxygen carrier reacts with the gasification products of the solid fuel generated inside the fuel reactor. Additionally, in the process called Chemical-Looping with Oxygen Uncoupling (CLOU), the oxygen-carrier is able to release gaseous oxygen for the combustion of the solid fuel.

For hydrogen production, the regeneration of the oxygen-carrier can be done using air or steam. When air is used for regeneration, it can be differentiated: the Steam Reforming integrated to Chemical-Looping Combustion process (SR-CLC), where CLC is used to give the energy required for usual catalytic steam reforming; and the Chemical-Looping Reforming process (CLR) where primary products from the Chemical-Looping system are H_2 and CO.

Other processes use the property of some oxygen depleted materials to react with steam to produce hydrogen, also known as "water splitting". In this category it can be found the Chemical-Looping Hydrogen (CLH) or "One Step Decarbonization" (OSD) process, and the so-called "Chemical-Looping Gasification" technologies: the Syngas Chemical-

Looping process (SCL) and the Coal Direct Chemical-Looping process (CDCL). Usually these processes need several oxidation steps using air for the final regeneration of the oxygen carrier.

This review focuses in the main development of the "Chemical-Looping" processes where the oxygen-carrier material is regenerated by air, i.e. CLC and CLR. Common features involve these processes both for combustion or hydrogen production, mainly focused on the oxygen-carrier material. More information about processes based on "water splitting" can be found elsewhere [19-21].

This section shows an overview of the history of the above referred Chemical-Looping processes giving the main milestones reached during last years in the development of the technology. The basic idea can be first attributed to Lewis and Gilliland [22] who presented a patent entitled "Production of pure carbon dioxide" in 1954 [23] which describes a concept similar to the current known CLC process. They also introduced the concept of oxygen-carrier for the used oxide, the possibility to use different fuels to reduce it, and the use of two interconnected fluidized beds for the solids circulation. Later, Richter and Knoche [24] proposed in the early eighties the principle of CLC process to increase the thermal efficiency in fossil fuel fired power plants. They suggested a fuel oxidation reaction scheme involving two intermediate reactions with a metal oxide (copper oxide, nickel oxide or cadmium oxide) as oxygen-carrier. However, Ishida et al. [25] were the first ones to introduce the name of Chemical-Looping Combustion in their thermodynamic study to reduce the exergy loss caused by the conversion of fuel energy to thermal energy in conventional power plants using natural gas. Some years later, Ishida and Jin [26,27] proposed CLC as a process for CO_2 capture using Fe- and Ni-based oxygen-carriers.

In 1997, Hatanaka et al. [28] proposed the "MERIT" (Mediator Recirculation Integrating Technology) as a method to contribute the settlement of environmental problems, including NO_x emissions. This system divides combustion into two reactions: oxidation of metal by air at high temperature and reduction of metal oxide by fuel at low temperature.

In 2000, Copeland et al. [29] introduced the concept of "Sorbent Energy Transfer System" (SETS) by using a standard combined cycle in which the combustor is replaced by the oxidation and reduction reactors. The main difference with respect to the CLC process is that SETS uses a thermal neutral reducing reactor. They pointed out that SETS can make major reductions in greenhouse gas emissions, since it can be used with any fossil fuel and can be sited anywhere.

However, CLC was no more than a paper concept in early 2000. The process had never been demonstrated in continuous plants and only a limited number of oxygen-carrier materials had been tested in simple tests during few cycles.

During those years, a great number of ideas and technologies related with the CO_2 capture concept were emerging. The CO_2 Capture Project (CCP) funded research programs in the European Union (EU) during the period 2001 to 2003 [13] to promote a number of 'proof of concept' for CO_2 capture with the objective to develop technologies that will achieve a step change in the cost of capture and separation of carbon dioxide. In this context, the Grangemouth Advanced CO_2 Capture Project (GRACE) was the first trial that supported an important advance in the development of the CLC technology [30]. More than 300 different particles were evaluated within the project [31,32], two of which were produced in large quantities for testing in a 10 kW_{th} Chemical-Looping combustor unit built specifically for the project. Within this project, Lyngfelt and Thunman [33] at Chalmers University of Technology (CHALMERS) presented the first

demonstration of the technology by showing the firsts 100 hours of continuous operation in the 10 kW_{th} CLC plant with the same batch of nickel particles. The fuel used was natural gas, and a fuel conversion efficiency of 99.5% was obtained using a Ni-based oxygen-carrier. Neither decrease in reactivity nor in mechanical strength of the carrier material was seen during the test period. Moreover, the design concept for a large scale CLC boiler was accomplished [34].

In parallel, another EU project –Capture of CO_2 in Coal Combustion (CCCC)– analysed the possibility to develop the CLC technology for syngas from coal gasification [35]. A 300 W_{th} CLC reactor system was constructed and operated successfully during 30-70 h using three different carriers based on nickel, iron and manganese oxides [36].

At the same time, Ryu et al. [37,38] at the Korea Institute of Energy Research (KIER) operated a 50 kW_{th} unit during 28 h with methane as fuel and oxygen-carriers based on nickel and cobalt oxides.

Adánez et al. [39,40] at Institute of Carboquímica (ICB-CSIC) presented the first long term operation (120 h) with copper particles in their 10 kW_{th} CLC plant. Until then, Cu-based materials had been rejected as potential candidates for CLC as a consequence of their agglomeration in fluidized-bed reactors. However, the tests showed a good behaviour of the oxygen-carriers reaching 100 % of CO_2 capture at 800 ºC in the fuel-reactor, without any agglomeration problem.

Further development of the CLC with gaseous fuels was accomplished within the EU project "Chemical Looping Combustion CO_2-Ready Gas Power" (CLC Gas Power) [41]. Among the main results it must be mentioned the scale-up of the CLC process up to 120 kW_{th} on a unit built at Vienna University of Technology (TUWIEN) [42]; the scale-up of the carrier production by using spray-drying [43] and impregnation [44] methods; the successfully long-term operation during more than 1000 hours at

CHALMERS using Ni-based particles manufactured by spray-drying of commercial raw materials [43]; and the testing of the effect of gas impurities such as H_2S and light hydrocarbons over the nickel oxide particles at ICB-CSIC [44-46].

In parallel to the development of the technology for combustion of gaseous fuels, other options based on Chemical-Looping cycles for integrated H_2 production and CO_2 capture have risen. The idea of H_2 production from hydrocarbons using the chemical looping principles started in the late 19th and early 20th century by means of the steam-iron process. A more detailed description of that and other related processes during the 20th century can be found in the work of Li et al. [47]. More recently, in early 21st century, Lyon and Cole [48] proposed the unmixed combustion to supplying heat to endothermic reactions, as for example, the steam reforming. In this process, fuel and air alternately pass over a catalyst that undergoes oxidation and reduction, storing heat from oxidation step and delivering it during fuel reforming.

However, the biggest development in this area was obtained within the EU project "Carbon Dioxide Capture and Hydrogen Production from Gaseous Fuels" (CACHET) [49]. The aim was the development of technologies which will significantly reduce the cost of CO_2 capture from power generation and H_2 production using natural gas as fuel. CACHET focused on 4 promising technologies: advanced steam methane reforming, Chemical-Looping, metal membranes and sorption enhanced water gas shift (SEWGS). Within Chemical-Looping, CACHET considered the production of syngas using three process variants. In the first approach, the autothermal reforming of methane is carried out in a so-called Chemical-Looping Reforming (CLR) system [50]. The second one involves H_2 production by Steam Reforming coupled with CO_2 capture by Chemical-Looping Combustion (SR-CLC) [51]. This process uses the benefits of CLC regarding the CO_2 capture by integrating a CLC unit with the widely used catalytic Steam

Reforming process for H_2 production [50]. The third process, called One-Step Decarbonisation (OSD) or Chemical-Looping Hydrogen generation (CLH), features direct H_2 production with CO_2 capture [21,52]. The OSD process, originally proposed by Eni company, is based on the use of a circulating "redox" solid material that can be oxidised via water splitting, thereby producing H_2, and reduced by a hydrocarbon fuel, producing CO_2 [53].

The CACHET project was focused in: (1) the development of Ni-based oxygen-carriers suitable for the CLR and SR-CLC processes based on different industrial production methods such as spray-dying and impregnation; (2) the determination of the effect of pressure for CLR process; (3) the demonstration of the CLR process in a comparably large (140 kW_{th}) Chemical-Looping reactor under similar conditions to those believed to be preferred in a real-world facility; and (4) the development of suitable redox materials for the OSD process.

The development of CO_2 capture technologies in a global context of power generation processes should include also solid fuels as energy sources. In this context, CLC can directly use solids fuels without the need of a previous gasification. Lyon and Cole [48] proposed in 2000 unmixed combustion for solid fuels. The first experiments in a CLC system with solids fuels were accomplished by Lyngfelt´s research group at CHALMERS in 2005 as part of the EU project "Enhanced Capture of CO_2"(ENCAP) [54,55]. They tested the combustion of a bituminous coal and petcoke in a 10 kW_{th} experimental rig for solid fuels. The major changes to adapt CLC to solid fuels are related with the fuel-reactor design and the type of oxygen-carrier. In this case, ilmenite was selected as the oxygen-carrier. Moreover, a first concept design of a 455 MW_e CLC solid fuel power plant was also accomplished within the project.

The development of the CLC technology for use of solids fuels continued within the EU project "Emission Free Chemical Looping Coal Combustion Process" (ECLAIR), which started in 2008. The key issues considered in the project are related to i) verification of oxygen-carrier performance, ii) demonstration of the technology in a 1 MW_{th} CLC system and iii) finding adequate technical solutions to the reactors and surrounding systems [56]. Within this project, another technology valid for solid fuels is also under development: the Chemical-Looping with Oxygen Uncoupling (CLOU) process. This new process was proposed by Mattisson et al. [57] based on the CuO decomposition properties already noted by Lewis and Gilliland [23].

The chemical looping processes has been also developed in USA. The research group of Prof. Fan at the Ohio State University (OSU) has been involved in several American projects with the main objective to develop the coal direct chemical looping (CDCL) process [20,58] by using iron oxide as oxygen carrier. The fuel reactor consists of a moving-bed and the air reactor is an entrained flow reactor. This technology can be used to produce electric power or H_2 if the oxidation is carried out by air or steam, respectively.

ALSTOM worked in a multi-phase program to develop the "Hybrid Combustion-Gasification Chemical Looping Process" where $CaSO_4$ is used as oxygen-carrier for heat generation, syngas production or hydrogen generation [59, 60]. Substantial work began in 2003 with the construction of a small-scale pilot facility of 65 kW_{th} (Process Development Unit, PDU) in Windsor, Connecticut. Later phases include the design, construction and operation of a 3-MWth prototype facility that it was expected to be operational in 2011.

The interest in CLC technologies is continuously increasing because of the promising results showed above. Chemical-Looping processes had about 3500 hours of operational experience in continuous plants of different size, with 36 different materials tested. Considering that the experimental experience of this technology is less than 10 years old, the development of the process can be considered very successful. This is also supported by the increasing number of papers, patents [23,61-77], and PhD Thesis [78-97] in subjects related with CLC and CLR. Patents cover different aspects of the technology development including oxygen-carrier manufacture, reactor configuration, plant optimization and even new processes related to CLC. A quick overview of the status of the development of the Chemical-Looping processes was done by Lyngfelt et al. in 2008 [98]. In the same year, Hossain and de Lasa [99] reviewed the progress reached in the development of oxygen-carrier materials. Later, the applications of Chemical-Looping technologies for fossil energy conversion were briefly overviewed by Fan and Li [19], and Fang et al. [52]. A deeper description of Chemical-Looping technologies has been done recently by Fan [20] and by Brandvoll [100]. Finally, Lygnfelt [101] have made a compilation of the operational experience on CLC.

This review covers the main achievements reached during the last years. Section 2 and 3 explains the Chemical-Looping Combustion process using gaseous and solid fuels, respectively. Section 4 covers the application of Chemical-Looping for H_2 production, known as Chemical-Looping Reforming (CLR). Section 5 deals with the status of the development of CLC prototypes. Advances on mathematical models and kinetic determination are presented in Section 6. Finally, future research and prospects are marked in Section 7.

2. Chemical-Looping Combustion of gaseous fuels

This section explains the fundamentals of the Chemical-Looping Combustion process using metal oxides as oxygen-carriers, being mainly focused in description of results obtained with gaseous fuels, although references to the solid fuelled CLC and CLR are done in some cases.

2.1. Process fundamentals

The process is based on the transfer of oxygen from air to the fuel by means of a solid oxygen-carrier avoiding direct contact between fuel and air. Fig. 1 shows a general scheme of this process.

In a first step, the fuel is oxidized to CO_2 and H_2O by a metal oxide (Me_xO_y) that is reduced to a metal (Me) or a reduced form Me_xO_{y-1}. If the composition of the fuel gas is expressed as $C_nH_{2m}O_p$, the global reduction process is given by reaction (1). The gas produced in this first step contains primarily CO_2 and H_2O. After water condensation and purification, a highly concentrated stream of CO_2 ready for transport and storage is achieved. This concept is the main advantage of the process in relation with other CO_2 capture technologies. In this sense, CLC is a combustion process with inherent CO_2 separation, i.e. avoiding the need of CO_2 separation units and without any penalty in energy.

The metal or reduced metal oxide is further oxidized with air in a second step, and the material regenerated is ready to start a new cycle (reaction 2). The flue gas obtained contains N_2 and unreacted O_2. The net chemical reaction over the two steps, and therefore the combustion enthalpy, is the same to conventional combustion where the fuel is burned in direct contact with oxygen from air (reaction 3). Therefore, the total amount of heat evolved in the CLC process is the same as in conventional combustion.

$$(2n+m-p)\ Me_xO_y + C_nH_{2m}O_p \rightarrow (2n+m-p)\ Me_xO_{y-1} + n\ CO_2 + m\ H_2O \quad \Delta H_r \quad (1)$$

$$(2n+m-p)\ Me_xO_{y-1} + (n+m/2-p/2)\ O_2 \rightarrow (2n+m-p)\ Me_xO_y \quad \Delta H_o \quad (2)$$

$$C_nH_{2m}O_p + (n+m/2-p/2)\ O_2 \rightarrow n\ CO_2 + m\ H_2O \quad \Delta H_c = \Delta H_r + \Delta H_o \quad (3)$$

2.1.1. CLC concepts

The Chemical-Looping concept showed in Fig. 1 has been proposed to be accomplished in different type of reactors and configurations, namely (a) two interconnected moving or fluidized-bed reactors; (b) alternated packed or fluidized-bed reactors; or (c) a rotating reactor. Fig. 2 shows a scheme of the different configurations.

The majority of the CLC plants existing worldwide at the moment use the configuration composed of two interconnected fluidized-bed reactors, one of them being the fuel-reactor and the other the air-reactor. In the so-called fuel-reactor conversion of the fuel happens (reaction 1), whereas the regeneration of the oxygen-carrier (reaction 2) is carried out in the air-reactor. In addition, two loop-seal devices must be used in order to avoid gas leakage between reactors.

First designs using these concepts were developed for combustion of gaseous fuels at atmospheric pressure. Several works have been carried out to study the more appropriated design of the system. In 2001 Lyngfelt et al. [102] proposed a design based on the circulating fluidized bed (CFB) principle. This configuration has several advantages over alternative designs, considering that the process requires a good contact between gas and solids as well as a flow of solid material between the fuel-reactor and air-reactor. Other works [103-106] showed that CLC can be carried out in a variety of configurations, mainly composed of a high velocity riser and a low velocity bubbling fluidized bed as the air- and fuel-reactors, respectively. The preference for this type of

configuration is based on carrier reactivities [33,37] considering that most oxygen-carriers demand a higher particle residence time for the reduction reaction than for the oxidation. The riser has to fulfil two objectives: to give the driving force for the solid material circulation and shall provide sufficient oxygen to the carrier for complete fuel conversion in the fuel-reactor. Other authors have considered both reactors in the bubbling fluidized regime [39,107].

More recently, a dual circulating air-reactor and fuel-reactor directly connected by fluidization (DCFB) are used in the 120 kW_{th} unit at TUWIEN [105]. In this system the fuel-reactor is in the turbulent regime improving in this way the gas-solid contact compared to the bubbling regime. The air-reactor is a fast bed with pneumatic transport of solids. In this configuration the solid holdup is stabilized by the direct hydraulic link between the two reactors. Moreover the solid circulation rate is only dependent on the air flow. Compared with other CLC configurations, this unit features very high solids circulation rate with low solids inventory.

A different design was used by Son and Kim [108] in a 1 kW_{th} annular shape reactor with double CFB loops for investigation into CLC. It is composed of two bubbling fluidized bed zones in the core and annular sections and two risers where the oxygen-carrier particles are circulated through each section. The annular shape of the reactor was designed to optimize heat transfer from the oxidation reactor to the reduction reactor.

Shen et al. [109] designed a 10 kW_{th} CLC plant for biomass or coal with a spout-fluid bed instead of a bubbling bed for the fuel-reactor. The spout-fluid bed has two compartments; the major compartment is called as reaction chamber, and the minor one is the inner seal. The reaction chamber allows the combination of coal gasification and oxygen-carrier reduction with coal syngas to proceed inside the spouted-fluidized bed.

In contrast with these designs, a new concept of two interconnected bubbling beds and independent solid flow control has been proposed. At IFP-France, a 10 kW_{th} unit with three interconnected bubbling beds (one fuel-reactor and two air-reactors) and independent solid flow control has been designed and constructed. The solid circulation rates can be achieved independently of the gas flow and solids inventory in each reactor by means of pneumatic L-valves [110]. In parallel, Ryu et al. [107] developed a 50 kW_{th} unit with control of the solids flow using solid injection nozzles inside each reactor.

In this sense, SINTEF and NTNU (Norway) have proposed a second generation 150 kW_{th} CLC unit with focus on pressurization [111]. The unit has a double loop circulating fluidized beds operating in the fast fluidization regime. A compact design for the prospective of pressurized operation was developed in order to integrate the CLC unit into a gas turbine power cycle. However, at the moment just a full scale atmospheric cold flow version of the rig has been built and tested and solutions to improve its design have been proposed.

The more complex configuration using fluidized beds has been developed by ALSTOM for its hybrid combustion-gasification chemical looping system [59]. This system needs to operate three interactive solids transport loops (oxidizer, reducer, and sorbent calciner) at elevated temperatures, which requires advanced control systems [60].

Li and Fan [112] proposed the use of a moving bed for the CLC process. Due to its solid plug flow, the use of this reactor configuration is based on the theoretical higher solid conversion in a moving bed than in a fluidized bed, reducing in this way the needed reactor volume. However, results from their coal direct Chemical-Looping process tested in a 2.5 kW_{th} moving bed unit at Ohio State University using an iron-based oxygen carrier are still missing. More recently, Schwebel et al. [113] had also suggested the use of a new reactor concept for implementing CLC using a parallel arrangement of

a moving-bed fuel-reactor and a fluidized-bed air-reactor, especially for solid fuels. The authors claimed that this configuration avoids fuel segregation together with a less char at the reactor exit and less power demand for fluidization. However, this approach has a restricted thermal power per unit approximately of 20 MW_{th}.

With respect to power cycle burning gaseous fuels, to achieve competitive energy efficiencies it is necessary to operate at high temperatures and high pressures (1-3 MPa) [114,115]. In this sense, operating pressurised CLC plants using interconnected fluidized bed technology could have some technical difficulties to maintain a stable solid circulation between the reactors. With the aim to work under pressure, dynamically operated packed-bed reactors have been proposed [116,117]. At least two reactors in parallel working alternately must be used to assure a continuous high temperature gas stream supply to the downstream gas turbine. The process consists of alternate oxidation and reduction cycles in two separate reactors, intermittently alternated with short periods of mild fluidization of the bed after each cycle to level off temperature and concentration profiles. The main advantages of packed-bed reactor technology are that the separation of gas and particles is intrinsically avoided and the possibility to work under pressure. Disadvantages of the concept include the necessity to use a high temperature, high flow gas switching system. A full scale power plant using this technology would need a sophisticated system of valves for different feeds and outlet gases that might be a problem and also the pulsed operation for the gas turbines. Moreover the heat transfer in a packed bed must be carefully analysed, being this characteristic very important for the process. A first evaluation of the concept was made with a Cu-based oxygen-carrier and CH_4 as fuel [116,117]. However higher temperature differences and deeper radial temperature profiles can be expected working with oxygen-carriers based on nickel or iron in CH_4 combustion.

Dennis et al. [118,119] have proposed the use of a cycling fed-batch operation for solid fuels in order to reduce the attrition problems associated with the conveying of large quantities of solids in the interconnected fluidized beds configuration. In this operation mode, three consecutive periods of time (fuel feeding, char combustion without fuel feed, and oxygen-carrier regeneration with air) are carried out in only one fluidized reactor. However, for industrial practice, several reactors at different stages would be needed in order to load the power cycle. This scheme has just been experienced at lab-scale.

Finally, a rotating reactor was proposed by Dahl et al. [120,121]. In this reactor, the oxygen-carrier material is rotated between different gas streams flowing radially outwards through the metal oxide bed. Between the two reacting streams one inert gas is introduced to avoid mixing of the two reacting gases. The main challenge in this reactor concept is to avoid gas mixing between fuel and air streams, which at the moment are unavoidable.

2.1.2. Thermodynamical analysis

To identify the solid compounds that have the capacity to transfer oxygen in a CLC system is an essential task. To be considered as oxygen-carrier for CLC, a compound must show a favourable tendency toward high conversion of fuel gas to CO_2 and H_2O. Jerndal et al. [122] showed a broad thermodynamic analysis of different redox systems considered for CLC. They identified oxides of Cu, Ni, Co, Fe and Mn with favourable thermodynamics for CH_4, H_2 and CO conversion. At temperatures and pressures relevant for CLC, CH_4 is not thermodynamically stable and variable amounts of CO_2, H_2O, CO, and H_2 could appear depending on the redox system. Fig. 3 shows the equilibrium constant for the reduction reaction with H_2 and CO with different redox systems. Higher equilibrium constant means a higher conversion of the reducing gas.

The selectivity towards CO_2 and H_2O –which is affected by the equilibrium constant for CO and H_2, respectively– depends on the redox system.

Three different behaviours can be identified by analysis of the equilibrium constants for CO and H_2 showed in Fig. 3. Redox systems with equilibrium constants higher than 10^3 show almost complete conversion to CO_2 and H_2O. CuO-Cu, Mn_3O_4-MnO and Fe_2O_3-Fe_3O_4 are typical redox systems with this behaviour at common CLC conditions. For copper, the redox systems Cu_2O-Cu and those involving copper aluminates also show high conversion of gases. The redox system should be Cu_2O-Cu at temperatures higher than 950 ºC because of the decomposition of CuO to Cu_2O; in addition copper aluminate can appear if Al_2O_3 is used as supporting material.

In a second category of redox systems, those with an equilibrium constant of about 10^2 are included. In these cases, small amounts of CO and H_2 can be found. For NiO carriers a conversion in the range 99-99.5 % for H_2 and 98-99% for CO is obtained at equilibrium conditions. When Al_2O_3 is used as supporting material, the formation of $NiAl_2O_4$ is favourable at CLC conditions, which has a lower conversion of these gases (93-98 %). For CoO/Co system thermodynamics is less favourable with maximum conversion of 95-97 % for H_2 and 87-95 % for CO. In this case, full conversion could be obtained in the redox system Co_3O_4-CoO, but oxidation to Co_3O_4 is unfavoured in air at temperatures higher than 880 ºC. The redox system $CaSO_4$-CaS for CLC application also has been considered by several authors, having similar thermodynamic limitations for conversion of H_2 and CO as NiO.

The system Fe_2O_3-FeO also gives values of equilibrium constant in this category. This redox system has been used by Leion et al. [123] to justify the high gas conversions obtained for reduction deeper than Fe_3O_4. Nevertheless, Fe_3O_4 appears usually as an intermediate product in the Fe_2O_3 reduction, and further reduction of Fe_3O_4 to FeO

results in low conversion of gas. Alternatively, the presence of Al_2O_3 or TiO_2 modifies the thermodynamic for reduction of Fe_2O_3 because the formation of $FeAl_2O_4$ or $FeTiO_3$. In these cases, the reduction of Fe(III) to Fe(II) allows obtaining almost complete conversion of H_2 and CO to H_2O and CO_2.

The Fe_3O_4-FeO and FeO-Fe pairs are representative of the third category of redox systems, i.e. equilibrium constants lower than 10. Thus, these redox systems should be avoided in a CLC system based on interconnected fluidized-beds configuration. Nevertheless, reduction of Fe_2O_3 to FeO or Fe systems could be exploited with full combustion if special configurations of fuel reactor was used, e.g. with counterflow of gas and solids [20,58]. This configuration has been proposed in chemical looping processes involving an intermediate step of oxidation to Fe_3O_4 with steam for hydrogen production. However, oxidation of FeO or Fe to Fe_2O_3 with air shows ussually agglomeration of particles in CLC systems [80].

Some of the systems above showed (CuO-Cu_2O, Mn_2O_3-Mn_3O_4, Co_3O_4-CoO) have the capacity to release oxygen at the fuel-reactor at high temperature. These materials have been proposed to be used in CLC for solid fuel applications as will be discussed later on.

2.1.3. Mass and heat balances

The CLC concept is based on the transport of oxygen from the air to the fuel by means of an oxygen-carrier. For a CLC system based on two interconnected fluidized beds the circulation rate between them must be high enough to transfer the oxygen necessary for the fuel combustion and the heat necessary to maintain the heat balance in the system, if necessary.

Mass balance. The mass balance determines the oxygen carrier circulation rate between the fuel and air reactors which depends on the type of oxygen-carrier and fuel used.

Taking as a reference 1 MW_{th} of fuel, and assuming full conversion of gas ($\Delta X_f = 1$), the solids circulation flow rate, $\dot{m}_{OC}$, is obtained as [124],

$$\dot{m}_{OC} = \frac{1}{R_{OC}\Delta X_s}\frac{2dM_O}{\Delta H_c^0} \tag{4}$$

d being the stoichiometric coefficient for O_2 in reaction (3), M_O the atomic weight of oxygen, and ΔH_c^0 the standard combustion heat of the fuel. ΔX_s is the difference in solids conversion between the inlet and the outlet of the fuel or air reactors. The solid conversion of the oxygen-carrier is defined as,

$$X_s = \frac{m - m_r}{m_o - m_r} = \frac{m - m_r}{R_{OC} m_o} \tag{5}$$

where m is the instantaneous mass and the denominator is the maximum oxygen transport between the fully oxidized, m_o, and reduced, m_r, oxygen-carrier. The oxygen transport capacity of the material R_{OC}, defined by equation (6), depends on the oxygen transport capability of oxide, R_O, and the fraction of the active compound for the oxygen transport, x_{OC}.

$$R_{OC} = x_{OC} R_O \tag{6}$$

It must be considered that the metal oxides are combined with an inert [27]. Thus, the effective value of oxygen transport capacity of an oxygen-carrier depends on the fraction of active material for oxygen transport, x_{OC}. The oxygen transport capability, R_O, defined by equation (7), is dependent on the metal oxide and redox reactions considered.

$$R_O = \frac{m_o - m_r}{m_o} \tag{7}$$

Fig. 4 shows the value of R_O for some redox systems of interest. Higher R_O values correspond to $CaSO_4$, Co_3O_4, NiO and CuO. The interaction of the metal oxide with the support material can affect to the oxygen transport capacity of the oxygen-carrier. For

example, for Fe-based oxygen-carriers supported on Al_2O_3 or TiO_2 the reduction of Fe(III) in Fe_2O_3 to Fe(II) in iron aluminate ($FeAl_2O_4$) or iron titanate ($FeTiO_3$) can be exploited and still reach almost complete combustion to CO_2 and H_2O in CLC system. In these cases, the oxygen transport capacity is increased because the higher utilization of oxygen in the iron oxide with respect to the restricted transformation Fe_2O_3/Fe_3O_4 in a CLC system.

Oxygen transport capacity, R_{OC}, is one characteristic of the oxygen-carrier which is important for process design and operation. R_{OC} is one indicator of the amount of oxygen that can be transferred by the oxygen-carrier between reactors. Thus, the solid circulation rate necessary to fulfil the mass balance increases with decreasing the oxygen transport capacity of the oxygen-carrier (see equation 4), either by a lower value of R_O for the redox pair or by a lower fraction of the active compound in the oxygen-carrier. Fig. 5 shows the circulation rates, $\dot{m}_{OC}$, necessary for the combustion of different fuel gases (CH_4, CO, H_2) as a function of the oxygen transport capacity of the oxygen-carrier, R_{OC}, and on the conversion difference, ΔX_s, obtained during operation. The differences in $\dot{m}_{OC}$ as a consequence of the fuel gas used are linked with the oxygen needed for the reaction of each fuel gas. Thus, to obtain 1 MW_{th}, 1.25 mol CH_4 s^{-1}, 3.53 mol CO s^{-1}, or 4.14 mol H_2 s^{-1} are necessary as a consequence of their different combustion enthalpies (see Table 2), together with oxidant flow rates, $\dot{m}_O$, of 80, 56, or 66 g/s of oxygen, respectively. Usually, the ratio between the molar oxygen flow transported by the oxygen carrier and the stoichiometric amount for complete combustion of the fuel, is defined as the oxygen-carrier to fuel ratio, ϕ, [39,40] given by

$$\phi = \frac{R_{OC}\dot{m}_{OC}}{\dot{m}_O M_O} \tag{8}$$

From a practical point of view, circulation rates must also consider other aspects related with the hydrodynamic behaviour, especially in the riser, and with the heat balance in the whole system. The circulation rate in a CFB system depends on the operating conditions and configuration of the riser. Abad et al. [124] selected 16 kg/s MW_{th} as the maximum circulation rate feasible in a CLC plant at atmospheric pressure without increased costs according to commercial experience. Assuming this value, oxygen-carriers with oxygen transport capacity values lower than ≈ 0.4 % could not be used for CLC because it would not be possible to transfer the required oxygen to fully convert the fuel to CO_2 and H_2O. Thus, an amount of 2 wt% of NiO or CuO in the materials can be enough due to their high transport capacity. However, higher metal oxide contents are required for Mn_3O_4 (> 6 wt%) or Fe_2O_3 (> 12 wt%) due to their lower transport capacity. Higher values of R_{OC} can be necessary for a pressurized CLC system if the upper limit for the solids circulation rate is lower than at atmospheric conditions. Wolf et al. [125] estimated a value for the solids circulation rate corresponding to about 7 kg/s per MW_{th} at 1.3 MPa, although the actual value would be highly dependent on the properties of the oxygen-carrier particles.

The solids circulation rate will also have consequences on the solids inventory of the CLC plant. It must be considered that the fuel gas conversion depends on the gas-solid reaction rate in the reactor, and this is affected by the oxygen-carrier reactivity and the mean residence time of the particles in the reactor [124,126]. The effect of reactivity in the calculation of solids inventories will be further explained in Section 6.5.

Heat balance. The heat release over the two reactors in a CLC system is the same as normal combustion, although the distribution between the fuel- and air-reactors depends both on the fuel gas and the material to transport the oxygen used. Table 2 shows the oxidation and reduction enthalpies for the different redox systems. The oxidation

reaction is always exothermic with subsequent heat release. However, the reduction reaction is exothermic or endothermic depending on the redox system. The energy involved during the reduction with CH_4 is significantly different to that involved in the reduction with H_2 or CO. Thus, in most of the cases the reduction with CH_4 is endothermic, whereas the reduction with H_2 or CO usually is exothermic, as can be seen in Table 2. When the reduction reaction is endothermic, the oxidation reaction has a higher heat of reaction than conventional combustion of the fuel gas with air.

The interaction of the metal oxide with the support material can change the thermodynamic of the redox system. This fact is relevant for the CuO/Al_2O_3 system. In this case, the copper aluminate compound can be formed ($CuAl_2O_4$), which varies the reduction of Cu(II) to Cu with methane from exothermic to endothermic. The opposite trend is observed for the Fe_2O_3/Al_2O_3 system.

Thermal integration among the air-reactor and fuel-reactor has consequences on the system operation [122,124,127,128]. Fig. 6 shows the adiabatic temperature difference in the fuel-reactor for different metal oxides and fuel gases (CH_4 and syngas) as a function of the difference of the mass conversion, $\Delta\omega$, which depends on the oxygen transport capacity and the difference of solids conversion as:

$$\Delta\omega = R_{OC}\Delta X_s \tag{9}$$

Opposite trends in the thermal balance of the fuel-reactor happens when the reduction reaction is endothermic or exothermic. The reduction reactions with H_2 and CO are always exothermic, as well as the reduction of CuO with CH_4. These cases result in an increase in the fuel-reactor temperature and the solids circulation rate is not limited by the heat balance. Depending on the oxygen-carrier and operating conditions, it can be necessary to remove heat from the fuel-reactor to avoid an excess of temperature in this reactor [127,128]. Especial care has to be done using Cu-based oxygen-carriers, because

the increase of temperature in the fuel-reactor could cause the melting of metallic copper.

On the contrary, when the reduction reaction is endothermic the fuel-reactor is heated by the circulating solids coming from the air-reactor at higher temperature. In this case there is a temperature drop in the fuel-reactor, as is shown in Fig. 6 [122,124,127]. However, high temperatures are preferred to have a fast reaction between the fuel gas and the oxygen-carrier and a high energetic efficiency of the CLC process. To avoid a large temperature drop in the fuel-reactor, a high solids circulation rate is desired, which in practice means a low $\Delta\omega$. Thus, limitations in the variation of solids conversion can happen to maintain a relatively high temperature in the fuel-reactor. Alternatively, if the fuel-reactor temperature is fixed, the temperature in the air-reactor is increased. Nevertheless, very high temperatures in the air-reactor temperature should be avoided in order to prevent the appearance of operational problems. For example, agglomerates have been observed at temperatures as high as 1180 ºC using Ni-based oxygen-carriers [129]. Thus, for Ni-based materials low values of $\Delta\omega$ should be required to avoid a large difference on temperature between both reactors. This means that either the NiO content or the conversion of NiO should be low.

Moreover, to maintain the energy balance in the system a fraction of thermal power around 50-65% must be removed from the air-reactor –or somewhere between the fuel- and air-reactor [130-132]–. Therefore, the heat recovery system in a CLC unit should be designed both to remove the required energy and to optimize the steam cycle [115].

2.2. Oxygen-carrier fundamentals

The key issue in the system performance is the oxygen-carrier material. The oxygen-carrier must accomplish the following characteristics:

(i) sufficient oxygen transport capacity,

(ii) favourable thermodynamics regarding the fuel conversion to CO_2 and H_2O in CLC,

(iii) high reactivity for reduction and oxidation reactions, to reduce the solids inventory in the reactors, and maintained during many successive redox cycles,

(iv) resistance to attrition to minimize losses of elutriated solids,

(v) negligible carbon deposition that would release CO_2 in the air-reactor reducing CO_2 capture efficiency,

(vi) good fluidization properties (no presence of agglomeration),

(vii) limited cost,

(viii) environmental friendly characteristics.

The first two characteristics are intrinsically dependent on the redox system, and they have been analyzed in the previous section. The cost and the environmental characteristics have also relation with the type of metal oxide used. The quality of the other required characteristics must be experimentally determined for each specific material.

Normally, the pure metal oxides do not fulfil the above characteristics and reaction rates quickly decreased in a few cycles [133,134], showing the need of using a support. A porous support provides a higher surface area for reaction, a binder for increasing the mechanical strength and attrition resistance, and also increases the ionic conductivity of solids [27].

In this sense, the method used in the preparation of the materials strongly affects the properties of the oxygen-carrier. The distribution of the metal oxide on the support and the possible interaction between them will affect the oxygen-carrier reactivity, as well as the strength and material stability during the consecutive redox cycles. Several preparation methods can be found in the literature. There are methods in which powders of metal oxide and support are mixed (mechanical mixing and extrusion, freeze

granulation, spray drying, or spin flash). In other methods, a solution of the active metal and support are used as original products in the preparation. In this case, the solid compounds are generated by precipitation (co-precipitation, dissolution, sol-gel, solution combustion). Finally, there is the impregnation method where a solution containing the active metal is deposited on a resistant and porous solid support. More specific information about the oxygen-carrier prepared by different methods can be found in the works referenced in Tables A1-A8 of Annex.

An important feature of the preparation method is the scale. Most of the preparation methods cited above are developed for laboratory scale production. At the moment, the preparation methods planned for oxygen-carrier preparation at large-scale production are spray drying, spin flash and impregnation. As an example, Fig. 7 shows photographs of two oxygen-carriers prepared by spray drying and impregnation methods.

2.2.1. Economic costs

Besides reactivity, other important feature of an oxygen-carrier is the economic cost, especially for synthetic materials. The cost of an oxygen-carrier will be the sum of several factors including the cost of the metal oxide, the inert, and the manufacturing cost. When industrial methods are used, the manufacturing costs of the oxygen-carrier are rather low and the final cost is mainly given by the price of the raw materials. Fig. 8 shows the evolution of price of the metals necessary to produce the oxygen-carriers during the last 5 years. Average annual values have been taken from the Mineral Commodity Summaries 2010 [135]. Cobalt and nickel are the more expensive metals, followed by copper. Manganese and iron exhibit the lowest prices.

Abad et al. [124] presented an evaluation of the impact of the cost of the metal oxide on the CO_2 capture cost based on the reactivity and lifetime of the materials. The whole cost of the oxygen-carrier in the process will depend on the lifetime of the particles.

Considering the makeup flow of the particles as the main cost associated with the process, a lifetime of the particles of about 300 h represents the same cost of material than the makeup of amine in the commercial MEA adsorption technology of CO_2 capture. In addition, particles with lifetime under 100 h would fulfil the target range of 20-30$ per tonne of CO_2 avoided proposed for future CO_2 capture processes. Lifetime values much higher than those have been inferred from several works during long operation in continuous CLC pilot plants [33,39]. Therefore, it can be concluded that the cost of the particles does not represent a limitation to the technology development [33,124].

2.2.2. Environmental aspects

Environmental and health issues must be considered to ensure the process meets future high standards of environmental performance and workplace safety. However, little information has been published related to the possible environment and health problems derived from the use of the above materials in CLC process.

In general, nickel and cobalt are considered the materials exhibiting the highest risk during operation. Emissions containing nickel particles from the air-reactor deserve special attention since nickel derived compounds have carcinogenic properties, and the effects and health impacts on the surroundings have to be considered. Cobalt is also expensive and involves health and safety aspects. On the contrary, iron and manganese are considered as non-toxic materials for CLC applications.

The unique work regarding environmental aspects in the handling of materials useful for CLC processes was carried out by García-Labiano et al. [136] who made a study about the solid waste management of a CLC plant using Cu-based oxygen-carriers. They concluded that the solid residue finally obtained after a recovery process can be classified as a stable nonreactive waste acceptable at landfills for nonhazardous wastes.

Although more work regarding environmental aspects is necessary for the scale-up of CLC technology, it can be said that these aspects have not been identified as immediate showstoppers of the process.

2.2.3. Attrition

The attrition behaviour of the solids is an important characteristic for its use in fluidized-bed reactors. For this purpose, crushing strength of the oxygen-carrier is a preliminary indicator. Standard test for attrition behaviour of fluidizable solid give a more relevant indication because conditions are relevant for industrial operation [137]. However it is necessary to consider that chemical stress due to redox reactions is present together with physical attrition effects. Thus attrition behaviour obtained during multicycle redox reactions in a batch fluidized bed or in a continuously operated CLC unit is a good indicator of the expected behaviour in a CLC system.

Lifetime of oxygen-carriers is an important parameter to be evaluated at full scale. The lifetime of the oxygen-carriers can be defined as the mean time that a particle must be under reaction (reduction or oxidation) in the system without any reactivity loss or without suffering the attrition/fragmentation processes that produce particle elutriation out of the system. Normally, loss of fines is defined as the loss of particles smaller than 45 μm [33]. It is assumed that particles of this size have a short residence time in a commercial unit and thus are of little use in the process. To determine their value with accuracy, operation in continuous CLC units during long time periods is necessary. The economical cost of the makeup stream of solids to replace loss of fines will depend on the lifetime of particles and on the cost of the oxygen-carrier, which is mainly affected by the metal used and its content in the solid.

Table 3 shows the lifetime data available in literature during long time tests in continuous units. The highest experience corresponds to Ni-based oxygen-carriers. High

lifetime values were derived for these particles. It must be remarked that the lifetime of particles prepared by spray drying and a total NiO content about 60 wt% was 33000 h [43], which was calculated from extrapolation of data obtained during 1016 h of continuous operation. Lower lifetime values have been obtained for $NiO/NiAl_2O_4$ particles prepared by spin flash or for impregnated Cu-based materials. Investigations to obtain high resistant copper particles to operate at high temperature gave lifetime values up to 2700 h [138] for impregnated particles with 13 wt% CuO and 3 wt% NiO.

2.2.4. Carbon deposition

The carbon deposited on the oxygen-carrier in the fuel-reactor can flow on the particles to the air-reactor and be burnt by air. Therefore, carbon deposition on the oxygen-carrier particles reduces the efficiency of the CO_2 capture and should be avoided. Carbon deposition can also produce catalyst deactivation as it is well known in the literature and industrial practice with catalysts.

Some works have analyzed carbon deposition on oxygen-carriers at lab-scale [144-166]. It has been found that carbon deposition is dependent on metal oxide, inert material and H_2O/fuel ratio. The main ways for carbon formation are decomposition of hydrocarbons, e.g. CH_4, or disproportionation of CO to C and CO_2, i.e. Boudouard reaction. The carbon formation has been systematically observed in batch mode reactors –TGA, fixed bed or fluidized bed– for Ni-based particles because both reactions can be catalyzed by metallic nickel [144-158]. Carbon formation was strongly dependent on the availability of oxygen. Usually carbon deposition appears more prominent at the end of the reduction period when more than 80% of the available oxygen was consumed [154]. Thus, rapid carbon formation happens when fuel gas combustion cannot take place, at least substantially.

Similar results to that obtained with nickel materials were found for Cu-based carriers at metal oxide conversions higher than 75 % [166]. On the contrary, for iron particles no or very little carbon was formed, even when the fuel conversion was very low [154].

The conditions for carbon formation depends on the amount of oxygen added to the fuel gas, either by the oxygen-carrier [122,147] or by H_2O or CO_2 [152,159-162]. Thus, conditions where carbon formation is avoided have been determined for NiO/bentonite oxygen-carrier [165] and for NiO/YSZ oxygen-carriers [159]. If carbon is deposited on the oxygen-carrier surface, this can be eliminated by gasification with H_2O or CO_2 [163] or the solid-solid reaction between carbon and the lattice oxygen from the particles [147]. Therefore, there is a balance between carbon formation and disappearance by oxidation or steam gasification. If these reactions are faster than carbon generation, then carbon deposition is not observed, e.g. when the temperature is high enough [153,164]. So, it can be considered that carbon is an intermediate product for the reforming reaction or for the reduction of NiO.

Nevertheless, the effect of the operating conditions is different for the reactions involved in carbon deposition and the net effect is difficult to extrapolate from batch tests to continuous operation. In fact, carbon formation in continuously operated CLC system has never been observed, even when the oxygen supply by the oxygen-carrier was close to the stoichiometric for conversion of CH_4 to CO_2 and H_2O [33,39,40,141,167-169]. As thermodynamic calculations showed, no carbon formation should be expected as long as more than one-fourth of the oxygen needed for complete oxidation of CH_4 is supplied [122,147]. This situation is exceeded in CLC systems, where full conversion to CO_2 and H_2O is desirable, and also for autothermal CLR systems where a certain excess of oxygen over the stoichiometric to give CO and H_2 must be transferred to fulfil the energy balance to the system [170]. At these conditions,

carbon is not accumulated on the oxygen-carrier particles. Therefore, it can be concluded that problems with carbon formation are not expected in a well-mixed fluidized-bed reactor.

2.2.5. Agglomeration

Particles agglomeration must be avoided in CLC with two interconnected fluidized beds because it can lead to bed defluidization that causes solids circulation disturbances and channelling of the gas stream through the bed. Channelling turns the contact between gas and particles less efficient.

Agglomeration behaviour has been investigated for some Ni-, Fe-, Mn- and Cu-based oxygen-carriers. Combinations of metal content, type of support and calcination conditions have been found to avoid agglomeration problems in these oxygen-carriers.

In general, Ni-based oxygen-carriers do not exhibit agglomeration problems at typical temperatures (950 ºC) tested in batch and continuous facilities. NiO particles with various binder materials, such as Al_2O_3, $NiAl_2O_3$, TiO_2, and ZrO_2, has been tested regarding agglomeration in fluidized beds [31,147,150,171] and it was concluded that no tendency to sinter during reaction, except for the pair NiO/TiO_2 [147]. Further, materials supported on $NiAl_2O_4$ or $MgAl_2O_4$ were tested in 10-120 kW_{th} continuous units for long term and defluidization by agglomeration of the oxygen-carrier was not found [33,139,167]. Tests at higher temperatures were also performed with some of the materials. Kuusik et al. [129] found that NiO supported on $MgAl_2O_4$ particles did not form agglomerates and did not de-fluidize in any of the tests carried out up to 1175-1190 ºC.

For Mn-based particles, the agglomeration phenomenon was detected when ZrO_2 was used as support in batch fluidized bed [31]. Johansson et al. [172] tested several materials using ZrO_2 doped with Ca, Mg, and Ce. They found that metal content and

calcination temperature affected the agglomeration tendency. One of these materials supported on $MgO-ZrO_2$ was successfully used in a CLC reactor for 70 hours without defluidization [130].

In the case of iron, the effect of the conversion range on agglomeration was clearly shown by Cho et al. [171]. Defluidization occurred during oxidation periods after long reduction periods in which significant reduction of magnetite (Fe_3O_4) to wustite (FeO) occurred yielding hard agglomerates [171,173]. However in continuous CLC operation defluidization is not expected enabling high carrier conversion. In fact, agglomeration was not detected in a 300 W_{th} CLC unit using a Fe-based material [131]. Similar results were found with the natural mineral ilmenite ($FeTiO_3$) for CLC applications [174,175].

Cu-based oxygen-carriers had a higher tendency to defluidization by the low melting temperature of Cu (1085 ºC) [176]. Some preliminary studies have reported agglomeration problems during fluidized bed operation [177,178] and eliminated CuO as potential active compound for oxygen-carriers. Cho et al. [178] found strong agglomeration with freeze granulated carriers containing 60 wt% CuO during reduction at 850 ºC. Chuang et al. [179] prepared oxygen-carriers with variable fractions of CuO on Al_2O_3 by mechanical mixing, wet-impregnation, and co-precipitation for testing in batch fluidized bed. Particles made by mechanical mixing and wet impregnation were rejected, because they agglomerated. They attributed agglomeration to the fact that CuO was not well dispersed throughout the Al_2O_3. Co-precipitated carriers, with 82.5% of CuO, did not agglomerate after 18 cycles of operation at 800 ºC with CO. However when this material was used in redox cycles to determine reaction kinetics at temperatures from 250 to 900 ºC [180], they found some carrier had become tightly stuck on the walls and distributor of the fluidized bed even working with small batches (10-30 mg) added to a sand bed.

An intensive work in developing Cu-based oxygen-carriers to avoid agglomeration problems was carried out by the research group at ICB-CSIC. de Diego et al. [166], investigated the preparation conditions and oxygen-carrier characteristics to avoid the agglomeration of the Cu-based materials supported on alumina. It was observed that the CuO content in the oxygen-carrier, the calcination temperature used in the preparation, and the conversion reached by the oxygen-carrier during the reduction period affected the agglomeration process. CuO fractions lower than 20 wt% were necessary in all cases to avoid bed agglomeration. A selected oxygen-carrier was tested at 800 ºC in a 10 kW_{th} CLC prototype using methane as fuel, showing good particle behaviour during 100 h of continuous operation [39,40]. Further studies in a 500 W_{th} CLC unit showed no agglomeration of several Cu-based oxygen-carriers using different supports (α–Al_2O_3, γ–Al_2O_3, $MgAl_2O_4$ and $NiAl_2O_4$) prepared by impregnation at temperatures of 900 ºC in the fuel-reactor and 950 ºC in the air-reactor [138].

In summary, it is possible to prepare oxygen-carriers without agglomeration problems using adequate inert materials, metal oxide content and preparation method for the typical metal oxides used in CLC.

2.3. Development of oxygen-carriers

Many efforts have been made to develop oxygen-carriers suitable for the different processes. A selection of oxygen-carrier materials for natural gas and syngas combustion has been summarized by Lyngfelt et al. [98] and Hossain and de Lasa [99]. Most of the oxygen-carriers proposed in the literature are synthetic materials. The active metal oxides (CuO, Fe_2O_3, NiO, Mn_3O_4 or CoO) are supported on different inert materials such as Al_2O_3, $MgAl_2O_4$, SiO_2, TiO_2, ZrO_2 or stabilized ZrO_2 (with yttria, MgO or CaO), bentonite, sepiolite, etc. Major contributors are Chalmers University of

Technology (CHALMERS), Institute of Carboquímica belonging to Spanish National Research Council (ICB-CSIC), Tokyo Institute of Technology (TITECH) and Korea Institute of Energy Research (KIER). In addition, on the basis of lower cost with respect to synthetic materials, there are some studies on the suitability of using some minerals as iron ore, ilmenite, manganese ore or waste materials coming from steel industry and alumina production.

Thus, more than 700 carriers have been developed and tested. Tables A1-A8 of Annex give an overview of the development work on oxygen-carrier materials made in the past, including synthetic materials, mixed oxides, minerals and waste materials. These tables give information about the metal oxide content, support, preparation method, as well as the laboratory installation or facility where it has been tested, the reacting gases and the application for which it has been directed. Similar materials prepared with different metal oxide content or calcination temperatures have been grouped. A compilation of the methods used for oxygen carrier preparation can be found elsewhere [20].

An important aspect of the oxygen-carrier materials is the suitability to be used in continuous CLC units during long periods of time. However, the number of materials tested in this kind of units is limited. Table 4 shows a summary of those oxygen-carriers tested in continuous CLC units specifying the operation time of each material. In short, Table 5 shows a summary of the operation hours in continuous plant depending on the metal oxide, and application for the works published up to the end of 2010.

2.3.1. Ni-based oxygen-carriers

Ni-based oxygen-carriers have been the most extensively materials analyzed in the literature. Ni-based oxygen-carriers have shown very high reactivity and good

performance working at high temperatures (900-1100 ºC). Near complete CH_4 conversion was obtained in a CLC process, although thermodynamic restrictions result in a small presence of CO and H_2 in the gas outlet of the fuel-reactor. Nickel is more expensive than other metal oxides, although this problem may be solved using particles with low nickel content, high reactivity, and low attrition rate. Moreover, the use of Ni-based oxygen-carriers may require safety measures because of its toxicity.

Table A1 summarizes Ni-based particles investigated by different authors and the testing conditions to evaluate their feasibility for use as oxygen-carriers for a CLC system. Pure NiO particles have low reaction rate due to their low porosity [27,134]. To increase the reactivity and regenerability of the oxygen-carrier particles, a number of Ni-based solid particles fashioned by different preparation methods and using different compounds as support material have been tested. Spray drying [181], incipient impregnation [151], and mechanical mixing [37] has been used considering the capability of scaling-up for industrial application and the potential to reduce particle production costs.

The use of alumina-based compounds as support material has been extensively investigated in the literature. In comparison with other metal oxides, most of the oxygen-carriers supported on Al_2O_3 compounds showed very high reactivity with all fuel gases, no agglomeration problems, low attrition rates during operation in fluidized beds, and avoidance of carbon deposition at CLC conditions.

However, reduction of NiO/Al_2O_3 particles was limited by the partial transformation of NiO into $NiAl_2O_4$ spinel compound [165,211], which has poor reactivity for CLC [212]. Oxygen-carriers prepared by Ni–Al–O mixtures consisted of cubic NiO and $NiAl_2O_4$ spinel. Nevertheless, high reactivity and low $NiAl_2O_4$ formation was found in some cases using mechanical mixing or impregnation methods [32,150,176,213,214].

However, particles prepared by mechanical mixing were rejected due to their low crushing strength [32,108].

As consequence of $NiAl_2O_4$ formation, excess of NiO must be used during particle preparation to get free NiO inside the particle. Thus, NiO particles over $NiAl_2O_4$ support have demonstrated to be very reactive although the Ni content in the particle must be very high (up to 80 wt%) to have a NiO free content of 60 wt%.

The formation of the spinel depends on the crystalline nature of the support. Therefore, the use of γ-Al_2O_3 leads to formation of important amounts of $NiAl_2O_4$. To avoid or to minimize the interaction of NiO with alumina some modifications of the support via thermal treatment or chemical deactivation can be accomplished.

Thermal treatment of γ-Al_2O_3 at 1150 ºC produced the phase transformation to α-Al_2O_3. Ni-based oxygen-carriers prepared by impregnation on α-Al_2O_3 showed very high reactivity, showing low attrition rates and agglomeration avoidance problems during operation in fluidized beds [150]. However, thermal treatments do not avoid completely the formation of the spinel compound. Dueso et al. [215] observed that reactivity of these particles prepared by impregnation was dependent on the conversion reached during the reduction stage. These differences were attributed to the different free NiO and $NiAl_2O_4$ contents on the sample. They concluded that about the 80% of the Ni reduced in the fuel-reactor was oxidised to free NiO while the remaining Ni was oxidised into $NiAl_2O_4$.

Chemical deactivation of the support can be also used to avoid the spinel formation. This method consists in precoating the support with other compounds (Mg, Ca, La and Co) increasing the inert function of the support. Addition of CaO or MgO to the NiO/Al_2O_3 mixture improved the stability of the support material by formation of a spinel structure i.e. $MgAl_2O_4$ or $CaAl_2O_4$, and improves regenerability upon repeated

redox cycles at temperatures up to 950 ºC [150]. Excellent reactivity and regenerability were found for particles using supports modified by Co and La, although these oxygen-carriers have only been tested at temperatures below 700 ºC [216-220].

In general, the use of other compounds as support material has shown problems with reactivity, mechanical strength, defluidization or carbon formation. Particles using zirconia (ZrO_2) [32,147] or YSZ [221] as inert material presented good reactivity, but mechanical strength values were low. Lower reactivity was shown using bentonite as support [108] especially at temperatures above 800 ºC [153,165,22,223]. Very slow or no reaction was found for TiO_2 and MgO support materials as a consequence of the formation of stable complex compounds, $NiTiO_3$ and $Mg_{0.4}Ni_{0.6}O$, respectively [108,147,156,159], except for those prepared by mechanical mixing that were calcined at temperatures in the range 1100-1200 ºC [32]. Also low reactivity, deactivation as a function of the cycle or low mechanical strength was seen for NiO supported on SiO_2 [32,224] or sepiolite [32].

Main part of oxygen-carriers shown in Table A1 has been investigated by TGA and in batch fluidized-bed reactors. However, limited information can be obtained from discontinuous experiments. To gain a more adequate understanding of the behaviour and usefulness of the particles in CLC process, tests are needed in real systems where the particles are continuously circulated between the air-and fuel-reactor. Only a small group of selected Ni-based oxygen-carriers with very promising properties at laboratory scale (high reactivity during reduction and oxidation reactions, regeneration capacity for repeated redox cycles, and durability) has been investigated in continuous units at different scales from 300 W_{th} to 120 kW_{th}, (see Table 4).

Ryu et al. [37,153,165] at Korea Institute of Energy Research tested in a 50 kW_{th} CLC unit an oxygen-carrier prepared by mechanical mixing with 60 wt% NiO on bentonite.

The material presented high attrition rates and only a few operational hours were reported. A different NiO oxygen-carrier prepared by spray drying was later prepared and tested during more than 50 hours obtaining good operational results [107].

Lyngfelt et al. [33,188] at Chalmers University of Technology (CHALMERS) initially developed and tested oxygen-carriers prepared by freeze granulation in 300 W_{th} and 10 kW_{th} units. A Ni-based oxygen-carrier, 40 wt% free NiO on $NiAl_2O_4$, was satisfactorily tested during 100 h in a 10 kW_{th} CLC unit. It must be remarked that these experiments were the first demonstration of the technology during long periods of time. They reported loss of fines by attrition of 0.0023 % per hour, which gives a lifetime of the particles of 40000 hours.

Later, an oxygen-carrier with 40 wt% free NiO on $NiAl_2O_4$ prepared by spray drying was tested during long term operation (> 1000 h) in the same 10 kW_{th} CLC plant located at CHALMERS [43,168]. Firstly, 405 h were accomplished using a single batch of these particles. The last 611 h were achieved using a mixture of the above particles and a second batch with similar oxygen-carrier containing a small amount of MgO. No decrease in reactivity of the oxygen-carrier was seen during the test period. Based on the loss of fines measurements, a lifetime of 33000 h was estimated. However, it must be considered that the first batch of particles presented agglomeration in some cases during operation. Previous tests showed that these particles started to agglomerate at 1125 ºC and defluidized at 1150 ºC [43,129]. Addition of particles modified with MgO improved the methane conversion. These results agree with those of Johansson et al. [188,196] and Jerndal [225] using Ni-based particles with addition of MgO or the use of $MgAl_2O_4$ as support material. These materials did not form agglomerates and did not defluidize in any case up to 1175-1190 ºC [43,129].

These materials were further tested in a 120 kW_{th} unit at Vienna University of Technology to demonstrate the process at pilot scale and to determine the effect of the operating conditions on the process performance [42,167,192,194,195]. Experimental runs in the range of 60-145 kW_{th} fuel power, operating temperatures in the range of 800-950 ºC, and high global solids circulation rates up to 1.8 kg/s (13 kg/s per MW_{th}) were tested. The mixture of NiO-$NiAl_2O_4$ and NiO-$MgAl_2O_4$ particles showed better performance than the use of only NiO-$NiAl_2O_4$ particles. Depending on the oxygen-carrier and operating conditions, full CH_4 conversion and a CO_2 yield value up to 0.94 was reached.

Besides spray drying particles, Linderholm et al. [140] at CHALMERS tested the suitability of Ni-based oxygen-carrier prepared by spin-flash during 160 h in a 10 kW_{th} CLC system. The fuel conversion to CO_2 was as high as 99%. The CO fraction was found to follow the thermodynamic equilibrium for all fuel-reactor temperatures investigated, 660-950 ºC. After 160 h of operation the fractional loss of fines was 0.022 % per hour, corresponding to a particle life time of 4500 h.

Shen et al. [186] at Southeast University in China carried out experiments using Ni-based oxygen-carriers prepared by co-precipitation in a 10 kW_{th} unit during 100 h using coal as fuel. No significant change in the morphology of the Ni-based oxygen-carrier was observed at a fuel-reactor temperature ≤ 940 ºC, but loss of surface area and porosity of reacted oxygen-carriers happened when the fuel-reactor temperature exceeded 960 ºC.

Adánez et al. [141,169] at ICB-CSIC in Spain tested the suitability of Ni-based oxygen-carriers prepared by impregnation of α-Al_2O_3 for methane and syngas combustion in a continuously operated 500 W_{th} CLC unit. The main operating variables affecting the combustion efficiencies, i.e., the oxygen-carrier to fuel ratio, the solids inventory and

the fuel-reactor temperature, were analyzed. Tests carried out during continuous operation in the CLC prototype allowed one to determine the conditions necessary to obtain a high efficiency during the methane combustion using this Ni-based oxygen-carrier. At 880 ºC, an oxygen-carrier to fuel ratio, ϕ, higher than 1.5 and a solid inventory in the fuel-reactor of 600 kg per MW_{th} were necessary to reach combustion efficiencies close to the maximum allowed by the thermodynamic constraint. The solids inventory and fuel-reactor temperature had a high relevance to the combustion efficiency, whereas the solids circulation rate also became more important at $\phi < 1.5$-2. During 100 h of operation, the oxygen-carrier particles never showed agglomeration problems or carbon deposition in the fuel-reactor with low attrition rates (0.01 % per hour). The estimated lifetime would be 10000 h. No changes in the physical properties of the particles were observed. The results obtained in these works showed that the use of a Ni-based oxygen-carrier prepared by impregnation is suitable for methane combustion in a continuously operated CLC system.

Other important characteristic of the Ni-based materials is their behaviour with respect to sulfur present in the fuel. Reactivity deactivation by the presence of H_2S in the fuel gas has been observed [45,226]. Using an impregnated Ni-based oxygen-carrier in a 500 W_{th} unit, nickel sulphide was always formed when H_2S was present in the fuel gas [45]. From their results, a maximum value of 100 ppmv H_2S in the fuel gas was inferred for a good performance of Ni-based oxygen-carriers in CLC.

2.3.2. Cu-based oxygen-carriers

Cu-based oxygen-carriers have shown high reaction rates and oxygen transfer capacity, and have no thermodynamic restrictions for complete fuel conversion to CO_2 and H_2O. In addition, copper is cheaper than other materials used for CLC such as nickel and cobalt and its use in oxygen-carriers has less environmental problems than those.

Table A2 summarizes a review of most Cu-based particles investigated and the testing conditions to evaluate their feasibility as oxygen-carrier for a CLC system. Pure CuO have been investigated in some studies carried out by TGA during reaction with fuel gases or directly with coal [133,227-231]. This metal exhibits high reactivity, even at low temperatures [228] although the oxidation reaction rate of pure CuO decreased quickly with the increasing number of cycles [133].

To improve CuO performance, a number of Cu-based materials have been prepared using different compounds as support materials (Al_2O_3, bentonite, BHA, $CuAl_2O_4$, MgO, $MgAl_2O_4$, sepiolite, SiO_2, TiO_2 and ZrO_2) and different preparation methods (mechanical mixing, co-precipitation, spray drying, freeze granulation and impregnation). If alumina is used, an interaction between CuO and the support to give $CuAl_2O_4$ has been observed [166,176,179]. However this material is highly reducible showing very high reduction reaction rates similar to that of CuO. The majority of these investigations were carried out using TGA, batch fluidized bed or fixed-bed reactors (see Table A2).

Cu-based materials have exhibited very high reactivities with all the supports and preparation methods. Oxygen-carriers prepared by impregnation on SiO_2, TiO_2 or γ-Al_2O_3 [29,133,176] or co-precipitation with Al_2O_3 [179] have excellent chemical stability, maintaining mechanical strength after multicycle testing. On the contrary, particles using other supports or preparation methods showed a substantial decay in the mechanical properties to unacceptable levels during preparation [32] or after repeated redox cycles [133].

However, the main concern on the use of Cu-based oxygen-carriers was related with the agglomeration problems due to the low melting point of Cu (1085 ºC) [176-180]. The major advancements in the development of Cu-based materials for its use in CLC were

carried out at ICB-CSIC [166]. The preparation conditions were optimized to avoid the agglomeration of the Cu-based materials during their operation in a fluidized bed which was the main reason adduced in the literature to reject this kind of materials for their use in a CLC process. The optimum preparation method was the impregnation on $\alpha-Al_2O_3$, $\gamma-Al_2O_3$, $MgAl_2O_4$ or $NiAl_2O_4Al_2O_3$ [138,166]. CuO content lower than 20 wt% was required to avoid agglomeration during fluidization.

From a previous screening carried out by de Diego et al. [166], a 15 wt% CuO impregnated on γ-Al_2O_3 oxygen-carrier was selected to be tested in 500 W_{th} and 10 kW_{th} CLC units for syngas and CH_4 combustion. Very successful operation was obtained in a continuous 10 kW_{th} CLC prototype using methane as fuel during 120 h both regarding methane combustion efficiency and particle behaviour [39,40]. Adánez et al. [39] analyzed the effect of the operating conditions (oxygen-carrier to fuel ratio, fuel gas velocity, oxygen-carrier particle size, and fuel-reactor temperature) on fuel conversion. It was found that the most important parameter was the oxygen-carrier to fuel ratio, ϕ. Complete methane conversion, without CO or H_2 emissions, was obtained with this oxygen-carrier working at 800 °C and $\phi > 1.4$. During operation, no carbon deposition, agglomeration, or any other type of operational problems was observed. The attrition rate was high at the beginning of the experimental run and rapidly decreased. After 50 h of operation a low and constant value of the attrition rate was obtained (0.04 wt%/h), which gave a particle lifetime of 2400 h [40]. Similar results were obtained by Forero et al. [201] with the same particles for syngas combustion in a 500 W_{th} CLC unit, as well as when variable amounts of light hydrocarbons [203], i.e. ethane and propane, were present in the fuel gas. In addition, Forero et al. [202] found that the sulfur impurities present in the feed gas did not affect the reactivity of the oxygen-carrier and full CH_4 conversion can be reached in the fuel-reactor.

There is a concern about the safe temperature to operate CLC with Cu-based oxygen-carriers. Cu-based materials had been proved to fulfil the requirements for an oxygen-carrier at temperatures lower than 800 ºC in the fuel-reactor. This temperature was recommended to avoid agglomeration problems derived from the low melting point of the metallic copper (1085 ºC). However, higher operating temperatures would be preferred to obtain high energetic efficiencies in the system. Thus, information about the high temperature resistance of the oxygen-carriers would be needed. By temperature resistance is meant the ability to withstand high temperature without defluidizing or agglomerating, with low attrition rate and stable reactivity.

Recently, the high temperature resistance of some impregnated Cu-based oxygen-carriers has been investigated in a continuous CLC unit of 500 W_{th} during long-term tests using methane as fuel gas. Forero et al. [142] analysed the behaviour of a Cu-based oxygen-carrier with γ–Al_2O_3 and fuel-reactor temperatures up to 900 ºC and air-reactor temperatures up to 950 ºC. Stable operation for more than 60 h was only feasible at T_{FR} = 800 ºC and T_{AR} = 900 ºC. In addition, Gayán et al. [138] investigated the effect of the support (α–Al_2O_3, γ–Al_2O_3, $MgAl_2O_4$, and NiO-Al_2O_3) on the oxygen-carrier behaviour using temperatures up to 900 ºC in the fuel-reactor and 950 ºC in the air-reactor. They found that at these high temperatures, stable operation for more than 67 h was only feasible using the oxygen-carrier with γ–Al_2O_3 modified with a small amount of NiO (3 wt%) as support.

A waste management study from a CLC plant was carried out by García-Labiano et al. [136] using the Cu-based material obtained in the 10 kW_{th} CLC plant. Both the recovery and recycling of the used material and the disposal of the waste was analysed. The copper lost by elutriation was recovered and used for later impregnation of particles, decreasing the amount of raw materials (Cu and Al_2O_3) employed in a CLC power plant

as well as the waste generated in the process. In addition, the solid residue finally obtained in the CLC plant (composed of Al_2O_3 and $CuAl_2O_4$) can be classified as a stable nonreactive waste acceptable at landfills for nonhazardous wastes.

2.3.3. Fe-based oxygen-carriers

Because of its low cost and environmental compatibility, Fe-based oxygen-carriers are considered an attractive option for CLC applications, in spite of its weak redox characteristics, as low methane conversion and oxygen transport capacity. In this sense, iron oxide is cheaper than other metal oxides [124] and it is not toxic.

For Fe-based oxygen-carriers, different oxidation states can be found when Fe_2O_3 is reduced (Fe_3O_4, FeO, or Fe). Due to thermodynamic limitations, only the transformation from hematite to magnetite (Fe_2O_3-Fe_3O_4) may be applicable for industrial CLC systems based on interconnected fluidized-beds. Further reduction to wustite (FeO) or Fe would produce a high decrease in the CO_2 purity obtained in the fuel-reactor because of the increase in the equilibrium concentrations of CO and H_2 [122]. When alumina or titania is present in the particles, $FeAl_2O_4$ or $FeTiO_3$ can be formed as reduced compound –which corresponds to Fe(II)– in order to fully convert the gas to CO_2 and H_2O [174,232,233]. Reduction of Fe_2O_3 to FeO or Fe systems could be exploited with full combustion if special configurations of the fuel reactor was used, e.g. with counterflow of gas and solids in moving beds [20,58]. Besides the thermodynamic limitations mentioned above, some authors have found agglomeration problems in the bed associated with the phase change from wustite to magnetite [171,234] when oxidized in air.

As for the reactivity, several works have shown that Fe-based oxygen-carriers have enough reactivity both at atmospheric [32,124,173,235] and pressurized conditions [236], especially for H_2 and CO fuel gases, being lower for CH_4. Other chemical

characteristics are advantageous for the use of Fe-based oxygen-carriers: low tendency to carbon formation [154] and no risk of sulphide or sulphate formation at any sulfur-containing gas concentration or operating temperature [122].

Table A3 provides a summary of the current knowledge about the development and behaviour of Fe-based oxygen-carriers for the different CLC applications. As it can be seen, more than 60 different materials based on Fe have been evaluated in the past 10 years. The preparation methods varied from the easy physical mixing to freeze granulation, together with impregnation. The metal content ranged between 20 to 100 wt% metal oxide. Most of the works used materials with contents higher than 60 wt% due to the low oxygen transport capability of this metal oxide. Even 20% of the total different materials were pure Fe_2O_3. Abad et al. [124] pointed out that metal contents lower than 10 wt% of Fe_2O_3 were not recomended in CLC operation due to physical limitations of the solid circulation rate of interconnected fluidized-bed reactors.

A variety of materials has been used as supports for this kind of oxygen-carriers (Al_2O_3, $MgAl_2O_4$, SiO_2, TiO_2, Zr-based, etc.), alumina being the most usual. As mentioned above, the use of alumina as support has a positive effect on the oxygen transport capacity of the oxygen-carrier if $FeAl_2O_4$ is formed [232]. In general, Fe-based materials exhibited good reactivities, especially with CO and H_2. An exception would be the Fe_2O_3/SiO_2 system. The reactivity of this material decreased drastically as a function of the number of cycles due to the formation of unreactive iron silicates [237].

The majority of the works have been performed in laboratory reactors in a batch-wise mode (TGA and fluidized-bed reactors) using predominantly gaseous fuels (usually methane) to CLC application, although three Fe-based materials were analyzed for CLR application. However, tests in continuously circulated units are needed to gain a more adequate understanding of the behaviour and usefulness of these particles. As it can be

seen in Table 4, only four works have examined the behaviour of Fe-based oxygen-carriers in a continuous way using gaseous fuels, and one for solid fuels. Different pilot plants ranging from 300 W_{th} to 10 kW_{th} have been used.

Abad et al. [131] used an oxygen-carrier of 60 wt% of Fe_2O_3 and Al_2O_3 prepared by freeze granulation in 300 W_{th} continuous unit at temperatures from 800 to 950 ºC. Tests using natural gas or syngas as fuel were carried out for a total of 40 h in combustion conditions, without any sign of deactivation, agglomeration, carbon deposition, and very little attrition. This oxygen-carrier was better suited for syngas than for methane combustion. The combustion efficiency of syngas was high, about 99% for all experimental conditions. For natural gas combustion, methane was detected in the gas from the reactor and combustion efficiencies ranged up to 94%.

Tests with a Fe-based oxygen-carrier were made in a 10 kW_{th} CLC pilot plant by Lyngfelt and Thunman [33] using methane as fuel during 17 h of continuous operation. Similar results to that obtained in the above 300 W_{th} unit were found in this system. High outlet concentration of CH_4 and CO were measured (2-8%) even working at low fuel flows, high circulation rates or high fuel-reactor temperatures. Similar conclusions were reached by Son and Kim [108] in their 1 kW_{th} CLC unit with a Fe_2O_3/bentonite oxygen-carrier.

Ortiz et al. [204] used a Fe-based oxygen-carrier prepared by impregnation on Al_2O_3 in a 500 W_{th} CLC unit. The objective was to analyze their behaviour regarding to the combustion of a simulated tail gas from a PSA unit (CH_4, CO, CO_2 and H_2). The prototype was running during 50 hours with no carbon formation, agglomeration or defluidization problems. They found that CH_4 is the most difficult gas to burn. Nevertheless, complete combustion of the PSA-offgas components, i.e. CH_4, H_2 and

CO, was obtained working with the Fe_2O_3/Al_2O_3 material at high oxygen-carrier to fuel ratios ($\phi > 4$), and fuel-reactor temperature of 880 ºC.

An option to obtain high CH_4 combustion efficiencies with lower solid inventories is the addition of small amounts of a Ni-based oxygen-carrier to increase the reaction rate for the reforming reaction [238]. Using this idea, Fe-based oxygen carriers with small addition of Ni-based particles has been proposed to be useful for CLR [158]. A deeper analysis of these mixtures of particles will be made in Sections 2.3.6. and 4.2.

The application of CLC to solid fuels has been focussed on the use of pure iron oxides as oxygen-carriers. Table A3 shows that no more than 9 materials were evaluated using different solid fuels (char, coal, petcoke, and biomass), usually in TGA or batch reactors. $Fe_2O_3/MgAl_2O_3$ materials showed good performance in a batch fluidized bed [239], whereas Fe_2O_3 supported on Fe_3O_4 particles showed loss of reactivity after 20 redox cycles [240]. Lower reactivity was found for no-supported particles prepared from pure Fe_2O_3 powder [109,241]. Usually, most of gasification products were burnt, being the char gasification the rate-limiting step in the coal conversion [241].

2.3.4. Mn-based oxygen-carriers

Similar to the Fe-based materials, interest has been found in the literature in the development of Mn-based materials because this metal oxide is considered a non-toxic and cheap material. Moreover, the oxygen transport capacity is higher when it is compared to iron compounds. However, only few works deal with the use of Mn-based materials as oxygen-carrier for CLC, see Table A4.

Several oxidation states could be involved in the manganese redox reactions. The highest oxidized manganese compound, MnO_2, decompose at ≈ 500 ºC, whereas Mn_2O_3 is thermodynamically stable in air at temperatures lower than 900 ºC [242]. However, at

temperatures higher than 800 ºC, surprisingly, only the presence of Mn_3O_4 could be established [243]. Therefore, the transformation between only Mn_3O_4 and MnO is considered for CLC applications.

The use of particles consisting of pure manganese oxide has shown low reactivity with methane or coal [227,230]. Several inert compounds have been tested as supporting material for the particle preparation of Mn-based oxygen-carrier to improve its performance. The use of SiO_2, TiO_2, Al_2O_3 or $MgAl_2O_4$ as inert material was rejected because of the formation of highly irreversible and un-reactive phases [32,176,178,224,237], as well as the use of sepiolite because of the low mechanical strength showed by particles [32].

By contrast, the use of bentonite as binder has revealed promising results from TGA reactivity tests [226]. Particles exposed to a mixture of H_2 and CO showed good reactivity. In addition, the reactivity was very sensitive to the presence of H_2S in the gas mixture, simulating the composition of coal-derived synthesis gas.

Particles prepared with ZrO_2 as supporting material showed good reactivity as well as stability through consecutive redox cycles [244]. In addition to reactivity tests in TGA, this kind of particle has been exposed to repeated reduction and oxidation cycles in batch fluidized-bed reactors. During heat treatment and reactivity testing, Mn-based particles with ZrO_2 underwent a phase transformation which produced cracks in the structure [245]. Similar materials showed agglomeration and most of the particles were stuck to the reactor wall [31,145]. To avoid these problems, new oxygen-carriers were prepared with ZrO_2 stabilized by addition of MgO, CaO or CeO_2 [245]. These materials showed high reactivity, limited physical changes during redox reactions, and avoidance of agglomeration. The oxygen-carrier that seemed less affected by the continuous redox reactions and at the same time showed high reactivity was the one stabilized with MgO.

Mn-based oxygen-carriers supported on ZrO_2 stabilized with MgO has shown good reactivity with syngas components, i.e. H_2 and CO [246], but lower reactivity has been found for CH_4 [244]. These particles have been also tested in a continuously operated 300 W_{th} CLC unit [130]. Absence of agglomeration and low attrition rate were observed. These particles were better suited for syngas than for methane combustion, according to the higher reactivity showed with syngas. Thus, very high efficiencies (>99.9 %) were obtained at temperatures in the range 800-950 ºC for syngas combustion. For natural gas combustion, some methane was detected in the gas outlet from the fuel-reactor and combustion efficiencies ranged from 88 to 99%.

2.3.5. Co-based oxygen-carriers

Cobalt oxide was considered as a possible oxygen-carrier due to its high transport capacity even considering its high cost and environmental concerns.

Several oxidation states can be involved in the redox reactions with cobalt. However, it must be considered that Co_3O_4 is unstable above 900 ºC, and it is converted into CoO. Therefore, the transformation between CoO and Co only is considered for CLC applications although in this case the thermodynamics is less favourable with maximum conversion of ≈95-97% for H_2 and ≈87-97% for CO in the temperature range 800-1200 ºC.

All these reasons explain why only few works deal with the development of this type of materials, as it can be observed in Table A5. Jin et al. [144,152] developed Co-based oxygen-carriers over several supports, and tested their behaviour on a TGA during a few cycles. The authors observed that CoO/YSZ oxygen-carrier exhibited good reactivity and low carbon deposition in their TGA studies. When using Al_2O_3, TiO_2 and MgO as inert, metal oxide and support suffered a strong interaction to form unreactive compounds such as $CoAl_2O_4$, $CoTiO_3$ and $Mg_{0.4}Co_{0.6}O$. The same conclusion was

obtained by Mattisson et al. [176] with an oxygen-carrier prepared by impregnation using Al_2O_3 as support, and concluded that the material was not suitable for CLC.

The most relevant advance obtained with this type of carriers was obtained by Ryu et al. [38,247] who reported 25 hours of continuous operation in their 50 kW_{th} CLC unit using a Co-based material supported on $CoAl_2O_4$. They reported a 99.6% of CH_4 conversion although they concluded that attrition resistance should be improved to accomplish long-term CLC operation.

2.3.6. Mixed oxides and perovskites as oxygen-carriers

It is well-know that complex metal oxides may sometime provide better properties than those of individual metal oxides. So, oxygen-carriers based on mixed oxides have been prepared, characterized and tested to evaluate its performance in the CLC process. The investigations have been performed either by mixing different active metal oxides into the same particle (showed in Table A6) or mixing different oxygen-carriers composed by single metal-oxides. The main objectives desired using mixed oxides instead of an oxygen-carrier based on a single metal oxide can be some of the following:

- To increase the reactivity and/or stability of particles.
- To improve the conversion of the fuel gas.
- To improve the mechanical strength and to decrease the attrition rate of particles.
- To minimize the carbon deposition.
- To decrease the preparation cost of the oxygen-carrier, using cheaper metal oxides.
- To minimize the use of toxic metals, as for example nickel oxide.

Materials containing Cu and Fe with the spinel structure (see Table A6) prepared by different methods were tested in a TGA apparatus and in a batch fluidized-bed reactor [161,162,248-250]. Rifflart et al. [250] found that the best working spinel formulation was $Cu_{0.95}Fe_{1.05}AlO_4$, with high oxygen transfer capacity, high oxidation rate, but a

relatively low reduction rate compared with a reference Ni-based oxygen-carrier ($NiO60NiAl_2O_4$). Lambert et al. [248] found that impregnating NiO on this spinel material increased both oxygen-carrier capacity and reactivity of the resulting material. However, the addition of CuO on the spinel produced agglomeration and defluidization of the bed during the reduction and oxidation.

Lambert et al. [251] studied Fe-Mn mixed oxides to check for eventual cooperative effects between both metals. Ksepko et al. [252] also prepared oxygen-carriers consisting of Fe_2O_3-MnO_2 supported on ZrO_2 and sepiolite and observed that both carriers exhibited excellent reaction performance and thermal stability for CLC process at 800 ºC. They also found that the support had an important effect on the reaction rate. The sepiolite appeared to be a better support than ZrO_2. Moreover, Fe-Mn-O mixed oxides have oxygen uncoupling properties, as well as Ni-Mn-O materials. In these cases, $NiMn_2O_4$ or $Fe_xMn_{(1-x)}O_3$ can be formed suggesting that Mn(III) can be exploited as CLOU material [253]. The use of Fe-Mn-O and Ni-Mn-O systems has been also evaluated for methane conversion [253]. From this screening, only one Mn-Fe-O material showed enough high values of reactivity and mechanical strength to be used as oxygen-carrier.

Jin et al. [144,160] prepared a CoO-NiO supported on YSZ oxygen-carrier. They found that the reduction and oxidation reaction rates of this oxygen-carrier were slightly lower than those of the individual metal oxides because a solid solution ($NiCoO_2$) between NiO and CoO was formed. However, the double metal oxides provided an excellent performance with good reactivity, complete avoidance of carbon deposition, and significant regenerability for repeated cycles of reduction and oxidation. Hossain et al. [216,217] also prepared a bimetallic Co-NiO/Al_2O_3 oxygen-carrier which was tested at temperatures up to 750 ºC. The oxygen-carrier displayed excellent reactivity and

stability. The addition of Co enhanced the reducibility of the oxygen-carrier by minimizing the formation of nickel aluminate, and inhibited metal particle agglomeration.

Adánez et al. [146] prepared stable bimetallic Cu-Ni/Al_2O_3 particles and observed that the presence of NiO in the oxygen-carrier stabilized the CuO phase. The use of salts of K or La in the preparation of the bimetallic Cu-Ni oxygen-carriers did not produce any improvement in their behaviour during CLC testing. Further, long-term tests in a 500 W_{th} CLC unit under continuous operation using methane as fuel and high temperature were carried out using a Cu-based oxygen-carrier (13 wt% CuO) prepared using γ-Al_2O_3 as support modified with a small NiO addition (3 wt%) [138]. These particles showed high metal oxide utilization, complete CH_4 combustion, and low and stable attrition rate after 67 h of operation at high temperature (T_{AR} = 950 ºC and T_{FR} = 900 ºC). A particle lifetime of 2700 h was estimated for those particles. Agglomeration was not observed and particles maintained their structural integrity and original homogeneity in copper distribution. This is the first time that a Cu-based oxygen-carrier, prepared by a commercial manufacturing method, exhibits good behaviour at these temperatures.

Bimetallic Fe-Ni oxygen-carriers have been prepared by different researchers. Lagerbom et al. [254] tested in a TGA a bimetallic Fe-Ni/Al_2O_3 oxygen-carrier and observed that addition of NiO to Fe_2O_3/Al_2O_3 particles improved the activity but decreased the mechanical strength. Son and Kim [108] carried out experiments in a continuous CFB using different Fe-Ni/bentonite particles. They found that the reactivity of the oxygen-carrier particles increased with increasing NiO content. The optimum ratio of NiO/Fe_2O_3 was found to be 3 (NiO/Fe_2O_3=75:25).

The addition of Ni-based particles in a bed of Fe-based particles has been also investigated. Johansson et al. [238] found that a bed of iron oxides with only 3 wt% nickel oxides was sufficient to give a very high CH_4 conversion. In addition, these researchers showed that the mixed-oxide system produced significantly more CO_2 than the sum of the metal oxides run separately, thus giving evidence of the synergy in using nickel oxide together with iron oxide. Very similar findings were also observed by Rydén et al. mixing NiO60-$MgAl_2O_4$ either in a bed of $Fe_2O_3$60-$MgZrO_2$ [234], in a bed of ilmenite [255] or waste products from the steel industry [256]. The positive effect of the Ni addition was also found in continuous units. Ortiz et al. [204] reported an increase in the combustion efficiency in a continuous 500 W_{th} CLC prototype using PSA as fuel gas.

In addition to mixed oxides with the spinel structure and bimetallic oxygen-carriers, other more complex metal oxides with perovskite structure (see Table A7) have been proposed to be used as oxygen-carriers for the CLC process [158,257,258]. Several materials including mixtures of several metals oxides (La, Sr, Co, Fe, Cu, Cr or Ni) has been tested. $La_xSr_{1-x}Fe_yCo_{1-y}O_{3-d}$ was found to be feasible for CLC, whereas $La_xSr_{1-x}FeO_{3-d}$ perovskite was found to be well suited for CLR.

However, long-term chemical and mechanical properties of perovskite particles are largely unknown and further investigation with these new materials is needed to know its behaviour in continuous fluidized-bed reactors.

Also a perovskite type structure can be formed when calcium and manganese are present in the particles. In these cases, Mn(IV) appears to be the oxidized form, whereas deeper reduction of Mn(III) should be avoided in order to preserve the perovskite structure [259]. The perovskite type Mn-Ca-O materials have oxygen uncoupling properties, which have been considered also to be used with gaseous fuels. A perovskite

type material, $CaMn_{0.875}Ti_{0.125}O_3$, showed good methane conversion values and chemical stability in batch and continuous CLC systems [259,260].

2.3.7. Low cost materials as oxygen-carriers

Increasing interest is being shown in low cost materials as oxygen-carriers as the option to process a solid fuel in the CLC system. Thus, in the in-situ gasification in the fuel-reactor [261] –the so-called iG-CLC– the solid fuel, e.g. coal, is physically mixed with the oxygen-carrier, with a predictable partial loss of oxygen-carrier particles in the waste stream of coal ash. In this context, the use of natural minerals or industrial waste products seems to be very promising. Nevertheless, as these materials have good reactivity with gasification products as H_2 or CO, low cost materials are also being considered for their use with gaseous fuels [123,262].

The use of ilmenite has been extensively analyzed as oxygen-carrier. Ilmenite is mainly composed of $FeTiO_3$ ($FeO{\cdot}TiO_2$), where iron oxide is the active phase that behaves as oxygen-carrier. There are an interesting number of recent studies showing an acceptable performance of ilmenite as oxygen-carrier in CLC at different scales. Norwegian and Australian ilmenites had higher reactivity when compared to one from South Africa or one provided by ArcelorMittal Eisenhüttenstadt GmbH [113,263,264]. Moreover, the South African ilmenite showed a tendency to agglomerate [263]. Norwegian ilmenite has been the most used material. Comparing the performance of several natural iron ores and industrial products, Norwegian ilmenite was among the materials which showed higher reactivity for both gaseous and solid fuels [123,265].

Although ilmenite particles have initially a rather low reactivity, it undergoes an activation process after several redox cycles. An increase in porosity and reactivity of ilmenite particles occur with increasing the redox cycles, accompanied with an increase in its reactivity remarkably for H_2, CO and CH_4 as reacting gases [266]. Adánez et al.

[266] found that the number of consecutives redox cycles to activate ilmenite depended on the reduction degree reached for each fuel gas in every cycle. Eventually, a constant reactivity was reached. When the variation of solids conversion was low (lower than 20%), the oxygen transport capacity was barely affected by the number of cycles [206]. However, if the variation of solids conversion in every cycle was higher (about 50%), the oxygen transport capacity decreased from the original value of 4% down to 2.1% after 100 redox cycles because of Fe segregation from the titanium-rich phase [266]. The activation of ilmenite particles has been confirmed also during continuous operation in a 500 W_{th} CLC unit using coal as fuel [206]. A short activation period has been found, so a previous activation step of ilmenite particles would not be necessary in industrial operation.

The ilmenite material has been tested for CLC systems with gaseous or solids fuels. The gas conversion shown by activated ilmenite was similar to one synthetic $Fe_2O_3/MgAl_2O_4$ material selected from prior works [267]. Thus, ilmenite has high conversion of CO and H_2 for syngas applications, but moderate conversion of CH_4 for the use of natural gas as fuel [174,266]. The good conversion of syngas using ilmenite has been shown in dual fluidized bed CLC systems [208,209]. Additionally, ilmenite showed good mechanical stability and good fluidizing properties.

In addition, the performance of ilmenite in continuously operated CLC system has been analyzed with various solid fuels in the input thermal power range of 500 W_{th} [206] and 10 kW_{th} [54,55]. From results obtained in a 10 kW_{th} CLC unit, it was concluded that the low tendency for attrition or agglomeration of this material and its low market price make it one interesting option for use in the iG-CLC process.

The use of different ores also has been evaluated to be used as oxygen-carrier. The main component of fresh iron ore is hematite (Fe_2O_3), and the pre-treatment only consisted of

crushing, sieving and calcination. Mattisson et al. [268] found that iron ore has sufficient reaction rate for reduction and oxidation to be employed in a CLC system. Further, a screening of different iron ores identified several materials as suitable oxygen-carriers for CLC both for syngas [123] and for solid fuels [265]. The effect of pressure on the reaction rate with coal gasification products of an iron ore was analyzed by Xiao et al. [269-271] in a fixed-bed reactor. The reactivity of particles increased and stabilized after approximate 10 cycles and agglomeration was not observed. The particles become porous after experiments with coal but maintain its structure and size after several cycles. Furthermore, to evaluate the performance of natural iron ore as an oxygen-carrier for CLC of coal, the continuous operation has been accomplished in a 1 kW_{th} CLC reactor [143]. No tendency to decrease reactivity was observed during 10 h of operation. Indeed, an activation of this material with increasing the number of redox cycles was found and stabilized after 10 cycles [270]. However, moderate fragmentation/attrition in the interconnected fluidized beds was detected. The rate of loss of fine particles was 0.0625%/h, corresponding to a particles lifetime of 1600 h.

Leion et al. [123] and Fossdal et al. [262] analyzed the behaviour of several iron and manganese ores, as well as iron and manganese industrial products, during repeated redox cycles at fluidizing conditions using syngas or methane as fuel gases. Regarding the reactivity of materials, Fossdal et al. [262] found a Mn ore as the most promising for CLC applications. However, Leion et al. [123] concluded that manganese ores showed poor mechanical stability and poor fluidizing properties making them unsuitable as oxygen-carriers.

Among the industrial by-products tested for CLC application, remarkable results were obtained with materials based on iron oxide, e.g. oxide scales from rolling of steel sheets [123,265] or red mud, a waste product of the alumina production [210]. On the

one hand, oxide scales had higher reaction rates compared to iron ore or ilmenite and showed a small increase in reactivity for every cycle in a batch fluidized bed when syngas or methane was used as fuel [123]. On the other hand, the coarse fraction of the red mud –particles of 150 μm called "sand process"– has been used in a 500 W_{th} CLC unit to burn syngas, CH_4 or PSA tail gas [210]. Particles maintained their properties (reactivity, no agglomeration, high durability, etc.) after more than 110 h of continuous operation. Particles showed sufficient reactivity to fully convert syngas to CO_2 and H_2O at 880 ºC with 400 kg/MW_{th}. However, the combustion efficiency ranged from 75% to 80% with methane containing fuels because of the lower reactivity of this gas compared to CO and H_2.

Recently, interest on the use of $CaSO_4$ as oxygen-carrier has been shown by several research groups in China. For example, $CaSO_4$ from natural anhydrite is a low cost material and has much higher oxygen transport capacity than other proposed materials [272,273] (see Fig. 4). The general reactions for the $CaSO_4$ reduction in the fuel-reactor are the following:

$$CaSO_4 + 4\,H_2 \rightarrow CaS + 4\,H_2O \quad (10)$$

$$CaSO_4 + 4\,CO \rightarrow CaS + 4\,CO_2 \quad (11)$$

$$CaSO_4 + CH_4 \rightarrow CaS + CO_2 + 2\,H_2O \quad (12)$$

These reactions have exhibited low reaction rates [274-278]. In addition, simulation results based on chemical equilibrium show that small fractions of CO and H_2 can not be converted [278,279].

ALSTOM is developing the Hybrid Combustion-Gasification Chemical Looping Process where $CaSO_4$ is used as oxygen-carrier for heat generation, syngas production or hydrogen generation [59,280]. For heat generation complete combustion of solid fuel is required, but partial oxidation happens if syngas is the desired product. The

production of hydrogen can be accomplished by coupling a $CaCO_3$/CaO cycle to the $CaSO_4$/CaS cycle with the use of an additional reactor, i.e. the calciner.

A drawback for the use of $CaSO_4$ is the possible formation of CaO by side–reactions evolving SO_2 to the reacting gases [272]. The formation of CaO can happen by several mechanisms either in the air-reactor or in the fuel-reactor, see reactions (13-19). The reactions (13-15) could happen in the fuel-reactor. Whereas the reduction of $CaSO_4$ to CaS is preferred to reactions (13) and (14) at CLC conditions [278], the decomposition with CO_2 and steam –reactions (15) and (16)– can be of importance in the fuel-reactor [281]. In addition, the relative reaction rate between the $CaSO_4$ reduction to CaS and the solid-solid reaction (17) primarily determines the fraction of Ca converted to CaO, which is dependent on the operating conditions, e.g. temperature and gas composition [273,282]. Reactions (18) and (19) are favoured in the air-reactor at higher temperatures than 1200 ºC [282], although some fractions of CaO and SO_2 can appear even at 1000 ºC during oxidation, which constrains the temperature of the air-reactor [279].

$$CaSO_4 + H_2 \rightarrow CaO + H_2O + SO_2 \quad (13)$$

$$CaSO_4 + CO \rightarrow CaO + CO_2 + SO_2 \quad (14)$$

$$CaS + 3\,H_2O \rightarrow CaO + 3\,H_2 + SO_2 \quad (15)$$

$$CaS + 3\,CO_2 \rightarrow CaO + 3\,CO + SO_2 \quad (16)$$

$$3\,CaSO_4 + CaS \rightarrow 4\,CaO + 4\,SO_2 \quad (17)$$

$$CaS + 3/2\,O_2 \rightarrow CaO + SO_2 \quad (18)$$

$$CaSO_4 \rightarrow CaO + SO_2 + 1/2\,O_2 \quad (19)$$

If CaO is generated either in the fuel-reactor or in the air-reactor, the oxygen transport capacity of $CaSO_4$ is eliminated, thus requiring the addition of fresh particles into the CLC system to replace the spent material [277]. To minimize the SO_2 release, the optimum temperature was determined to be 1050-1150 ºC in the air-reactor and 900-950

ºC in the fuel-reactor [283]. Thus, no sulphur release as either sulphur dioxide (SO_2) or hydrogen sulphide (H_2S) has been reported by ALSTOM working at temperatures up to 980 ºC [59].

Nevertheless, the conditions at which CaO is formed in a CLC system are not completely understood, and additional research are required in a continuously operated CLC system to evaluate the relevance of side-reactions for CaO generation in both air- and fuel-reactors.

2.4. Effect of fuel gas composition

Several gases have been considered as potential fuels for CLC including natural gas, refinery gas or syngas from coal gasification. Commonly, the investigations are carried out with synthetic gases simulating the composition of these fuels. However, real fuel gases contain variable amounts of light hydrocarbons (LHC), i.e. C_2-C_5, and sulfur compounds, such as H_2S, COS, mercaptans, and thioaromatics. These compounds can produce strong environmental and operational problems, which will affect the design of the CLC plant. This problem is also maintained in the most recent application of CLC with solid fuels, some of them characterized by their high sulfur content.

Recently, biogas generated from municipal solid waste, wastewater, animal manure and agricultural wastes has been also considered as an option to be used in a CLC process [249]. Moreover, the application of CLC for heat production from liquid fuels such as heavy hydrocarbons proceeding from oil and refinery industry has been also established [284]. The use of liquid fuels raises specific problems of implementation in an industrial plant that are very different from the extensively studied gaseous and solid fuels. However, the research on liquids fuels is in a very initial stage of development.

2.4.1. Fate of sulfur

Usually all fuels (natural gas, syngas, refinery gases and coal) contain sulfur compounds in variable amounts. Natural gas contains very small amounts of H_2S (≈ 20 vppm). H_2S content in refinery fuel gas can vary depending on the site but contents up to 800 vppm can be found, and this value can be increased up to 8000 vppm for raw syngas obtained from coal gasification [285].

The design of an industrial CLC plant can be affected by the presence of these sulfur compounds in a double way, and depending on the oxygen-carrier used. From the environmental point of view, the sulfur fed into the system can be released as SO_2 in the air-reactor gas outlet stream and must fulfil the legislation about gaseous emissions, or be emitted in the fuel-reactor gas stream affecting the quality of the CO_2 with important consequences for the compression, transport and storage [286,287]. Pipitone and Bolland [288] give some examples of quality specifications for CO_2 transport and storage of some industrial companies operating at the moment.

From an operational point of view, the sulfur compounds may react with the active metal oxide to form several metal sulphides that are poisonous to the oxygen-carrier, decreasing their reactivity. This process is especially important when Ni-based oxygen-carriers are used [45]. Moreover, the low melting point of some sulphides could produce agglomeration and affect the solids circulation pattern between the interconnected fluidized-bed reactors [147].

Several works have shown thermodynamic calculations about the fate of H_2S in a CLC process depending on the metal oxide selected as oxygen-carrier, the operating conditions (temperature, pressure, and H_2S concentration), and the fuel gas (CH_4, CO or H_2).

Mattisson et al [147] carried out a thermodynamic study about the fate of H_2S in a CLC system using a Ni-based oxygen-carrier and CH_4 as fuel. They found that H_2S may be oxidized to SO_2 in the fuel-reactor by oxidants such as H_2O, CO_2 and even the NiO. The degree of conversion to SO_2 is enhanced at high temperatures and low pressures. Both SO_2 and H_2S could react with the active metal (NiO or Ni) to form sulphides or sulphates (NiS, NiS_2, Ni_3S_2 or $NiSO_4$). They found out that $NiSO_4$ is not formed at the conditions which may be encountered in the fuel-reactor, and Ni_3S_2 was the thermodynamically most stable sulphide.

Jerndal et al [122] and Wang et al. [289] carried out a thermodynamic investigation about carbon deposition and sulfur evolution in CLC for most of the metal oxides used as oxygen-carriers and several fuel gases. They detected several sulphides (Ni_3S_2, $Fe_{0.84}S$, $CoS_{0.89}$) as the most possible solid sulfur compounds that can be formed at partial pressures and temperatures which may be encountered in a CLC fuel-reactor. For CuO, the Cu_2S was the most thermodynamically favored under oxygen-deficient conditions. $MnSO_4$, instead of sulphides, was found as the predominant solid species for Mn-based as oxygen-carrier, at both oxidizing and reducing conditions.

Tian et al. [226] have carried out a thermogravimetric study about the effect of H_2S present in syngas on the behaviour of several bentonite-supported metal oxides based on iron, nickel, manganese and copper during 10 redox cycles. They found that the rates of reduction and oxidation decreased in the presence of H_2S for all four metal oxides, with the highest decrease for NiO and the lowest for Mn_2O_3.

It must be noted that the thermodynamic analysis considers the final condition reached at equilibrium. However the results are difficult to extrapolate to a flow reactor with continuously changing conditions and with kinetic constraints. Therefore, experimental data are necessary to know the real consequences in a CLC process. However, only few

studies have been made in continuous units to analyze the effect of sulfur using NiO and CuO oxygen-carriers under different operating conditions.

García-Labiano et al. [45] and Forero et al. [202] have analyzed the behaviour of oxygen-carriers based on nickel and copper, respectively, during CH_4 combustion in a 500 W_{th} CLC pilot plant under continuous operation. They analyzed the influence of temperature and H_2S concentration on the gas product distribution and combustion efficiency, oxygen-carrier deactivation, sulfur splitting between fuel-reactor and air-reactor, and material agglomeration. Based on the experimental results these authors propose the most probable reactions involving sulfur compounds both in the fuel-reactor and air-reactor.

García-Labiano et al. [45] found that nickel sulphide, Ni_3S_2, was formed at all operating conditions in the fuel-reactor, which produced an oxygen-carrier deactivation and lower combustion efficiencies. Fig. 9 shows the CO_2 concentration at the fuel-reactor outgoing gas stream when methane was used as fuel gas and different amounts of H_2S (ranging from 0 to 1000 vppm) were added. It can be seen that the CO_2 concentration decreased as the H_2S concentration was increased. This fact was due to a lower conversion of methane as the H_2S concentration was increased because of the oxygen-carrier deactivation by sulphide formation and accumulation in the system. Despite the high sulphides formation in some extreme cases, agglomeration problems were never detected. The sulphides transported to the air-reactor were oxidized by air and SO_2 was released, thus requiring a desulfurization step for the air-reactor gas stream. In the case that nickel sulphide was fully decomposed in the air-reactor, it would be possible to return the oxygen-carrier fully regenerated to the fuel-reactor to start a new cycle. In fact, this regeneration process was experimentally observed after removal of sulfur feed. Thus, no accumulation of nickel sulphide and no oxygen-carrier deactivation would

occur in the CLC system. The gas produced in the fuel-reactor would contain a few ppm of sulfur and no problems with CO_2 purity are expected. Considering both operational and environmental aspects, fuels with sulfur contents below 100 vppm H_2S can be tolerated in an industrial CLC plant using a Ni-based oxygen-carrier. The implementation of a desulfurization step previous to fuel combustion would be necessary for fuels with higher sulfur content. It must be considered that desulfurization of the fuel gas can be preferred to a desulfurization step in the gas stream exiting the air-reactor because the sulfur dilution in depleted air.

The situation was different for a Cu-based oxygen-carrier. Forero et al. [202] found that the great majority (~95%) of sulfur in the fuel is released in the fuel-reactor as SO_2 under normal operating conditions, affecting mainly the quality of the CO_2 produced. Nevertheless, the cleaning of this stream is easier than the stream from the air-reactor because it has lower flow rates and higher concentrations. Formation of copper sulphide, Cu_2S, was not observed at typical operating conditions. Cu_2S was only detected during operation at low values of oxygen-carrier to fuel ratios, although this fact did not produce any agglomeration problem in the system. In addition, the oxygen-carrier was fully regenerated in a H_2S-free environment. In all cases, full CH_4 conversion was reached with low oxygen excess ($\phi \geq 1.5$) even working with a fuel containing 1300 vppm H_2S.

More recently, attention has been focusing on solid fuels such as, for instance, coal or petroleum coke. The sulfur contained in these solid fuels already may play an important role in the CLC process. Berguerand and Lyngfelt [207] investigated the CLC process of petroleum coke using ilmenite as oxygen-carrier in a 10 kW_{th} unit. The sulfur was emitted as H_2S and SO_2 in the fuel-reactor. No data on the effect of sulfur on the oxygen-carrier were presented and more studies are necessary in the future.

2.4.2. Fate of light hydrocarbons

Gaseous fuels can contain variable amounts of light hydrocarbons (LHC), i.e., C_2-C_5. In addition to methane, the LHC content may be up to 10 vol% in crude natural gas [290] and up to 30 vol% in refinery gas [291].

The concerns about the presence of these LHC in the fuel gas are related with the reactivity of the oxygen-carrier with respect to these LHC as well as on possible carbon formation during operation. Depending on the reactivity of the oxygen-carrier with the hydrocarbons, incomplete fuel conversion could happen, which would have a significant effect on the CLC process efficiency and in the CO_2 quality. It must be considered that the presence of some hydrocarbons in the CO_2 stream may increase the compression and transmission energy consumption because of changes in density and compressibility relative to pure CO_2 [286]. However, the tolerance limits of hydrocarbons in the CO_2 stream is not as restrictive as other impurities, and values < 5 vol% would be admissible [292]. Although non-converted hydrocarbons could be addressed in different ways, e.g. adding some oxygen at the fuel-reactor outlet to oxidize minor amounts of unconverted fuel [293] or separating hydrocarbons from the CO_2 gas stream, it would be desirable to get full conversion of hydrocarbons in the CLC system.

Adánez et al. [46] and Gayán et al. [203] presented experimental results in a continuous CLC plant (500 W_{th}) using LHC in concentrations up to 14.3 vol% C_2H_6 or 10 vol% C_3H_8 with oxygen-carriers based on nickel and copper prepared by impregnation. In both cases, similar conclusions were reached. Neither carbon formation nor agglomeration problems were detected during operation. Moreover, unburnt hydrocarbons never appeared at the outlet stream. Even in those cases of low solids circulation rates, the lower combustion efficiency was due to the presence of CO and H_2

but no unburnt LHC were detected at the outlet stream. They concluded that no special measures should be adopted due to the presence of light hydrocarbons in the fuel gas of a CLC plant using Ni- or Cu-based oxygen-carriers.

3. Chemical-Looping Combustion of solid fuels

Chemical-Looping Combustion (CLC) with gaseous fuels has been developed in the last years, but CLC with solid fuels has recently gained a great interest. The use of coal in CLC is very attractive in the future sceneries with restriction in CO_2 emissions, since coal will keep on being a main energy source in the medium-term. In addition, other solid fuels could be used in a CLC system, as pet-coke, solid wastes or biomass. In the case of using biomass as fuel, the CO_2 captured can be considered as a negative emission because this CO_2 was already removed from atmosphere through a photosynthesis process in the plants. In this section, different options to process solid fuels in a CLC system are described. In each case, the specific way in which the solid fuel is being converted will determine the design of the CLC system, as well as the selection of the suitable oxygen-carrier material.

There are two approaches for the use of the CLC technology with coal (see Fig. 10). The first one is to first carry out coal gasification and subsequently to introduce the syngas produced in the CLC system [18,279,294], i.e. the syngas fuelled CLC (syngas-CLC). The second approach is the direct feeding of the solid fuel to the fuel reactor in a CLC process (solid fuelled-CLC). In this last case two options have been proposed for CLC with solid fuels. On the one hand, the solid fuel is gasified in-situ by H_2O or CO_2 supplied as fluidization agent [261], i.e. the in-situ Gasification Chemical-Looping Combustion (iG-CLC). On the other hand, Mattisson et al. [57] proposed the so-called

Chemical-Looping with Oxygen Uncoupled (CLOU) process, where the solid fuel is burned with gaseous oxygen released by the oxygen-carrier in the fuel-reactor.

The main reactions involved in each process are depicted in Fig. 11. When the coal is previously gasified, the fuel-reactor is fed by syngas, mainly composed of CO and H_2 as reducing agents. In this case, the CLC design should be similar to that for any gaseous fuel, such as natural gas. In the iG-CLC, prior to reaction with the oxygen-carrier, the solid fuel is devolatilized and gasified by H_2O or CO_2 in the fuel-reactor. These gases may be used as fluidizing gas in the fuel-reactor. Eventually, volatiles and gasification products react with the oxygen-carrier particles to produce the combustion products, i.e. CO_2 and H_2O. Lastly, the CLOU process is characterized by the use of an oxygen-carrier that evolves gaseous oxygen in the fuel-reactor environment. The subsequent combustion of coal is similar to that for normal combustion with air.

3.1. Syngas fuelled Chemical-Looping Combustion (Syngas-CLC)

This way to process a solid fuel in a CLC system is schematized in Fig. 10(a). In this case, the solid fuel is gasified to produce a syngas which is fed to the fuel-reactor. To supply the energy required for the endothermic gasification process, oxygen must be used as gasifying agent to ensure that nitrogen is not present together with the CO_2 stream. Another approach is to supply the energy directly from the CLC system, e.g. introducing the gasifier inside the air-reactor [295], with the corresponding heat transfer difficulties between these reactors.

As syngas is a gaseous fuel, benefits of the experience gained using natural gas as fuel can be taken. In this option, a highly reactive synthetic oxygen-carrier is preferred in order to decrease the solids inventory in the CLC system. Several synthetic oxygen-carriers based on Ni, Cu, Fe and Mn oxides have shown good reactivity with syngas components, i.e. H_2 and CO, at atmospheric [36,232] and pressurized conditions

[223,236,294]. Special care must be done on sulphur in the syngas, especially for Ni-based oxygen-carriers due to partial deactivation of the material by H_2S [226].

The use of syngas in a CLC system has been successfully accomplished in 300-1000 W_{th} continuous CLC units using Ni-, Cu- and Mn-based oxygen-carriers [130,131,169,184,188,201]. Lower conversion was obtained for an iron on alumina oxygen-carrier [131]. In addition, the use of natural ores or industrial waste has also been suggested as oxygen-carriers for syngas combustion [123,174,175,296]. Worse performance was obtained processing syngas in a 120 kW_{th} facility with a natural ilmenite than using a Ni-based oxygen-carrier [191,208], but the low price and the environmental friendly behaviour of ilmenite are the main reasons to be considered as oxygen-carrier. Lower reactivity was found for $CaSO_4$ based oxygen-carriers [273,275,277,283].

Integrating the coal Gasification, CLC and gas turbine Combined Cycle, the process namely ICLC-CC, would have similar efficiencies as the system with conventional IGCC application [295,297] but without CO_2 capture. As the separation of CO_2 is expected to substantially decrease the net power efficiency in an IGCC system, the CLC systems have a potential of being more efficient. Hence, an additional gain of 5–10% points can be achieved compared to conventional IGCC with CO_2 recovery [294]. However, the ICLC-CC process includes the use of interconnected pressurized Chemical-Looping reactors, which is currently a challenge for the development of this technology.

3.2. In-situ Gasification Chemical-Looping Combustion (iG-CLC)

The second approach for the use of coal in CLC is the direct gasification of the solid fuel in the CLC process avoiding the need of a gasifier and the corresponding gaseous oxygen requirement [48,241,261]. The general scheme for the iG-CLC configuration is

shown in Fig. 10(b). In this option, the solid fuel is physically mixed with the oxygen-carrier in the fuel-reactor and the carrier reacts with volatiles and the gas products from char gasification, where H_2 and CO are the main components. The fuel-reactor is fluidized by H_2O, CO_2 or mixtures of these gases, which act as gasifying agents. If CO_2 is used, the energy required for steam production is avoided. CO_2 can be re-circulated from the flue gases. The use of CO_2 has been proposed for highly reactive solid fuels, such as low-rank coals or biomass [119]. Otherwise, special considerations should be given when using CO_2 as gasification agent depending on the design configuration because of the slow gasification rate with CO_2, as will be discussed later. To reduce the external energy requirements for the steam generation, coal slurry instead of dry coal particles has been proposed to be introduced into the fuel-reactor [298]. In this way the pyrolysis and gasification of coal is enhanced by the intense exchange of heat and mass when the coal slurry is in contact with the hot oxygen-carrier. However, the solids recirculated from the air-reactor must transport an additional energy to vaporize the water coming with the coal slurry stream.

In the iG-CLC, the solid fuel gasification proceeds first according to reactions (20-22) and the resulting gases and volatiles are oxidized through reduction of the oxidized oxygen-carrier, Me_xO_y, by means of reaction (23). The water-gas shift (WGS) equilibrium –see reaction (24)– can also affect the gas composition obtained in the reactor [299]. The oxygen-carrier reduced by volatiles and gasification products, Me_xO_{y-1}, is oxidized with oxygen from air following reaction (25). Thus the oxygen-carrier is regenerated to start a new cycle. The net chemical reaction is the same as in usual combustion with the same combustion enthalpy.

$$\text{Coal} \rightarrow \text{Volatile matter} + \text{Char} \quad (20)$$

$$\text{Char (mainly C)} + H_2O \rightarrow H_2 + CO \quad (21)$$

$$\text{Char (mainly C)} + CO_2 \rightarrow 2\,CO \quad (22)$$

$$H_2, CO, \text{Volatile matter} + n\,Me_xO_y \rightarrow CO_2 + H_2O + n\,Me_xO_{y-1} \quad (23)$$

$$H_2O + CO \leftrightarrow H_2 + CO_2 \quad (24)$$

$$Me_xO_{y-1} + ½\,O_2 \rightarrow Me_xO_y \quad (25)$$

Initial calculations have shown that the iG-CLC process has the potential to obtain higher power efficiencies and lower costs than other evaluated technologies [15], with a net efficiency of the process of about 41-42% [300,301]. To increase the energy efficiency, the iG-CLC process can be performed at pressurized conditions. The effect of pressure on oxygen-carrier and char reactivity can be very important [299]. On the one hand, an increase of pressure does not lead to the expected increase in reaction rates of the oxygen-carrier [236]. On the other hand, the char gasification rate increase with pressure is not relevant above a certain pressure [269,271].

Two different iG-CLC concepts have been proposed. Most of the works demonstrating the iG-CLC technology have been carried out using two interconnected fluidized-bed reactors [54,187,206]. Another alternative is to use a batch of an appropriate oxygen-carrier in a single fluidized bed with three stages [118,119]. The process would consist of several fluidized-bed reactors operating in parallel and out of phase with one another to achieve a continuous supply of energy. The number of reactors could be high to avoid instabilities from unsteady state operation.

The benefits of circulating fluidized-bed technology commonly used in CLC are the fuel flexibility associated with current CFB boilers and that they operate at steady-state, thus supplying energy continuously. Thus, different solid fuels could be used such as coal, pet–coke, biomass or solid wastes [228]. Most of the work found in the literature refers to the use of coal or pet–coke as fuels. On the other hand, biomass has been shown to have a relatively fast conversion rate [228,265,302]. The use of biomass in a

continuously operated CLC system has been recently communicated [109], showing promising results for further development of a biomass-fueled CLC system. Fig. 12 shows a general scheme of the iG-CLC system using two interconnected fluidized-bed. Thus, reactions (20)-(24) proceed in the fuel-reactor, i.e. the solid fuel devolatilization and gasification, as well as subsequent oxidation of the gases generated. The oxygen-carrier reduced in the fuel-reactor, Me_xO_{y-1}, is transferred to the air-reactor where it is regenerated to be later transferred to the fuel-reactor and start a new cycle.

Ideally, the CO_2 capture is inherent to this process, because the air is never mixed with the fuel, and no additional costs or energy penalties for gas separation are required, as was the case for gaseous fuels. However, the CO_2 capture efficiency can be reduced if some char particles are by-passed to the air-reactor. The gasification process has been identified as the controlling step in the iG-CLC concept [303,304]. Indeed, the char gasification is usually a slow process, and the solids stream exiting from the fuel-reactor could contain some unconverted char together with the oxygen-carrier and ash. Thus, char particles need a long enough residence time in the fuel-reactor to be gasified. To increase the residence time of char particles in the fuel-reactor, without excessive increase of the reactor size, several options can be found:

- the separation of the char particles from oxygen-carrier particles and their recirculation to the fuel-reactor. So, the amount of carbon transferred from the fuel-reactor to the air-reactor is reduced. Based on the different fluidizing properties of remaining char and oxygen-carrier particles, a carbon stripper has been proposed as a feasible equipment to carry out the separation of char, as showed in Fig. 12 [261,301].
- to modify the design of the fuel-reactor to approach plug flow instead of the perfect mixing related to fluidized-bed [54]. For example, this can be accomplished by

several fluidized-bed reactors in series. Thus, the residence time of char particles is homogenized and the loss of particles with low residence time related to the perfect mixing of solids is reduced.

When char particles pass to the air-reactor, they will be burnt when exposed to air. Therefore, the gas stream exiting the air-reactor can contain some CO_2 together with the oxygen-depleted air. In this case, the efficiency of CO_2 capture is reduced. Although the total energy released in the CLC system is unchanged, char by-passing to the air-reactor changes the energy balance in each reactor, i.e. the air- and fuel-reactors. Nevertheless, it has been reported that there is a preferential oxidation of the oxygen-carrier over the oxidation of char using a highly reactive Cu-based oxygen-carrier [305]. Thus, this kind of material would allow oxidizing the oxygen-carrier in the air-reactor but only burning a small fraction of char, the remaining coming back to the fuel-reactor. In this way, the fraction of non-captured CO_2, i.e. CO_2 exiting from the air-reactor, could be low enough to maintain a high efficiency in the CO_2 capture of the CLC system.

In addition, some energy would be lost if unburnt compounds (CO, H_2, CH_4, volatiles) appear in the combustion gases from the fuel-reactor, which contain primarily CO_2 and H_2O. Unburnt compounds can come from inefficient conversion of volatiles released or from gasification products. As in a fluidized-bed reactor solid flow is perfectly mixed, reducing gases are generated in the whole reactor. Thus, some of gasification products can be generated at a point in the reactor near to the reactor exit where the contact time with the oxygen-carrier is not enough to fully convert to CO_2 and/or H_2O. So, it could be difficult to reach complete gas conversion with solid fuel even using highly reactive oxygen-carrier materials or high solids inventory, merely because the type of solid and gas flows in the reactor. This situation is completely different to the case of using gaseous fuels, where the gas has a feeding point in the lower part of the fluidized bed

and thereafter reacts with the solids present in the reactor. Different possibilities have been proposed to process the unburnt compounds: (a) an oxygen polishing step after the cyclone to complete gas combustion to CO_2 and H_2O; (b) separation and recirculation of unburnt compounds; or (c) a fuel-reactor in series where exhaust gases are fed. Most likely, an oxygen polishing step could be added to the fuel-reactor down-stream. Thus, unburnt components are fully burnt to CO_2 and H_2O with oxygen, which requires a small air separation unit (ASU). Usually, the term *oxygen demand* is used to define the percentage of oxygen supplied by the ASU with respect to the stoichiometric oxygen required for complete combustion of fuel.

The feasibility of the process has been proven during continuous operation in CLC units ranging from 500 W_{th} to 10 kW_{th}. Mainly, unburned compounds can come from two processes happening in the fuel-reactor: devolatilization or char gasification. Continuous operation using solid fuels has shown that the concentration of CO and H_2 in the flue gases due to unconverted gasification products is in the range 0.7-1.5 vol%, which corresponds to an oxygen demand of 5-9% in the oxygen polishing step [207]. Similar amounts of unconverted gases from volatiles have been detected using ilmenite [206,304] or a highly Ni-based oxygen-carrier [185,187]. Unconverted gases were mainly H_2, CO and some CH_4, with tars being fully converted by the oxygen-carrier [118,206]. In addition, when a high-sulfur content fuel was used, high concentration of H_2S was present in the gases, indicating partial conversion to SO_2 and closely doubling the oxygen demand [207].

The combustion efficiency in the fuel-reactor, the efficiency of char separation in the carbon stripper, and the separation of ash from the oxygen-carrier seem to be key factors for the development of this process. The efficiency of char combustion will depend on the char conversion in the reactor and on the reactivity of the oxygen-carrier

with the volatiles and gasification gases. Thus, both factors must be considered to understand the whole behaviour of the iG-CLC process [119].

3.2.1. Coal conversion in the fuel-reactor

Most of the works about the iG-CLC process have been focused on the char conversion. The direct solid-solid reaction between char and oxygen-carrier has been observed in TGA apparatus using Cu-, Ni-, Mn-, Fe- and Co-based oxygen-carriers [227,229,306,307]. However, the solid-solid reaction could be disguised when a gasifying agent is used as fluidization gas, which is the case for CLC. Experiments in fluidized beds using ilmenite as oxygen-carrier have shown that the gasification rate by H_2O or CO_2 had higher relevance than the conversion rate by direct solid-solid reaction using low reactive bituminous coals or pet-coke [119,239,304]. Therefore, the reaction path involving H_2 and CO from char gasification as intermediate products would be the prevailing mechanism in the char conversion in a fluidized bed when CO_2 and/or H_2O are used as fluidizing gas.

The char gasification rate was showed to be the time controlling step in the coal conversion. Sub-bituminous and lignite coal char have shown CO_2 gasification rates as high as for H_2O [308]. Therefore, the use of these types of coals could be advantageous because recirculated CO_2 could be used as a fluidizing agent. Indeed, dry gasification of a lignite [118] was found to be as fast as the steam gasification of bituminous coal [309] using Fe-based oxygen-carriers. On the contrary, works using bituminous Colombian coal show that the conversion rate of char using CO_2 as fluidizing agent is about 5 times lower than that using H_2O [304,309]. In this case, whereas the steam coal gasification at 900 ºC proceeds in minutes, the CO_2 gasification time is of the order of hours. The CO_2 concentration in the fluidizing gas would be limited to 20% in order to maintain a high gasification rate with that bituminous coal [304]. The main effect of the low gasification

rate is an increase in the char concentration in the fuel-reactor. The carbon stripper should be optimized to separate char from a solid stream highly concentrated in it. Moreover, loss of carbon in elutriated char particles could be higher when the char concentration increases. However, the gasification rate could not be a limiting factor in the carbon capture efficiency if efficient carbon separation systems both in the gaseous and oxygen-carrier streams are accomplished in iG-CLC. In this case, either H_2O or CO_2 could be used as fluidization agent. In addition, the presence of SO_2 in a CO_2 stream has been reported to increase the gasification rate to values as high as that for H_2O [239]. Thus, CO_2 recirculation can be an interesting option when highly reactive solid fuels –e.g. sub-bituminous coal, solid waste or biomass– or high-sulfur coals are used, or if the recovery of char particles exiting the fuel-reactor is highly efficient.

The in-situ gasification is favoured by the presence of the oxygen-carrier particles. It has been determined that oxygen-carrier does not have catalytic activity on the char gasification reaction [303]. The increase of the gasification rate when char is mixed with the oxygen-carrier particles is based on the continuous consumption of gasification products by reaction with the oxygen-carrier [228,239,265,267,304]. It is well known that the gasification products, i.e. H_2 for steam gasification or CO for gasification by CO_2, are inhibitors for the char gasification reactions [308]. Thus, the gasification rate depends on the oxygen-carrier reactivity, i.e. more reactive particles are more efficient in converting H_2 and CO, and therefore the gasification rate is increased because of the reduced inhibitory effect of these gases [310].

The temperature of the reactor greatly affects the char conversion [206,207,267,311,312] and temperatures about 1000 ºC are preferred. Equally, the conversion of CO and H_2 produced during gasification also increases with the temperature although in a lower amount [109].

3.2.2. Operational experience of oxygen-carriers for iG-CLC

As for gaseous fuels, suitable oxygen-carriers for solid fuels in the CLC process must have high selectivity towards CO_2 and H_2O, enough oxygen transport capacity, high reactivity, high mechanical strength, attrition resistance and negligible agglomeration. All these characteristics must be maintained during many reduction and oxidation cycles. There are several studies on the reactivity of synthetic oxygen-carriers based on CuO [228,303,305,313], Fe_2O_3 [118,229,239,299] and NiO [185,187,314,315] for in-situ gasification of the solid fuel. In addition, natural minerals or waste products from different industries have been proposed as oxygen-carrier materials.

Cu-based materials have shown to be very reactive, obtaining full combustion of gasification products with a mass ratio of oxygen-carrier to solid fuel of 10:1 at 850 ºC [313]. In addition, the combined pyrolysis-reduction and gasification-reduction reactions are exothermic for Cu-based materials. Thus, the heat release during CuO reduction compensates for the endothermic reactions suffering the solid fuel, i.e. pyrolysis and gasification [228]. In some cases, the cyclic redox reactions alternating Cu2O and Cu have been tested when the oxidation temperature is high enough to prevent oxidation to CuO [303,305].

Ni-based materials have also shown a high reactivity with the gasification products [314]. The reactivity of Ni-based materials tested was highly dependent on temperature. Thus, the fraction of CO_2 in the exiting gases increased with temperature. Good performance of Ni-based oxygen-carrier particles was reported in continuous operation in CLC systems using bituminous coal as fuel [185,187], although full conversion of gasification gases was not observed because of the segregation of char particles in the upper part of the fuel-reactor –which was a spouted bed– with low contact efficiency between pyrolysis products and solid particles. However, the use of Ni-based materials

with solid fuels could be restricted to low-sulfur fuels, because the carrier can be deactivated by the presence of sulfur [45,226,315]. In addition, Ni-based materials are less interesting for the use with solid fuels because of their high price and toxicity. Their toxicity will require extreme safety measurements to avoid the pollution by drained ash containing nickel oxide.

Synthetic Fe-based materials have shown lower reactivity. In this case, a mass ratio of oxygen-carrier to solid fuel higher than 100:1 should be necessary to fully convert the gasification products to CO_2 and H_2O [118,239].

Considering all the above aspects, Fe- and Cu-materials are preferred for their use in the iG-CLC process because these materials are harmless when they are found in the ash, as opposed to Ni-based materials. In addition, it is expected that the lifetime of these materials would be limited by the loss of solids in the drained stream rather than by its degradation. As a consequence of the ash present in the solid fuel it is necessary to drain the ash from the system to avoid its accumulation in the reactors. Ash can be separated from the oxygen-carrier on the basis of density and particle size differences. By controlling the gas velocity in a fluidized bed, e.g. the fuel-reactor itself, fly ash particles can be elutriated and can be recovered by use of a cyclone [261]. However, the drained stream will also contain some amount of oxygen-carrier and a partial loss with the fuel ash is expected. Thus, low cost materials or materials which could be easily separated from the ashes, e.g. Fe-based materials with magnetic properties, are to be preferred for use with coal.

The use of cheap natural minerals for this option seems to be very interesting, with ilmenite being an appropriate material. Leion et al. [267] analyzed the reactivity of ilmenite in a batch fluidized bed for solid fuels combustion, obtaining high conversion of gasification products. The conversion rate of the fuel was in the same order of

magnitude as that obtained using highly reactive oxygen-carriers, such as a Ni-based material [315], because in both cases the conversion rate was limited by the char gasification step. Berguerand and Lyngfelt operated a 10 kW_{th} Chemical-Looping combustor using coal and petroleum coke as solid fuels [54,55,207,312,316]. Good performance of the iG-CLC concept for CLC of solid fuels was described, and they concluded that ilmenite appeared to be a suitable material to be used for solid fuel combustion in a CLC system. Experiments in a smaller CLC unit (500 W_{th}) showed that unburnt tars or volatile matter was not present in the fuel-reactor outlet, except CH_4 which was found at low concentration [206]. Gasification products were near fully converted to CO_2 and H_2O but unconverted CO and H_2 proceeding from coal devolatilization were outgoing from the fuel-reactor. Combustion efficiencies from 85 to 95 % were obtained in all the experimental works.

Regarding the good behaviour showed by natural ilmenite, synthetic ilmenite has been produced and studied. Although in general synthetic ilmenites have better CO and H_2 conversion than natural ilmenites, these last showed sufficiently good performance to be considered as suitable oxygen-carriers for the iG-CLC process [263]. Other low-cost materials such as natural ores and industrial wastes products have also been analyzed [123,265,317]. Some Fe- and Mn-based materials have been found to meet the criteria for use as oxygen-carrier in the iG-CLC process. Continuous operation in a 1 kW_{th} CLC reactor using a natural iron ore (hematite) [143] gave similar values of coal combustion efficiency than a highly reactive Ni-based oxygen-carrier [185]. The combustion efficiency was in the range of 82% to 87%, with CO and CH_4 as the only unburnt gases.

Considering the low cost of iron, synthetic Fe-based materials have also been proposed as oxygen-carriers in the iG-CLC process. Dennis et al. [241] tested the feasibility of using pure iron oxide and a lignite fuel gasified by CO_2 in a batch fluidized-bed reactor.

They stated that although the oxygen-carrier used (pure Fe_2O_3) was not optimized, it was still able to burn most of the CO produced by the gasification of the carbon, indicating that gasification is probably the rate-limiting step. Besides, Gao et al. [240] used a mixture of Fe_2O_3/Fe_3O_4 as an oxygen-carrier during CLC of coal in a batch fluidized bed, where steam acted as the gasification-fluidization medium. H_2 and CH_4 had the maximum and minimum reactivity in the process, respectively. However, the reactivity of the oxygen-carrier with gasification products significantly decreased after 20 redox cycles because of the sintering on external surface of the oxygen-carrier particles.

Leion et al. [239] investigated the feasibility of CLC of petroleum coke using an oxygen-carrier composed of 60 wt% of Fe_2O_3 and $MgAl_2O_4$ as inert in a batch fluidized-bed reactor. They stated that the solid–solid reaction between Fe_2O_3 and carbon does not proceed at an appreciable rate in the fluidized-bed reactor although high reactivity was found with the gasification products, H_2 and CO. In this line, char was used by Rubel et al. [229,318] to evaluate solid CLC without gasification of the solid fuel. They used a TGA to directly oxidize a high carbon coal char in an inert gas, i.e. solid to solid CLC, using a high-purity Fe_2O_3 powder as the only source of oxygen. They reported low utilization efficiency due to the slow reaction rate observed.

Biomass as solid fuel was evaluated by Shen et al. [109] in a continuous 10 kW_{th} CLC combustor using an oxygen-carrier prepared from iron oxide powders. A long-term experiment of 30 h was accomplished with the same batch of iron oxide particles. The effect of the fuel-reactor temperature (740-920 ºC), and the biomass conversion to CO_2 in the fuel-reactor was investigated using CO_2 as gasification medium. The CO concentration in the fuel-reactor flue gas increased with the fuel-reactor temperature, since biomass gasification with CO_2 was more temperature dependent than CO

oxidation with iron oxide. A low reactivity of the oxygen-carrier particles used was found due to the grains sintering on the particle surface. To avoid this sintering process, an air staging in the air-reactor was proposed by the authors.

$CaSO_4$ from natural anhydrite ore has been widely analyzed as an oxygen-carrier in the iG-CLC process. Low reactivity has been shown with all the reducing gases (H_2, CO and CH_4) [274-278]. However, this should not be an important problem in the iG-CLC process because the conversion rate of the fuel is limited by the slow gasification step. Thus high conversion of gasification products, i.e. CO and H_2, to CO_2 and H_2O was observed at temperatures higher than 1000 ºC using a ratio of coal to oxygen-carrier of 1:30 [281]. Nevertheless, lower conversion of pyrolysis products could be obtained with $CaSO_4$ than with other more reactive materials.

In the iG-CLC process, special attention must be paid to the effect of accumulated ash mixed with the oxygen-carrier particles in the reactors. During the time that ash and the oxygen-carrier particles are mixed, harmful effects on the oxygen-carrier performance could be produced, e.g. loss in the reactivity or appearance of agglomeration. Several works have analyzed the effects of long time contact between ash and oxygen-carrier particles. In general, no problems were observed with agglomeration or reactivity loss involving ash and carrier particles when the ash concentration was low [186,303]. When the ash content was increased up to values of 20 wt%, an increase in the reactivity was shown using Fe-based oxygen-carriers [318]. However, it was not definitively determined if this increase was due to an activation of the solids, similar to ilmenite, or was due to a synergetic effect of ash. Nevertheless, the deposit of ash on the surface of the oxygen-carrier can be rubbed off under the fluidization conditions of the reactors [186]. Exceptionally, some problems of agglomeration have been found using biomass as fuel and a Cu-based material as oxygen-carrier. Probably the formation of low-

melting eutectics between the oxygen-carrier and metals from the biomass ash are the responsible for the agglomeration [313].

3.3. Chemical-Looping with Oxygen Uncoupling (CLOU)

To overcome the low reactivity of char gasification stage in the iG-CLC process, an alternative option has been recently proposed. Lyngfelt and coworkers [57] made use of the idea first proposed by Lewis and Gilliland [22,23] to produce CO_2 from solid carbonaceous fuels by using gaseous oxygen produced by the decomposition of CuO. They discovered the importance of carriers in CLC that dissociated to produce oxygen and designated this process as Chemical-Looping with Oxygen Uncoupling (CLOU).

The CLOU process is based on the use of an oxygen-carrier which release gaseous oxygen in the fuel-reactor thereby allowing the solid fuel to burn with gas-phase oxygen (see Fig. 11). In this way, the slow gasification step in the iG-CLC process is avoided giving a much faster solid conversion. Likely, this process has the implication that much less oxygen-carrier material is needed in the system, which will also reduce the reactor size and associated costs. Moreover, in the direct combustion of solid fuels in the standard CLC process, the fuel-reactor must be fluidized by H_2O or H_2O+CO_2 mixtures, which also acts as gasification agents. In the CLOU process, this fluidization gas can be recycled CO_2, reducing in this way the steam duty of the plant and the corresponding energy penalty.

In the CLOU process several reactions take place in the fuel reactor:

$$2\ Me_xO_y \leftrightarrow 2\ Me_xO_{y-1} + O_2 \quad (26)$$

$$\text{Coal} \rightarrow \text{Volatiles} + \text{Char} + H_2O \quad (27)$$

$$\text{Char (mainly C)} + O_2 \rightarrow CO_2 \quad (28)$$

$$\text{Volatiles} + O_2 \rightarrow CO_2 + H_2O \quad (29)$$

First the oxygen-carrier releases oxygen according to reaction (26) and the solid fuel begins devolatilization producing a porous solid (char) and a gas product (volatiles), reaction (27). Then, the char and volatiles are burnt as in usual combustion according to reactions (28) and (29). A scheme of this process can be seen in Figure 11. After that the oxygen-carrier is re-oxidized in the air-reactor.

For the design of CLOU systems, it is important to consider the relation among the different reactions taking place in the fuel-reactor. If the oxygen-carrier decomposition rate is very rapid compared to the combustion rate of fuel, the O_2 concentration in the fuel-reactor will be close to equilibrium and thus the kinetics of the char combustion will determine the operating conditions on the fuel-reactor. In this case, it is likely that specifications of CO_2 purity for compression and sequestration could not be fulfilled as some oxygen will be present in the gas outlet of the fuel-reactor. By contrast, if the combustion rate of fuel is faster than the oxygen release rate, the O_2 concentration in the fuel-reactor will be close to zero. Accordingly, the operating conditions in the fuel-reactor should maximize this release although some unburnt compounds will be present. Thus, the CLOU system must be designed having enough amount of oxygen-carrier to release the oxygen to burn the fuel, and high enough amount of solid fuel to avoid an excess of oxygen in the flue gases from the fuel-reactor. The optimum oxygen concentration in the fuel-reactor will be a compromise between the O_2 generation rate by the oxygen-carrier and the oxygen consumption by the fuel.

The suitable materials that have the property of releasing oxygen are limited. Besides O_2 release, the process must be reversible as the oxygen-carrier must be oxidized again in the air-reactor. Thus a special requirement is needed for the oxygen-carrier to be used in the CLOU process in comparison with the oxygen-carriers for normal CLC where the fuel (gaseous or solid) reacts directly with the oxygen-carrier without any release of gas

phase oxygen. Therefore, only those metal oxides that have a suitable equilibrium partial pressure of gas phase oxygen at temperatures of interest for combustion (800-1200 ºC) can be used as active compounds for CLOU. Three metal oxide systems have so far been identified: CuO/Cu_2O, Mn_2O_3/Mn_3O_4, and Co_3O_4/CoO [57]. These systems can release oxygen in the gas phase through the following reversible reactions:

$$4\ CuO \leftrightarrow 2\ Cu_2O + O_2\ (g) \qquad \Delta H_{850} = 263.2\ kJ\ /mol\ O_2 \qquad (30)$$

$$6\ Mn_2O_3 \leftrightarrow 4\ Mn_3O_4 + O_2(g) \qquad \Delta H_{850} = 193.9\ kJ\ /mol\ O_2 \qquad (31)$$

$$2\ Co_3O_4 \leftrightarrow 6\ CoO + O_2(g) \qquad \Delta H_{850} = 408.2\ kJ\ /mol\ O_2 \qquad (32)$$

The oxygen transport capability of the oxygen-carriers, R_O, is very different depending on the reaction pairs, being 0.1, 0.03 and 0.066 for the pairs CuO/Cu_2O, Mn_2O_3/Mn_3O_4, and Co_3O_4/CoO, respectively.

Fig. 13 shows the partial pressure of oxygen at equilibrium conditions as a function of the temperature for these metal oxide systems. It is clear from this figure that the air- and fuel-reactor temperatures in the process must be selected based on the thermodynamic equilibrium of each metal system.

The equilibrium concentration of oxygen during carrier decomposition will be given by the temperature in the fuel-reactor, which is determined by the temperature of the incoming particles, the circulation rate in the system, as well as the heat of reaction in the fuel-reactor. A high equilibrium partial pressure of oxygen together with a very reactive oxygen-carrier will promote the overall conversion rate of the solid fuel in the fuel-reactor. In addition, the combustion of the fuel will decrease the oxygen concentration in the reactor and can improve the decomposition reaction of the metal oxide particles.

For Cu- and Mn-based oxygen-carriers, the reactions with carbon taking place in the fuel-reactor are exothermic, reactions (33) and (34). Thus, it is possible to operate at

lower temperatures in the air-reactor, which results in a significantly lower partial pressure of O_2 at equilibrium conditions at the air-reactor exit. This fact improves the use of O_2 in the air stream.

$$C + 4\,CuO \rightarrow 2\,Cu_2O + CO_2 \qquad \Delta H_{850} = -133.8 \text{ kJ/mol C} \qquad (33)$$

$$C + 6\,Mn_2O_3 \rightarrow 4\,Mn_3O_4 + CO_2 \qquad \Delta H_{850} = -203.1 \text{ kJ/mol C} \qquad (34)$$

$$C + 2\,Co_3O_4 \rightarrow 6\,CoO + CO_2 \qquad \Delta H_{850} = 11.2 \text{ kJ/mol C} \qquad (35)$$

On the contrary, the reaction of carbon with Co_3O_4 is endothermic, reaction (35). Therefore, the temperature in the air-reactor must be higher than that in the fuel-reactor, and also higher than the one needed when Cu- or Mn-based oxygen-carriers are used.

A distinguishing characteristic of the CLOU process, relative to normal CLC, is the especially constrained operating conditions for the air-reactor due to the thermodynamic limitations of the oxygen-carrier oxidation. To maintain high power plant efficiency it is important to keep the outlet partial pressure of O_2 from the air-reactor as low as possible. The oxygen concentration from the air-reactor will depend on the oxygen-carrier reactivity for oxidation reaction and the equilibrium concentration of each metal oxide system at the actual air-reactor temperature (see Fig. 13).

Thus, the temperature in the air-reactor to oxidise the oxygen-carrier should be lower for Mn- and Co-based oxygen-carriers than for Cu-based oxygen-carriers, according to Fig. 13. This high temperature dependency of the oxygen concentration in the CLOU process makes the thermal integration between fuel-reactor and air-reactor a key aspect in the development of the technology.

Although the oxygen transport capability of the cobalt metal oxide is high (6.6 g O_2 per 100 g Co_3O_4), the great endothermicity of the decomposition reaction and the high cost of the material makes this metal oxide hardly attractive. The most promising metal oxide systems for the CLOU process have found to be CuO/Cu_2O and Mn_2O_3/Mn_3O_4

[57]. Copper oxide has the highest oxygen transport capability (10 g O_2 per 100 g CuO compared to 3 g O_2 per 100 g Mn_2O_3) and manganese the highest heat of reaction with carbon. Regarding Cu-based materials, agglomeration problems could be overcome in the CLOU process because the oxygen-carrier is never reduced to metallic Cu, the product with lower melting point (1085 ºC). It must be considered that the solids involved in the CLOU process, i.e. both CuO and Cu_2O, have high melting temperatures, 1446 ºC and 1235 ºC, respectively. In this sense, high copper contents are preferred in the oxygen-carrier developed for the CLOU process (see Table 6) as the oxygen transport capacity is half that of CuO/Cu in the CLC process.

Table 6 shows an overview of the materials proposed in the literature as oxygen-carriers for the CLOU process. As this new option for Chemical-Looping with solid fuels was proposed recently, there is a small number of works dealing with the use of Cu- [57,319-323], and Mn-based [253,259,260,324,325] based materials.

In the research group of ICB-CSIC [322], a screening study considering more than 25 different Cu-based oxygen-carriers prepared using different methods, copper contents and supports was carried out (see Table 6). The reaction rates for oxygen release and oxygen-carrier regeneration were determined carrying out successive cycles in a TGA system at different reaction temperatures and oxygen concentrations. Selected materials were tested by redox decomposition-regeneration cycles in a batch fluidized-bed reactor working at different temperatures and reacting atmospheres. The maximum oxygen concentration detected during experiments was the equilibrium composition. The fluidization behaviour affecting agglomeration and attrition during a high number of cycles was also determined. Two promising Cu-based oxygen-carriers prepared by pelletizing by pressure (60 wt% CuO supported on $MgAl_2O_4$, and 40 wt% CuO supported on ZrO_2) were selected for further studies using coal as fuel. These materials

exhibited high reactivity during successive redox cycles, absence of agglomeration and low attrition rate.

In the research group at Chalmers University of Technology, 20 different CLOU materials were tested in TGA and batch fluidized bed using gas (CH_4) or solid fuels [57,253,259,260,320,324,325]. Best results were obtained using an oxygen-carrier based on CuO and ZrO_2 as support. Although there was some defluidization phenomenon during some parts of the experiments, no permanent agglomerations were detected. Their results using six different solid fuels show that the differences in reactivity between fuels were more pronounced in the iG-CLC than in CLOU process [319]. This fact was explained by the difference in the reaction paths between both processes since in their CLOU experiments the limiting reaction rate was the oxygen release from the oxygen-carrier particle and also because of the high dependency on the solid conversion rate with the reaction temperature. Experiments carried out at 980 ºC using petroleum coke as fuel [320] showed that CLOU process can increase the fuel conversion by a factor of 45 with respect to the conversion found when the same fuel was gasified with steam and using Fe-based oxygen-carriers which do not release oxygen in the fuel-reactor. Eyring et al. [321], based on previous results of Lewis et al. [22] using a Cu-based oxygen-carrier, obtained maximum increases in conversion rates over those for the $C+CO_2$ reactions of 24 and 32 at 845 and 890 ºC, respectively. Therefore, the role of oxygen uncoupling in accelerating the conversion of solid fuels was also confirmed. Based on these preliminary studies, Mattisson et al. [320] found an important reduction in the fuel-reactor inventories using a Cu-based oxygen-carrier (120-200 kg/MW_{th}) compared to those needed using Fe-based oxygen-carriers (2000 kg/MW_{th}), using a low reactive petroleum coke in both cases.

Regarding the use of manganese oxides for CLOU process, Shulman et al. analyzed the CLOU properties of different Mn-based materials combined with Fe_2O_3, NiO or SiO_2 [253] prepared by freeze granulation. They found that some Mn/Fe oxygen-carriers showed very high reactivity towards methane. The authors apply this quality to open the possibility to combine benefits of CLOU and CLC processes in the future. Further, other Mn/Fe materials prepared by spray drying method were tested by the same research group [324,325]. A manganese ore was also tested for CLOU by Rydén et al. [325], but this material was much less reactive than synthetic Mn/Fe particles. Another material with a spinel perovskite-like type structure, $CaMn_{0.875}Ti_{0.125}O_3$, [259,260] was evaluated as an oxygen-carrier for the CLOU process. In this case, the improved conversion rate was lower than using a Cu-based CLOU material [320], although it was still higher compared to normal CLC with solid fuels. However, the authors pointed out as an advantage of this new material a likely lower price compared to Cu-based oxygen-carriers, despite the complex preparation method required, (see Table 6), and the oxidation temperature not being so limited by thermodynamics.

The proof of concept of the CLOU process with coal was demonstrated in a 1500 W_{th} unit located at ICB-CSIC consisting of two interconnected fluidized-bed reactors [323]. The experiments were carried out at 900-960 ºC in the fuel-reactor with a Cu-based oxygen-carrier and a bituminous Colombian coal "El Cerrejón" as fuel. A total of 15 hours of continuous operation feeding coal and 40 hours of continuous fluidization were carried out. Neither agglomeration nor any other type of operational problems were detected during the whole experimental work. Unburnt volatile matter was not present in the fuel-reactor outlet, which was composed of only CO_2 and H_2O. Coal conversion in the fuel-reactor was determined by the char combustion, which was mainly affected by the temperature and the solid mean residence time. High char conversion (>97%)

and carbon capture efficiency were obtained in all the experimental conditions tested in the continuously operated CLOU system, in spite of the lack of a carbon stripper. It is remarkable that a char conversion value as high as 99% was reached at temperatures higher than 940 ºC.

These recent studies show that this technology is very promising although their status of development is, at the moment, far from that accomplished using the iG-CLC process, as can be seen comparing facilities in Table 4 and Table 6. A drawback of this technology compared to normal CLC for solid fuels, where natural ores are being developed as oxygen-carriers, is the cost of the oxygen-carrier even considering the lower solid inventory needed for the CLOU process. This higher cost of the CLOU materials must be compensated with a very high particle lifetime, a high and stable reactivity, and a high resistance towards ash fouling.

4. Chemical-Looping Reforming (CLR)

CO_2 capture and storage (CCS) technologies have great potential to reduce CO_2 emissions from large point sources such as power plants and large industries. However, CO_2 capture technology applied to the transport sector is more complex, being the use of H_2 as fuel a promising option to reduce the CO_2 emissions from mobile sources. In addition to the transport sector, H_2 could be also used for power generation and as an intermediate for the production of other important products (ammonia, methanol, petrochemical processes, etc).

H_2 can be produced from renewable energy sources through water electrolysis, from solid fossil fuels via gasification, or from gaseous fossil fuels via reforming, mainly from natural gas. The reforming processes have many advantages as this technology has been operated for decades and the H_2 production cost is less than that produced from

renewable energy sources or from solid fossil fuels via gasification. Today, steam reforming of natural gas, where the reforming takes place in tubular reactors packed with a catalyst, is the most widely used technology for H_2 production. The syngas produced in the tubes must undergo a process to separate H_2 and CO_2 using typical absorption or adsorption technologies. However, the heat needed for the endothermic reforming reactions is provided by burning a fuel outside the tubes. This method produces large amounts of CO_2 mixed with N_2 that must be captured to avoid its emission. These CO_2 emissions could be eliminated by using physical or chemical absorption, by using a substantial part of the hydrogen as fuel for the heat demand in the reforming process, or by using pure oxygen to burn the fuel.

In any case, a CO_2 capture technology integrated with H_2 production is available today although with a high cost, being this fact the main barrier to its use. The integration of CO_2 capture technologies with H_2 production systems for power generation and fuel applications were studied in the CACHET project [49]. The overall goal of this project was to develop innovative technologies to reduce the cost of CO_2 capture whilst simultaneously producing H_2 from natural gas. Two of the technologies investigated were based on Chemical-Looping concept: Steam Reforming integrated with Chemical-Looping Combustion (SR-CLC) and Autothermal Chemical Looping Reforming (a-CLR). The general schemes for air- and fuel-reactors of these processes are presented in Fig. 14. The SR-CLC process avoids the need of any CO_2 capture step from the exhaust gases produced in the heating of the reformer tubes whereas the a-CLR process avoids the ASU required in the conventional autothermal reforming.

4.1. Steam Reforming integrated with Chemical-Looping Combustion (SR-CLC)

Steam Reforming integrated with Chemical-Looping Combustion (SR-CLC) was proposed by Rydén and Lyngfelt [51,89] and it is a process where steam and hydrocarbons are converted into syngas by conventional catalytic reforming. The main difference with respect to conventional steam reforming is that a CLC system is used to provide heat for the endothermic reforming reactions and to capture CO_2. The reformer tubes are located inside the fuel-reactor (see Fig. 14a) or in a fluidized bed heat exchanger connected to the Chemical-Looping system, a procedure which provides very favourable conditions for the important heat transfer needed. From the operational point of view, some uncertainties could arise from the allocation of steam reformer inside the fluidized-bed reactors. More details can be found in the works of Rydén et al. [51,89,326].

For H_2 production, the SR-CLC unit is integrated with Water-Gas Shift (WGS) and Pressure Swing Adsorption (PSA) units. The offgas leaving the PSA unit, composed of CH_4, CO, CO_2, and H_2 can be used as fuel in the fuel-reactor of the CLC system. So, the integrated process provides almost 100% CO_2 capture without any extra penalty in efficiency.

The working conditions and the oxygen-carriers used in the CLC system could be the same as those summarised in Section 2 for conventional CLC. The offgas is rich in H_2 which shows high reactivity with oxygen-carriers, the main difference being that there is not much experience on the behaviour of the oxygen-carriers working with offgas from PSA units as fuel. Recently, Ortiz et al. [204,210] analyzed the behaviour of several Fe-based materials, a synthetic and a waste product (redmud), as oxygen-carriers in a continuous 500 W_{th} unit using a simulated PSA-offgas as fuel. They found that, for the same operating conditions, the combustion efficiency was higher using

PSA-offgas as fuel than using pure CH_4. Moreover, the addition of a Ni-based oxygen-carrier to both Fe-based oxygen-carrier materials had a positive effect on the combustion efficiency [204].

4.2. Auto-thermal Chemical-Looping Reforming (a-CLR)

Auto-thermal Chemical-Looping Reforming (a-CLR, or simply CLR) utilizes the same basic principles as CLC, the main difference being that the desired product in CLR is not heat but H_2 and CO. Fig. 14b) shows a scheme of the process. In the CLR process the air to fuel ratio is kept low to prevent the complete oxidation of the fuel to CO_2 and H_2O. Thus, N_2 free gas stream concentrated in H_2 and CO is obtained from the fuel-reactor. Moreover, the ASU required in the conventional auto-thermal reforming for CO_2 capture is here avoided. When a WGS reactor is used downstream, the H_2 yield in this process can reach 2.7 mol H_2 per mol of CH_4 [327], but with the advantage that the CO_2 capture is inherently accomplished and no additional energy from an external source is needed. Auto-thermal CLR, as described in Fig. 14b), was initially proposed by Mattisson and Lyngfelt in 2001 [328]. Later, Rydén and Lyngfelt [89,329] conducted a system analysis of some atmospheric and pressurized processes for H_2 production using a-CLR. They found that the efficiencies at atmospheric pressure were similar to those obtained for the conventional reforming process with CO_2 capture by amine scrubbing. Atmospheric a-CLR processes have high H_2 yield but the power needed to compress the product is considerable. Rydén [89] carried out a thermodynamic analysis of atmospheric and pressurized a-CLR processes for H_2 production. They concluded that pressurized CLR has potential to achieve much higher overall efficiency, about 5% higher, because pressurized systems reduce the energy penalty for H_2 compression. Siriwardane et al. [223] and García-Labiano et al. [236] studied, in a packed reactor and in a TGA, the effect of the pressure on the behaviour of several oxygen-carriers for

CLC. In both works, it was showed that the pressure had a positive effect on the reaction rates, although the increase was not as high as expected.

In the a-CLR process, the steam methane reforming is an important reaction in the fuel-reactor. Thus, Ni-based oxygen-carriers can be considered as a first good choice. The main reactions happening in the fuel-reactor of a CLR system when using a Ni-based oxygen-carrier are the following:

$$CH_4 + 4\,NiO \longrightarrow 4\,Ni + CO_2 + 2\,H_2O \qquad \Delta H_{1200K}=135\ kJ/mol\ CH_4 \qquad (36)$$

$$CH_4 + H_2O \xleftrightarrow{Ni} CO + 3\,H_2 \qquad \Delta H_{1200K}=228\ kJ/mol\ CH_4 \qquad (37)$$

The appearance of CO and H_2 as primary products in CH_4 conversion can also be considered.

$$CH_4 + NiO \longrightarrow Ni + CO + 2\,H_2 \qquad \Delta H_{1200K}=213\ kJ/mol\ CH_4 \qquad (38)$$

If an excess of oxygen is transferred to the fuel-reactor, the CO_2 and H_2O can appear as products of combustion of H_2 and CO to some extent:

$$CO + NiO \longleftrightarrow Ni + CO_2 \qquad \Delta H_{1200K}= -48\ kJ/mol\ CO \qquad (39)$$

$$H_2 + NiO \longleftrightarrow Ni + H_2O \qquad \Delta H_{1200K}= -15\ kJ/mol\ H_2 \qquad (40)$$

and the water gas shift equilibrium modifies the composition of gases:

$$CO + H_2O \longleftrightarrow CO_2 + H_2 \qquad \Delta H_{1200K}= -33\ kJ/mol\ CO \qquad (41)$$

In the air-reactor the oxygen-carrier is regenerated by oxidation in air:

$$2\,Ni + O_2 \longrightarrow 2\,NiO \qquad \Delta H_{1200K}= -468\ kJ/mol\ O_2 \qquad (42)$$

The same reaction scheme can be found for other metal oxides, although the relative importance of reforming reaction (37) could be lower than for Ni-based materials. The major advantage of this process is that the heat needed for converting CH_4 to H_2 is supplied without costly oxygen production, without mixing of air with carbon containing fuel gases or without using part of the H_2 produced in the process.

An important aspect to be considered in the a-CLR system is the heat balance. The oxidation reaction (42) of the metal oxide is highly exothermic, whereas the reduction reactions (36) and (38) and the steam reforming (reaction 37) are endothermic. So, the heat for the endothermic reduction reactions is supplied by the circulating solids coming from the air-reactor at higher temperature. The heat generated in the air-reactor must be high enough to fulfil the heat balance in the system without requirement of any external energy source for the process. The thermodynamics and the heat balance of the fuel- and air-reactors using Cu- and Ni-based oxygen-carriers were studied by Mattisson et al. [329]. They found that, in order to maintain a high temperature and CH_4 conversion, the fraction of oxygen supplied by the steam should not exceed approximately 0.3 of the total oxygen added to the fuel-reactor. Recently, Ortiz et al. [327] have carried out detailed mass and heat balances to determine the operating conditions that maximise H_2 production in the a-CLR process using an oxygen-carrier based on nickel. It was found that the oxygen-to-methane molar ratio should be higher than 1.25 to reach auto-thermal conditions, which means that the H_2 yield is 2.7 mol H_2/mol CH_4.

A key issue for the CLR technology development is the selection of an oxygen-carrier with suitable properties: enough reactivity through cycles to reduce solids inventory; high resistance to attrition to minimize losses of elutriated solid; complete fuel conversion to CO and H_2; negligible carbon deposition that would release CO_2 in the air-reactor and good properties for fluidization (no presence of agglomeration). In addition, other characteristics such as simple preparation methods would be desirable to reduce costs.

Fe-, Ni-, Cu-, and Mn-based oxygen-carriers supported on different inert materials, such as Al_2O_3, SiO_2, Mg-ZrO_2 and prepared by different methods, have been investigated to be used in a a-CLR system. Different oxygen-carriers consisting of oxides of Fe, Mn, Ni

and Cu supported on $MgAl_2O_4$ and SiO_2 were tested by Zafar et al. [224,237] in a laboratory fluidized-bed reactor and in a TGA. They observed that working at high temperature all of the $MgAl_2O_4$-supported oxygen-carriers showed high reactivities during reduction and oxidation. However, the oxygen-carriers supported on SiO_2 underwent considerable reactivity deactivation and/or agglomeration with the redox cycles. The Ni-based oxygen-carriers showed the highest selectivity towards H_2 and CO, while oxygen-carriers based on Fe-, Cu- and Mn- suffered from poor selectivity and produced mostly CO_2, H_2O and unconverted CH_4. In other work [329] it was determined that the selectivity towards H_2 production was higher with a NiO/SiO_2 oxygen-carrier than with a CuO/SiO_2 oxygen-carrier. Also, the authors pointed out that the use of Fe-based carriers in a-CLR will need additional measures to transform CH_4 to syngas. Addition of 1% NiO on $Fe_2O_3/MgAl_2O_4$ particles was found to have useful properties for CLR due to the great increase of both CH_4 reactivity and selectivity towards CO and H_2. Later, Rydén et al. [158] tested the $Fe_2O_3/MgAl_2O_4$ material as oxygen-carrier in a fixed-bed reactor with or without $NiO/MgAl_2O_3$ addition. They found that $Fe_2O_3/MgAl_2O_4$ has properties that could be useful for a-CLR in both cases if the reduction of Fe_3O_4 to FeO or Fe is exploited.

Ni appears to be the most interesting metal due to its strong catalytic properties. In fact, metallic Ni is used as a catalyst in most commercial steam reforming processes. The support used to prepare the oxygen-carriers has an important influence in the behaviour of the oxygen-carriers. Johansson et al. [157] compared two different Ni-based oxygen-carriers, $NiO/NiAl_2O_3$ and $NiO/MgAl_2O_4$, using both continuous and pulse experiments in a batch laboratory fludized bed. They found that $NiO/MgAl_2O_4$ had a higher methane conversion, better reforming properties and lesser tendency for carbon formation.

de Diego et al. [330] studied in a TGA and in a batch fluidized-bed reactor the behaviour of several Ni-based oxygen-carriers prepared by deposition-precipitation and by impregnation on γ-Al_2O_3, θ-Al_2O_3, and α-Al_2O_3 for the a-CLR process. They found that the preparation method and support type had an important effect on the reactivity of the oxygen-carrier, on the gas product distribution, and on the carbon deposition. The oxygen-carrier impregnated on γ-Al_2O_3 showed the lowest reactivity and the one on α-Al_2O_3 showed the highest reactivity during the reduction reaction. All oxygen-carriers exhibited very high reactivity during oxidation. The low reduction reactivity of the NiO/γ-Al_2O_3 was due to the solid state reaction between the metal and the support to form $NiAl_2O_4$. The high reduction reactivity of NiO/α-Al_2O_3 was due to the minimization of the interaction between the NiO and the support was reduced. In addition, it was found that the oxygen-carriers prepared by a deposition-precipitation method had a higher tendency to increase the carbon deposition than the oxygen-carriers prepared by impregnation, and the maximum conversions without carbon deposition were reached with the oxygen-carrier supported on α-Al_2O_3. They observed that an increase in the reaction temperature and in the H_2O/CH_4 molar ratio produced a decrease in the carbon deposition during the reduction period.

Atmospheric continuous a-CLR process working with Ni-based oxygen-carriers has been demonstrated by Rydén et al. [182,197,198] and by de Diego et al. [170] in continuous units, and by Pröll et al. [195] in a 140 kW_{th} pilot plant. A summary of the oxygen-carriers used in these installations together with the operational experience is showed in Table 7. Rydén et al. [182,197,198] used a 500 W_{th} continuous laboratory reactor consisting of two interconnected fluidized beds with Ni-based oxygen-carries supported on $MgAl_2O_4$, γ-Al_2O_3, α-Al_2O_3, and Mg-ZrO_2. Complete conversion of natural gas and high selectivity towards H_2 and CO was achieved for all cases. The gas

composition leaving the fuel-reactor was reasonably close to thermodynamic equilibrium of the water-gas shift reaction. Formation of solid carbon was noticed for some experiments with dry gas, but this was reduced or eliminated by adding steam or CO_2 to the natural gas. These authors confirmed that the a-CLR concept is feasible and should be further investigated.

Oxygen-carriers of NiO supported both on γ-Al_2O_3 and α-Al_2O_3 were also tested by de Diego et al. [170] in a 900 W_{th} CLR prototype. These authors analyzed the effect of different operating variables, like fuel-reactor temperature (800 to 900 ºC), H_2O/CH_4 molar ratio (0 to 0.5) and solid circulation rate, on CH_4 conversion and gas product distribution. For all operating conditions, the CH_4 conversion was very high (>98%) with both oxygen-carriers. For the same NiO/CH_4 molar ratio, an increase in the reduction reaction temperature produced a slight increase in the CH_4 conversion and CO_2 and H_2O concentrations and a slight decrease in the H_2 and CO concentrations. An increase in H_2O/CH_4 molar ratio produced a small increase in the CO_2 and H_2 concentrations and a small decrease in the CO concentration (see Fig. 15). The most important operating variable affecting the gas product distribution was the oxygen-carrier circulation rate, that is, the NiO/CH_4 molar ratio. An increase in the NiO/CH_4 molar ratio produced an increase in the CO_2 and H_2O concentrations and a decrease in the H_2, CO and CH_4 concentrations. In that work, only the oxygen reacted was considered to evaluate the results. A $NiO_{reacted}/CH_4$ molar ratio of ≈ 1.3 (air to fuel ratio ≈ 0.32) was calculated to be the minimum value necessary to fulfil the heat balance for the a-CLR process without any heat losses to the environment. At this condition, a dry gas product composition of about 65 vol% H_2, 25 vol% CO, 9 vol% CO_2, and 1-1.5 vol% CH_4 was obtained working with both oxygen-carriers (see Fig. 15). If heat losses

are present, the $NiO_{reacted}/CH_4$ molar ratio must be higher and, as a consequence, the H_2 and CO concentrations decrease and the CO_2 and H_2O concentrations increase.

Recently, a-CLR was demonstrated by Pröll et al. [195] in a 140 kW_{th} dual circulating fluidized bed installation. They used natural gas as fuel and a mixture 50:50 (by weight) of two different Ni-based oxygen-carriers supported on $NiAl_2O_4$ and $MgAl_2O_4$ as oxidant. The experimental work was carried out at temperatures between 750 and 900 ºC and global air to fuel ratios lower than 1.1. It was found that the natural gas conversion was very high with the residual amount of methane decreasing with increasing fuel-reactor temperature. The fuel-reactor exhaust gas was in thermodynamic equilibrium, and no carbon species were detected in the air-reactor exhaust gas. This is remarkable because no steam was added to the natural gas feed, excepting that used for lower loop seal fluidization that might have been directed back into the fuel-reactor. The minimum air-to-fuel ratios to work under a-CLR conditions without feed preheating were between 0.46-0.52. At these conditions, a dry gas product composition of about 55 vol% H_2, 28 vol% CO, and 17 vol% CO_2 was obtained at 900 ºC. In addition, a valuable stream of N_2 was obtained from the air-reactor.

In all these works, the oxygen-carriers did not show any agglomeration or defluidization problems and the loss of fine particles due to attrition was negligible. Moreover, no noticeable changes in the reactivity, surface texture and the solid structure of the oxygen-carrier particles were detected after operation. So, these results suggest that Ni-based oxygen-carriers supported on $MgAl_2O_4$ or Al_2O_3 could have a high lifetime, being suitable oxygen-carriers for a a-CLR system.

All above works were done at atmospheric pressure. However, it is stated the benefits from the use of pressurized a-CLR regarding the energetic efficiency of the process. The performance of pressurized a-CLR system was studied by Ortiz et al. [331] in a

semicontinuous pressurized fluidized-bed reactor. The effect of total pressure on the CLR process using CH_4 as fuel and oxygen-carriers of NiO supported on γ-Al_2O_3, and α-Al_2O_3 was analyzed. These oxygen-carriers were previously tested by de Diego et al. [170] in the atmospheric 900 W_{th} CLR prototype. The effect of different operating variables, like reduction reaction temperature and oxygen-carrier to fuel molar ratio, on CH_4 conversion and gas product distribution was analyzed at pressures up to 10 bars. A very high CH_4 conversion (>98%) was observed for both oxygen-carriers at all operating pressures tested. An increase in the operating pressure did not produce any important change in the gas product distribution of the a-CLR process and no carbon formation was detected. The measured gas outlet concentrations were near to that given by thermodynamic equilibrium. Negligible changes in the surface texture and the solid structure of the oxygen-carrier particles were detected after operation. The results were almost the same as those found by de Diego et al. [170] at atmospheric pressure, suggesting that these oxygen-carriers could have a high durability, being suitable as oxygen-carriers for a pressurized a-CLR system. However, pressurized circulating fluidized bed combustion is not yet a standard technology and some research and development effort will be necessary to make such systems work reliably.

Although Ni-based oxygen-carriers have shown good behaviour in the a-CLR process, other active phases than NiO have been examined to find cheaper and environmentally sound oxygen-carriers with high reactivity and selectivity towards CO and H_2. Rydén et al. [158] tested in a fixed-bed reactor $La_xSr_{1-x}FeO_{3-\delta}$ perovskites. They found that perovskites provided very high selectivity towards CO and H_2 and should be well suited for a-CLR but long-term chemical and mechanical properties of the perovskite particles are largely unknown. However, further investigation with these new materials is needed

to know its behaviour in continuous fluidized-bed reactors, in order to analyze effects like agglomeration, attrition, etc.

5. Status development of Chemical-Looping technologies

Although there was a patent on a process to produce pure carbon dioxide in the 1950s [23], the principle of CLC was first introduced by Richter and Knoche [24] in 1983 using two interconnected fluidized beds as a medium to increase the thermal efficiency of the combustion process. But it was not until the 90s that the process was seen as an option for CO_2 capture [27].

Most of the CLC plants existing worldwide at the moment use the configuration composed of two interconnected fluidized-bed reactors working at atmospheric pressure. Alternative reactor concepts for CLC described in Section 2.1.1 have only been tested at lab-scale. One important advantage of the use of a fluidized bed configuration for the CLC process is that CFB technology is mature and has been used for decades for other processes such as solid fuel combustion (coal, biomass, and residue) or fluid catalytic cracking (FCC). Currently, CFB is a serious option for its use in full scale utility units.

Several CLC units for gaseous fuels can be found in the literature, ranging from the 10 kW_{th} units located at Chalmers University of Technology and Institute of Carboquímica (ICB-CSIC), to the 120 kW_{th} pilot plant located at Vienna University of Technology (see Table 8 and Fig. 16). The main operational experience is based on the use of methane and natural gas, although a great effort is being made in the development of CLC for solid fuels.

Long operation times were successfully conducted in two different 10 kW_{th} prototypes built at CHALMERS and ICB-CSIC. The 10 kW_{th} unit at CHALMERS was operated

during more than 1300 h using different Ni- and Fe-based oxygen-carriers using natural gas as fuel [33,140,168,189]. These authors presented the first long-time demonstration of the CLC technology during 100 h of continuous operation with the same batch of Ni-based oxygen-carrier particles. Moreover, long-term tests (>1000 h) using Ni-based oxygen-carriers has also carried out in this unit to analyze the integrity of the particles with respect to reactivity and physical characteristics. No leakage between reactors and a high fuel conversion (98-99%) was reported. The experiments were successful and the used particles showed limited changes.

The 10 kW_{th} unit at ICB-CSIC operated during 200 h, 120 h of which in combustion, using a Cu-based oxygen-carrier prepared by impregnation on Al_2O_3 and methane as fuel [39,40]. The CLC plant designed allowed an easy variation and accurate control of the solid circulation flow rate between both reactors. These tests were the first long-term demonstration of the use of copper materials under continuous operation in a CLC process. Complete methane conversion with 100% selectivity to CO_2 and H_2O was achieved. Although some CuO losses were observed during the first 50 h of operation, no deactivation of the particles or agglomeration problems in the reactors were detected at 800 ºC.

IFP-France and TOTAL has operated a 10 kW_{th} unit using a Ni-based oxygen-carrier and methane as fuel gas. Successful operation was reported with high methane conversions to CO_2 [110].

Operation in a pressurised CLC system at Xi'an Jiaotong University in China [205] has been recently reported. The system maximum operating temperature was 950 ºC and the pressure was maintained at 0.3 MPa during the whole experiment. The pressurized CLC unit was in continuous operation with coke oven gas for 15 h. The oxygen carrier, Fe_2O_3/CuO supported on $MgAl_2O_4$, showed high reactivity in the system as well as

reasonable crushing strength and resistance toward agglomeration and fragmentation. The maximum fuel conversion reached was 92.3%.

ALSTOM Power Boilers [332] operated a 15 kW_{th} rig with natural gas and different nickel oxides in a two interconnected circulating fluidized beds to study the attrition behaviour of the oxygen-carriers. A limited attrition has been measured with four different oxygen-carriers using natural gas as fuel.

A 50 kW_{th} unit at the Korea Institute of Energy Research, KIER-1 [37,38] was operated during 28 h with methane as fuel and oxygen-carriers based on nickel and cobalt oxides. The same authors have published the second generation 50 kW_{th} unit, KIER-2, [107] with more than 300 h of operation using natural gas and syngas as fuel with Ni-based and Co-based oxygen-carriers. This new unit has two interconnected bubbling beds without loop-seals, riser nor transport lines. The solid flow control is independent using solid injection nozzles inside each reactor. They found a steady and smooth solid circulation between reactors during long-term operation with high fuel conversion.

At Vienna University of Technology, TUWIEN, [167,191] a dual circulating fluidized bed pilot plant of 120 kW_{th} was successfully operated using methane and syngas as fuels and two kinds of Ni-based oxygen-carriers and a natural mineral (ilmenite). More than 90 hours of operation experience was accomplished with Ni-based materials [193]. The CH_4 conversion measured was almost identical to that determined in the 10 kW_{th} unit at CHALMERS with the same materials [168]. In addition, the results found in the plant revealed ilmenite as a potential oxygen-carrier for H_2-rich fuels. The authors suggested that the results found in this plant can be assigned to large plants since commercial CLC power plants are likely to feature two fast fluidized bed reactors.

The potential of the Chemical-Looping Reforming process (a-CLR) has been evaluated in the 140 kW_{th} pilot plant at TUWIEN using a Ni-based oxygen-carrier [195]. Almost

full CH_4 conversion was reached and the fuel-reactor exhaust gas was in thermodynamic equilibrium. In the air-reactor, a potential valuable side stream consisting of N_2 and Ar was obtained. Promising CLR results were found at atmospheric pressure with the oxygen-carrier tested. Authors pointed out the main challenges of this technology as the effective dust removal and the operation at increased pressure because pressurized CFB is not yet a standard technology.

Recently, a number of researchers have investigated the use of solid fuels in CLC systems (iG-CLC process). At CHALMERS, ilmenite as oxygen-carrier was tested in a 10 kW_{th} Chemical-Looping combustor using coal and petroleum coke as solid fuels [54,55]. Temperatures above 1000 ºC were tested in some cases [207]. The results obtained confirmed that ilmenite appeared to be a suitable material to be used for solid fuel combustion in a CLC system. The CO_2 capture obtained with petroleum coke fuel (68-87%) was lower compared to the ones obtained with coal (82-96%) which was a consequence of the lower reactivity of this fuel. The authors pointed out different approaches to improve the CO_2 capture in the plant: an optimized carbon stripper, a better performance of the fuel-reactor cyclone which recirculates unburnt particles, a new fuel-reactor configuration to improve the contact between the oxygen-carrier and the fuel particles or an increase of the solids residence time in the fuel-reactor. In addition, a relevant amount of unburnt compounds were found at the fuel-reactor exit. To fully oxidize unburnt compounds to CO_2 and H_2O, they propose an ‘‘oxygen polishing’’ step downstream, that is, injection of pure oxygen to the gas flow after the fuel-reactor cyclone.

At the Southeast University in China, Shen et al. [109,186,187] have carried out CLC experiments using biomass or coal as fuels with an iron oxide or a Ni-based oxygen-carrier, respectively, in a 10 kW_{th} pilot plant of two interconnected fluidized beds of

which the fuel-reactor was a spouted-fluidized bed. They observed a reactivity deterioration of the Ni-based oxygen-carrier prepared by coprecipitation during coal fuelled CLC due to sintering of nickel. However, the effects of coal ash and sulfur were negligibles.

Ohio State University (OSU) is developing an iron oxide-based chemical looping process for retrofit on existing coal-fired power plants. The sub-pilot scale (25 kW_{th}) CDCL unit includes the integration of a moving-bed for the fuel reactor and an entrained bed as the combustor [58]. This plant has been also used for H_2 production when oxidation is carried out with steam [20].

ALSTOM has successfully demonstrated the coal combustion in a 65 kW_{th} pilot plant for the hybrid combustion-gasification chemical looping process using $CaSO_4$ as oxygen carrier [280]. High gasification rates were obtained even with low reactive coals.

The next step in the development of the CLC technology is the scaling-up of the process. Two CLC plants are planned to be operative in 2011 for solid fuels: a 1-MW_{th} coal fuelled CFB unit at Darmstadt University of Technology, TUD [56] within the frame of the EU ECLAIR project; and the 3-MW_{th} for the ALSTOM hybrid combustion-gasification process [59,280].

The demonstration of CLC at 1-3 MW_{th} scale is necessary to reach the next level of maturity for the scale-up step before the pre-commercial units. ALSTOM Power Boilers developed a design concept for a 200 MW_{th} (70 MW_e) CLC fired with refinery gas [34]. Later, a conceptual design for an industrial demonstration unit of 20-50 MW_e was prepared [335], together with the first environmental assessment of a full scale CLC boiler. As well, the design of a 455 MW_e CLC power plant with solid fuels was accomplished within the project ENCAP [301].

6. Modelling

The modelling of the fuel- and air-reactors is helpful for the design, optimization, and scale-up of the CLC process. An interesting number of works can be found in the literature for the modelling of the reactors involved in a CLC system, as is presented in Table 9. Most of them are developed for the two interconnected fluidized-bed reactors concept. As commented in Section 2.1.1., this is the most used configuration for a CLC system. The air-reactor is designed as a high-velocity riser and the fuel-reactor as low-velocity bubbling fluidized bed. Nevertheless, the fuel-reactor can be operated in the fast fluidization regime, where the gas velocity is higher than in the bubbling regime, to increase the fuel load [167].

Modelling of fluidized-bed reactors can be divided into three main fields, which are closely connected: fluid dynamics, reaction scheme and kinetics, and heat balance. Fluid dynamics describe the kind of contact between reacting gases and solids. The reaction scheme must consider the relevant reactions happening in the reactor taking into account the kinetics of every reaction. Finally, the heat balance is necessary to know the distribution temperature in the reactors and the heat flux that must be extracted from the reactors. Fluid dynamics, mass balances and heat balances in the reactor must be solved simultaneously because of the variation of reaction rates and gas properties. Thus, the actual reaction rate in every position inside the reactor, the appearance of side-reactions, the possible gas expansion as fuel is converted (e.g. when methane or coal is used), the growth of the bubble size, or relevance of reactions in the freeboard are other factors to be considered.

The mathematical modelling of each reactor will improve the understanding of the fluid dynamics coupled with the complex chemistry happening in the reactors. In addition,

the solids circulation flow rate and the solids inventory in the CLC reactors can be evaluated.

6.1. Fluid dynamics

Fluid dynamics of the reactor must depict both the flow and distribution of gaseous compounds and solid particles in the reactors. It is well known that restrictions for the gas-solids contact –e.g. the resistance to gas diffusing between bubble and emulsion phases in the dense bed– are relevant in a fluidized bed. For CLC, experimental results obtained in lab-scale fluidized-bed reactors have been adequately predicted by models neglecting these physical processes [303]. But it is likely that these assumptions will not be fulfilled for CLC systems at higher scale because of the use of highly reactive oxygen-carriers and the high velocity of gas related to most gas flowing through the bubbles. The predicted solids inventories to fully convert the fuel gas to CO_2 and H_2O considering diffusional resistances have been found to be between 2 and 10 times higher than those found when these effects were neglected [200]. These results reveal the importance of considering the mechanisms limiting the gas-solids contact in the fluidized-bed reactors.

Based on the description of the fluid dynamics of the reactor, mainly two categories of models can be differentiated, as it is shown in Table 9: macroscopic fluid dynamics models, and computational fluid dynamics models (CFD). These models consider the complex gas flow and solids distribution in the reactors involved in a CLC system.

The macroscopic models consider the distribution of the gas flow among emulsion and bubbles as well as the distribution of solids concentration in the bed by using empirical equations. The more complete models also include the solids distribution in the freeboard region above the dense bed, see Table 9. An attempt to consider the diffusion resistance between bubbles and emulsion was done by Kolbitsch et al. [336] by using a

model parameter, $\phi_{s,core}$, which simulates an effective amount of solids exposed to gas phase. This simple model describes the behaviour of both the fuel- and air-reactors and how the conversion of solids is coupled by the reaction in these reactors. However, it is difficult to know the actual value of this parameter in a fluidized bed, which could be different in different zones of the reactor.

Models based on the two-phase theory for bubbling fluidized beds [355] or for fluidized beds in the turbulent or fast fluidization regime [356] have been used for CLC simulation. These models were developed to predict the fluid dynamics of large fluidized bed reactors. Actually, the vertical profile of solids predicted by the model described by Pallarés and Johnsson [356] showed good agreement with the experimental data for units as large as 226 MW circulating fluidized beds (CFB) and adequately predicted the combustion efficiency burning biomass in a 12 MW_{th} CFB boiler [357]. Thus, the macroscopic models have a great potential to be used for the simulation, design and optimization of large fluidized-bed reactors in CLC systems. These models integrate the complex chemistry where a fuel gas, e.g. natural gas, reacts with a continuously circulated oxygen-carrier, with the complex fluid dynamics of large fluidized-bed reactors, using low computing time (order of minutes). In this way, modelling and simulation of the fuel-reactor for CH_4 as fuel gas has been developed for a 10 kW_{th} bubbling fluidized bed and a 120 kW_{th} high-velocity fluidized bed [200,341]. These models have been validated against experimental results obtained in the CLC units built at ICB-CSIC and TUWIEN, respectively.

The computational fluid dynamic codes (CFD) are based on the first principles of momentum, heat and mass transfer and do not required detailed assumptions in the modelling procedure. These models can simulate the behaviour of the reactor during a transient time until the steady-state is reached. To date few CFD simulations have been

performed of a full CFB due to the complexities in geometry and the flow physics, requiring a large computational effort (order of several hours). The task of simulating a full scale CFB is very challenging, and improvement of CFD methods for modelling full scale fluidized beds is in development [358]. However, with the improvement of numerical methods and more advanced hardware technology, the use of CFD codes is becoming more affordable. CFD models for commercial scale bubbling fluidized bed has been recently presented [359,360]. Therefore, the use of CFD models can be of interest for the development of the CLC technology in the near future.

The fluid dynamics for the full loop, i.e. air-reactor, cyclone and fuel-reactor, in a small scale cold-flow model has been successfully modelled by using CFD codes [361-363]. Fig. 17 shows the solids distribution in the system predicted by the CFD model in the whole loop [363]. However, limited works have been carried out using CFD codes to simulate a CLC system. CFD models are being developed for bubbling fluidized beds, being very sensitive to the bursting of bubbles at the top of the bed and the fluctuations in the concentration of gas at the reactor exit are predicted [344,347,348]. However, these models either do not consider the solids fraction in the freeboard, or it is under-predicted because of the low conversion of gas predicted in this zone by CFD models. Notice that gas-solids reaction in freeboard has been revealed of high importance to predict the high fuel conversion experimentally observed [200]. Most of CFD models have been developed for reactors in batch mode, without solids circulation, or for small scale CLC systems (300–1000 W_{th}). Important progress has been done validating the CFD models with experimental results obtained in small-scale facilities using gaseous fuels [351-353], or coal [354]. Up to date, the more complete modelling of a CLC system using CFD codes is the simulation of a bubbling fluidized bed for the fuel-

reactor coupled to a riser for the air-reactor using methane as fuel and Mn- or Ni-based oxygen-carriers [349,350].

The relatively complex processes affecting the reaction of fuel gas with the oxygen-carrier –such as full fluid dynamics, reactivity of the oxygen-carrier, the reaction pathway and the effect of solids circulation rate– has not yet been modelled using CFD codes in the range of the status of the CLC technology (10-150 kW_{th}). Until CFD codes for CLC process are more accessible and robust, the macroscopic models are effective tools for the simulation, design and optimization of CFB technologies.

6.2. Reaction scheme

To develop a mathematical model suitable for the design, simulation and optimization of a CLC system, a mass balance is required considering the kinetics of the reduction and oxidation reactions of the oxygen-carrier for the fuel-reactor and air-reactor, respectively. The mass balance in the reactor must be included in the model according to the reaction scheme proposed. Considering that scheme, the kinetic of the reactions involved in the fuel-reactor must be calculated. In most of the cases, the oxidation reaction can be represented by the simple reaction (43). In general, the oxidation reaction rates are high, and do not depend on the gas used for the reduction [126,236].

$$2\ Me_xO_{y-1} + O_2 \rightarrow 2\ Me_xO_y \quad (43)$$

In the fuel-reactor, the overall reactions of an oxygen-carrier with the CH_4, CO and H_2 present in the fuel gases are described by the reactions (44)-(47). These reactions involve the oxidation of main compounds in gaseous fuels, e.g. natural gas or syngas. Altough the mechanistic steps can involve the presence of other intermediate products, e.g. radicals, these overall reactions are often used for modelling purposes. Moreover, other reactions can be relevant in the fuel-reactor either in gas phase or catalyzed by solids. In some cases, the reforming of methane -reactions (48) and (49)- has been found

to be relevant, specially if Ni-based oxygen-carriers are used. The dry reforming of methane with CO_2 -reaction (50)- is usually slower than the steam reforming by H_2O. Thus, for modelling purposes, the dry reforming reaction can be neglected [341]. Another reaction which has been analyzed in several studies is that of carbon formation which could be promoted when Ni-based oxygen-carriers are used because the catalytic activity of Ni (see more details in Section 2.2.4.). There are two possible ways of carbon formation: methane decomposition favoured at high temperature, reaction (51); and the reverse Boudouard reaction favoured at low temperature, reaction (52). Indeed, carbon formation could be an intermediary during the conversion of methane or CO. Thus, carbon formed on the oxygen-carrier surface can be gasified by steam, reaction (53) or oxidised by lattice oxygen, reaction (54), given CO and H_2 as gaseous products. In addition, the water-gas shift (WGS) equilibrium is usually considered when CO_2, H_2O, CO and H_2 are present in the reacting gas (reaction 55).

$$4\ Me_xO_y + CH_4 \longrightarrow 4\ Me_xO_{y-1} + CO_2 + 2\ H_2O \quad (44)$$

$$Me_xO_y + CH_4 \longrightarrow 4\ Me_xO_{y-1} + CO + 2\ H_2 \quad (45)$$

$$Me_xO_y + CO \longleftrightarrow Me_xO_{y-1} + CO_2 \quad (46)$$

$$Me_xO_y + H_2 \longleftrightarrow Me_xO_{y-1} + H_2O \quad (47)$$

$$CH_4 + H_2O \overset{Ni}{\longleftrightarrow} CO + 3\ H_2 \quad (48)$$

$$CH_4 + 2\ H_2O \overset{Ni}{\longleftrightarrow} CO_2 + 4\ H_2 \quad (49)$$

$$CH_4 + CO_2 \overset{Ni}{\longleftrightarrow} 2\ CO + 2\ H_2 \quad (50)$$

$$CH_4 \overset{Ni}{\longleftrightarrow} C + 2\ H_2 \quad (51)$$

$$2\ CO \longleftrightarrow C + CO_2 \quad (52)$$

$$C + H_2O \longleftrightarrow CO + H_2 \quad (53)$$

$$Me_xO_y + C \longrightarrow Me_xO_{y-1} + CO \quad (54)$$

$$CO + H_2O \longleftrightarrow CO_2 + H_2 \quad (55)$$

Main combustible compounds in syngas are CO and H_2, which is generally accepted to react in one-step with the oxygen-carrier as it was showed in reactions (46) and (47). In contrast to the simple reaction mechanism accepted for H_2 and CO, especial attention about the primary products in CH_4 conversion is necessary, which could depend on the metal oxide used in the oxygen-carrier. Using Cu-based oxygen-carriers, Abad et al. [200] assumed that the conversion of methane takes place through H_2 and CO following the general scheme showed in reaction (45), followed by reactions (46) and (47). Thus, a model predicted adequately the presence of H_2 and CO during CH_4 conversion in a 10 kW_{th} CLC unit in the cases when it was not fully converted [39].

Using Fe-based oxygen-carriers, during the reduction period of Fe_2O_3 to Fe_3O_4, the majority of CH_4 converted goes to CO_2 and H_2O, but CO and H_2 also appear in variable amounts [131,173-175,208,233,235,268,364]. For $CaSO_4$ as oxygen-carrier, CO_2 and H_2O have been proposed as direct products of CH_4 combustion [283]. However, it could proceed with H_2 and CO as intermediate products due to the relatively large amounts of these gases observed during CH_4 conversion [272,276]. Thus, a similar approach to the methane conversion with CuO, Fe_2O_3 and $CaSO_4$ can be assumed, being CO and H_2 primary products in the conversion of CH_4 by the oxygen-carrier.

The direct reaction of CH_4 to CO_2 and H_2O as showed in reaction (44) can be assumed when the incoming methane is partially converted to form only CO_2 and H_2O, i.e. CO and H_2 are not present in the product gases. This is the case for Mn-based particles [130,245]. The reduction can be considered in one-step process towards H_2O and CO_2, as it was used in the model presented by Mahalatkar et al. [351].

Also, CO_2 and H_2O have been found to be the primary products in the conversion of CH_4 with supported NiO [365]. Thus, the direct reaction (44) of CH_4 towards CO_2 and H_2O has been shown to be adequate to predict the gas distribution in a 120 kW_{th} CLC unit [341]. In other work, Iliuta et al. [164] also considered the partial oxidation to H_2 and CO. However, they found that the formation of CO_2 prevails over the formation CO at temperatures of interest in CLC, and they assumed that the primary products of the CH_4 reacting with NiO were H_2 and CO_2. Thus, different mechanism for methane conversion using Ni-based materials have been proposed, but more research is needed in order to determine the actual set of equations to be included in the mathematical model.

Together with the gas-solid reactions between fuel gas and oxygen-carrier, side-reactions also can be relevant in the fuel-reactor. There is evidence that the reforming reactions (48) and (49) can be decisive in CH_4 conversion when Ni-based oxygen-carriers are used. For Ni-based oxygen-carriers the unconverted products were H_2 and CO when the temperature was low [160] or the oxygen in the particles was depleted [145-147,153,162,172,215]. In some cases, even though methane was fully converted, H_2 and CO can be significantly high for low reactive oxygen-carriers [150,151,157]. These fact have been related to that H_2 and CO are produced as intermediate products by the steam reforming of methane, and then they react to H_2O and CO_2 following reactions (46) and (47). Therefore, the mechanism for CH_4 conversion via steam reforming can be of higher relevance than the direct conversion of CH_4 to CO_2 and H_2O under certain conditions, i.e. when H_2 and CO are the main unconverted products. However, the conversion of methane by steam reforming decreases with the increase in the total pressure [160] and the reverse reaction (48), i.e. methanation, is promoted [294]. Moreover, the degree of the reduction of the NiO particles has shown a very

strong influence on the catalytic activity for methane reforming. A high degree of oxidation results in an almost complete deactivation of the Ni sites for CH_4 adsorption, decreasing the catalytic activity of the material [365]. As a result, the product selectivity for methane conversion changes during the oxygen-carrier reduction. During the early seconds of NiO reduction the product gas showed unconverted CH_4 [149,157,161,162,181,215], which disappeared as the reduction reaction progressed. This suggested that the steam reforming of methane was catalyzed by metallic nickel formed during reduction. This interpretation was also proposed by Kolbitsch et al. [167] to justify the results obtained during methane combustion in a 120 kW_{th} CLC unit. They found that as the oxygen-carrier was more reduced, the methane conversion was higher, although more CO and H_2 unconverted were observed. Correspondingly, Abad et al. [341] developed a model for the 120 kW_{th} CLC unit including a factor for the catalytic activity which increased with the reduction degree of the oxygen-carrier. In this way, the gas conversion in the unit was adequately predicted by the model.

In opposition to Ni-based oxygen-carriers, at conditions where methane was partially converted the main unconverted product with Cu- [166], Fe- [131,173] and Mn- [130,245] based oxygen-carriers was methane itself. This fact suggests that the reforming reactions of methane were of low relevance in these cases.

The carbon deposition is in clear competition with the main reduction reaction of the oxygen-carrier by CH_4 or CO. Recently Chiron et al. [163] have shown that carbon formation does not block the active sites. If carbon is deposited on the oxygen-carrier surface, this can be cleared by gasification with H_2O or CO_2 [163] -reaction (52) and reverse (53)- or the solid-solid reaction between carbon and the lattice oxygen from the particles [147] -reaction (54)-. If these reactions are faster than carbon generation, then carbon deposition is not observed, e.g. when the temperature is high enough [153,164].

So, it can be considered that carbon is an intermediary product for the reforming reaction or for the reduction of NiO [163], as reaction (48) is the sum of reactions (51) and (53), whereas reaction (44) can be considered as the sum of reactions (48), (49), (51), and (54). Nevertheless, as carbon formation has been never observed in continuously operated CLC system, the carbon formation could be neglected in the reaction scheme.

Thus, different paths can drive to obtain a mixture of CO_2, H_2O, CO and H_2 during CH_4 conversion. Therefore, for modelling purposes the reaction kinetics of reduction by H_2 and CO are needed even when CH_4 is used as fuel gas. The reaction of H_2 and CO mixtures with the oxygen-carrier has shown two different behaviours. Addition of the individual rates for H_2 and CO has been confirmed for Cu- and Fe-based oxygen-carriers [232], as well as for $CaSO_4$ [275]. By contrast, for a Ni-based material the reaction rate corresponded to that of the gas reacting faster, H_2 or CO, depending on the actual gas concentration [232].

Finally, the analysis of the relevance of the WGS reaction (55) is done. WGS reaction is relatively fast at temperatures involved in CLC systems using Ni- or Cu-based oxygen-carriers, and can be considered to be at equilibrium conditions [200,341]. This reaction changes the gas concentration profiles in the reactor and, therefore, the reaction rate of the oxygen-carrier. Usually, reaction with H_2 is faster than with CO. Thus, the disappearance of the highest reactive gas by the reaction with the solid is partially compensated by that generated by the WGS reaction. The consequence of this fact is an increase in the average reaction rate of the oxygen-carrier in the reactor [232]. In contrast, experimental evidence has been found that the gas composition is far from WGS equilibrium condition using Fe-based oxygen-carriers [131].

For solids fuelled CLC, two options have been proposed: (1) in–situ gasification CLC (iG–CLC); and (2) the Chemical–Looping with Oxygen Uncoupling (CLOU). The particular chemical processes happening during the solid fuel conversion in the fuel-reactor affects to the conversion of the fuel in the reactor. Particularly, in the iG–CLC the pyrolysis and gasification of coal take place in the fuel-reactor according to reactions (20)-(22), and the oxygen-carrier reacts with the gaseous products, where H_2, CO and volatile matter are the main components, as in common CLC for gaseous fuels by means of reactions (44)-(47), together possible side-reactions (48)-(55). Thus, in addition to the kinetics of gaseous compounds with the oxygen-carrier, the kinetics of char gasification with H_2O and CO_2 is also needed.

With this reaction scheme, Mahalatkar et al. [354] simulated the behaviour of a small batch fluidized bed for coal conversion using a Fe-based oxygen-carrier. They used the gasification kinetics and the reduction kinetics of the oxygen-carrier with pyrolysis and gasification products. The theoretical results agreed with the experimental results. In addition, Ströhle et al. [334] presented a simulation of 1 MW_{th} iG-CLC unit. They showed the need of a carbon stripper in order to reach high values of char conversion in the fuel-reactor because of the slow gasification reaction. Volatiles and gasification products were highly converted using ilmenite as oxygen-carrier.

The reduction of metal oxides with solid carbon could also be a true solid-solid reaction, which has been found at very low absolute pressure [366]. It was widely assumed that the metal oxides reduction by carbon should be negligible at temperatures lower than 1000 ºC [367-369]. However, Siriwardane et al. [227,370] showed the direct reduction of CuO, NiO, Mn_2O_3, Fe_2O_3 and Co_3O_4 by carbon in TGA at lower temperatures. The faster conversion was obtained for Cu and Co, for which the conversion rate was in the range 8-10%/min, i.e. in the lower range of the values obtained when char is gasified by

H_2O in presence of an oxygen-carrier [303,265,267,304]. On the contrary, results obtained in fluidized-bed reactors showed that the reduction by gasification products, i.e. H_2 and CO, had a higher relevance that the direct solid-solid reaction [119,239,304]. Even though N_2 was used as fluidizing gas, eventually the char conversion through CO_2 gasification can be the relevant reacting mechanism. Dennis and Scott [303] and Cao et al. [228] suggest that direct solid-solid reaction to give CO_2 as reaction product can happen in some extent using highly reactive sub-bituminous coal and lignite in nitrogen. Nevertheless, they suggested that small amounts of CO_2 act as a precursor of the processes involved in the iG-CLC system, i.e. gasification by CO_2 followed by oxidation of CO by reaction with the oxygen-carrier, to give more CO_2. Indeed, modelling of char conversion in a fluidized bed adequately predicted experimental results even if the solid-solid reaction was not included in the reaction scheme [119].

So, the mechanism for direct coal conversion is not well understood. Contact between char and oxygen-carrier particles seems to be a fundamental factor [370]. In a TGA, the particles are small and static, and contact between char and oxygen-carrier particles could favour the solid-solid reaction. On the contrary, in the fluidized bed particles are larger and continuously moving, reducing the surface of contact and the contact time at short intervals. These factors can affect the mechanism of char conversion. At fluidized bed conditions solid-solid reaction should be noticeable when the fluidizing gas is not a gasifying agent –e.g. in N_2–, which is not relevant for CLC application. However, when the fluidizing gas is H_2O or CO_2, the main path for char conversion should be gasification.

In the CLOU process, the relevant reactions in the fuel-reactor are the direct combustion of volatiles and char with the gaseous oxygen evolved from the oxygen-carrier [320], via the reactions (26)-(29).

It is expected and desirable that the gas in the fuel-reactor is lean in oxygen. Thus, a balance among the generation of gaseous oxygen and the oxygen reacted with volatiles and char should be looked for. In addition, the volatiles proceeding from coal pyrolysis could react directly with the oxygen-carrier, as in the iG-CLC process [303,305]. A more complete scheme could include the coal gasification, due to the fact that CO_2 and H_2O are present in the fluidizing gases, although this reaction path should be slower than the char combustion with gaseous oxygen.

6.3. Reaction kinetic

The solids inventory in the fuel- and air-reactors predicted by models is linked and depends on the reactivity of the materials and on the oxygen transport capacity of the oxygen-carrier [102,124]. To account for the reaction rate of gases and solids, the kinetic of the reactions is included in the model according to the reaction mechanism proposed.

An intensive work has been done in the past about the reactivity and kinetic determination of the reduction and oxidation of metal oxides –supported or un-supported– for metallurgical applications and catalyst characterization [366]. However, the application of the experience achieved for metallurgical applications can not be directly applied to the reactions involved in the CLC process for several reasons, namely: (i) the oxidized and reduced compounds can not be the same as that for CLC, especially for Fe- [286] and Mn-based oxygen-carriers; (ii) the analysis of the reduction or oxidation was limited to the use of fresh or pre-treated particles, but in a CLC system the solid particles suffer repeated reduction and oxidation cycles, which can affect their chemical and physical properties; and (iii) the experimental condition –e.g. temperature, particle size, gas composition– are usually different than those required for CLC. Thus,

the reaction kinetics for the oxidation and reduction should be determined for oxygen-carriers at typical conditions in a CLC system.

To adequately design the CLC reactors, the knowledge of the reaction kinetics of the solid oxygen-carrier with the reducing gases and oxygen in air are required. The kinetics for all the reactions involved in the reaction scheme must be determined. For example, if H_2 and CO were intermediate products during CH_4 conversion, reaction kinetic for reduction with H_2 and CO must be considered.

Reactivity data for a huge number of materials have been reported in the literature, but usually they are obtained for one single operational condition [98]. Limited information can be extracted for design purposes from the reactivity data, although they can be used for comparison purposes among different oxygen-carriers. It must be considered that the oxygen-carrier will be found in different environments during their stage in the fuel- and air-reactors. Thus, it is necessary to determine the reaction rate under different operating conditions of temperature and gas concentration.

The reactions involved in the fuel- and air-reactors with the oxygen-carrier can be considered as non-catalytic gas-solid reactions. Different models for gas-solid reactions have been used to predict the time dependence of the conversion of oxygen-carrier particles and the effect of operating conditions on the reaction rate. The most frequently used models are the Changing Grain Size Model (CGSM), the Shrinking Core Model (SCM), and nucleation and nuclei growth models, see Fig. 18.

6.3.1. Changing Grain Size Model (CGSM)

A common feature of all gas-solid reactions is that the overall process may involve several intermediate steps [371]. Typically, these intermediate steps involve the following: (1) gaseous diffusion of the reactants from the bulk of the gas phase to the surface of the reacting solid particle, the so-called film diffusion; (2) diffusion of

gaseous reactants through the pores of a solid particle and/or the product layer formed during the reaction; (3) adsorption of the gaseous reactants on the solid surface; and (4) the actual chemical reaction between the gas and the solid. Eventually, if gaseous compounds are produced during the reaction, desorption and diffusion until the bulk of the gas phase happens through steps (1)-(3) in the opposite direction. In addition, several other phenomena may affect the progress of gas-solid reactions, including heat transfer and changes in the solid structure, such as sintering.

The Changing Grain Size Model (CGSM) [372] considers most of steps involved in gas-solid reactions. This model assumes that the particle consists of a number of non-porous grains of uniform characteristic length, r_0. As the reaction proceeds, the grain size changes, r_1, while the size of the unreacted core shrinks, r_2, because of the different volume of the product formed per unit volume of reactant. Each grain reacts following a Shrinking Core Model (SCM). The SCM is characterized by a clearly defined interphase of reaction in the unit of reaction, here a grain. Initially, the reaction happens in the external surface of the grain. As the reaction proceeds, a layer of the solid product is formed around an unreacted core inside. At the same time, the unreacted core diminishes in size. The border area delimiting both zones –product layer and unreacted core– is the boundary where the chemical reaction happens. The reacting gas must overcome the following resistances until reaction: film transfer, diffusion through the interstices among the grains –i.e. the pores –, diffusion through the product layer around the grain and chemical reaction on the interface in the grain. The unsteady-state mass transfer equation considering the diffusion through pores and reaction within a spherical particle is

$$\frac{1}{R^2}\frac{\mathrm{d}}{\mathrm{d}R}\left(D_g R^2 \frac{\mathrm{d}C_g}{\mathrm{d}R}\right) - (-r_g) = \frac{\mathrm{d}C_g}{\mathrm{d}t} \tag{56}$$

C_g being the gas concentration at a radial position R in the particle, D_g the effective diffusional coefficient of gas in the pores, and ($-r_g$) the reaction rate of gas with the solid. Because of the possible diffusional resistance through the solid product layer in the grain, the gas concentration in the pores could be not the same as that existing at the reaction interface. To find that relation, a mass balance on the grain must be performed, whose analytical solution allows us to express the local reaction rate in terms of the gas concentration in the pores by this equation

$$(-r_g) = \frac{S_o (r_2 / r_0)^2}{1 + \frac{k_s}{D_s} r_2 \left(1 - \frac{r_2}{r_1}\right)} k_s C_g \tag{57}$$

S_o being the specific surface area, k_s the kinetic constant and D_s the effective diffusional coefficient in the product layer around the grain. The relative importance of these factors depends on the properties of the solid particles –particle size, porosity and reactivity– and the operating conditions –temperature, gas concentration and gas flow–. Moreover, the rate controlling step can change in the course of the reaction. García-Labiano et al. [373] used a non-isothermal Changing Grain Size Model (CGSM) to estimate the relative relevance of different steps in the reaction of oxygen-carrier particles in CLC applications. The resistance to heat and mass transfer in the gas film and inside the particle together with the chemical reaction on the particle surfaces were considered for the oxidation and the reduction reactions with different fuel gases (CH_4, H_2 and CO) and materials (Ni, Cu, Fe, Mn and Co). Under typical conditions present in a CLC system, with particle sizes lower than 300 μm, 40 wt% of metal oxide content and full reaction times of 30 s, the particles can be considered isothermal with conversion and temperature profiles inside the particles of low significance. Also, the external mass and heat transfer hardly affected the reaction rate for these conditions. These results agree with the results shown by Ishida et al. [221] and Hossain and de

Lasa [217]. Accordingly, Erri and Varma [374] showed that the reduction reaction of Ni-based oxygen-carrier particles supported on $NiAl_2O_4$ (40 wt% NiO, particle size up to 425 μm) were not limited by diffusion effects. The resistance to the mass or heat transfer can be relevant for larger particle sizes, higher metal oxide content or reaction rates. As example, Fig. 19 shows the maximum increase in the particle temperature during oxidation or reduction of several materials. Thus, maximum increases in the particle temperature of 90 ºC were predicted when 1 mm particles of a Ni-based oxygen-carrier were oxidized. The temperature increase during oxidation followed the order Ni ≈ Co > Cu > MnO > Fe_3O_4 due to the heat involved in each reaction, i.e. the enthalpy of reaction, see Section 2.1.3.

A simplified solution to the mass balance –equations (56) and (57)– considers an effectiveness factor, η_r, for the reaction rate, which takes into account the gas diffusion in the pores. Here we refer to this model as the diffusion-reaction model, DRM [375]. The true reaction rate of the particle, $\left(-r\right)_{true}$, is calculated as

$$\left(-r_g\right)_{true} = \eta_r \left(-r_g\right)_{C_{g,0}} \tag{58}$$

$\left(-r\right)_{C_{g,0}}$ being the reaction rate with the gas concentration at the particle surface, $C_{g,0}$.

For a first-order, isothermal, irreversible reaction occurring within a spherical particle, the effectiveness factor is calculated as

$$\eta_r = \frac{3\Phi_{Th}\left(\coth\Phi_{Th} - 1\right)}{\Phi_{Th}^2} \qquad \Phi_{Th} = R_p\sqrt{\frac{k_s}{D_g}} \tag{59}$$

Φ_{Th} being the Thiele modulus, R_p the radius of the particle. For small Φ_{Th} the impact of diffusion is small and η_r is close to unity. For large Φ_{Th} diffusional limitations reduce significantly the observed reaction rate. Chuang et al. [180] applied the effectiveness factor to relatively large particles (355–500 μm and 850–1000 μm) and a high copper

content (82.5 wt%). The effectiveness factor η was between 0.9 and 0.07, suggesting a transition of the controlling mechanism from intrinsic kinetics at the lower temperatures (150-600 ºC) to diffusion and reaction inside pores at high temperatures (600–900 ºC).

Another approximation towards a simplified solution of the CGSM is following the concept that the time accounting for all the resistances is obtained simply by summing the time for each one separately as it was proposed by Szekely et al. [366] in the grain model.

$$t = t_{film,p} + t_{pl,p} + t_{pl,g} + t_{reac,g} = \tau_{film,p} f_{F_p}(X) + \tau_{pl,p} p_{F_p}(X) + \tau_{pl,g} p_{F_g}(X) + \tau_{reac,g} g_{F_g}(X) \quad (60)$$

Table 10 shows the expressions for the conversion functions $p_{F_p}(X)$, $p_{F_g}(X)$ and $g_{F_g}(X)$.

In most of cases related to oxygen-carrier particles, the rate of diffusion thought the film, pores and product layer presents a negligible resistance. In this case, particles can be considered as an agglomerate of individual grains reacting in the absence of mass transport resistance and the solids conversion is uniform throughout the solid. In this case, no dependence with the particle size is happening. The model corresponds to a Shrinking Core Model in the grains (SCMg), considering only the last term in Equation (60). The SCMg was used to calculate the kinetic parameters of the reduction and oxidation reactions for Cu-, Ni-, and Fe-based oxygen-carriers [124,126,232,276].

Usually, spherical grains has been assumed (F_p = 3). The model for plate-like geometry (F_p = 1) was used for impregnated Cu-based particles [126]. This case is characterized by a straight conversion vs. time curve. Straight conversion vs. time curves also has been obtained for particles for which the plate-like geometry can not be assumed [243,377]. The linearity of the curves may indicate that the oxygen coverage on the surface is constant during the reducing period, meaning that oxygen atoms diffuse

through the product layer of metal onto the surface where the reaction occurs [377]. Moreover, the diffusion of oxygen is not the rate-limiting step. This model is referred as the Chemical Reaction at Surface Model (ChRSM).

Diffusional resistance in the product layer was also included during reduction of $NiAl_2O_4$ [94]. In this case, initially the reaction was controlled by chemical reaction and suddenly a sharp decrease in the reaction rate was observed at a certain conversion. To predict this behaviour, a diffusion coefficient dependent on solid conversion was used. This behaviour has been observed for reduction of Cu- and Ni-based oxygen-carriers at low temperatures [126,376]. However, this sharp decrease in the reaction rate did not take place at high temperatures typically used in CLC systems. Therefore, only the chemical reaction control was considered in these cases.

6.3.2. Shrinking Core Model (SCM)

When the resistance to gas diffusion in the un-reacted particle is very high, the Shrinking Core Model (SCM) in the particle has been considered. Thus, a layer of the solid product is formed around an unreacted core inside the particle. The time required to reach a certain conversion is calculated in a similar way as that in the grain model – see Equation (60)– but replacing the radius of the grain, r_g, by the radius of the particle, R_p. If one of these steps controls the reaction, then only the corresponding term in Equation (61) will be considered.

$$t = t_{film} + t_{pl} + t_{reac} = \tau_{film} X_i + \tau_{pl}\, p_{F_p}\left(X_i\right) + \tau_{reac}\, g_{F_p}\left(X_i\right) \tag{61}$$

The SCM has been used to calculate the kinetic parameters for reduction with H_2 and oxidation of millimetre-sized Ni-based particles [221]. The conversion vs. time curves indicate that reduction was controlled by chemical reaction, but oxidation was in the intermediate regime between chemical reaction control and product layer diffusion control. According to the SCM, the reaction rate is first order in R_p for chemical

reaction control, second order for product layer diffusion control, and in the interval 1.5-2.5 order in R_p for gas film diffusion. This fact was properly analyzed by Ishida et al. [221] for particle sizes from 1 to 3.2 mm. The SCM has been able to predict experimental data for smaller particles [108,222]. However, uncertainty arises about the suitability of the SCM in these cases because of the high porosity and small size of the particles, in the order of 100 μm.

6.3.3. Nucleation and nuclei growth models

In many gas-solid reactions with formation of a solid product, oxidation and reduction of oxygen-carrier particles can be addressed by a nucleation process. According to the nucleation and nuclei growth models, the process proceeds with the generation of metallic nuclei, which subsequently grow and finally overlap. The reaction rate increases as the number of nuclei increases during the first moment of reaction, the so-called the induction period. After this point the reaction will occur uniformly over the solid surface, and the reaction front advances uniformly into the inner part of the grain. Thus, the conversion vs. time curves are characterized by a sigmoid behaviour, often described by the Avrami–Erofeev Model (AEM) [217].

$$\frac{\mathrm{d}X_s}{\mathrm{d}t} = k_s^{'}(T) C_g^n f(X_s) \tag{62}$$

The general equation for the function of the solids conversion is

$$f(X_s) = \nu(1-X_s)\left[-\ln(1-X_s)\right]^{(\nu-1)/\nu} \tag{63}$$

where ν is the Avrami exponent indicative of the reaction mechanism and crystal growth dimension. Thus, the Random Nucleation Model (RNM) is given by a value of $\nu = 1$, and when $\nu = 2$ and 3 the nuclei growth is assumed to be 2-dimensional or 3-dimensional, respectively. When $\nu = 1$, an induction period is not present.

An equivalent expression to that for the RNM can be obtained from the Power Law Model (PLM) or a Modified Volumetric Model (MVM). These models have been used when the reaction occurs uniformly all through the particle, i.e. no diffusion resistance exists. The rate of reaction per unit volume of the particle for PLM is represented as

$$\left(-r_g\right) = k_s^{'} C_g^n C_s^m \tag{64}$$

When the reaction order regarding the solid concentration, C_s, is m = 1, the integrated equation can be expressed as

$$t = -\frac{1}{k_s^{'} C_g^n} \ln\left(1 - X_s\right) \tag{65}$$

corresponding to a homogeneous model, which takes the same form as the RNM.

The Avrami–Erofeev Model has been applied to the reduction and oxidation of Ni-based oxygen-carriers [217]. Temperature programmed reduction (TPR) or oxidation (TPO) was performed to obtain the kinetic parameters, using a heating rate of 10 ºC/min. Reduction reaction proceeds from 300 ºC to 600 ºC, above which the reduction is complete. A lower temperature was necessary for oxidation (from 200 ºC to 500 ºC). The RNM, with ν = 1 in Equation (63), was found to give the best fit. Son and Kim [108] used the same time-conversion dependence for the MVM to obtain kinetic parameters for the reduction with CH_4 of Ni- and Fe-based oxygen-carriers.

Nucleation effects are often significant in systems such as reduction of metallic oxides [366]. These models have been widely used in reduction of Ni-based catalyst at low temperatures. Thus, the induction period has been clearly evidenced at solids conversions lower than 0.1-0.2 and temperatures lower than ~300 ºC [371]. The nucleation process is accelerated as the temperature increases. For example, at 340 ºC the induction period was imperceptible. Sedor et al. [214] found that the reaction starts immediately, with no induction period, at temperatures above 600 ºC.

In a CLC system, temperatures of about 600-800 ºC could be sufficient for industrial process such as refineries but higher temperatures in the range (900-1200 ºC) should be necessary to get high electrical efficiency [115,378]. For the temperature range involved in CLC the nucleation process could be relatively fast and of low relevance regarding the conversion of the bulk solids. When the nucleation occurs rapidly over the entire solid surface, the models described above in Sections 6.3.1 and 6.3.2 –which deal with interfacial chemical reactions– can be applied [366]. Actually, both the Shrinking Core Model and the RNM have been shown to fit the same experimental data reasonably well [214].

6.3.4. Kinetic data

The kinetics of reaction for the reduction with the main reducing gases present in a CLC system, i.e. CH_4, CO and H_2, and the oxidation with oxygen have been determined for Cu-, Ni-, Fe- and Mn-based oxygen-carriers, as is shown in Table 11. Most of experimental studies have been done in a thermogravimetric analyzer (TGA). In these experiments, the absence of external mass transfer control was checked. The temperature programmed reduction or oxidation (TPR, TPO) technique also has been used for kinetic determination, but in these cases the reaction kinetics were obtained at a quite low temperature. Others facilities, as fluidized-bed or fixed-bed reactors has been also used, but taking measures to reduce mass transfer limitations [180,380,382] or by using a reactor model accounting for the mass transfer processes [164].

To consider kinetic determination useful for modelling purposes, both the activation energy and the reaction order must be determined for every reaction involved in the reaction scheme, which is not always available. Thus, the effect of temperature and gas concentration on the reaction rate will be adequately predicted. In general, the reaction order was found to be in the range 0.8–1.0. The activation energy seems to follow the

tendency $CH_4 > H_2 > CO \approx O_2$. Nevertheless, an important dispersion in the values for each kind of metal-based oxygen-carriers was observed. The interaction among the metal oxide and the support affect the activation energy. Reducing the affinity of the metal oxide with the support reduces the activation energy, reflecting the increased ease of reducing the metal oxide [217,376]. Thus, it is necessary to determine the kinetic parameters for every specific oxygen-carrier.

The majority of kinetic determination has been done for synthetic oxygen-carriers supported on an inert material. Only a limited number of studies were found about the reaction kinetics of natural minerals, such as ilmenite ($FeTiO_3$) or anhydrite ($CaSO_4$). Less are the studies focused on the kinetics of one certain oxygen-carrier with all the reducing gases when natural gas, syngas or coal is used as fuel, mainly CH_4, CO and H_2. It is necessary to point out that CO and H_2 can appear as intermediate products during the reaction of CH_4 or coal, and it is necessary to know the reaction kinetics with CO and H_2 even if CH_4 or coal is used as fuel gas [200,296,341]. Furthermore, the kinetics for the oxidation reaction also is required for the air-reactor design, and thus optimization the CLC system by integrating air- and fuel-reactors [124,336].

In addition, natural gas or refinery gas can contain a certain amount of light hydrocarbons. Similar reactivity as for methane has been found for these compounds with Cu- and Ni-based oxygen-carriers [46,203]. In addition, the use of liquid hydrocarbon feedstocks has been proposed as fuel for CLC systems [383]. However, no kinetic data about the reaction rate of oxygen-carriers with higher hydrocarbons has been found in the literature.

The effect of the concentration of a gas product on the reduction reaction rate has been barely analyzed. At low temperature, it was observed that the presence of steam delayed the reduction of NiO by H_2 at 295 ºC [384]. Nevertheless, at temperatures of interest for

CLC, the H_2O or CO_2 content does not affect the observed reduction rate in most of cases [27,126,200,218,232,296]. However, in few cases a negative effect of the gaseous products for the reduction with methane has been observed, i.e. H_2O in Fe_2O_3 on Al_2O_3 particles [124] and CO_2 on NiO/bentonite particles [199]. Nevertheless, the effect of the gaseous products can be relevant when the gas composition is approaching to the equilibrium condition, especially with Ni- or Co-based oxygen-carriers. Ishida and Jin [27] also detected a negative effect of H_2O on the oxidation reaction of NiO/YSZ particles, which was more pronounced as the particle size increased. The presence of steam in the air stream can be of interest in order to increase the energetic efficiency of the overall process, as it was proposed for the Chemical-Looping Saturated Air (CLSA) process [26].

Very limited kinetic information was found about the decomposition of Cu-, Mn- or Co-based oxygen-carriers, which is of interest for its use in CLOU. This reactions has shown to have a relatively large activation energy, E_r = 313 kJ/mol, for CuO decomposition [385]. For the oxidation of Cu_2O to CuO, Chuang et al. [380] found a value of E_r = 60 kJ/mol. Further research about the decomposition and re-oxidation of oxygen-carriers for CLOU is needed in the future.

When mixed-metal oxides are used, Moghtaderi et al. [379] related the pre-exponential factor, activation energy and reaction order with those for the individual components. Thus, the results obtained by Son and Kim [108] with Ni-Fe oxygen-carriers were adequately predicted. These authors also fitted the kinetics parameters for dual systems of Cu-, Ni-, Fe-particles. In this case, the mixture was obtained by physically mixing single-oxide particles, and there is no clear effect of physically mixing different particles on the resulting kinetics of the mixture.

The kinetic data showed in Table 11 were obtained at atmospheric pressure. For the design of CLC at pressurized conditions, it is recommendable to determine the kinetic parameters at the same operating pressure to be used in the CLC plant. Few works on the behaviour of the oxygen-carriers under pressurized conditions has been done. In general, the total reaction rate is increased with the increase of total pressure [223,236,386]. However, García-Labiano et al. [236] showed that this increase in the reaction rate was lower than the expected increase considering the increase of the partial pressure of reacting gases. If data at pressurized conditions are not available, the equation proposed by García-Labiano et al. [236] to calculate the apparent kinetic rate constant at pressure P, k_P, from kinetic data at atmospheric pressure, k, can be used, as showed in Fig. 20.

6.4. Residence time distribution in the reactor

The appropriate distribution of solids residence time in the reactor must be considered in the reactor model. The particle residence time distribution (RTD) in the reactor influences the reaction rate of solids in the reactor. Thus, very different conversion of gas were obtained using different distribution functions for the solids conversion, even though they may have the same average conversion [340]. Three different approximations have been proposed to consider the distribution of solids conversion in the reactor: (1) homogeneous conversion of solid particles in the reactor, which has been used mainly in CFD models; (2) a population balance to the solid particles [339,340]; and (3) a residence time distribution of solids in the reactor [124,200,341]. Usually, it is considered that the solids are in perfect mixing inside fluidized-bed reactors, which has shown to be true for mixing among solids in the dense bed and the freeboard zone [104]. Exceptionally at low fluidizing velocities, u_g/u_{mf} < 10-15, this assumption can not be maintained because the appearance of stagnant zones [104]. At

these conditions the use of a homogeneous conversion in the reactor could drive to unsuitable results.

The average reaction rate of the particles having a RTD function $E(t)$ in the fuel- or air-reactor can be calculated by

$$\left(\overline{-r_O}\right) = R_{OC}\int_0^{\tau_c} \frac{\mathrm{d}X_s}{\mathrm{d}t} E\left(t\right)\mathrm{d}t \tag{66}$$

The average reactivity has been expressed to consider that the oxygen-carrier is introduced into the fuel- and air-reactor partially converted, with a mean conversion $\overline{X}_{s,in}$. The variation of solids conversion proceeds from $X_s = 0$ at $t = 0$ to $X_s = 1 - \overline{X}_{s,in}$ at $t = \tau_c$. [124,126]. Abad et al. [124] introduced the characteristic reactivity of the reactor, Φ_j, to calculate the average reaction rate from the known rate of oxygen transfer at $X_s = 0$, $\left(-r_O\right)$.

$$\left(\overline{-r_O}\right) = \frac{\Phi_j}{\delta}\left(-r_O\right) \tag{67}$$

Table 12 shows the algebraic equations for the characteristic reactivity, Φ_j, as a function of the solid conversion at the inlet of the reactor, $\overline{X}_{s,in}$, and the conversion variation in the reactor, ΔX_s. Perfect mixing of solids was assumed. The parameter δ is a constant from derivation of the conversion with time equation, see values in Table 12. The value of characteristic reactivity, Φ_j, is limited between 0 and δ. As an example, Fig. 21 shows a plot for the calculation of Φ_j introducing the values of $\overline{X}_{s,in}$ and ΔX_s. when the kinetic model is the SCM or SCMg with spherical geometry.

The variation of Φ_j –and therefore the average reaction rate of solids– with ΔX_s is not linear. When ΔX_s is decreased from 1 to ~0.5, the value of Φ_j approaches its maximum value, i.e. δ. Further decrease in ΔX_s results in lower increases of Φ_j value [200], and the average reaction rate asymptotically approaches to the $\left(-r_O\right)$ value.

6.5. Modelling results

The mathematical model for the air- or fuel-reactor must describe the behaviour of a gas-solid reactor –usually a fluidized bed– to process a fuel with continuous circulation of an oxygen-carrier. The main inputs of the model are related to the reactor geometry, the operational conditions and the solids and gas properties. The main outputs of the model consist of the fluid dynamical structure of the reactor –solids concentration profiles and gas flow distribution between bubbles and emulsion phases–, axial profiles of gas flow and composition, gas composition at the reactor exit, and conversion of the oxygen-carrier in the reactor. Fig. 22 shows examples of axial profiles for gas and solid concentration in the fuel-reactor predicted by using a macroscopic model. Also, maps of gas and solids concentration by using a CFD model are shown.

6.5.1. Fuel-reactor modelling

A fundamental part of the reliability of a CLC system is based on the behaviour of the fuel-reactor. A good fuel-reactor design looks for the complete conversion of fuel gas. If the fuel gas is not fully converted, additional actions must be taken. These include the recirculation of the unburned gases, e.g. CO, H_2 or CH_4, after removing H_2O and CO_2 from the flue gas, or the use of a final gas polishing step with pure oxygen. Thus, most of the models available in the literature are focused in the fuel-reactor using gaseous fuels in a bubbling fluidized-bed, see Table 9. In this case, models predicted that about half of the gas conversion in the dense bed occurs close to the gas distributor plate because of the highest rates of reaction and high gas-solid mass transfer in this region. However, the gas conversion is reduced in upper parts of the dense bed due to limitations in the gas transfer between bubble and emulsion. Thus, a relevant fraction of unconverted fuel bypasses the dense bed through bubbles [344,347]. The conversion in the freeboard region above the dense bed –where the gas-solids contact is improved– is

decisive to reach high conversion efficiency, except if the gas velocity was low [200]. When a high-velocity fluidized-bed is considered, the fractional conversion in the dense bed was lower than in a bubbling fluidized-bed. In this case, most of fuel gas is converted in the freeboard region [341].

The effect of several operating parameters has been predicted by modelling. Factors affecting the oxygen-carrier reactivity –such as temperature, solids circulation flow rate or particle size– have been shown to have important impact on the CLC performance. So, the fuel conversion is improved by an increase in temperature [200,341,344] or solids circulation flow rate [200]; or by a decrease in the particle size [344]. Nevertheless, when the reaction rate is not affected by the particle size, a slight increase in the combustion efficiency was predicted as the particle size increases due to a lower fraction of gas passing through the bubbles for higher particle sizes [200]. At a constant oxygen-carrier to fuel ratio, a moderate increase in the fuel flow has low relevance on the combustion efficiency because the excess of gas bypassing the dense bed is compensated by a higher amount of solids in the freeboard.

Very limited works can be found related with CLC modelling for solid fuels. Modelling of the iG-CLC process has shown that the process is limited by the rate of char gasification [334,354]. The decisive importance of the separation efficiency of unconverted char from the oxygen-carrier stream to the air-reactor to reach high carbon capture efficiency has been also evidenced [334,387]. In addition, higher solids inventories are needed to get high char conversions in the fuel-reactor –thus having high carbon capture efficiency– than to reach high conversion of gases to CO_2 and H_2O [387].

6.5.2. Air-reactor modelling

The most common design of a CLC plant includes a high-velocity riser for the air-reactor [102]. In a typical configuration of a CLC system, the air-reactor must be properly designed to have enough gas velocity to carry out the necessary flow of solids to the fuel-reactor. Thus, the air-reactor is often designed to give the required solids circulation rate by changing the air flow [104,388,389]. However, an increase in the air flow means that the temperature in the air-reactor is reduced [378]. In addition, the air-reactor must provide a long enough residence time to take up the required oxygen for the fuel gas. In this case, the power capacity of the CLC system could depend on the maximum amount of oxygen which can be taken up by particles in the air-reactor [340].

When simulated, the air-reactor has been considered as a riser [349,350]. Cloete et al. [349] found that a low conversion of the oxygen-carrier (3.6%) was obtained with a reactor height of 11 m. This means that the solids circulation rate should be high and that most of metal oxide present in the particles is not being used. In this sense, the use of particles with high reactivity and low content of metal oxide could be advantageous [141]. A dense bed could be necessary under the dilute region in the riser to give a long enough residence time for particles to be oxidized to a high degree [378]. Indeed, there are experimental evidence that low oxidation conversion in the air-reactor limits the fuel conversion in the fuel-reactor [192], even though enough oxygen in the solid material was transported to convert the fuel to CO_2 and H_2O. The effect of low oxidation degree on the fuel-reactor performance has been adequately predicted by modelling [341].

The limitation among the air flow supplied and the solids circulation rate can be decoupled in other CLC configurations recently proposed, either by recirculating a fraction of the solids from the cyclone to the air-reactor [56,283,390,391] or by independent control of the solids circulation from the air- and fuel-reactors [333,392].

6.5.3. Air- and fuel-reactor linkage

Experimental results have shown that the operating condition of one reactor affects the behaviour of the other reactor [167]. Thus, the solids circulation rate affects the variation of solids conversion and the average conversion of solids in every reactor. In addition, temporary fluctuations in the solids circulation rate because of the fluid dynamics of the system had important effects on the temperature and solids conversion in the reactors [350]. If the fuel flow was changed, a constant ratio of the fuel flow to the solids inventory in the air-reactor is recommended as scale-up factor [339], in order to have enough residence time for oxygen-carrier particles to uptake the required oxygen in air-reactor.

Abad et al. [124] introduced a simplified method to evaluate the effect of operating conditions on the performance of the CLC system. This method is based on the calculation of the average reaction rate of particles, $\left(\overline{-r_O}\right)$, as a function of the variation of the solids conversion, ΔX_s, and the average conversion of solids at the reactor inlet, $\overline{X}_{s,in}$, see Equation (70) together with Table 12 and Fig. 21. Using this method, an inventory of solids in a CLC system is calculated as a function of these variables (ΔX_s and $\overline{X}_{s,in}$). Thus, the effect of operating conditions on the calculated solids inventory can be qualitatively analyzed [124,200,232,243,376]. The calculated solids inventory is the minimum that could be necessary in a perfectly stirred reactor because this method does not consider the bubble-emulsion gas transfer resistance in the bed, and it can be used for comparison purposes among different oxygen-carriers. When gas transfer resistance is considered, as it is the case in a real fluidized bed, the required solids inventory to fully convert the fuel gas can be multiplied by a factor from 2 to 10 [200].

The total solid inventory is dependent on the solid conversion at the inlet of fuel- and air-reactors, as shown in Fig. 23a. The solids inventory increases in the air-reactor as the

oxygen-carrier is forced to be more oxidized; correspondingly, the solids inventory increases in the fuel-reactor as the oxygen-carrier is more reduced. The total solid inventory –sum of the solids in the air- and fuel-reactors– has an optimum which minimizes the amount of solids in both reactors. The optimum conditions are found in the intermediate range of $\overline{X}_{s,in}$, i.e. the solids should be neither fully oxidized in the air-reactor nor fully reduced in the fuel-reactor.

In addition to the solids inventory needed to fully convert the fuel, the circulation rate of solids should be high enough to transport the oxygen required by the fuel from the air-reactor, see Section 2.1.3. The circulation rate of solids directly affects to the variation of solids conversion between the reactors, ΔX_s, and therefore the calculated solids inventory. Indeed, ΔX_s has been used to determine the solids circulation rate in a continuously operated CLC unit [192]. Fig. 23b shows that low values of ΔX_s gave high circulation rates and low solids inventory. Oppositely, high values of ΔX_s gave low circulation rates, but high solids inventory. The optimum values of ΔX_s to get low circulation rates and low solids inventory could be about 0.2–0.6.

Considering the individual effect of $\overline{X}_{s,in}$ and ΔX_s on the solids inventory in the air- and fuel-reactor, it has been showed that different pairs $\overline{X}_{s,in}$–ΔX_s can give the same value of total amount of solids in both reactors [124]. Thus, a diagram can be displayed where level curves for the same solids inventory are plotted as a function of $\overline{X}_{s,in}$ and ΔX_s, see Fig. 24. The minimum solids inventory in every reactor is obtained for the limiting case for $\Delta X_s \rightarrow 0$. For any value of ΔX_s the minimum solids inventory is found at values around $\overline{X}_{o,outAR} = 0.5+\Delta X_s/2$, being $\overline{X}_{o,outAR}$ the oxidation degree of solids in the air-reactor and equal to the conversion at the fuel-reactor inlet, $\overline{X}_{o,inFR}$.

Accordingly, Kolbitsch et al. [336] analyzed the dependence of the distribution of a certain amount of solids among the air- and fuel-reactors on the CLC performance. They concluded that there is an intermediate region –around when the solids are shared fifty-fifty– where the gas conversion is less sensitive to the shifting of solids inventory between air- and fuel-reactors. However, when one reactor has much more solids inventory than the other, the conversion of the gas decreases. At optimum conditions, the oxygen-carrier is not fully oxidized in the air-reactor nor fully reduced in the fuel-reactor.

Predictions of the models are usually interpreted at the steady state of the system, which is useful for design and optimization purposes. However, dynamic models can be used to simulate transition periods between stationary periods. Thus, modelling can help to identify strategies for off-design operation, as the start-up, shutdown and part-load periods [393-395]. Balaji et al. [396] presented a non-stationary model used for control purposes. A thermodynamic equilibrium based mathematical model was used to predict the non-steady and non-isothermal transition period after a perturbation is introduced in the CLC system –e.g. a change in the air or fuel flow rate or the addition of fresh material– until the steady state is reached again in both the air- and fuel-reactors. They concluded that the linkage between the two reactors is strong, i.e. a disturbance in one reactor greatly affects the other reactor.

In conclusion, to optimize a CLC system it is necessary to develop design tools for the air-reactor and fuel-reactor, and further integrate the models to simulate the performance of the whole CLC cycle. Also it will be valuable to couple the reactors with other components, as cyclones and loop seals.

6.5.4. Model validation

Mathematical models have been used for different purposes. In some cases, reactor models in the CLC field have been used to predict experimental results at lab-scale or determine the kinetics of an oxygen-carrier, see Table 9. However, the most important purpose of a mathematical model is using it to design and optimize a CLC plant. Validation of the models against experimental results obtained in continuously operated CLC system is an important step before use them for design, optimization and scale-up purposes. The scale-up of the reactors must consider the change in the reactor height, which can affect to the gas transference among bubbles and emulsion phases. However, few models have been validated against experimental results in continuously operated CLC units.

CFD models have been used to simulate the performance of small facilities up to 1 kW_{th} [351-353] showing a good fit between experimental results and theoretical predictions. However, it is doubtful that these models can be valid for scale-up without important modifications. Macroscopic models have been used to predict the performance of the fuel-reactor at bubbling and high-velocity fluidized beds [200,341] at a scale up to 120 kW_{th}, i.e. the largest scale built and operated for a CLC system up to the present.

Once a model has been validated, it can be used to design a new reactor and to optimize the operation of an existing CLC plant. Thus, the solids inventory needed to fully convert the fuel in the fuel-reactor can be calculated as a function of the operating conditions. As an example, Fig. 25 shows the minimum inventory of solids per MW_{th} of fuel predicted by a macroscopic model [200] to fully convert CH_4 as a function of the solids circulation rate at different temperatures. The oxygen-carrier was 14 wt% in CuO. It can be seen that the solids inventory increases rapidly with a decrease of the temperature or the solids circulation rate.

6.5.5. Modelling of alternative CLC concepts

In addition to the interconnected fluidized-beds reactors, other concepts have also been analyzed to carry out the CLC process, although at lower scale. In these concepts the oxygen-carrier material is static and air and methane are planned to flow alternatively through the reactor, which can be formed by coated monoliths [343], packed bed [116] or fluidized bed [119]. To optimize these systems, modelling and simulations are required by fixing the time period which the air and the fuel are fed, and the time whenever the flue gases is directed towards a CO_2 storage unit [343]. In addition, when this configuration is used for solids fuel, it is necessary to provide a period of time for gasification of the accumulated char in the bed before the regeneration step in order to optimize the carbon capture efficiency [119]. Also, the energy balance is coupled to the extension of oxidation and reduction during the cycles [116].

Simulation of the process in a packed-bed reactor shows that the maximum temperature is independent of the gas mass flow rate or the oxidation kinetics of the oxygen-carrier, offering a high flexibility to changes in the production capacity and little disturbance by changes in the reaction kinetics. Moreover, the cyclic steady state was obtained after only a small number of oxidation/reduction cycles, and continuous power generation can be reached with only two packed-bed reactors in parallel [116]. However, a high flow rate gas switching system and high pressure drops in the reactor would be needed. In addition, the appearance of severe profiles of temperature in the reactor during every step (oxidation or reduction) should be analyzed for sizes at commercial scale.

6.5.6. CLC integration and part-load analysis

Finally, it must be remembered that the CLC system replaces the combustor in a process for energy generation. Thus, the integration of the CLC system with the equipments of the system for energy generation is a key factor to obtain a high efficiency converting

chemical energy in the fuel. Simulation studies show CLC as a promising technology with relatively high energetic efficiency in power/heat generation with inherent capture of CO_2 [14, 15,17]. Exergy analysis has been used as a method to identify key parameters in the integration of CLC system in a power plant [24-26,297]. The destruction of fuel exergy in the unmixed combustion in a CLC system is decreased compared to similar systems with conventional combustion of fuel where the combustion is carried out by mixing fuel and air [25,26,297]. Thus, the net power efficiency is increased in the case of CLC systems. Additional advantages can arise when CO_2 capture is considered, because the CO_2 is inherently separated from the rest of gases in the CLC process providing a relatively low cost for the CO_2 capture [14,17,397]. Furthermore, the relative improvement of the net plant efficiency of the CLC combined cycle is increased when the power plant is operated at part-load, which could happen frequently during the life time of the plant [394]. In this case, gas leakages between reactors could happen if there is a pressure difference between the two reactors, which is undesirable in a CLC system. To overcome this problem, the use of a compressor with variable inlet guide vanes was proposed in order to allow normal CLC operation at off-design conditions [393-395].

Design and operating parameters of the CLC system –e.g. the pressure drops, temperature and combustion efficiency in the CLC system– affect to the whole performance of the plant. Several configurations have been proposed to optimize the integration of the CLC reactors with a combined cycle. The Chemical-Looping principle may be applied either in a gas turbine cycle with pressurized oxidation and reduction reactors, or in a steam turbine cycle with atmospheric pressure in the reactors. At atmospheric pressure, the use of a steam cycle could achieve about 40-42% efficiency when using gaseous or solid fuels [300,398] including energy demands for CO_2

compression before transport and sequestration. The compression of CO_2 reduces the efficiency by about 2% [115]. The calculated CLC efficiency is similar to that achieved by currently atmospheric power plants, which does not include energy penalty for CO_2 capture.

The energetic efficiency of a CLC-based power plant is increased when the system is pressurized and a gas turbine is used for power generation. However, up to the present there is no proper design of a pressurized (1-3 MPa) CLC plant using two interconnected pressurized fluidized beds. Systems composed by a combined cycle have been analyzed in depth [393,398]. Additionally, the use of an air-based gas turbine and a CO_2-turbine with an integrated heat recovery system was analyzed [25,26,114]. Theoretical calculations show that the total pressure and the pressure ratio of the gas turbine has little effect on the overall efficiency of the CLC process in a pressure range from 1 to 2 MPa [114,115]. The efficiency decreased below 1.3 MPa, and it barely increased for futher increases in total pressure. Thus, a pressure in a CLC system above 1.3 MPa is not recommended [115]. Also, the inclusion of a CO_2 turbine has no substantial impact on the energetic efficiency of the process. This was mainly due to the higher compression work needed after decompression in the CO_2 turbine to pressurize the CO_2 stream to sequestration conditions.

On the contrary, the temperature of the air-reactor –which depends on the air flow and the solids circulation rate– has a great impact on the efficiency of the combined cycle because it defines the turbine inlet temperature [378,394]. Thus, the energetic efficiency of the CLC process increases as the air-reactor temperature increases [114,378,393,394]. The use of saturated air in the air-reactor has been also proposed to increase the energetic efficiency, as in the CLSA process [26].

In earlier studies, it was identified that a higher difference in temperature between the air- and fuel-reactors decreases the exergy losses [25]. This means that the temperature in the fuel-reactor should be as low as possible. Very low temperatures in the fuel-reactor (200 ºC) were proposed for methanol as fuel and Fe-based oxygen-carriers, obtaining a net overall efficiency as high as 56.8% without considering the losses in the further compression of CO_2 [399]. Thus, endothermic reactions in the fuel-reactor would be preferred to exothermic ones [25], because the exergy loss is reduced when a higher amount of energy is released in the air-reactor at high temperature. When the heat released at high temperature is efficiently utilized, it is theoretically possible to increase the overall power efficiency [297]. However, attention must be paid to the oxygen-carrier reduction reactivity at low temperature.

Later calculations have shown that the temperature in the fuel-reactor can be increased to have high reaction rates between gas and solids without substantial effects in efficiency [114,115]. Furthermore, in the case that a combined cycle was used –i.e. air-based, CO_2 and steam turbines–, the overall efficiency increases as the fuel-reactor temperature increases [115]. In this sense, the fact that the reduction reaction was exothermic or endothermic has residual effect on the net efficiency [400]. Thus, the fuel-reactor temperature would be determined by an optimized design of the fuel-reactor to minimize the solids inventory rather than to achieve a high efficiency. If low fuel-reactor temperature means low reactivity of oxygen-carrier material, then the solids inventory must be increased to reduce unburnt compounds at the fuel-reactor outlet streams. On the one hand, the thermodynamic advantage of CLC is lost if pressure drops in the CLC system are significantly larger than the conventional combustor [378]. By the other hand, partial oxidation of the fuel can reduce the overall efficiency.

Simulations showed that there is a 0.5% efficiency drop for each 1% decrease in fuel conversion [398], although the advantage of CO_2 separation would still remain [297].

When temperature is constrained by limitation of the oxygen-carrier particles, e.g. with copper materials, top-firing can be an option to further increase the inlet temperature of the gas turbine [378]. However, the CO_2 capture efficiency in this case can decrease by up to 50% [400,401]. Another proposed strategy is to use multi-stage CLC [402]. In this option, reheat is introduced into the air turbine by employing several CLC reactors in series. Fig. 26 shows that using single (SR-CLCCC) or double reheat (DR-CLCCC), i.e. two or three CLC systems, a similar efficiency is obtained when the turbine inlet temperature (TIT) is decreased by about 200 ºC relative to the use of a single CLC reactor system (CLCCC). This solution has shown to be also promising for the use of CLC joined to an IGCC [403].

The efficiency of power generation using natural gas as fuel, and including CO_2 compression, has been calculated to be in the range 52-53 % [115,378,393,402], which is about 3-5 percentage points more efficient that a natural gas combined cycle with the state-of-the-art technology for CO_2 capture [17,397,402]. If coal is used as fuel, a value of 42% in the efficiency of power generation has been reported for a CLC system, which is only 2% lower than the reference case of a pulverized fuel fired power plant without CO_2 capture [297]. Higher energy penalties were found for pre-combustion or oxy-fuel technologies. When CLC is adapted to an IGCC, the overall efficiency calculated was about 44% [295], which is similar to that obtained for available IGCC systems without CO_2 capture [15,403].

Therefore, CLC process has been revealed as a promising technology to produce energy by combustion of fuels with CO_2 capture at low cost and low energy penalty.

7. Future research and prospects

Chemical-Looping Combustion (CLC) and Chemical-Looping Reforming (CLR) have arisen during last years as very promising technologies for power plants and industrial applications with CO_2 capture. The advantages of these technologies come from their inherent CO_2 capture which avoids the energetic penalty of this process in other competing technologies.

Most of the experience has been gained for the use of gaseous fuels with long term tests (up to 1000 h) and operation in continuous plants up to 120 kW_{th}. An important background has been reached in the development of the oxygen-carriers, with the testing of more than 700 different materials mainly based on nickel, copper and iron. The total time of operational experience in continuous units including all fuels and technologies is about 3500 h at the end of 2010.

CLC have possible applications in the oil and gas industry to replace conventional CO_2 capture systems in heaters and boilers. For example, refinery gas and fuel oil are used at the moment to deliver their internal energy requirements. In the case of CLC using refinery gas as fuel, the selection of the solid material could be determined by the effect of minor compounds present in the fuel, i.e. sulfur and light hydrocarbons, on the oxygen-carrier behaviour.

In addition, the oil industry is showing great interest in the use of liquid fuels, such as heavy hydrocarbons, in a CLC system for heat and steam generation. Possible applications can be found in a refinery complex or in the in-situ extraction of heavy oil seams. However, limited studies with oxygen-carriers to process liquid fuels are present in the open literature.

Regarding the intensive use of coal for energy generation, there is an increasing interest in the use of CLC for solid fuels. In fact, this is the more relevant application field of

CLC technology at this moment. Direct combustion of coal in the CLC process is investigated to avoid the oxygen needed in coal gasification for further CLC syngas combustion. In situ gasification of coal in the fuel-reactor using cheap oxygen-carriers as natural minerals or industrial waste products is very promising. This technology needs to improve combustion efficiency in order to reduce the intensity of an oxygen polishing step, and to optimize the carbon stripper design to maximise the CO_2 capture efficiency. The use of the CLOU process for solid fuel combustion using oxygen-carriers that can release oxygen at high temperature is another promising alternative. This process facilitates the implementation of the technology because the carbon stripper is avoided. Relevant advances in this technology are now under way, especially in the development of materials with CLOU properties.

Regarding H_2 production by Chemical-Looping technologies, a-CLR has been demonstrated at scales up to 140 kW avoiding the need of oxygen in the process. The economy of this technology will be highly improved if pressurised reactors are used. The steam reforming integrated with Chemical-Looping Combustion (SR-CLC) has an important potential although needs to be demonstrated at higher scale.

A cornerstone in the successful development of all the CLC technologies is the oxygen-carrier material. It must be considered that cost of the oxygen-carrier is the main added cost of this technology. An economic balance should consider the cost of the raw materials, the cost of particle preparation, the oxygen-carrier lifetime, disposal and environmental costs. Therefore, it is important to have a portfolio of oxygen-carriers, both synthetic and low cost materials, with specific characteristics adequate for different fuels (coal, natural gas, refinery gas, syngas, liquid fuels, etc.) and Chemical-Looping processes (CLC, CLR).

CLC technology has suffered a great advance in different aspects such as material development and process design. Until now, CLC/a-CLR has been demonstrated at scales up to 120-140 kW_{th} with natural gas and the operation of 1 MW_{th} CLC plant with coal is currently underway. The scale up of the technology is a very important issue that needs to be accomplished. Demonstration of the CLC process with different fuels at demo scale and an examination of the impact of high temperatures on materials and engineering components need further consideration. This would result in a more reliable and safer operation. In addition, a life cycle assessment and the environmental impact of the Chemical-Looping technologies are aspects to be analyzed.

At the moment, most of the know-how is based on operation at atmospheric pressure. However, higher energetic efficiency is obtained with pressurized operation by means of the use of combined cycles for electricity generation. This is especially important for the use of gaseous fuels in power industry because of the competition with gas turbine combined cycle plants with conventional CO_2 capture. Therefore, CLC and CLR under pressure is an important challenge for natural gas combustion and reforming. Key elements will be the development of control systems for solid circulation between interconnected fluidized beds.

Given that a price must be paid to implement CO_2 capture from fossil fuel power plants, CLC seems to be an economical alternative in comparison to other proposed approaches. As a consequence, the future of the Chemical-Looping technologies will be very promising during the next years and commercial scale implementation will certainly occur in the medium term.

Acknowledgements

The authors want to thank the European Commission, CO_2 Capture Project (CCP), Spanish National R&D&I Plan, and Gobierno de Aragón for their financial support on projects that helped the research in Chemical-Looping Technologies.

Abbreviations

AEM	Avrami-Erofeev Model
AR	Air-Reactor
ASU	Air Separation Unit
a-CLR	Autothermal Chemical-Looping Reforming
bFB	Batch Fluidized Bed
BFB	Bubbling Fluidized Bed
BHA	Barium-hexaaluminate
CACHET	Carbon Dioxide Capture and Hydrogen Production from Gaseous Fuels
CAM	Citric Acid Method
CCCC	Capture of CO_2 in Coal Combustion
CCP	CO_2 Capture Project
CCS	CO_2 Capture and Storage
CDCL	Coal Direct Chemical Looping
CFB	Circulating Fluidized Bed
CFC	Chlorofluorocarbon
CFD	Computing Fluid Dynamics
CGSM	Changing Grain Size Model
CHALMERS	Chalmers University of Technology
CLC	Chemical-Looping Combustion
CLCCC	CLC-Combined Cycle
CLCs	Solid fuelled Chemical-Looping Combustion
CLCp	Pressurized Chemical-Looping Combustion
CLH	Chemical-Looping Hydrogen
CLOU	Chemical-Looping with Oxygen Uncoupling

CLR	Chemical-Looping Reforming
COP	Coprecipitation
CREC	Chemical Reactor Engineering Centre
C&S	Crush and Sieve
ChRSM	Chemical Reaction at Surface Model
DCFB	Dual Circulating Fluidized Bed
DIS	Dissolution
DP	Deposition-Precipitation
DR-CLCCC	Double reheat CLC-combined cycle
DRM	Diffusion-Reaction Model
DSC	Differential Scanning Calorimeter
ECLAIR	Emission Free Chemical-Looping Coal Combustion Process
ENCAP	Enhanced Capture of CO_2
EXT	Extrusion
EU	European Union
FB	Fluidized Bed
FG	Freeze Granulation
FR	Fuel-Reactor
FxB	Fixed Bed
GHG	Greenhouse Gas
GRACE	Grangemouth Advanced CO_2 Capture Project
GWP	Global Warming Potential
HC	Hydrocarbon
HCD	Homogeneous Conversion Distribution
HIMP	Hot Impregnation

HS	Hydrothermal Synthesis
ICB-CSIC	Institute of Carboquímica (Consejo Superior de Investigaciones Científicas)
ICLC-CC	Integrated Chemical-Looping Combustion Combined Cycle
iG-CLC	In-situ Gasification Chemical-Looping Combustion
IGCC	Integrated Gasification Combined Cycle
IMP	Impregnation
IPCC	Intergovernmental Panel on Climate Change
KIER	Korea Institute of Energy Research
LHC	Light Hydrocarbons
LME	London Metal Exchange
MEA	Methil Ethanolamine
MERIT	Mediator Recirculation Integrating Technology
MM	Mechanical Mixing
MS	Mass Spectrometer
MVM	Modified Volumetric Model
n.a.	not available
n.g.	natural gas
NTNU	Norwegian University of Science and Technology
OC	Oxygen-Carrier
OSD	One Step Decarbonization
OSU	Ohio State University
pFxB	Pressurized Fixed Bed
pTGA	Pressurized Thermogravimetric Analyzer
P	Precipitation

PLM	Power Law Model
PB	Population Balance
PE	Pelletizing by Extrusion
PP	Pelletizing by Pressure
PSA	Pressure Swing Adsorption
PSR	Perfectly Stirred Reactor
RNM	Random Nucleation Model
RTD	Residence Time Distribution
scFB	Semi-continuous Fluidized Bed
SC	Solution Combustion
SCL	Syngas Chemical Looping
SCM	Shrinking Core Model
SCMg	Shrinking Core Model in the grain
SD	Spray Drying
SEM	Scanning Electron Microscope
SETS	Sorbent Energy Transfer System
SEWGS	Sorption Enhanced Wager Gas Shift
SfC	Spot for Cathodes
SF	Spin Flash
SG	Sol-Gel
SINTEF	Foundation for Scientific and Industrial Research
SP	Spray Pyrolysis
SR	Steam Reforming
SR-CLC	Steam Reforming integrated with Chemical-Looping Combustion
SR-CLCCC	Single reheat CLC-combined cycle

TGA	Thermogravimetric Analyzer
TIT	Turbine Inlet Temperature
TITECH	Tokyo Institute of Technology
TPO	Temperature Programmed Oxidation
TPR	Temperature Programmed Reduction
TUD	Darmstadt University of Technology
TUWIEN	Vienna University of Technology
UNFCCC	United Nations Framework Convention on Climate Change
WGS	Water Gas Shift
XRD	X-ray Diffraction
YSZ	Yttria Stabilized Zirconia

Nomenclature

b = stoichiometric coefficient for reaction of gas with the oxygen-carrier, mol solid reactant (mol fuel)$^{-1}$

C_g = gas concentration, mol m^{-3}

C_s = concentration of solid reactant, mol m^{-3}

d = stochiometric factor in the fuel combustion reaction with oxygen, mol O_2 per mol of fuel

d_p = particle diameter, m

D_g = gas diffusion coefficient, m^2 s^{-1}

D_s = coefficient of gas diffusion in the product solid layer, m^2 s^{-1}

E_r = activation energy, kJ mol^{-1}

F_g = shape factor for the grain

F_p = shape factor for the particle

k_g = coefficient gas diffusion in the particle outside, m s^{-1}

k_p = kinetic constant at pressurized conditions, mol^{1-n} m^{3n-2} s^{-1}

k_s = chemical reaction rate constant based on surface area, mol^{1-n} m^{3n-2} s^{-1}

$k_s^{'}$ = chemical reaction rate constant, $(mol\ m^{-3})^{-n}$ s^{-1}

K_{eq} = equilibrium constant

L_p = characteristic length of the particle, m

m = instantaneous mass of the oxygen-carrier, kg

m_o = mass of the fully oxidised oxygen-carrier, kg

m_r = mass of oxygen-carrier in the reduced form, kg

$\dot{m}_O$ = flow of oxygen required for complete combustion of the fuel, (kg O) s^{-1} MW_{th}^{-1}

$\dot{m}_{OC}$ = circulation rate oxygen-carrier as fully oxidized mass based, (kg OC) s^{-1} MW_{th}^{-1}

M_O = atomic weight of oxygen, 16 g mol^{-1}

n = reaction order respect to gas

P = pressure, atm

r_0 = initial grain radius, m

r_1 = grain radius, m

r_2 = un-reacted core radius, m

$(-r_g)$ = reaction rate of gas, mol m^3 s^{-1}

$(-r_s)$ = reaction rate of solid, (g oxygen) $(kg\ OC)^{-1}$ s^{-1}

R = radial position in a spherical particle, m

R_O = oxygen transport capability of the metal oxide

R_{OC} = oxygen transport capacity of the oxygen-carrier

R_p = particle radius, m

s = reaction order respect to solid

S_0 = specific surface area, $m^2\ m^{-3}$

t = time, s

x_{OC} = mass fraction of active material in the fully oxidized oxygen-carrier

X_s = solid conversion

Z = volume expansion factor between solid product and reactant

Greek letters

δ = constant in Eq. (67)

ε = porosity of particle

ΔH_c^0 = standard heat of combustion of the gas fuel, kJ mol^{-1}

ΔX_f = variation of the fuel conversion

ΔX_s = variation of the solid conversion

$\Delta\omega$ = variation in the mass conversion of the oxygen-carrier

ϕ = ratio of oxygen-carrier to fuel

Φ_j = characteristic reactivity of solids in the reactor j

Φ_{th} = Thiele modulus

η_r = effectiveness factor for the reaction rate

ρ_m = molar density of the solid reactant, mol m^{-3}

ρ_{OC} = density of active phase in the oxygen-carrier, kg m^{-3}

ρ_s = solid density, kg m^{-3}

ν = Avrami exponent

τ = reacting time to reach full conversion of solids, s

τ_c = reacting time to reach full conversion of solids if initially it was partially reacted, s

ω = mass based conversion

References

[1] IPCC. Climate Change 2007: Synthesis Report. IPCC; 2007.

[2] IPCC. Climate change and biodiversity. IPCC technical paper V. IPCC; 2002.

[3] IPCC. Climate Change 2001. The third Assesment Report of the Intergovernmental Panel on Climate Change (IPCC). Cambridge, UK: Cambridge University Press; 2001.

[4] Shine KP, Derwent RG, Wuebebles DJ, Morcrette JJ. Radiative forcing of climate. In: JT Houghton, GJ Jenkins, JJ Ephraums, editors. Climate Change: the IPCC scientific assessment, Cambridge, UK: Cambridge University press; 1990. p. 41-68.

[5] Archer D. Fate of fossil fuel CO_2 in geologic time. J Geophys Res 2005;110, C09S05, doi:10.1029/2004JC002625.

[6] Tans P. Trends in carbon dioxide. NOAA/ESRL. Available in http://www.esrl.noaa.gov/gmd/ccgg/trends/.

[7] Kyoto protocol to the United Nations framework convention on climate change. United Nations; 1998.

[8] IPCC. IPCC special report on carbon dioxide capture and storage, Cambridge, UK: Cambridge University Press; 2005.

[9] International Energy Agency (IEA). World energy outlook 2007. IEA Publications; 2007.

[10] International Energy Agency (IEA). Energy technology perspectives: Scenarios and strategies to 2050. París, France: OECD/IEA; 2006.

[11] International Energy Agency (IEA). Energy policies review. The European Union. 2008.

[12] Toftegaard MB, Brix J, Jensen PA, Glarborg P, Jensen AD. Oxy-fuel combustion of solid fuels. Prog Energy Combust Sci 2010;36:581-625.

[13] Thomas DC, Benson SM. Carbon dioxide capture for storage in deep geologic formations– Results from the CO_2 capture project, Oxford, UK: Elsevier; 2005. Vol 1 and 2.

[14] Kerr HR. Capture and separation technology gaps and priority research needs. In: Thomas DC, Benson SM, editors. Carbon dioxide capture for storage in deep geologic formations– Results from the CO_2 capture project, Oxford, UK: Elsevier; 2005, vol. 1, Chapter 38.

[15] Ekström C, Schwendig F, Biede O, Franco F, Haupt G, de Koeijer G, Papapavlou C, Røkke PE. Techno–economic evaluations and benchmarking of pre–combustion CO_2 capture and oxy–fuel processes developed in the european ENCAP project. Energy Procedia 2009;1:4233–40.

[16] Petrakopoulou F, Boyano A, Cabrera M, Tsatsaronis G. Exergoeconomic and exergoenvironmental analyses of a combined cycle power plant with chemical looping technology. Int J Greenhouse Gas Control 2010;5:475-82.

[17] Thambimuthu K, Soltanieh M, Abanades JC. Capture of CO_2. In: Metz B, Davidson O, de Coninck HC, Loos M, Meyer LA, editors. IPCC special report on

carbon dioxide capture and storage, Cambridge. UK: Cambridge University Press; 2005, chapter 3.

[18] Anthony EJ. Solid looping cycles: a new technology for coal conversion. Ind Eng Chem Res 2008;47:1747-54.

[19] Fan & Li. Chemical Looping technology and its fossil energy conversion applications. Ind Eng Chem Res 2010; 49:10200-11.

[20] Fan L-S. Chemical looping systems for fossil energy conversions. Hoboken, New Jersey, USA: John Wiley & Sons, Inc; 2010.

[21] Mizia F, Rossini S, Cozzolino M, Cornaro U, Tlatlik S, Kaus I, Bakken E, Larring Y. One step decarbonization. In: Eide LI, editor. Carbon dioxide capture for storage in deep geological formations– Results from the CO_2 capture project, UK: CPL Press; 2009, vol. 3. Chapter 15.

[22] Lewis, W. K., Gilliland, E. R., Sweeney, W. P. Gasification of carbon metal oxides in a fluidized power bed. Chem Eng Prog 1951; 47: 251-6.

[23] Lewis WK, Gilliland ER. Production of pure carbon dioxide. Patent 2665972; 1954.

[24] Richter HJ, Knoche KF. Reversibility of combustion process. In: Gaggioli RA, editors. Efficiency and Costing, Second law Analysis of Process. ACS Symposium Series 235, American Chemical Society: Washington DC; 1983, pp. 71-85.

[25] Ishida M, Zheng D, Akehata T. Evaluation of a chemical-looping-combustion power-generation system by graphic exergy analysis. Energy 1987;12:147-54.

[26] Ishida M, Jin H. A new advanced power-generation system using chemical-looping combustion. Energy 1994;19:415-22.

[27] Ishida M, Jin H. A novel combustor based on chemical-looping reactions and its reaction kinetics. J Chem Eng Jpn 1994;27:296-301.

[28] Hatanaka T, Matsuda S, Hatano H. A new-concept gas–solid combustion system "MERIT" for high combustion efficiency and low emissions. Proc of the 32nd Intersociety Energy Conversion Eng Conf (IECEC-97). Honolulu, Hawaii; 1997. p. 944-8.

[29] Copeland RJ, Alptekin G, Cesario M, Gebhard S, Gershanovich Y. A novel CO_2 separation system. Proc 8th Int Symp on Transport Phenomena and Dynamics of Rotating Machinery (ISROMAC-8). Honolulu, Hawaii; 2000.

[30] Lyngfelt A, Kronberger B, Adánez J, Morin J-X, Hurst P. The Grace Project. Development of oxygen carrier particles for chemical-looping combustion, design and operation of a 10 kW chemical-looping combustor. Proc 7th Int Conf Greenhouse Gas Control Technology (GHGT-7). Vancouver, Canada; 2004.

[31] Adánez J, García-Labiano F, de Diego LF, Gayán P, Abad A, Celaya J. Development of oxygen carriers for chemical-looping combustion. In: Thomas DC, Benson SM, editors. Carbon dioxide capture for storage in deep geologic formations formations – Results from the CO_2 capture project, Oxford, UK: Elsevier; 2005, vol. 1, Chapter 34.

[32] Adánez J, de Diego LF, García-Labiano F, Gayán P, Abad A. Selection of oxygen carriers for chemical-looping combustion. Energy Fuels 2004;18:371-7.

[33] Lyngfelt A, Thunman H. Construction and 100 h of operational experience of a 10-kW chemical-looping combustor. In: Thomas DC, Benson SM, editors. Carbon dioxide capture for storage in deep geologic formations– Results from the CO_2 capture project, Oxford, UK: Elsevier; 2005, vol. 1, Chapter 36.

[34] Morin JX, Béal C. Chemical looping combustion of refinery fuel gas with CO_2 capture. In: Thomas DC, Benson SM, editors. Carbon dioxide capture for storage in deep geologic formations– Results from the CO_2 capture project, Oxford, UK: Elsevier; 2005, vol. 1, Chapter 37.

[35] Mattisson T, García-Labiano F, Kronberger B, Lyngfelt A, Adánez J, Hofbauer H. CO_2 capture from coal combustion using chemical-looping combustion. Proc 8th Int Conf Greenhouse Gas Control Technologies (GHGT-8). Trondheim, Norway; 2006.

[36] Mattisson T, García-Labiano F, Kronberger B, Lyngfelt A, Adánez J, Hofbauer H. Chemical-looping combustion using syngas as fuel. Int J Greenhouse Gas Control 2007;1:158-69.

[37] Ryu HJ, Jin G-T, Yi C-K. Demonstration of inherent CO_2 separation and no NO_x emission in a 50 kW chemical-looping combustor: Continuous reduction and oxidation experiment. Proc 7th Int Conf Greenhouse Gas Control Technology (GHGT-7). Vancouver, Canada; 2004.

[38] Ryu H-J, Jin G-T, Bae D-H, Yi C-K. Continuous operation of a 50 kWth chemical-looping combustor: long-term operation with Ni- and Co-based oxygen carrier particles. Proc 5th China-Korea Joint Workshop on Clean Energy Technology, Qingdao University, China; 2004. p. 221-30.

[39] Adánez J, Gayán P, Celaya J, de Diego LF, García-Labiano F, Abad A. Chemical looping combustion in a 10 kW prototype using a CuO/Al_2O_3 oxygen carrier: effect of operating conditions on methane combustion. Ind Eng Chem Res 2006;45:6075-80.

[40] de Diego LF, García-Labiano F, Gayán P, Celaya J, Palacios JM, Adánez J. Operation of a 10 kWth chemical-looping combustor during 200 h with a CuO-Al_2O_3 oxygen carrier. Fuel 2007;86:1036-45.

[41] Eide LI. Carbon dioxide capture for storage in deep geological formations– Results from the CO_2 capture project, UK: CPL Press; 2009, vol. 3.

[42] Pröll T, Kolbitsch P, Bolhàr-Nordenkampf J, Hofbauer H. Demonstration of chemical-looping combustion at relevant operating conditions. In: Eide LI, editor. Carbon dioxide capture for storage in deep geological formations– Results from the CO_2 capture project, UK: CPL Press; 2009, vol. 3. Chapter 7.

[43] Linderholm C, Lyngfelt A, Béal C, Trikkel A, Kuusink R, Jerndal E, Mattisson T. Chemical-looping combustion with natural gas using spray-dried NiO-based oxygen carriers. In: Eide LI, editor. Carbon dioxide capture for storage in deep geological formations– Results from the CO_2 capture project, UK: CPL Press; 2009, vol. 3. Chapter 6.

[44] Adánez J, García-Labiano F, Abad A, de Diego LF, Gayán P, Dueso C. NiO-based oxygen carriers impregnated on Al_2O_3-based materials for chemical-looping combustion. In: Eide LI, editor. Carbon dioxide capture for storage in deep geological formations– Results from the CO_2 capture project, UK: CPL Press; 2009, vol. 3. Chapter 8.

[45] García-Labiano F, de Diego LF, Gayán P, Adánez J, Abad A, Dueso C. Effect of fuel gas composition in chemical-looping combustion with Ni-based oxygen carriers. 1. Fate of sulphur. Ind Eng Chem Res 2009;48:2499-508.

[46] Adánez J, Dueso C, de Diego LF, García-Labiano F, Gayán P, Abad A. Effect of fuel gas composition in chemical-looping combustion with Ni-based oxygen carriers. 2. Fate of light hydrocarbons. Ind Eng Chem Res 2009;48:2509-18.

[47] Li F, Zeng L, Ramkumar S, Sridhar D, Iyer M, Fan L-S. Chemical looping gasification using gaseous fuels. In: Fan L-S, editor. Chemical looping systems for fossil energy conversions. Hoboken, New Jersey, USA: John Wiley & Sons, Inc; 2010. Chapter 4.

[48] Lyon RK, Cole JA. Unmixed combustion: an alternative to fire. Combust Flame 2000;121:249-61.

[49] Beavis R. Introduction to Cachet. A pre-combustion technology, development program, co-funded by the EU and CCP. In: Eide LI, editor. Carbon dioxide capture for storage in deep geological formations– Results from the CO_2 capture project, UK: CPL Press; 2009, vol. 3. Chapter 10.

[50] Rydén M, Lyngfelt A, Schulman A, de Diego LF, Adánez J, Ortiz M, Pröll T, Bolhàr-Nordenkampf J, Kolbitsch P. Developing chemical looping steam reforming and chemical looping autothermal reforming. In: Eide LI, editor. Carbon dioxide capture for storage in deep geological formations– Results from the CO_2 capture project, UK: CPL Press; 2009, vol. 3. Chapter 14.

[51] Rydén M, Lyngfelt A. Using steam reforming to produce hydrogen with carbon dioxide capture by chemical-looping combustion. Int J of Hydrogen Energy 2006;31:1271-83.

[52] Fang H, Haibin L, Zengli Z. Advancements in development of chemical looping combustion: A review. Int J of Chem Eng 2009. doi:10.1155/2009/710515.

[53] Sanfilippo D, Mizia F, Malandrino A, Rossini S. Process for the production of hydrogen and the coproduction of carbon dioxide. Patent US2005/0232859.

[54] Berguerand N, Lyngfelt A. Design and operation of a 10 kW_{th} chemical-looping combustor for solid fuels - Testing with South African coal. Fuel 2008;87:2713-26.

[55] Berguerand N, Lyngfelt A. The use of petroleum coke as fuel in a 10 kW chemical-looping combustor. Int J Greenhouse Gas Control 2008;2:169-79.

[56] Beal C, Epple B, Lyngfelt A, Adánez J, Larring Y, Guillemont A, Anheden M. Development of metal oxides chemical looping process for coal–fired power plants. Proc 1st Int Conf on Chemical Looping. Lyon, France; 2010.

[57] Mattisson T, Lyngfelt A, Leion H. Chemical-looping with oxygen uncoupling for combustion of solid fuels. Int J Greenhouse Gas Control 2009;3:11-9.

[58] Coal direct chemical looping retrofit to pulverized coal power plants for in-situ CO_2 capture. Ohio State University. NETL project NT005289.

[59] ALSTOM´s chemical looping combustion prototype for CO_2 capture from existing pulverized coal-fired power plants. Alstom Power. NETL project NT0005286.

[60] Development of computational approaches for simulation and advanced controls for hybrid combustion-gasification chemical looping. Alstom Power. NETL project NT43095.

[61] Neuschaefer CH, Lou X. Integrated controls design optimization. Alstom Technology Ltd. Patent WO 2009/114309; 2009.

[62] Chiu JH, Andrus HE, Liljedahl GN, Thibeault PR. System for hot solids combustion and gasification. Alstom Technology Ltd. Patent WO 2010/014938; 2010.

[63] Dennis J, Hayhurst A, Scott S. Solid fuel combustion method and apparatus. Cambridge Enterprise Limited. Patent WO 2007/107730; 2007.

[64] Thomas TJ, Fan L, Gupta P, Velázquez-Vargas LG. Combustion looping using composite oxygen carriers. Patent US 2005/0175533; 2005.

[65] Adánez J, de Diego LF, García-Labiano F, Gayán P, Abad A. NiO/Al_2O_3 oxygen carrier, method for obtaining same and use thereof. CSIC. Patent WO 2009/022046 ; 2009.

[66] Adánez J, de Diego LF, García-Labiano F, Gayán P, Abad A. Solid NiO/Al_2O_3 oxygen carrier that is useful for methane reforming, method for producing same and applications thereof. CSIC. Patent WO 2009/101233; 2009.

[67] Fan Z, Hack H, Robertson A, Seltzer A. Method of and a plant for combusting carbonaceous fuel by using a solid oxygen carrier. Foster Wheeler Energy Corporation. Patent WO 2009/013647; 2009.

[68] Becue T, Marchand K, Lambert A, Lebas E. Redox active mass for a chemical looping combustion process. IFP. Patent US 2007/0049489; 2007.

[69] Lambert A. Use of a redox mass having a spinel type structure for a looping redox process. IFP. Patent WO 2009/074729; 2009.

[70] Forret A, Pelletant W, Hoteit A. Chemical-looping process for the combustion of heavy liquid hydrocarbon fractions. IFP. Patent WO 2009/138588; 2009.

[71] Lambert A, Gauthier T. Oxidation-reduction active mass and chemical-loop combustion method. IFP. Patent WO 2009/138595; 2009.

[72] Gauthier T, Hoteit A. Method and installation for chemical looping combustion with independent control of the circulation of solids. IFP. Patent WO 2011/007055; 2011.

[73] Cichanowicz JE, Muzio LJ. Rotary regenerative chemical-looping combustion. Patent US 2009/0265978; 2009.

[74] Dahl IM, Blom R. Chemical looping combustion. Sinvent AS. Patent WO 2008/044942; 2008.

[75] Ishida M, Jin H. Chemical-looping combustion power generation plant system. Tokyo Electric Power Co. Patent US 5447024; 1995.

[76] Pröll T, Kolbitsch P, Bolhàr-Nordenkampf J, Hofbauer H. Fluidized-bed reactor system. Technische Universität Wien. Patent WO 2009/021258; 2009.

[77] Pröll T, Kolbitsch P. The present invention relates to a method for producing carbon dioxide and hydrogen from hydrocarbons using chemical looping reforming (CLR). Technische Universität Wien. Patent WO 2010/0099555; 2010.

[78] Wolf J. CO_2 mitigation in advanced power cycles – chemical looping combustion and steam-based gasification. PhD Thesis. KTH- Royal Institute of technology, Stockholm, Sweden; 2004.

[79] Brandvoll Ø. Chemical looping combustion—fuel conversion with inherent CO_2 capture. PhD thesis. Norwegian University of Science and Technology (NTNU), Trondheim, Norway; 2005.

[80] Cho P. Development and characterization of oxygen-carrier materials for chemical-looping combustion. PhD Thesis. Chalmers University of Technology, Göteborg, Sweden; 2005.

[81] Johansson E. Fluidized-Bed reactor systems for chemical-looping combustion with inherent separation of CO_2. PhD Thesis. Chalmers University of Technology, Göteborg, Sweden; 2005.

[82] Kronberger B. Modelling analysis of fluidised bed reactor systems for chemical-looping combustion. PhD Thesis. Vienna University of Technology, Vienna, Austria; 2005.

[83] Luisser M. Chemical looping combustion – Simulation of the fuel oxidation reactor. PhD Thesis. Vienna University of Technology, Vienna, Austria; 2006.

[84] Naqvi R. Analysis of natural gas-fired power cycles with chemical looping combustion for CO_2 capture. PhD Thesis. Norwegian University of Science and Technology (NTNU), Trondheim, Norway; 2006.

[85] Celaya J. Combustión de CH_4 en lecho fluidizado con separación inherente de CO_2 por medio de transportadores sólidos de oxígeno de base cobre. PhD Thesis. Universidad de Zaragoza, Zaragoza, Spain; 2007.

[86] Johansson M. Screening of oxygen-carrier particles based on iron-, manganese-copper- and nickel oxides for use in chemical-looping technologies. PhD Thesis. Chalmers University of Technology, Göteborg, Sweden; 2007.

[87] Zafar Q. Oxygen carrier materials for chemical-looping technologies. PhD Thesis. Chalmers University of Technology, Göteborg, Sweden; 2007.

[88] Leion H. Capture of CO_2 from solid fuels using chemical-looping combustion and chemical-looping with oxygen uncoupling. PhD Thesis. Chalmers University of Technology, Göteborg, Sweden; 2008.

[89] Rydén M. Hydrogen production with fossil fuels with carbon dioxide capture, using chemical-looping technologies. PhD Thesis. Chalmers University of Technology, Göteborg, Sweden; 2008.

[90] Bolhàr-Nordenkampf J. Chemical looping for synthesis gas and power generation with CO_2 capture - pilot plant study and process modelling. PhD Thesis. Vienna University of Technology, Vienna, Austria; 2009.

[91] Berguerand N. Design and operation of a 10 kWth chemical-looping combustor for solid fuels. PhD Thesis. Chalmers University of Technology, Göteborg, Sweden; 2009.

[92] Kolbitsch P. Chemical looping combustion for 100% carbon capture - Design, operation and modelling of a 120 kW pilot rig. PhD Thesis, Vienna University of Technology, Vienna, Austria; 2009.

[93] Jerndal E. Investigation of nickel- and iron-based oxygen carriers for chemical-looping combustion. PhD Thesis. Chalmers University of Technology, Göteborg, Sweden; 2010.

[94] Dueso C. Chemical looping combustion of gaseous fuels with NiO-based oxygen carriers. PhD Thesis. University of Zaragoza, Zaragoza, Spain; 2011.

[95] Forero CR. Combustión de gas con captura de CO_2 mediante transportadores sólidos de oxígeno basados en CuO. PhD Thesis. University of Zaragoza, Zaragoza, Spain; 2011.

[96] Ortiz M. Reformado de metano con transportadores sólidos de oxígeno. "Chemical looping reforming". PhD Thesis. Universidad de Zaragoza, Zaragoza, Spain; 2011.

[97] Linderholm . CO_2 capture using Chemical-Looping Combustion – Operational experience with gaseous and solid fuels. PhD Thesis. Chalmers University of Technology, Göteborg, Sweden; 2011.

[98] Lyngfelt A, Johansson M, Mattisson T. Chemical-looping combustion- Status of development. Proc 9th Int Conf on circulating fluidized beds (CFB-9). Hamburg: Germany; 2008.

[99] Hossain MM, de Lasa HI. Chemical-looping combustion (CLC) for inherent CO_2 separations-a review. Chem Eng Sci 2008;63:4433-51.

[100] Brandvoll ϕ. Chemical looping combustion. Saarbrücken, Germany: Lambert Academic Publishing; 2010.

[101] Lyngfelt A. Oxygen carriers for chemical looping combustion - 4000 h of operational experience. Oil & Gas Sci Technol 2011;66:161-72.

[102] Lyngfelt A, Leckner B, Mattisson T. A fluidized-bed combustion process with inherent CO_2 separation, application of chemical-looping combustion. Chem Eng Sci 2001;56:3101-13.

[103] Kronberger B, Johansson E, Löffler G, Mattisson T, Lyngfelt A, Hofbauer H. A two-compartment fluidized bed reactor for CO_2 capture by chemical-looping combustion. Chem Eng Technol 2004;27:1318-26.

[104] Kronberger B, Lyngfelt A, Löffler G, Hofbauer H. Design and fluid dynamic analysis of a bench-scale combustion system with CO_2 separation-chemical-looping combustion. Ind Eng Chem Res 2005;44:546-56.

[105] Kolbitsch P, Pröll T, Bolhàr-Nordenkampf J, Hofbauer H. Design of a chemical looping combustor using a dual circulating fluidized bed reactor system. Chem Eng Technol 2009;32:1-7.

[106] Johansson E, Lyngfelt A, Mattisson T, Johsson F. Gas leakage measurements in a cold model of an interconnected fluidized bed for chemical-looping combustion. Powder Technol 2003;134:210-7.

[107] Ryu H-J, Jo S-H, Park Y, Bae DH, Kim S. Long term operation experience in a 50 kWth chemical looping combustor using natural gas and syngas as fuels. Proc 1st Int Conf on Chemical Looping. Lyon, France; 2010.

[108] Son SR, Kim SD. Chemical-looping combustion with NiO and Fe_2O_3 in a thermobalance and circulating fluidized bed reactor with double loops. Ind Eng Chem Res 2006;45:2689-96.

[109] Shen L, Wu J, Xiao J, Song Q, Xiao R. Chemical-looping combustion of biomass in a 10 kW reactor with iron oxide as an oxygen carrier. Energy Fuels 2009;23:2498-505.

[110] Rifflart S, Hoteit A, Yazdanpanah M, Pelletant W, Surla K. Construction and operation of a 10kW CLC unit with circulation configuration enabling independent solid flow control. Proc 10th Int Conf Greenhouse Gas Technology (GHGT-10). Amsterdam, Netherlands; 2010.

[111] Bischi A, Langørgen Ø, Saanum I, Bakken J, Seljeskog M, Bysveen M, Morin, J-X, Bolland O. Design study of a 150 kW_{th} double loop circulating fluidized bed reactor system for chemical looping combustion with focus on industrial applicability and pressurization. Int J Greenhouse Gas Control 2011;5:467-74.

[112] Li F, Fan L. Clean coal conversion processes-progress and challenges. Energy Environ Sci 2008;1:248-67.

[113] Schwebel GL, Wiedenmann F, Krumm W. Reduction performance of ilmenite and hematite oxygen carriers in the context of a new CLC reactor concept. Proc 1st Int Conf on Chemical Looping. Lyon, France; 2010.

[114] Brandvoll O, Bolland O. Inherent CO_2 capture using chemical looping combustion in a natural gas fired power cycle. J of Eng for Gas Turbines and Power - Transactions of the ASME 2004;126:316-21.

[115] Wolf J, Anheden M, Yan J. Performance analysis of combined cycles with chemical looping combustion for CO_2 capture. Proc 18th Annual Int Pittsburg Coal Conf. New Castle, New South Wales, Australia; 2001, pp. 1122–1139.

[116] Noorman S, van Sint Annaland M, Kuipers H. Packed bed reactor technology for chemical-looping combustion. Ind Eng Chem Res 2007;46:4212-20.

[117] Noorman S, van Sint Annaland M, Kuipers JAM. Experimental validation of packed bed chemical-looping combustion. Chem Eng Sci 2010;65:92-7.

[118] Scott AA, Dennis JS, Hayhurst AN, Brown T. In situ gasification of a solid fuel and CO_2 separation using chemical looping. AIChE J 2006;52:3325-8.

[119] Brown TA, Dennis JS, Scott SA, Davidson JF, Hayhurst AN. Gasification and chemical looping combustion of a lignite char in a fluidized bed of iron oxide. Energy Fuels 2010;24:3034-48.

[120] Dahl I, Bakken E, Larring Y, Spejelkavik A, Hakonsem S, Blom R. On the development of novel reactor concepts for chemical looping combustion. Energy Procedia 2009;1:1513-9.

[121] Hakonsem S, Dahl I, Stange M, Spejelkavik A, Blom R. On the development of novel reactor concepts for chemical looping combustion-part 2. Proc 1st Int Conf on Chemical Looping. Lyon, France; 2010.

[122] Jerndal E, Mattisson T, Lyngfelt A. Thermal analysis of chemical-looping combustion. Chem Eng Res Des 2006;84:795-806.

[123] Leion H, Mattissson T, Lyngfelt A. Use of ores and industrial products as oxygen carriers in chemical-looping combustion. Energy Fuels 2009;23:2307-15.

[124] Abad A, Adánez J, García-Labiano F, de Diego LF, Gayán P, Celaya, J. Mapping of the range of operational conditions for Cu-, Fe- and Ni-based oxygen carriers in chemical-looping combustion. Chem Eng Sci 2007;62:533-49.

[125] Wolf J, Yan J. Parametric study of chemical looping combustion for tri-generation of hydrogen, heat, and electrical power with CO_2 capture. Int J Energy Res 2005;29:739-53.

[126] García-Labiano F, de Diego LF, Adánez J, Abad A, Gayán P. Reduction and oxidation kinetics of a copper-based oxygen carrier prepared by impregnation for chemical-looping combustion. Ind Eng Chem Res 2004;43:8168-77.

[127] Kronberger B, Löffler G, Hofbauer H. Simulation of mass and energy balances of a chemical-looping combustion system. Clean Air 2005;6:1-14.

[128] Abad A, Adánez J, de Diego LF, Gayán P, García-Labiano F. Design of chemical–looping combustion systems using syngas — Application of Cu–, Fe– and Ni–based oxygen carriers' reactivity. Proc Int Conf on Coal Sci and Technol (ICCS&T). Nottingham, UK; 2007.

[129] Kuusik R, Trikkel A, Lyngfelt A, Mattisson T. High temperature behaviour of NiO-based oxygen carriers for chemical looping combustion. Energy Procedia 2009;1:3885-92.

[130] Abad A, Mattisson T, Lyngfelt A, Rydén M. Chemical-looping combustion in a 300 W continuously operating reactor system using a manganese-based oxygen carrier. Fuel 2006;85:1174-85.

[131] Abad A, Mattisson T, Lyngfelt A, Johansson M The use of iron oxide as oxygen carrier in a chemical-looping reactor. Fuel 2007;86:1021-35.

[132] Bolhàr-Nordenkampf J, Pröll T, Kolbitsch P, Hofbauer H. Comprehensive modeling tool for chemical looping based processes. Chem Eng Technol 2009;32:410–7.

[133] de Diego LF, García-Labiano F, Adánez J, Gayán P, Abad A, Corbella BM, Palacios JM. Development of Cu-based oxygen carriers for chemical-looping combustion. Fuel 2004;83:1749-57.

[134] Ishida M, Jin H. A novel chemical-looping combustor without NO_x formation. Ind Eng Chem Res 1996;35:2469-72.

[135] Mineral commodity summaries 2010: U.S. Geological Survey. ISBN 978–1–4113–2666–8.

[136] García-Labiano F, Gayán P, Adánez J, de Diego LF, Forero CR. Solid waste management of a chemical-looping combustion plant using Cu-based oxygen carriers. Environ Sci Technol 2007;41:5882-7.

[137] ASTM D5757-95: Standard test method for determination of attrition and abrasion of powdered catalysts by air jets; ASTM: Philadelphia, PA, 1995.

[138] Gayán P, Forero CR, Abad A, de Diego LF, García-Labiano F, Adánez J. Effect of support on the behaviour of Cu-based oxygen carriers during long-term CLC operation at temperatures above 1073 K. Energy Fuels 2011;25:1316-26.

[139] Shulman A, Linderholm C, Mattisson T, Lyngfelt A. High reactivity and mechanical durability of $NiO/NiAl_2O_4$ and $NiO/NiAl_2O_4/MgAl_2O_4$ oxygen carrier particles used for over 1000 hours in a 10 kW CLC reactor. Ind Eng Chem Res, 2009;48:7400-5.

[140] Linderholm C, Abad A, Mattisson T, Lyngfelt A. 160 h of chemical-looping combustion in a 10 kW reactor system with a NiO-based oxygen-carrier. Int J Greenhouse Gas Control 2008;2:520-30.

[141] Adánez J, Dueso C, de Diego LF, García-Labiano F, Gayán P, Abad A. Methane combustion in a 500 Wth chemical-looping combustion system using an impregnated Ni-based oxygen carrier. Energy Fuels 2009;23:130-42.

[142] Forero CR, Gayán P, García-Labiano F, de Diego LF, Abad A, Adánez J. CuO-High temperature behaviour of a $CuO/\gamma Al_2O_3$ oxygen carrier for chemical-looping combustion. Int J Greenhouse Gas Control 2011;5:659-67.

[143] Wu J, Shen L, Hao J, Gu H. Chemical looping combustion of coal in a 1 kW_{th} reactor with iron ore as an oxygen carrier. Proc 1st Int Conf on Chemical Looping. Lyon, France; 2010.

[144] Jin H, Okamoto T, Ishida M. Development of a novel chemical-looping combustion: synthesis of a looping material with a double metal oxide of CoO-NiO. Energy Fuels 1998;12:1272-7.

[145] Adánez J, García-Labiano F, de Diego LF, Gayán P, Celaya J, Abad A. Characterization of oxygen carriers for chemical–looping combustion. Proc 7th Int Conf Greenhouse Gas Control Technology (GHGT-7). Vancouver, Canada; 2004.

[146] Adánez J, García-Labiano F, de Diego LF, Gayán P, Celaya J, Abad A. Nickel-copper oxygen carriers to reach zero CO and H_2 emissions in chemical-looping combustion. Ind Eng Chem Res 2006;45:2617-25.

[147] Mattisson T, Johansson M, Lyngfelt A. The use of NiO as an oxygen carrier in chemical-looping combustion. Fuel 2006;85:736-47.

[148] Mattisson T, Johansson M, Jerndal E, Lyngfelt A. The reaction of $NiO/NiAl_2O_4$ particles with alternating methane and oxygen. Can J Chem Eng 2008;86:756-67.

[149] Jerndal E, Mattisson T, Lyngfelt A. Investigation of different $NiO/NiAl_2O_4$ particles as oxygen carriers for chemical-looping combustion. Energy Fuels 2009;23:665-76.

[150] Gayán P, de Diego LF, García-Labiano F, Adánez J, Abad A, Dueso C. Effect of support on reactivity and selectivity of Ni-based oxygen carriers for chemical-looping combustion. Fuel 2008;87:2641-50.

[151] Gayán P, Dueso C, Abad A, Adánez J, de Diego LF, García-Labiano F. NiO/Al_2O_3 oxygen carriers for chemical-looping combustion prepared by impregnation and deposition-precipitation methods. Fuel 2009;88:1016-23.

[152] Jin H, Okamoto T, Ishida M. Development of a novel chemical-looping combustion: synthesis of a solid looping material of $NiO/NiAl_2O_4$. Ind Eng Chem Res 1999;38:126-32.

[153] Ryu HJ, Bae DH, Jin GT. Effect of temperature on reduction reactivity of oxygen carrier particles in a fixed bed chemical-looping combustor. Korean J Chem Eng 2003;20:960-6.

[154] Cho P, Mattisson T, Lyngfelt A. Carbon formation on nickel and iron oxide-containing oxygen carriers for chemical-looping combustion. Ind Eng Chem Res 2005;44:668-76.

[155] Corbella BM, de Diego LF, García-Labiano F, Adánez J, Palacios JM. Characterization study and five-cycle tests in a fixed-bed reactor of titania supported nickel oxide as oxygen carriers for the chemical-looping combustion of methane. Environ Sci Technol 2005;39:5796-803.

[156] Corbella BM, de Diego LF, García-Labiano F, Adánez J, Palacios JM, Performance in a fixed-bed reactor of titania-supported nickel oxide as oxygen Carriers for the chemical-looping combustion of methane in multicycle tests. Ind Eng Chem Res 2006;45:157-65.

[157] Johansson M, Mattisson T, Lyngfelt A, Abad A. Using continuous and pulse experiments to compare two promising nickel-based oxygen carriers for use in chemical-looping technologies. Fuel 2008;87:988-1001.

[158] Rydén M, Lyngfelt A, Mattisson T, Chen D, Holmen A, Bjørgum E. Novel oxygen-carrier materials for chemical-looping combustion and chemical-looping reforming, $La_xSr_{1-x}Fe_yCo_{1-y}O_{3-\delta}$ perovskites and mixed-metal oxides of NiO, Fe_2O_3 and Mn_3O_4. Int J Greenhouse Gas Control 2008;2:21-36.

[159] Ishida M, Jin H., Okamoto T. Kinetic behaviour of solid particle in chemical-looping combustion: suppressing carbon deposition in reduction. Energy Fuels 1998;12:223-9.

[160] Jin H, Ishida M. Reactivity study on natural-gas-fueled chemical-looping combustion by a fixed-bed reactor. Ind Eng Chem Res 2002;41:4004-7.

[161] Hoteit A, Chandel MK, Delabarre A. Nickel- and copper-based oxygen carriers for chemical looping combustion. Chem Eng Technol 2009;32:443-9.

[162] Chandel MK, Hoteit A, Delebarre A. Experimental investigation of some metal oxides for chemical looping combustion in a fluidized bed reactor. Fuel 2009;88: 898-908.

[163] Chiron F-X, Patience GS, Rifflart S. Kinetic mechanism derived through dosing reactants over NiO, Ni and Ni-C. Proc 1st Int Conf on Chemical Looping. Lyon, France; 2010.

[164] Iliuta I, Tahoces R, Patience GS, Rifflart S, Luck F. Chemical–looping combustion process: kinetics and mathematical modeling. AIChE J 2010;56:1063–79.

[165] Ryu HJ, Lim NY, Bae DH, Jin G-T. Carbon deposition characteristics and regenerative ability of oxygen carrier particles for chemical-looping combustion. Korean J Chem Eng 2003;20:157-62.

[166] de Diego LF, Gayán P, García-Labiano F, Celaya J, Abad A, Adánez J. Impregnated CuO/Al_2O_3 oxygen carriers for chemical-looping combustion: avoiding fluidized bed agglomeration. Energy Fuels 2005;19:1850-6.

[167] Kolbitsch P, Bolhàr-Nordenkampf J, Pröll T, Hofbauer H. Comparison of two Ni-based oxygen carriers for chemical looping combustion of natural gas in 140 kW continuous looping operation. Ind Eng Chem Res 2009;48:5542-7.

[168] Linderholm C, Mattisson T, Lyngfelt A. Long-term integrity testing of spray-dried particles in a 10 kW chemical-looping combustor using natural gas as fuel. Fuel 2009;88:2083-96.

[169] Dueso C, García-Labiano F, Adánez J, de Diego LF, Gayán P, Abad A. Syngas combustion in a chemical-looping combustion system using an impregnated Ni-based oxygen carrier. Fuel 2009;88:2357-64.

[170] de Diego LF, Ortiz M, García-Labiano F, Adánez J, Abad A, Gayán P. Hydrogen production by chemical-looping reforming in a circulating fluidized bed reactor using Ni-based oxygen Carriers. J Power Sources 2009;192:27-34.

[171] Cho P, Mattisson T, Lyngfelt A. Defluidization conditions for a fluidized bed of iron oxide-, nickel oxide-, and manganese oxide-containing oxygen carriers for chemical-looping combustion. Ind Eng Chem Res 2006;45:968-77.

[172] Johansson M, Mattisson T, Lyngfelt A. Comparison of oxygen carriers for chemical-looping combustion. Thermal Sci 2006;10:93-107.

[173] Mattisson T, Johansson M, Lyngfelt A. Multicycle reduction and oxidation of different types of iron oxide particles- Application to chemical-looping combustion. Energy Fuels 2004;18:628-37.

[174] Leion H, Lyngfelt A, Johansson M, Jerndal E, Mattisson T. The use of ilmenite as an oxygen carrier in chemical-looping combustion. Chem Eng Res Des 2008;86:1017-26.

[175] Cuadrat A, Abad A, Adánez J, de Diego LF, García-Labiano F, Gayán P. Behaviour of ilmenite as oxygen carrier in chemical–looping combustion. Proc 4th Int Conf on Clean Coal Technologies (CCT2009). Dresden, Germany; 2009.

[176] Mattisson T, Järdnäs A, Lyngfelt A. Reactivity of some metal oxides supported on alumina with alternating methane and oxygen-Application for chemical-looping combustion. Energy Fuels 2003;17:643-51.

[177] Copeland RJ, Alptekin G, Cesario M, Gershanovich Y. Sorbent energy transfer system (SETS) for CO_2 separation with high efficiency. Proc 27th Int Technical Conf on Coal Utilization & Fuel Systems. Clearwater, Florida, USA; March 4-7, 2002. (Vol. 2) pp. 719-29.

[178] Cho P, Mattisson T, Lyngfelt A. Comparison of iron-, nickel-, copper- and manganese-based oxygen carriers for chemical-looping combustion. Fuel 2004;83: 1215-25.

[179] Chuang SY, Dennis JS, Hayhurst AN, Scott SA. Development and performance of Cu-based oxygen carriers for chemical-looping combustion. Combust Flame 2008;154:109-121.

[180] Chuang SY, Dennis JS, Hayhurst AN, Scott SA. Kinetics of the chemical looping oxidation of CO by a co-precipitated mixture of CuO and Al_2O_3. Proc of the Combust Institute 2009;32:2633-40.

[181] Jerndal E, Mattisson T, Thijs I, Snijkers F, Lyngfelt A. Investigation of $NiO/NiAl_2O_4$ oxygen carriers for chemical-looping combustion produced by spray-drying. Int J Greenhouse Gas Control 2010;4:23-35.

[182] Rydén M, Lyngfelt A, Mattisson T. Chemical-looping combustion and chemical-looping reforming in a circulating fluidized-bed reactor using Ni-based oxygen carriers. Energy Fuels 2008;22:2585-97.

[183] Linderholm C, Jerndal E, Mattisson T, Lyngfelt A. Investigation of NiO-based mixed oxides in a 300-W chemical-looping combustor. Chem Eng Res Des 2010;88:661-72.

[184] Shen L, Zheng M, Xiao J, Xiao R. Sulfur behavior in chemical looping combustion with NiO/Al_2O_3 oxygen carrier. Combust Flame 2010;157:853-63.

[185] Shen L, Wu J, Gao Z, Xiao J. Characterization of chemical looping combustion of coal in a 1 kW_{th} reactor with a nickel-based oxygen carrier. Combust Flame 2010;157:934-42.

[186] Shen L, Wu J, Gao Z, Xiao J. Reactivity deterioration of NiO/Al_2O_3 oxygen carrier for chemical looping combustion of coal in a 10 kW_{th} reactor. Combust Flame 2009;156:1377-85.

[187] Shen L, Wu J, Xiao J. Experiments on chemical looping combustion of coal with a NiO based oxygen carrier. Combust Flame 2009;156:721-8.

[188] Johansson E, Mattisson T, Lyngfelt A, Thunman H. Combustion of syngas and natural gas in a 300 W chemical-looping combustor. Chem Eng Res Des 2006;84: 819-27.

[189] Johansson M, Mattisson T, Lyngfelt A. Use of $NiO/NiAl_2O_4$ particles in a 10 kW chemical-looping combustor. Ind Eng Chem Res 2006;45:5911-9.

[190] Ishida M, Yamamoto M, Ohba T. Experimental results of chemical-looping combustion with $NiO/NiAl_2O_4$ particle circulation at 1200 ºC. Energy Convers Mgmt 2002;43:1469-78.

[191] Kolbitsch P, Pröll T, Bolhar-Nordemkampf J, Hofbauer H. Operating experience with chemical looping combustion in a 120 kW dual circulating fluidized bed (DCFB) unit. Int J Greenhouse Gas Control 2010;4:180-5.

[192] Kolbitsch P, Pröll T, Bolhàr-Nordenkampf J, Hofbauer H. Characterization of chemical looping pilot plant performance via experimental determination of solid conversion. Energy Fuels 2009;23:1450-5.

[193] Bolhàr-Nordenkampf J, Pröll T, Kolbitsch P, Hofbauer H. Performance of a NiO-based oxygen carrier for chemical looping combustion and reforming in a 120 kW unit. Energy Procedia 2009;1:19-25.

[194] Pröll T, Kolbitsch P, Bolhar-Nordemkampf J, Hofbauer H. A novel dual circulating fluidized bed system for chemical looping processes. AIChE J 2009;55:3255-66.

[195] Pröll T, Bolhàr-Nordenkampf J, Kolbitsch P, Hofbauer H. Syngas and a separate nitrogen/argon stream via chemical looping reforming- A 140 kW pilot plant study. Fuel 2010;89:1249-56.

[196] Johansson E, Mattisson T, Lyngfelt A, Thunman H. A 300 W laboratory reactor system for chemical-looping combustion with particle circulation. Fuel 2006;85:1428-38.

[197] Rydén M, Lyngfelt A, Mattisson T. Synthesis gas generation by chemical-looping reforming in a continuously operating laboratory reactor. Fuel 2006;85:1631-41.

[198] Rydén M, Johansson M, Lyngfelt A, Mattisson T. NiO supported on $Mg\text{-}ZrO_2$ as oxygen carrier for chemical-looping combustion and chemical-looping reforming. Energy Environ Sci 2009;2:970-81.

[199] Ryu H-J, Park J, Lee S-Y, Park M-H. Effect of CO_2 concentration on reduction reactivity of oxygen carriers. Proc 1st Int Conf on Chemical Looping. Lyon, France; 2010.

[200] Abad A, Adánez J, García-Labiano F, de Diego LF, Gayán P. Modeling of the chemical-looping combustion of methane using a Cu-based oxygen carrier. Combust Flame 2010;157:602-15.

[201] Forero CR, Gayán P, de Diego LF, Abad A, García-Labiano F, Adánez J. Syngas combustion in a 500 W_{th} chemical-looping combustion system using an impregnated Cu-based oxygen carrier. Fuel Proc Technol 2009;90:1471-9.

[202] Forero CR, Gayán P, García-Labiano F, de Diego LF, Abad A, Adánez J. Effect of gas composition in chemical-looping combustion with copper-based oxygen carriers: Fate of sulphur. Int J Greenhouse Gas Control 2010;4:762-70.

[203] Gayán P, Forero CR, de Diego LF, Abad A, García-Labiano F, Adánez J. Effect of gas composition in chemical-looping combustion with copper based oxygen carriers: Fate of light hydrocarbons. Int J Greenhouse Gas Control 2010;4:13-22.

[204] Ortiz M, de Diego LF, Gayán P, Pans MA, García-Labiano F, Abad A, Adánez J. Hydrogen production coupled with CO_2 capture by chemical-looping using mixed Fe-Ni oxygen carriers. Proc 1st Int Conf on Chemical Looping. Lyon, France; 2010.

[205] Wang S, Wang G, Jiang F, Luo M, Li H. Chemical looping combustion of coke oven gas by using Fe_2O_3/CuO with $MgAl_2O_4$ as oxygen carrier. Energy Environ Sci 2010;3:1353-60.

[206] Cuadrat A, Abad A, García-Labiano F, Gayán P, de Diego LF, Adánez J. Ilmenite as oxygen carrier in a 500 W_{th} chemical-looping combustion system with coal. Proc 10th Int Conf Greenhouse Gas Technology (GHGT-10). Amsterdam, The Netherlands; 2010.

[207] Berguerand N, Lyngfelt A. Chemical-looping combustion of petroleum coke using ilmenite in a 10 kW_{th} unit- High-temperature operation. Energy Fuels 2009;23:5257-68.

[208] Pröll T, Mayer K, Bolhàr-Nordenkampf J, Kolbitsch P, Mattisson T, Lyngfelt A, Hofbauer H. Natural minerals as oxygen carriers for chemical looping combustion in a dual circulating fluidized bed system. Energy Procedia 2009;1:27-34.

[209] Bidwe AR, Mayer F, Hawthorne C, Charitos A, Schuster A, Scheffknecht G. Use of ilmenite as an oxygen carrier in chemical looping combustion-batch and continuous dual fluidized bed investigation. Proc 10th Int Conf Greenhouse Gas Technology (GHGT-10). Amsterdam, The Netherlands; 2010.

[210] Ortiz M, Gayán P, de Diego LF, García-Labiano F, Abad A, Pans MA, Adánez J. Hydrogen production with CO_2 capture by coupling steam reforming of methane and chemical-looping combustion: Use of and iron-based waste products as oxygen carrier burning a PSA tail gas. J Power Sources 2011;196:4370-81.

[211] Copeland RJ, Alptekin G, Cesario M, Gershanovich Y. A novel CO_2 separation system. Proc 1st National Conf on Carbon Sequestration. NETL. Washington D.C., USA; 2001.

[212] Villa R, Cristiani C, Groppi G, Lietti L, Forzatti P, Cornaro U, Rossini S. Ni based mixed oxide materials for CH_4 oxidation under redox cycle conditions. J Molecular Catal A: Chemical 2003;204-205:637-46.

[213] Sedor KE, Hossain MM, de Lasa HI. Reactivity and stability of Ni/Al_2O_3 oxygen carrier for chemical-looping combustion (CLC). Chem Eng Sci 2008;63:2994-3007.

[214] Sedor K, Hossain MM, de Lasa H.I. Reduction kinetics of a fluidizable nickel-alumina oxygen carrier for chemical-looping combustion. Can J Chem Eng 2008;86:323-34.

[215] Dueso C, Abad A, García-Labiano F, de Diego LF, Gayán P, Adánez J, Lyngfelt A. Reactivity of a NiO/Al_2O_3 oxygen carrier prepared by impregnation for chemical-looping combustion. Fuel 2010;89:3399-409.

[216] Hossain MM, Sedor KE, de Lasa HI. $Co\text{-}Ni/Al_2O_3$ oxygen carrier for fluidized bed chemical-looping combustion: Desorption kinetics and metal-support interaction. Chem Eng Sci 2007;62:5464-72.

[217] Hossain MM, de Lasa, HI. Reactivity and stability of $Co\text{-}Ni/Al_2O_3$ oxygen carrier in multicycle CLC. AIChE J. 2007;53:1817-29.

[218] Hossain MM, de Lasa HI. Reduction and oxidation kinetics of $Co\text{-}Ni/Al_2O_3$ oxygen carrier involved in a chemical-looping combustion cycles. Chem Eng Sci 2010;65:98-106.

[219] Hossain MM, Lopez D, Herrera J, de Lasa HI. Nickel on lanthanum-modified γ-Al_2O_3 oxygen carrier for CLC: reactivity and stability. Catal Today 2009;143:179-86.

[220] Quddus MR, Hossain MM; de Lasa HI. Chemical–looping combustion with $Ni\text{-}Co/La\text{-}\gamma Al_2O_3$ oxygen carrier in a fluidized bed reactor. Proc 1st Int Conf on Chemical Looping. Lyon, France; 2010.

[221] Ishida M, Jin H, Okamoto T. A fundamental study of a new kind of medium material for chemical-looping combustion. Energy Fuels 1996;10:958-63.

[222] Ryu H-J, Bae D-H, Han K-H, Lee S-Y, Jin G-T, Choi J-H. Oxidation and reduction characteristics of oxygen carrier particles and reaction kinetics by unreacted core model. Korean J Chem Eng 2001;18:831-7.

[223] Siriwardane R, Poston J. Chemical-looping combustion of simulated synthesis gas using nickel oxide oxygen carrier supported on bentonite. Energy Fuels 2007;21:1582-91.

[224] Zafar Q, Mattisson T, Gevert B. Redox investigation of some oxides of transition-state metals Ni, Cu, Fe, and Mn supported on SiO_2 and $MgAl_2O_4$. Energy Fuels 2006;20:34-44.

[225] Jerndal E, Mattisson T, Thijs I, Snijkers F, Lyngfelt A. NiO particles with Ca and Mg based additives produced by spray-drying as oxygen carriers for chemical-looping combustion. Energy Procedia 2009;1:479-86.

[226] Tian H, Simonyi T, Poston J, Siriwardane R. Effect of hydrogen sufide on CLC of coal-derived synthesis gas over bentonite-supported metal-oxide oxygen carriers. Ind Eng Chem Res 2009;48:8418-30.

[227] Siriwardane R, Tian H, Richards G, Simonyi T, Poston J. Chemical-looping combustion of coal with metal oxide oxygen carriers. Energy Fuels 2009;23:3885–92.

[228] Cao Y, Casenas B, Pan W-P. Investigation of chemical looping combustion by solid fuels. 2. Redox reaction kinetics and product characterization with coal, biomass and solid waste as solid fuels and CuO as an oxygen carrier. Energy Fuels 2006;20:1845-54.

[229] Rubel A, Liu K, Neathery J, Taulbee D. Oxygen carriers for chemical looping combustion of solid fuels. Fuel 2009;88:876-84.

[230] Roux S, Bensakhria A, Antonini, G. Study and improvement of the regeneration of metallic oxides used as oxygen carriers for a new combustion process. Int J of Chem Reactor Eng 2006;4:A38.

[231] Tian H, Chaudhari K, Simonyi T, Poston J, Liu T, Sanders T, Veser G, Siriwardane R. Chemical-looping combustion of coal-derived synthesis gas over copper oxide oxygen carriers. Energy Fuels 2008;22:3744-55.

[232] Abad A, García-Labiano F, de Diego LF, Gayán P, Adánez J. Reduction kinetics of Cu-, Ni- and Fe-based oxygen carriers using syngas ($CO+H_2$) for chemical-looping combustion. Energy Fuels 2007;21:1843-53.

[233] Corbella B, Palacios JM. Titania-supported iron oxide as oxygen carrier for chemical-looping combustion of methane. Fuel 2007;86:113-22.

[234] Rydén M, Cleverstam E, Johansson M, Lyngfelt A, Mattisson T. Fe_2O_3 on Ce-, Ca-, or Mg-stabilized ZrO_2 as oxygen carrier for chemical-looping combustion using NiO as additive. AIChE J 2010;56:2211-20.

[235] Johansson M, Mattisson T, Lyngfelt A. Investigation of Fe_2O_3 with $MgAl_2O_4$ for chemical-looping combustion. Ind Eng Chem Res 2004;43:6978-87.

[236] García-Labiano F, Adánez J, de Diego LF, Gayán P, Abad A. Effect of pressure on the behaviour of copper-, iron-, and nickel-based oxygen carriers for chemical-looping combustion. Energy Fuels 2006;20:26-33.

[237] Zafar Q, Mattisson T, Gevert B. Integrated hydrogen and power production with CO_2 capture using chemical-looping reforming-Redox reactivity of particles of CuO, Mn_2O_3, NiO, and Fe_2O_3 using SiO_2 as support. Ind Eng Chem Res 2005;44:3485-96.

[238] Johansson M, Mattisson T, Lyngfelt A. Creating a synergy effect by using mixed oxides of iron- and nickel oxides in the combustion of methane in a chemical-looping combustion reactor. Energy Fuels 2006;20:2399-407.

[239] Leion H, Mattisson T, Lyngfelt A. The use of petroleum coke as fuel in chemical-looping combustion. Fuel 2007;86:1947-58.

[240] Gao Z, Shen L, Xiao J, Zheng M, Wu J. Analysis of reactivity of Fe-based oxygen carriers with coal during chemical-looping combustion. J Fuel Chem Technol 2009;37:513-20.

[241] Dennis JS, Scott SA, Hayhurst AN. In situ gasification of coal using steam with chemical looping: a technique for isolating CO_2 from burning a solid fuel. J of the Energy Institute 2006;79:187–90.

[242] Stobbe ER, de Boer BA, Geus JW. The reduction and oxidation behaviour of manganese oxides. Catal Today 1999;47:161-7.

[243] Zafar Q, Abad A, Mattisson T, Gevert B, Strand M. Reduction and oxidation kinetics of Mn_3O_4/Mg-ZrO_2 oxygen carrier particles for chemical-looping combustion. Chem Eng Sci 2007;62:6556-67.

[244] Johansson M, Mattisson T, Lyngfelt A. Comparison of oxygen carriers for chemical-looping combustion of methane-rich fuels. Proc 19th Int Conf on FBC. Vienna, Austria; 2006.

[245] Johansson M, Mattisson T, Lyngfelt A. Investigation of Mn_3O_4 with stabilized ZrO_2 for chemical-looping combustion. Chem Eng Res Des 2006;84:807-18.

[246] Mattisson T, Johansson M, Lyngfelt A. CO_2 capture from coal combustion using chemical-looping combustion- Reactivity investigation of Fe, Ni and Mn based oxygen carriers using syngas. Proc of the Clearwater Clean Coal Conf. Clearwater, Florida, USA; 2006.

[247] Ryu H-J, Seo Y, Jin G-T. Development of chemical-looping combustion technology: Long-term operation of a 50 kW_{th} chemical-looping combustor with Ni- and Co-based oxygen carrier particles. Proc of the Regional Symp on Chem Eng. Hanoi, Vietnam; 2005.

[248] Lambert A, Briault P, Comte E. Spinel mixed oxides as oxygen carriers for chemical looping combustion. Proc 10th Int Conf Greenhouse Gas Technology (GHGT-10). Amsterdam, The Netherlands; 2010.

[249] Hoteit A, Chandel MK, Durécu S, Delebarre A. Biogas combustion in a chemical looping fluidized bed reactor. Int J Greenhouse Gas Control 2009;3:561-7.

[250] Rifflart S, Lambert A, Delebarre A, Salmi J, Durand B, Carpentier S. CLCMAT project – Material development for "chemical looping combustion". Proc 1st Int Conf on Chemical Looping. Lyon, France; 2010.

[251] Lambert A, Delquié C, Clémençon I, Comte E, Lefebvre V, Rousseau J, Durand B. Synthesis and characterization of bimetallic Fe/Mn oxides for chemical looping combustion. Energy Procedia 2009;1:375-81.

[252] Ksepko E, Siriwardane RV, Tian H, Simonyi T, Poston JA, Zinn A, Sciazko M. Effect of H_2S on chemical looping combustion of coal derived synthesis gas over Fe_2O_3-MnO_2 supported on ZrO_2/sepiolite. Proc 1st Int Conf on Chemical Looping. Lyon, France; 2010.

[253] Shulman A, Cleverstam E, Mattisson T, Lyngfelt A. Manganese/iron, manganese/nickel, and manganese/silicon oxides used in chemical looping with oxygen uncoupling (CLOU) for combustion of methane. Energy Fuels 2009;23:5269-75.

[254] Lagerbom J, Pikkarainen T, Kanerva U, Moilanen A, Koskinen P, Saastamoinen J, Kauranen P. Characteristics of various new oxygen carriers for CLC. Proc 1st Int Conf on Chemical Looping. Lyon, France; 2010.

[255] Rydén M, Johansson M, Cleverstam E, Lyngfelt A, Mattisson T. Ilmenite with addition of NiO as oxygen carrier for Chemical-Looping Combustion. Fuel 2010;89:3523-33.

[256] Rydén M, Cleverstam E, Lyngfelt A, Mattisson T. Waste products from the steel industry with NiO as additive as oxygen carrier for chemical-looping combustion. Int J of Greenhouse Gas Control, 2009;3:693-703.

[257] Readman JE, Olafsen A, Larring Y, Blom R. $La_{0.8}Sr_{0.2}Co_{0.2}Fe_{0.8}O_{3-\delta}$ as a potential oxygen carrier in a chemical looping type reactor, an in-situ powder X-ray diffraction study. J Mater Chem 2005;15:1931-7.

[258] Nalbandian L, Evdou A, Zaspalis V. $La_{1-x}Sr_xM_yFe_{1-y}O_{3-\delta}$ perovskites as oxygen-carrier materials for chemical-looping reforming. Proc 1st Int Conf on Chemical Looping. Lyon, France; 2010.

[259] Leion H, Larring Y, Bakken E, Bredesen R, Mattissson T, Lyngfelt A. Use of $CaMn_{0.875}Ti_{0.125}O_3$ as oxygen carrier in chemical looping with oxygen uncoupling. Energy Fuels 2009;23:5276-83.

[260] Rydén M, Lyngfelt A, Mattisson T. $CaMn_{0.875}Ti_{0.125}O_3$ as oxygen carrier for chemical oxygen combustion with oxygen uncoupling (CLOU) – Experiments in a continuously operating fluidized-bed reactor system. Int J of Greenhouse Gas Control 2011;5:356-66.

[261] Cao Y, Pan W-P. Investigation of chemical looping combustion by solid fuels. 1. Process analysis. Energy Fuels 2006;20:1836-44.

[262] Fossdal A, Bakken E, Øye BA, Schøning C, Kaus I, Mokkelbost T, Larring Y. Study of inexpensive oxygen carriers for chemical looping combustion. Int J Greenhouse Gas Control 2011;5:483-8.

[263] Azis MM, Jerndal E, Leion H, Mattisson T, Lyngfelt A. On the evaluation of synthetic and natural ilmenite using syngas as fuel in chemical-looping combustion (CLC). Chem Eng Res Des 2010;88:1505-14.

[264] Schwebel G, Hein D, Krumm W. Performance tests of ilmenite mineral as oxygen carrier in a laboratory fixed bed reactor-first step in developing a new technical approach of implementing chemical looping combustion. Proc 4th Int Conf on Clean Coal Technologies (CCT2009). Dresden, Germany; 2009.

[265] Leion H, Jerndal E, Steenari B-M, Hermansson S, Israelsson M, Jansson E, Johnsson M, Thunberg R, Vadenbo A, Mattisson T, Lyngfelt A. Solid fuels in chemical–looping combustion using oxide scale and unprocessed iron ore as oxygen carriers. Fuel 2009;88:1945-54.

[266] Adánez J, Cuadrat A, Abad A, Gayán P, de Diego LF, García-Labiano F. Ilmenite activation during consecutive redox cycles in chemical–looping combustion. Energy Fuels 2010;24:1402-13.

[267] Leion H, Mattisson T, Lyngfelt A. Solid fuels in chemical-looping combustion. Int J Greenhouse Gas Control 2008;2:180-93.

[268] Mattisson T, Lyngfelt A, Cho P. The use of iron oxide as an oxygen carrier in chemical-looping combustion of methane with inherent separation of CO_2. Fuel 2001;80:1953-62.

[269] Xiao R, Song Q, Song M, Lu Z, Zhang S, Shen L. Pressurized chemical-looping combustion of coal with an iron ore-based oxygen carrier. Combust Flame 2010;157:1140-53.

[270] Xiao R, Song Q, Zhang S, Zheng W, Yang Y. Pressurized chemical-looping combustion of chinese bituminous coal: cyclic performance and characterization of iron ore-based oxygen carrier. Energy Fuels 2010;24:1449-63.

[271] Song Q, Xiao R, Zhang S, Zheng W, Yang Y, Shen L. Effect of pressure on chemical–looping combustion of coal with iron ore as oxygen carrier. Proc 1st Int Conf on Chemical Looping. Lyon, France; 2010.

[272] Song Q, Xiao R, Deng Z, Shen L, Zhang M. Reactivity of a $CaSO_4$–oxygen carrier in chemical–looping combustion of methane in a fixed bed reactor. Korean J Chem Eng 2009;23:592–602.

[273] Tian H, Guo Q. Investigation into the behaviour of reductive decomposition of calcium sulphate by carbon monoxide in chemical-looping combustion. Ind Eng Chem Res 2009;48:5624-32.

[274] Xiao R, Song QL, Zheng WG, Deng ZY, Shen LH, Zhang MY. Reduction kinetics of a $CaSO_4$ based oxygen carrier for chemical–looping combustion. Proc 20th Int Conf on Fluidized Bed Combustion. Xian, China; 2009. p 519–26.

[275] Song Q, Xiao R, Deng Z, Shen L, Xiao J, Zhang M. Effect of temperature on reduction of $CaSO_4$ of simulated coal gas in a fluidized bed reactor. Ind Eng Chem Res 2008;47:8148-59.

[276] Song Q, Xiao R, Deng Z, Zhang H, Shen L, Xiao J, Zhang M. Chemical-looping combustion of methane with $CaSO_4$ oxygen carrier in a fixed bed reactor. Energy Convers and Mgmt 2008;49:3178-87.

[277] Song Q, Xiao R, Deng Z, Zheng W, Shen L, Xiao J. Multicycle study on chemical-looping combustion of simulated coal gas with a $CaSO_4$ oxygen carrier in a fluidized bed reactor. Energy Fuels 2008;22:3661-72.

[278] Jing C, Dejie C. Thermodynamic and kinetic analysis of Ca–based oxygen carrier in chemical–looping combustion. Int J of Chem Reactor Eng 2010;8:A46.

[279] Wang J, Anthony EJ. Clean combustion of solid fuels. Appl Energy 2008;85:73-9.

[280] Andrus HE, Chiu JH, Thiebeault PR, Brautsch A. Alstom´s calcium oxide chemical looping combustion coal power technology development. Proc. 34th Int Tech Conf on Clean Coal & Fuel Systems. Clearwater, Florida, USA; 2009.

[281] Zheng M, Shen L, Xiao J. Reduction of $CaSO_4$ oxygen carrier with coal in chemical–looping combustion: Effects of temperature and gasification intermediate. Int J of Greenhouse Gas Control 2010;4:716-28.

[282] Tian H, Guo Q, Chang J. Investigation into decomposition behaviour of $CaSO_4$ in chemical-looping combustion. Energy Fuels 2008;22:3915-21.

[283] Shen L, Zheng M, Xiao J, Xiao R. A mechanistic investigation of a calcium-based oxygen carrier for chemical looping combustion. Combust Flame 2008;154:489-506.

[284] Forret A, Hoteit A. Gauthier, T. Chemical looping combustion process applied to liquid fuels. Proc 4th European combustion meeting. Vienna, Austria; 2009. p. 235. Paper P810025.

[285] Hebden D, Strout HJF. Coal Gasification Processes. Chapter 24. In: Chemistry of Coal Utilization. Ed. Elliot MA. Wiley & Sons. 1981. New York.

[286] Sass B, Monzyk B, Ricci S, Gupta A, Hindin B, Gupta N. Impact of SOx and NOx in Flue Gas on CO_2 separation, compression, and pipeline transmission. In: Thomas DC, Benson SM, editors. Carbon dioxide capture for storage in deep geologic formations– Results from the CO_2 capture project, Oxford, UK: Elsevier; 2005, vol. 2, Chapter 17.

[287] Bryant S, Lake LW. Effect of impurities on subsurface CO_2 storage processes. In: Thomas DC, Benson SM, editors. Carbon dioxide capture for storage in deep geologic formations – Results from the CO_2 capture project, Oxford, UK: Elsevier; 2005, vol. 2, Chapter 18.

[288] Pipitone G, Bolland O. Power generation with CO_2 capture: Technology for CO_2 purification. Int J Greenhouse Gas Control 2009;3:528-34.

[289] Wang B, Yan R, Lee DH, Liang DT, Zheng Y, Zhao H, Zheng C. Thermodynamic investigation of carbon deposition and sulphur evolution in chemical looping combustion with syngas. Energy Fuels 2008;22:1012-20.

[290] Olafsen A, Daniel C, Schuurman Y, Råberg LB, Olsbye U, Mirodatos C. Light alkanes CO_2 reforming to synthesis gas over Ni based catalysts. Catal Today 2006;115:179-185.

[291] Middleton P, Hurst P, Walker G. GRACE: Pre-combustion de-carbonisation hydrogen membrane study. In: Thomas DC, Benson SM, editors. Carbon dioxide capture for storage in deep geologic formations– Results from the CO_2 capture project, Oxford, UK: Elsevier; 2005, vol. 1, Chapter 23.

[292] Fout T. Oxy-combustion: research, development and system analysis. Proc 3rd meeting of the oxy-fuel combustion network. Yokohama, Japan; 2008.

[293] Eide LI, Anheden M, Lyngfelt A, Abanades C, Younes M, Clodic D, Bill AA, Feron PHM, Rojey A, Giroudière F. Novel Capture Processes. Oil Gas Sci Technol 2005;60: 497-508.

[294] Jin H, Ishida M. A new type of coal gas fuelled chemical-looping combustion. Fuel 2004;83:2411-7.

[295] Xiang W, Wang S. Investigation of gasification chemical looping combustion combined cycle performance. Energy Fuels 2008;22:961-6.

[296] Abad A, Adánez J, Cuadrat A, García-Labiano F, Gayán P, de Diego LF. Reaction kinetics of ilmenite for chemical-looping combustion. Chem Eng Sci 2011;66:689-702.

[297] Anheden M, Svedberg G. Exergy analysis of chemical-looping combustion systems. Energy Convers Mgmt 1998; 39:1967-80.

[298] Shen L, Zheng M, Xiao J, Zhang H, Rui X. Chemical looping combustion of coal in interconnected fluidized beds. Science in China Series E: Technol Sci 2007;50:230-40.

[299] Yang J-B, Cai N-S, Li Z-S. Reduction of iron oxide as an oxygen carrier by coal pyrolysis and steam char gasification intermediate products. Energy Fuels 2007;21: 3360-8.

[300] Fillman B, Anheden M, Wolf J. Parameter study in order to reveal critical design issues in the design for a CLC power plant using solid carbon as fuel. Proc 1st Int Conf on Chemical Looping. Lyon, France; 2010.

[301] Morin JX, Béal C, Suraniti S. 455 MW_e CLC boiler / plant feasibility report and recommendations for the next step. Public Summary Report of ENCAP deliverable D4.2.4. Available in www.encapco2.org.

[302] Hossain MM, Quddus MR, Salaices E, de Lasa HI. Gasification of biomass and CO_2 capture using chemical–looping combustion. Proc 1st Int Conf on Chemical Looping. Lyon, France; 2010.

[303] Dennis JS, Scott SA. In situ gasification of a lignite coal and CO_2 separation using chemical looping with a Cu–based oxygen carrier. Fuel 2010;89:1623–40.

[304] Cuadrat A, Abad A, Adánez J, de Diego LF, García-Labiano F, Gayán P. Performance of ilmenite as oxygen carrier for chemical looping combustion using coal as fuel. Proc 1st Int Conf on Chemical Looping. Lyon, France; 2010.

[305] Dennis JS, Müller CR, Scott SA. In situ gasification and CO_2 separation using chemical looping with a Cu–based oxygen carrier: Performance with bituminous coals. Fuel 2010;89:2353-64.

[306] Zhao H, Liu L, Wang B, Xu D, Jiang L, Zheng C. Sol-gel-derived $NiO/NiAl_2O_4$ oxygen carriers for chemical-looping combustion by coal char. Energy Fuels 2008;22:898-905.

[307] Siriwardane R, Tian H, Miller D, Richards G, Simonyi T, Poston J. Evaluation of reaction mechanism of coal-metal oxide interactions in chemical–looping combustion. Combust Flame 2010;157:2198–208.

[308] Johnson JL. Fundamentals of Coal Gasification. Chapter 23. In: Chemistry of Coal Utilization. Ed. Elliot MA. Wiley & Sons. 1981. New York.

[309] Leion H, Lyngfelt A, Mattisson T. Effects of steam and CO_2 in the fluidizing gas when using bituminous coal in chemical–looping combustion. Proc 20th Int Conf on Fluidized Bed Combustion. Xian, China; 2009. p. 608–11.

[310] Leion H, Mattisson T, Lyngfelt A. Chemical-looping of solid fuels in a laboratory fluidized-bed reactor. Oil & Gas Sci Technol 2011;66:201-8.

[311] Berguerand N, Lyngfelt A. Batch testing of solid fuels with ilmenite in a 10 kWth chemical-looping combustor. Fuel 2010;89:1749-62.

[312] Berguerand N, Lyngfelt A, Mattisson T, Markström P. Chemical–looping combustion of solid fuels in a 10 kW_{th} unit. Oil & Gas Sci Technol 2011;66:181-91.

[313] Müller CR, Brown TA, Bohn CD, Chuang SY, Cleeton JPE, Scott SA, Dennis JS. Experimental investigation of two modified chemical looping combustion cycles using syngas from cylinders and the gasification of solid fuels. Proc 20th Int Conf on Fluidized Bed Combustion. Xian, China; 2009. p. 590–5.

[314] Gao Z, Shen L, Xiao J, Qing C, Song Q. Use of coal as fuel for chemical-looping combustion with Ni-based oxygen carrier. Ind Eng Chem Res 2008;47:9279-87.

[315] Leion H, Lyngfelt A, Mattisson T. Solid fuels in chemical–looping combustion using a NiO–based oxygen carrier. Chem Eng Res Des 2009;87:1543–50.

[316] Berguerand N, Lyngfelt A. Operation in a 10 kWth chemical-looping combustor for solid fuel-Testing with a Mexican petroleum coke. Energy Procedia 2009;1:407-14.

[317] Jerndal E, Leion H, Axelsson L, Ekvall T, Hedberg M, Johansson K, Källén M, Svensson R, Mattisson T, Lyngfelt A. Using low–cost iron–based materials as oxygen carriers for chemical–looping combustion. Oil & Gas Sci Technol 2011;66:235-48.

[318] Rubel A, Zhang Y, Liu K, Neathery J. Effect of ash on oxygen carriers for the application of chemical looping combustion to a high carbon char. Oil & Gas Sci Technol 2011;66:291-300.

[319] Leion H, Mattisson T, Lyngfelt A. Using chemical-looping with oxygen uncoupling (CLOU) for combustion of six different solid fuels. Energy Procedia 2009;1:447-53.

[320] Mattisson T, Leion H, Lyngfelt A. Chemical-looping with oxygen uncoupling using CuO/ZrO_2 with petroleum coke. Fuel 2009; 88:683-90.

[321] Eyring E, Konya G, Lighty J, Sahir A, Sarofim A, Whitty K. Chemical looping with copper oxide as carrier and coal as fuel. Oil & Gas Sci Technol 2011;66:209-21.

[322] Adánez-Rubio I, Gayán P, García-Labiano F, de Diego LF, Adánez J, Abad A. Development of CuO-based oxygen carrier materials suitable for chemical-looping with oxygen uncoupling (CLOU). Proc 10th Int Conf Greenhouse Gas Technology (GHGT-10). Amsterdam, The Netherlands; 2010.

[323] Adánez-Rubio I, Gayán P, Abad A, García-Labiano F, de Diego LF, Adánez J. CO_2 capture in coal combustion by chemical-looping with oxygen uncoupling (CLOU) with a Cu-based oxygen-carrier. Proc 5th Int Conf on Clean Coal Technologies (CCT2011). Zaragoza, Spain; 2011.

[324] Azimi G, Leion H, Mattisson T, Lyngfelt A. Chemical-looping with oxygen uncoupling using combined Mn-Fe oxides, testing in batch fluidized bed. Proc 10th Int Conf Greenhouse Gas Technology (GHGT-10). Amsterdam, The Netherlands; 2010.

[325] Rydén M, Lygfelt A, Mattisson T. Combined manganese/iron oxides as oxygen carrier for chemical-looping combustion with oxygen uncoupling (CLOU) in a circulating fluidized bed reactor system. Proc 10th Int Conf Greenhouse Gas Technology (GHGT-10). Amsterdam, The Netherlands; 2010.

[326] Rydén M, Lyngfelt A, Mattisson T. Two novel approaches for hydrogen production, chemical-looping reforming and steam reforming with carbon dioxide capture by chemical-looping combustion. Proc 16th World Hydrogen Energy Conf (WHEC). Lyon, France; 2006.

[327] Ortiz M, Abad A, de Diego LF, Gayán P, García-Labiano F, Adánez J. Optimization of a chemical-looping autothermal reforming system working with a Ni-based oxygen carrier. Proc 10th Int Conf Greenhouse Gas Technology (GHGT-10). Amsterdam, The Netherlands; 2010.

[328] Mattisson T, Lyngfelt A. Applications of chemical-looping combustion with capture of CO_2. Proc 2nd Nordic Minisymposium on Carbon Dioxide Capture and Storage. Göteborg, Sweden; 2001.

[329] Mattisson T, Zafar Q, Lyngfelt A, Gevert B. Integrated hydrogen and power production from natural gas with CO_2 capture. Proc 15th World Hydrogen Energy Conf (WHEC). Yokohama, Japan; 2004.

[330] de Diego LF, Ortiz M, Adánez J, García-Labiano F, Abad A, Gayán P. Synthesis gas generation by chemical-looping reforming in a batch fluidized bed reactor using Ni-based oxygen Carriers. Chem Eng J 2008;144:289-98.

[331] Ortiz M, de Diego LF, Abad A, García-Labiano F, Gayán P, Adánez J. Hydrogen production by auto-thermal chemical-looping reforming in a pressurised fluidized bed reactor using Ni-based oxygen carriers. Int J Hydrogen Energy 2010;35:151-60.

[332] Mattisson T, Adánez J, Proll T, Kuusik R, Beal C, Assink J, Snijkers F, Lyngfelt A. Chemical-looping combustion CO_2 ready gas power. Energy Procedia 2009;1:1557-64.

[333] Ryu H-J, Shun D, Jin G-T, Yi C-K. 2010b. Development of novel two–interconnected fluidized bed system for chemical looping combustion. Proc 1st Int Conf on Chemical Looping. Lyon, France; 2010.

[334] Ströhle J, Orth M, Epple B. Simulation of the fuel reactor of a 1 MW_{th} chemical looping plant for coal. Proc 1st Int Conf on Chemical Looping. Lyon, France; 2010.

[335] Assink J, Beal C. Chemical looping combustion (CLC) technology summary. In: Eide LI, editor. Carbon dioxide capture for storage in deep geological formations–Results from the CO_2 capture project, UK: CPL Press; 2009, vol. 3. Chapter 5.

[336] Kolbitsch P, Pröll T, Hofbauer H. Modeling of a 120 kW chemical looping combustion reactor system using a Ni-based oxygen carrier. Chem Eng Sci 2009;64:99-108.

[337] Adánez J, García-Labiano F, de Diego LF, Plata A, Celaya J, Gayán P, Abad A. Optimizing the fuel reactor for chemical looping combustion. Proc 17th Int Conf on Fluidized Bed Combustion. Jacksonville, Florida, USA; 2003.

[338] García-Labiano F, Adánez J, de Diego LF, Plata A, Celaya J, Gayán P, Abad A. Simulation of the reactor behavior for chemical looping combustion Systems. In: Macías-Machín A, Umbría J, editors. Chemical Industry and Environment IV. Las Palmas de Gran Canaria, Spain: Universidad de las Palmas de Gran Canaria; 2003, p. 233-242.

[339] Kronberger B, Löffler G, Hofbauer H. Chemical-looping combustion- Reactor fluidization studies and scale-up criteria. In: Thomas DC, Benson SM, editors. Carbon dioxide capture for storage in deep geologic formations– Results from the CO_2 capture project, Oxford, UK: Elsevier; 2005, vol. 1, Chapter 35.

[340] Xu M, Ellis N, Ryu H-J, Lim CJ. Modeling of an interconnected fluidized bed reactor for chemical looping combustion. Proc of the 2007 ECI Conference on The 12th Int Conf on Fluidization – New horizons in fluidization engineering. Vancouver, Canada; 2007. Paper 113.

[341] Abad A, Adánez J, García-Labiano F, de Diego LF, Gayán P, Kolbitsch P, Pröll T. CLC Modeling the fuel reactor at fast fluidization - Conversion of CH_4 using a NiO-based oxygen carrier in a 120 kW_{th} unit. Proc 1st Int Conf on Chemical Looping. Lyon, France; 2010.

[342] Pavone D, Rolland M, Lebas E. CO_2 capture using chemical looping combustion for gas turbine application. Proc 8th Int Conf Greenhouse Gas Control Technologies (GHGT-8). Trondheim, Norway; 2006.

[343] Pavone D. CO_2 capture by means of chemical looping combustion. Proc of the COMSOL Multiphysics User's Conference. Paris, France; 2005.

[344] Deng Z, Xiao R, Jin B, Song Q, Huang H. Multiphase CFD modelling for a chemical looping combustion process (Fuel reactor). Chem Eng Technol 2008; 31:1754-66.

[345] Deng Z, Xiao R, Jin B, Song Q. Numerical simulation of chemical looping combustion process with $CaSO_4$ oxygen carrier. Int J Greenhouse Gas Control 2009;3:368-75.

[346] Jin B, Xiao R, Deng Z, Song Q. Computational fluid dynamics modeling of chemical looping combustion process with calcium sulphate oxygen carrier. Int J Chem Reactor Eng 2009;7:A19.

[347] Jung J, Gamwo IK. Multiphase CFD-based models for chemical looping combustion process: Fuel reactor modelling. Powder Technol 2008;183:401-9.

[348] Shuai W, Yunchao Y, Huilin L, Jiaxing W, Pengfi X, Guodong L. Hydrodynamic simulation of fuel-reactor in chemical looping combustion process. Chem Eng Res Des 2011;89:1501-10.

[349] Cloete S, Johanse ST, Amini S. Multiphase CFD–based models for a chemical looping combustion process. Proc 1st Int Conf on Chemical Looping. Lyon, France; 2010.

[350] Kruggel-Emden H, Rickelt S, Stepanek F, Munjiza A. Development and testing of an interconnected multiphase CFD-model for chemical-looping combustion. Chem Eng Sci 2010;65:4732-45.

[351] Mahalatkar K, Kuhlman J, Huckaby ED, O'Brien T. Simulations of a circulating fluidized bed chemical looping combustion system utilizing gaseous fuel. Oil & Gas Sci Technol 2011;66:301-11.

[352] Mahalatkar K, Kuhlman J, Huckaby ED, O'Brien T. Computational fluid dynamic simulations of chemical looping fuel reactors utilizing gaseous fuels. Chem Eng Sci 2011;66:469-79.

[353] Mahalatkar K, O'Brien T, Huckaby ED, Kuhlman J. Simulation of the fuel reactor of a coal–fired chemical looping combustor. Powders and Grains: In: Proc 6th Int Conf on Micromechanics of Granular Media. Nakagawa M and Luding S (editors). American Institute of Physics; 2009. p. 83–6.

[354] Mahalatkar K, O'Brien T, Huckaby ED, Kuhlman J. Computational fluid dynamic simulation of the fuel reactor of a coal–fired chemical looping combustor. Proc 1st Int Conf on Chemical Looping. Lyon, France; 2010.

[355] Kunii D, Levenspiel O. Fluidized reactor models. 1. For bubbling beds of fine, intermediate, and large particles. 2. For the lean phase: freeboard and fast fluidization. Ind Eng Chem Res 1990;29:1226–34.

[356] Pallarès D, Johnsson P. Macroscopic modelling of fluid dynamics in large-scale circulating fluidized beds. Prog Energy Combust Sci 2006;32:539–69.

[357] Adánez, J., Gayán, P., de Diego, L. F., García-Labiano, F., Abad A. Combustion of wood chips in a CFBC. Modeling and validation. Ind Eng Chem Res 2003;42:987–99.

[358] Shah S, Klajny M, Myöhänen K, Hyppänen T. Improvement of CFD methods for modeling full scale circulating fluidized bed combustion systems. Proc 20th Int Conf on Fluidized Bed Combustion. Xian, China; 2009. p. 792–8.

[359] Blaser P, Chandran R. Computational simulation of fluidization dynamics inside a commercial biomass gasifier. Proc of the 2009 AIChE Annual Meeting. Nashville, TN, USA; 2009.

[360] Snider D, Clark S. CPFD Eulerian–lagrangian method for three dimensional thermal reacting flow - An example of a syngas gasifier. Proc of the 2009 AIChE Annual Meeting. Nashville, TN, USA; 2009.

[361] Snider D, Guenther C, Dalton J, Williams K. CPFD eulerian–lagrangian numerical scheme applied to the NETL bench–top chemical looping experiment. Proc 1st Int Conf on Chemical Looping. Lyon, France; 2010.

[362] Shuai W, Guodong L, Huilin L, Juhui C, Yurong H, Jiaxing W. Fluid dynamic simulation in a chemical looping combustion with two interconnected fluidized beds. Fuel Process Technol 2011;92:385-93.

[363] Shuai W, Guodong L, Huilin L, Juhui Ch, Yurong H, Jiaxing W. Fluid dynamic simulation in a chemical looping combustion with two interconnected fluidized beds. Fuel Proc Technol 2011;92:385–93.

[364] He F, Wang H, Dai Y. Application of Fe_2O_3/Al_2O_3 composite particles as oxygen carrier of chemical looping combustion. J Natural Gas Chem 2007;16:155-61.

[365] Dewaele O, Froment GF. TAP study of the mechanism and kinetics of the adsorption and combustion of methane on Ni/Al_2O_3 and NiO/Al_2O_3. J Catal 1999;184:499–513.

[366] Szekely J, Evans JW, Sohn HY. Gas–solid reactions. New York: Academic Press Inc; 1976.

[367] Dey SK, Jana B, Basumallick A. Kinetics and reduction characteristics of hematite–noncoking coal mixed pellets under nitrogen gas atmosphere. ISIJ Int 1993;33:735–9.

[368] Donskoi E, McElwain DLS, Wibberley LJ. Estimation and modeling of parameters for direct reduction in iron ore/coal composites: Part II. Kinetic parameters. Metallurgical Materials Transact B 2003;34B:255–66.

[369] Sohn I, Fruehan RJ. The reduction of iron oxides by volatiles in a rotary hearth furnace process: Part I. The role and kinetics of volatile reduction. Metallurgical Materials Transact B 2005;36B:605–12.

[370] Siriwardane R, Tian H, Miller D, Richards G, Simonyi T, Poston J. Investigation on reaction mechanism of chemical–looping combustion of coal utilizing oxygen carriers. Proc 1st Int Conf on Chemical Looping. Lyon, France; 2010.

[371] Szekely J, Lin CI, Sohn HY. A structural model for gas–solid reactions with a moving boundary — V An experimental study of the reduction of porous nickel–oxide pellets with hydrogen. Chem Eng Sci 1973;28:1975-89.

[372] Georgakis C, Chang CW, Szekely J. A changing grain size model for gas–solid reactions. Chem Eng Sci 1979;34:1072-5.

[373] García-Labiano F, de Diego LF, Adánez J, Abad A, Gayán P. Temperature variations in the oxygen carrier particles during their reduction and oxidation in a chemical-looping combustion system. Chem Eng Sci 2005;60:851-62.

[374] Erri P, Varma A. Diffusional effects in nickel oxide reduction kinetics. Ind Eng Chem Res 2009;48:4-6.

[375] Carberry JJ, Varma A. Chemical reaction and reactor engineering. New York: Marcel Dekker Inc; 1987.

[376] Zafar Q, Abad A, Mattisson T, Gevert B. Reaction kinetics of freeze-granulated $NiO/MgAl_2O_4$ oxygen carrier particles for chemical-looping combustion. Energy Fuels 2007;21:610-8.

[377] Readman JE, Olafsen A, Smith JB, Blom R. Chemical looping combustion using $NiO/NiAl_2O_4$: mechanisms and kinetics of reduction-oxidation (Red-ox) reactions from in situ powder X-ray diffraction and thermogravimetry experiments. Energy Fuels 2006;20:1382-7.

[378] Wolf J, Anheden M, Yan J. Comparison of nickel- and iron-based oxygen carriers in chemical looping combustion for CO_2 capture in power generation. Fuel 2005;84:993-1006.

[379] Moghtaderi B, Song H. Reduction properties of physically mixed metallic oxide oxygen carriers in chemical looping combustion. Energy Fuels 2010;24:5359-68.

[380] Chuang SY, Dennis JS, Hayhurst AN, Scott SA. Kinetics of the oxidation of a coprecipitated mixture of Cu and Al_2O_3 by O_2 for chemical-looping combustion. Energy Fuels 2010;24:3917-27.

[381] Chuang SY, Dennis JS, Hayhurst AN, Scott SA. Kinetics of the chemical looping oxidation of H_2 by a co-precipitated mixture of CuO and Al_2O_3. Chem Eng Res Des 2011;89:1511-23.

[382] Bohn CD, Cleeton JP, Müller CM, Scott SA, Dennis JS. Measuring the kinetics of the reduction of iron oxide with carbon monoxide in a fluidized bed. Proc 20th Int Conf on Fluidized Bed Combustion. Xian, China; 2009. p 555–561.

[383] Hoteit A, Forret A, Pelletant W, Roesler J, Gauthier T. Chemical looping combustion with different types of liquid fuels. Oil & Gas Sci Technol 2011;66:193-9.

[384] Bandrowski J, Bickling CR, Yang KH, Hougen OA. 1962. Kinetics of the reduction of nickel oxide by hydrogen. Chem Eng Sci 1962;17: 379–90.

[385] Chadda D, Ford JD, Fahim MA. Chemical energy storage by the reaction cycle CuO/Cu_2O. Int J Energy Res 1989;13:63–73.

[386] Jin H, Ishida M. Reactivity study on a novel hydrogen fueled chemical-looping combustion. Int J Hydrogen Energy 2001;26:889-94.

[387] Cuadrat A, Abad A, Gayán P, de Diego LF, García-Labiano F, Adánez J. Theoretical approach on the chemical-looping combustion performance with solid fuels: optimizing the solids inventory. Proc Int Conf on Coal Sci & Technol, (ICCS&T2011). Oviedo, Spain; 2011.

[388] Pröll T, Rupanovits K, Kolbitsch P, Bolhàr-Nordenkampf J, Hofbauer H. Cold flow model study on a dual circulating fluidized bed system for chemical looping processes. Chem Eng Technol 2009;32:1–8.

[389] Xu M, Ellis N, Jim Lim C, Ryu H-J. Mapping of the operating conditions for an interconnected fluidized bed reactor for CO_2 separation by chemical looping combustion. Chem Eng Technol 2009;3:404-9.

[390] Andrus HE, Chiu JH, Thibeault PR. Alstom's chemical looping combustion coal power technology development prototype. Proc 1st Int Conf on Chemical Looping. Lyon, France; 2010.

[391] Cheung JT, Ellis N, Lim CJ. Status of CLC at the University of British Columbia. Proc 1st Int Conf on Chemical Looping. Lyon, France; 2010.

[392] Yazdanpanah MM, Hoteit A, Forret A, Delebarre A, Gauthier T. Experimental investigations on a novel chemical looping combustion configuration. Oil & Gas Sci Technol 2011;66:265-75.

[393] Naqvi R, Bolland O, Wolf J. Off–design evaluation of a natural gas fired chemical looping combustion combined cycle with CO_2 capture. Proc of ECOS 2005. Trondheim, Norway; 2005.

[394] Naqvi R, Wolf J, Bolland O. Part-load analysis of a chemical looping combustion (CLC) combined cycle with CO_2 capture. Energy 2007;32:360-70.

[395] Chi J, Wang B, Zhang Z, Xiao Y. Off–design performance of a chemical looping combustion (CLC) combined cycle: effects of ambient temperature. J Thermal Sci 2010;19:87–96.

[396] Balaji S, Ilic J, Ydstie BE, Krogh BH. Control–based modelling and simulation of the chemical–looping combustion process. Ind Eng Chem Res 2010:49:4566-75.

[397] Kvamsdal HM, Jordal K, Bolland O. A quantitative comparison of gas turbine cycles with CO_2 capture. Energy 2007;32:10-24.

[398] Naqvi R, Bolland O, Brandvoll O, Helle K. Chemical looping combustion-Analysis of natural gas fired power cycles with inherent CO_2 capture. Proc of ASME Turbo Expo. Vienna, Austria; 2004.

[399] Zhang X, Han W, Hong H, Jin H. A chemical intercooling gas turbine cycle with chemical-looping combustion. Energy 2009;34:2131-6.

[400] Yu J, Corripio AB, Harrison DP, Copeland RJ. Analysis of the sorbent energy transfer system (SETS) for power generation and CO_2 capture. Adv Environ Res 2003;7:335-45.

[401] Consonni S, Lozza G, Pelliccia G, Rossini S, Saviano F. Chemical-looping combustion for combined cycles with CO_2 capture. J Eng for Gas Turbines and Power 2006;128:525-34.

[402] Naqvi R, Bolland O. Multi-stage chemical looping combustion (CLC) for combined cycles with CO_2 capture. Int J Greenhouse Gas Control 2007;1:19-30.

[403] Rezvani S, Huang Y, McIlven-Wright D, Hewitt N, Deb Mondol J. Comparative assessment of coal fired IGCC systems with CO_2 capture using physical absorption, membrane reactors and chemical looping. Fuel 2009;88:2463-72.

[404] Ishida M, Jin H. Fundamental study on a novel gas turbine cycle. J Energy Resources Technol 2001;123:10-14.

[405] Lee J-B, Park C-S, Choi S-I, Song Y-W, Kim Y-H., Yang H-S. Redox characteristics of various kinds of oxygen carriers for hydrogen fuelled chemical-looping combustion. J Ind Eng Chem 2005;11:96-102.

[406] Ishida M, Jin H. CO_2 recovery in a power plant with chemical looping combustion. Energy Convers Mgmt 1997;38:187-92.

[407] Baek J-I, Kim J-W, Lee JB, Eom TH, Ryu J, Ryu CK, Yi J. Effects of support on the performance of NiO-based oxygen carriers. Oil & Gas Sci Technol 2011;66:223-34.

[408] Baek J-I, Ryu CK, Kim J-W, Ryu J, Lee JB, Eom T-H, Yi J. Spray-dried NiO oxygen carrier with highly attrition resistance. Proc 1st Int Conf on Chemical Looping. Lyon, France; 2010.

[409] Johansson M, Mattisson T, Lyngfelt A. Comparison of oxygen carriers for chemical looping combustion. Int Symp: moving towards zero emission plants (CERTH/ISTFA). Leptokarya Piera, Greece; 2005.

[410] Solunke RD, Veser G. Nanocomposite oxygen carriers for chemical looping combustion of sulfur-contaminated synthesis gas. Energy Fuels 2009;23:4787-96.

[411] Ryu HJ, Shun D, Bae DH, Park MH. Syngas combustion characteristics of four oxygen carrier particles for chemical looping combustion in a batch fluidized bed reactor. Korean J Chem Eng 2009;26:523-7.

[412] Song KS, Seo YS, Yoon HK, Cho SJ. Characteristics of the NiO/Hexaaluminate for chemical looping combustion. Korean J Chem Eng 2003;20:471-5.

[413] Erri P, Varma A. Spinel-supported oxygen carriers for inherent CO_2 separation during power generation. Ind Eng Chem Res 2007;46:8597-601.

[414] Erri P, Varma A. Solution combustion synthesized oxygen carriers for chemical looping combustion. Chem Eng Sci 2007;62:5682-7.

[415] Snijkers F, Jerndal E, Thijs I, Mattisson T, Lyngfelt A. Preparation of oxygen carriers for chemical looping combustion by industrial spray drying method. Proc 1st Int Conf on Chemical Looping. Lyon, France; 2010.

[416] Pröll T, Kolbitsch P, Bolhàr-Nordenkampf J, Hofbauer H. Chemical looping pilot plant results using a nickel-based oxygen carrier. Oil & Gas Sci Technol 2011;66:173-80.

[417] Zhao H-b, Liu L-m, Xu D, Zheng C-G, Liu G-J, Jiang L-L. NiO/$NiAl_2O_4$ oxygen carriers prepared by sol-gel for chemical-looping combustion fuels by gas. J Fuel Chem Technol 2008;36:261-6.

[418] Lambert A, Briault P, Comte E. Chemical looping materials: Can NiO-$NiAl_2O_4$ carriers be outperformed?. Proc 1st Int Conf on Chemical Looping. Lyon, France; 2010.

[419] Brandvoll O, Kolbeinsen L, Olsen N, Bolland O. Chemical looping combustion. Reduction of nickel oxide/nickel aluminate with hydrogen. Chem Eng Transact 2003;3:105-10.

[420] Cao Y, Cheng ZX, Meng L, Riley JT, Pan WP. Reduction of solid oxygen carrier (CuO) by solid fuel (coal) in chemical looping combustion. Prepr ACS. Div Fuel Chem. 2005;50:99-102.

[421] Noorman S, Gallucci F, van Sint Annaland M, Kuipers HJAM. Experimental Investigation of a CuO/Al_2O_3 oxygen carrier for chemical-looping combustion. Ind Eng Chem Res 2010;49:9720-8.

[422] Forero CR, Gayán P, García-Labiano F, de Diego LF, Abad A, Adánez J. Effect of gas impurities on the behaviour of Cu-based oxygen carriers on chemical-looping combustion. Proc 1st Int Conf on Chemical Looping. Lyon, France; 2010.

[423] Corbella BM, de Diego LF, García-Labiano F, Adánez J, Palacios JM. Characterization and performance in a multicycle test in a fixed-bed reactor of silica-supported copper oxide as oxygen carrier for chemical-looping combustion of methane. Energy Fuels 2006;20:148-54.

[424] Corbella BM, de Diego LF, García-Labiano F, Adánez J, Palacios JM. The performance in a fixed bed reactor of copper-based oxides on titania as oxygen carriers for chemical looping combustion of methane. Energy Fuels 2005;19:433-41.

[425] Brown TA, Scala F, Scott SA, Dennis JS, Salatino P. Investigation of the attrition behaviour of an iron oxide oxygen-carrier under inert and reacting conditions. Proc 1st Int Conf on Chemical Looping. Lyon, France; 2010.

[426] Ishida M, Takeshita K, Suzuki K, Ohba T. Application of Fe_2O_3-Al_2O_3 composite particles as solid looping material of the chemical-loop combustor. Energy Fuels 2005;19:2514-8.

[427] Mattisson, T, Lyngfelt, A, Cho P. Possibility of using iron oxide as an oxygen carrier for combustion of methane with removal of CO_2 - Application of chemical-looping combustion. - Proc 5th Int Conf Greenhouse Gas Control Technologies (GHGT-5). Cairns, Australia; 2000.

[428] Cho P, Mattissson, Lyngfelt A. Reactivity of iron oxide with methane in a laboratory fluidized bed - application of chemical looping combustion. In: Proc 7th Int Conf on circulating fluidized beds (CFB-7). Niagara Falls, Ontario; 2002. pp 599-606.

[429] Linderholm C, Cuadrat A, Lyngfelt A. Chemical-looping combustion of solid fuels in a 10 kW_{th} pilot-batch tests with five fuels. - Proc 10th Int Conf Greenhouse Gas Technology (GHGT-10). Amsterdam, The Netherlands; 2010.

[430] Mendiara T, Abad A, de Diego LF, García-Labiano F, Gayán P, Adánez J. Red mud as oxygen carrier in chemical looping combustion of coal. Proc 5th Int Conf on Clean Coal Technologies (CCT2011). Zaragoza, Spain; 2011.

List of Tables

Table 1. Summary of the Chemical Looping processes for CO_2 capture.

Aim	Primary fuel	Process	Main features
Combustion	Gas	CLC	- Gaseous fuels combustion with oxygen-carriers
	Solid	Syngas-CLC	- Previous gasification of solid fuel - Oxygen requirement for gasification
	Solid	iG-CLC	- Gasification of the solid fuel inside the fuel-reactor - Low cost oxygen-carriers are desirable
	Solid	CLOU	- Use of oxygen-carriers with gaseous O_2 release properties - Rapid conversion of the solid fuel
H_2 production	Gas	SR-CLC	- Steam reforming in usual tubular reactors - Energy requirements for SR supplied by CLC fuelled by tail gas
	Gas	a-CLR	- Partial oxidation of fuel with oxygen carriers instead gaseous O_2 - Process can be fit to produce pure N_2 stream and the desired CO/H_2 ratio
	Gas	CLH (OSD)	- H_2 is produced by oxidation with steam of the oxygen-carrier - Three reactors are needed (FR, AR, and Steam reactor)
	Solid	SCL	- H_2 is produced by oxidation with steam of the oxygen-carrier - Previous gasification of solid fuel with O_2 - Three reactors are needed (Reducer, Oxidiser, and Combustor)
	Solid	CDCL	- H_2 is produced by oxidation with steam of the oxygen-carrier - Coal & O_2 are fed to the reducer reactor - Three reactors are needed (Reducer, Oxidiser, and Combustor)

Table 2. Standard heat of reaction (ΔH_r^0) for the reduction and oxidation reactions of different oxygen carriers. ΔH_r^0 data are referred to the chemical reaction balanced to one mol of CH_4, H_2, CO, C or O_2 and expressed as kJ/mol.

	ΔH_r^0 (kJ/mol gas or C)				
Redox system	CH_4	H_2	CO	C	O_2
$CaSO_4/CaS$	158.6	-1.6	-42.7	86.9	-480.5
Co_3O_4/Co	107.9	-14.3	-55.4	61.6	-455.1
Co_3O_4/CoO	-16.8	-45.5	-86.6	-0.8	-392.7
CoO/Co	149.5	-3.9	-45.0	82.4	-475.9
CuO/Cu	-178.0	-85.8	-126.9	-81.4	-312.1
CuO/Cu_2O	-236.6	-100.4	-141.6	-110.7	-282.8
Cu_2O/Cu	-119.5	-71.1	-112.3	-52.1	-341.4
$CuAl_2O_4/Cu{\cdot}Al_2O_3$	282.2	29.3	-11.8	148.7	-542.2
$CuAlO_2/Cu{\cdot}Al_2O_3$	-24.1	-47.3	-88.4	-4.4	-389.1
$CuAl_2O_4/CuAlO_2$	588.5	105.9	64.7	301.9	-695.4
Fe_2O_3/Fe_3O_4	141.6	-5.8	-47.0	78.4	-472.0
Fe_2O_3/FeO	318.4	38.3	-2.8	166.8	-560.3
$Fe_2O_3{\cdot}Al_2O_3/FeAl_2O_4$	-62.3	-56.8	-98.0	-23.5	-370.0
$Fe_2TiO_5/FeTiO_3$	106.5	-14.6	-55.8	60.9	-454.4
Mn_2O_3/MnO	-48.0	-53.3	-94.4	-16.4	-377.1
Mn_2O_3/Mn_3O_4	-396.6	-140.4	-181.6	-190.7	-202.8
Mn_3O_4/MnO	126.3	-9.7	-50.8	70.8	-464.3
NiO/Ni	156.5	-2.1	-43.3	85.9	-479.4
$NiAl_2O_4/Ni{\cdot}Al_2O_3$	158.6	-1.6	-42.8	86.9	-480.4

Table 3. Lifetime of oxygen-carriers based on attrition data.

Carrier	Facility	Operation time (h)	T (ºC)		Attrition rate (%/h)	Lifetime (h)	References
			FR	AR			
NiO /Al_2O_3	CLC 10 kW_{th}	100	≈ 900	1000	0.0023	40000	[33]
NiO / $NiAl_2O_4$+ $MgAl_2O_4$	CLC 10 kW_{th}	1016	≈ 940	1000	0.003	33000	[43,139]
NiO / $NiAl_2O_4$	CLC 10 kW_{th}	160	≈ 940	1000	0.022	4500	[140]
NiO / α–Al_2O_3	CLC 500 W_{th}	70	880	950	0.01	10000	[141]
CuO / γ–Al_2O_3	CLC 10 kW_{th}	100	800	800	0.04	2400	[40]
CuO / γ–Al_2O_3	CLC 500 W_{th}	60	800	900	0.09	1100	[142]
CuO / NiO-Al_2O_3	CLC 500 W_{th}	67	900	950	0.04	2700	[138]
Iron ore	CLCs 1 kW_{th}	10	950	1010	0.0625	1600	[143]

Table 4. Summary of the oxygen-carriers tested in continuously operated CLC and CLR units.

Metal oxide 1 (wt%)	Metal oxide 2 (wt%)	Support material	Preparation method	Application and facility	Reacting gas	Operation time (h)[a]	Reference
NiO							
18		α-Al_2O_3	IMP	CLC 300 W	n.g.	41	[182,183]
				CLC 500 W	CH_4	70	[141]
				CLC 500 W	H_2, CO, syngas	50	[169]
				CLC 500 W	C_2H_6, C_3H_8	40	[46]
				CLC 500 W	CH_4 + H_2S	45	[45]
				CLR 500 W	n.g.	36	[182]
				CLR 900 W	CH_4 + H_2O	40	[170]
21		γ-Al_2O_3	IMP	CLC 300 W	n.g.	5	[182]
				CLR 500 W	n.g.	37	[182]
				CLR 900 W	CH_4 + H_2O	40	[170]
35		Al_2O_3	COP	CLC 1 kW	Syngas + H_2S	n.a.	[184]
				CLCs 1 kW	Coal	30	[185]
				CLCs 10 kW	Coal	100	[186]
32.7		$NiAl_2O_4$	IMP	CLCs 10 kW	Coal	30	[187]
60		$NiAl_2O_4$	SF	CLC 10 kW	n.g.	160	[140]
60		$NiAl_2O_4$	FG	CLC 300 W	n.g.	8	[188]
40		$NiAl_2O_4$	FG	CLC 10 kW	n.g.	100	[33,189]
40		$NiAl_2O_4$	SD	CLC	H_2	n.a.	[190]
40		$NiAl_2O_4$	SD	CLC 300 W	n.g.	60	[183]
				CLC 10 kW	n.g.	1016	[168]
				CLC 65 kW	H_2, CO	n.a.	[191,192]
				CLC 120 kW	n.g.	90	[167,193,194]
				CLC 120 kW	CH_4	n.a.	[191,192]
40		$NiAl_2O_4$-MgO	SD	CLC 300 W	n.g.	40	[183]
				CLC 10 KW	n.g.	611[b]	[168]
				CLC 120 kW	n.g.	90	[167,193,194]
				CLR 140 kW	n.g.	18	[195]
20		$MgAl_2O_4$	FG	CLC 300 W	n.g.	10	[182]
				CLR 500 W	n.g.	49	[182]
60		$MgAl_2O_4$	FG	CLC 300 W	n.g.	30	[188,196]
				CLC 170 W	Syngas	30	[36,188]
				CLR 500 W	n.g.	40	[197]
60		Bentonite	MM	CLC 50 kW	CH_4	3.5	[37]
					Syngas	53	[107]
					n.g.	51	[107]
60		Bentonite	MM	CLC 1.5 kW	CH_4	n.a.	[108]
40		ZrO_2-MgO	FG	CLC 300 W	n.g.	16	[198]
				CLR 500 W	n.g.	24	[198]
OCN702-1100		n.a.	SD	CLC 50 kW	n.g.	n.a.	[199]
OCN703-1100		n.a.	SD	CLC 50 kW	n.g.	53	[107]
					Syngas	52	[107]
CuO							
15		α-Al_2O_3	IMP	CLC 500 W	CH_4	30	[138]
14		γ-Al_2O_3	IMP	CLC 10 kW	CH_4	120	[39,40,136,200]
				CLC 500 W	H_2, CO, syngas	40	[201]
				CLC 500 W	CH_4, H_2S	32	[202]
				CLC 500 W	CH_4, HC	30	[203]
				CLC 500 W	CH_4	89	[138,142]
12		$MgAl_2O_4$	IMP	CLC 500 W	CH_4	50	[138]
Fe_2O_3							
Pure				CLCs 10 kW	Biomass	30	[109]
20		Al_2O_3	IMP	CLC 300 W	PSA-offgas	40	[204]
60		Al_2O_3	FG	CLC 300 W	n.g., syngas	40	[36,131]
60		Bentonite	MM	CLC 1 kW	CH_4	n/a	[108]
n.a.		n.a.	n.a.	CLC 10 kW	n.g.	17	[33]

Mn_3O_4							
40		Mg-ZrO_2	FG	CLC 300 W	n.g., syngas	70	[130]
Co_3O_4							
n.a.		$CoAl_2O_4$		CLC 50 kW	n.g.	25	[38]
Mixed oxides							
CuO (13)	NiO (3)	γ-Al_2O_3	IMP	CLC 500 W	CH_4	67	[138]
Fe_2O_3 (45)	CuO (15)	$MgAl_2O_4$	MM	CLCp 10 kW	Coke oven gas	15	[205]
Fe_2O_3 (45)	NiO (15)	Bentonite	MM	CLC 1 kW	CH_4	n.a.	[108]
Fe_2O_3 (30)	NiO (30)	Bentonite	MM	CLC 1 kW	CH_4	n.a.	[108]
Fe_2O_3 (15)	NiO (45)	Bentonite	MM	CLC 1 kW	CH_4	n.a.	[108]
Low cost materials							
Ilmenite (Norway)				CLCs 500W	coal	26	[206]
				CLCs 10 kW	pet-coke	30	[55,207]
				CLCs 10 kW	coal	22	[54]
				CLC 120 kW	n.g., syngas	n.a.	[191,208]
Ilmenite (Australia)				CLC 1.3 kW	syngas	n.a.	[209]
Iron ore (Australia)				CLCs 1 kW	coal	10	[143]
Redmud				SR-CLC 500 W	CH_4, syngas, PSA-offgas	111	[210]

(a) the operation time corresponds to the period with fuel feeding

(b) partially mixed with $NiO/NiAl_2O_4$ particles (included in 1016 h in the above carrier)

Table 5. Summary of the experience time (in hours) on CLC and CLR in continuous units.

	CLC	CLCs	CLR	TOTAL
Nickel	2114	160	284	2558
Copper	391	--	--	391
Iron	97	30	--	127
Manganese	70	--	--	70
Cobalt	25	--	--	25
Mixed oxides	82	--	--	82
Low cost materials	111	88	--	199
TOTAL	2890	278	284	3452

Table 6. Summary of oxygen-carrier particles prepared and tested for CLOU application

Metal oxide 1 (wt%)	Metal oxide 2 (wt%)	Support material	Preparation method	Facility	Reacting fuel	Reference
CuO						
60		Al_2O_3	FG	bFB	CH_4, coke, air	[57]
40		ZrO_2	FG	bFB	Coke, coal, char, air	[319,320]
n.a.		SiO_2	n.a.	TGA, bFB	Coke, N_2, air	[321]
15		γ-Al_2O_3	IMP	TGA	N_2, CO_2, air	[322]
15		$MgAl_2O_4$	IMP	TGA	N_2, CO_2, air	[322]
33		γ-Al_2O_3	IMP	TGA	N_2, CO_2, air	[322]
80		Al_2O_3	MM+PE	TGA	N_2, CO_2, air	[322]
60		Al_2O_3	MM+PE	TGA	N_2, CO_2, air	[322]
80		Sepiolite	MM+PE	TGA	N_2, CO_2, air	[322]
80		SiO_2	MM+PE	TGA	N_2, CO_2, air	[322]
80		TiO_2	MM+PE	TGA	N_2, CO_2, air	[322]
80		ZrO_2	MM+PE	TGA	N_2, CO_2, air	[322]
60		$MgAl_2O_4$	MM+PP	TGA, bFB	N_2, CO_2, air	[322]
60		ZrO_2	MM+PP	TGA, bFB	N_2, CO_2, air	[322]
40		ZrO_2	MM+PP	TGA, bFB	N_2, CO_2, air	[322]
60		Sepiolite	MM+PP	TGA, bFB	N_2, CO_2, air	[322]
60		MgO	MM+PP	TGA, bFB	N_2, CO_2, air	[322]
60		$MgAl_2O_4$	SD	CLOU 1500 W	Coal	[323]
Mn_3O_4						
80		SiO_2	FG	bFB	CH_4,air	[253]
Mixed oxides						
Mn_3O_4 (80-60)	Fe_2O_3 (20-40)		FG	bFB	CH_4, air	[253]
Mn_3O_4 (20-80)	Fe_2O_3 (80-20)		SD	bFB, CLOU 300W	CH_4, Coke, coal	[324,325]
Mn_3O_4 (80)	NiO (20)		FG	bFB	CH_4, air	[253]
Perovskites						
$CaMn_{0.875}Ti_{0.125}O_3$			SD+FG	TGA, bFB, CLOU 300 W	CH_4, air	[259,260]
Low cost materials						
Manganese ore				bFB, CLOU 300 W	n.g.	[324]

Table 7. Oxygen carriers tested for CLR applications.

Metal oxide (%)	Support material	Preparation method	Laboratory facilities	Continuous plants	Operation time (h)[a]	Reference
NiO						
18	α-Al_2O_3	IMP		CLR 500 W	36	[182]
			TGA, bFB	CLR 900 W	40	[170,330,331]
21	γ-Al_2O_3	IMP		CLR 500 W	37	[182]
			TGA, bFB	CLR 900 W	40	[170,330,331]
20	$MgAl_2O_4$	FG		CLR 500 W	49	[182]
36	$MgAl_2O_4$	IMP	TGA			[224]
60	$MgAl_2O_4$	FG		CLR 500 W	40	[197]
40	$NiAl_2O_4$ + MgO	SD		CLR 140 kW	18	[195]
35	SiO_2	IMP	TGA, bFB			[224]
40	ZrO_2-MgO	FG	bFB	CLR 500 W	24	[198]
CuO						
43	$MgAl_2O_4$	IMP	TGA			[224]
40	SiO_2	IMP	TGA, bFB			[224,237,329]
Fe_2O_3						
32	$MgAl_2O_4$	IMP	TGA			[224]
40	$MgAl_2O_4$	FG	FxB			[158]
39	SiO_2	IMP	TGA, bFB			[224,237]
Mn_2O_3						
47	SiO_2	IMP	TGA, bFB			[224,237]
46	$MgAl_2O_4$	IMP	TGA			[224]
TOTAL					**284**	

[a] When used in continuous operation units

Table 8. Summary of chemical-looping units with power output higher than 10 kW_{th}.

Location	Unit size kW_{th}	Configuration	Fuel	Oxygen-carrier	Operation time hours[a]	References
Gaseous Fuels						
Chalmers University of Technology, CHALMERS, Sweden	10	Interconnected CFB-BFB	n.g.	NiO, Fe_2O_3	1350	[33,140,168,189]
Institute of Carboquimica, ICB-CSIC, Spain	10	Interconnected BFB-BFB	CH_4	CuO	200	[39,40]
IFP-TOTAL France	10	Interconnected BFB-BFB-BFB	CH_4	NiO	n.a.	[110]
Xi'an Jiaotong University China	10	Interconnected Pressurised CFB-BFB	Coke oven gas	Fe_2O_3/CuO	15	[205]
ALSTOM Power Boilers France	15	Interconnected CFB-BFB	n.g.	NiO	100	[332]
Korean Institute of Energy Research, KIER, Korea	50	Interconnected CFB-BFB (KIER-1) BFB-BFB (KIER-2)	 CH_4 CH_4, CO,H_2	 NiO, CoO NiO, CoO	 28 300	 [37,38] [107,333]
Technical University of Viena, TUWIEN, Austria	120 (CLC) 140 (CLR)	DCFB	CH_4, CO, H_2 CH_4	NiO, ilmenite NiO	>90 20	[167,191,193] [195]
Solid fuels						
Chamers University of Technology, CHALMERS, Sweden	10	Interconnected CFB-BFB	Coal, petcoke	ilmenite	90	[54,207]
Southeast University, China	10	CFB-spouted bed	Coal, biomass	NiO, Fe_2O_3	130	[109,186]
Ohio State University (OSU) Ohio, USA	25	Interconnected Moving bed-Entrained bed	Coal	Fe_2O_3	n.a.	[20,58]
ALSTOM Windsor, Connecticut, USA	65	Interconnected CFB-CFB	Coal	$CaSO_4$	n.a.	[280]
Darmstadt University of Technology, TUD, Germany	1 MW	Interconnected CFB-CFB	Coal	ilmenite	Operational in 2011	[56,334]
ALSTOM Windsor, Connectict, USA	3 MW	Interconnected CFB-CFB	Coal	$CaSO_4$	Operational in 2011	[280,390]

[a] The operation time corresponds to the period with particle circulation at high temperature.

Table 9. Summary of theoretical models for CLC.

	Reference	Oxygen–Carrier and Fuel		Reactor Model [1]		Solid distribution[1]	Reactor Size[2]
Macroscopics Models	Kolbitsch et al. [336]	OC: Fuel:	60 wt% NiO on Al_2O_3 CH_4	**FR&AR:**	Dense bed: single–phase Freeboard: exponential decay	HCD	120 kW_{th}
	Adánez et al. [337,338]	OC: Fuel:	60 wt% CuO on SiO_2 CH_4	**FR:**	Bubbling fluidized bed Dense bed: two phases Freeboard: exponential decay	RTD	6.5 MW_{th}
	Kronberger et al. [339]	OC: Fuel:	60 wt% NiO on Al_2O_3 CH_4	**FR:**	Bubbling fluidized bed Dense bed: two phases Freeboard: exponential decay	PB	10 kW_{th}
	Xu et al. [340]	OC: Fuel:	60 wt% NiO on YSZ H_2	**FR:** **AR:**	Bubbling fluidized bed Fast fluidization regime Dense bed: two phases Riser: core–annulus	PB	45 kW_{th}
	Abad et al. [200]	OC: Fuel:	14 wt% CuO on Al_2O_3 CH_4	**FR:**	Bubbling fluidized bed Dense bed: two phases Freeboard: exponential decay	RTD	10 kW_{th} (v)
	Abad et al. [341]	OC: Fuel:	40 wt% NiO on $NiAl_2O_4$ CH_4	**FR:**	Fast fluidization regime Dense bed: two phases Freeboard: core–annulus	RTD	120 kW_{th} (v)
	Iliuta et al. [164]	OC: Fuel:	15 wt% NiO on Al_2O_3 CH_4	**FR:**	Bubbling fluidized bed Dense bed: three phases Freeboard: no	HCD	batch mode (v)
	Brown et al. [119]	OC: Fuel:	Fe_2O_3 Char	**FR:**	Bubbling fluidized bed Dense bed: two phases Freeboard: no	HCD	batch mode (v)
	Ströhle et al. [334]	OC: Fuel:	Ilmenite Coal	**FR:**	Fast fluidization regime Dense bed: PSR Freeboard: PSR	HCD	1 MW
	Pavone et al [342,343]	OC: Fuel:	Ni coated monolith CH_4	**Alternating step** Flow through channels		--	batch mode
	Pavone et al., [342]	OC: Fuel:	Ni coated monolith CH_4	**Rotating reactor** Flow through channels		--	Continuous operation
	Noorman et al. [116, 117]	OC: Fuel:	CuO on Al_2O_3 CH_4	**Alternating step** Packed Bed		--	batch mode (v)
CFD Models	Deng et al. [344,345] and Jin et al. [346]	OC: Fuel:	$CaSO_4$ H_2	**FR:**	Bubbling fluidized bed Freeboard: no	HCD	batch mode
	Jung and Gamwo [347] Shuai et al. [348]	OC: Fuel:	58 wt% NiO on bentonite CH_4	**FR:**	Bubbling fluidized bed Freeboard: no	HCD	batch mode
	Cloete et al. [349]	OC: Fuel:	58 wt% NiO on bentonite CH_4	**FR:** **AR:**	Bubbling fluidized bed Freeboard: no Riser	HCD	12 kW_{th}
	Kruggel-Emden et al. [350]	OC: Fuel:	40 wt% Mn_3O_4 on Mg-ZrO_2 CH_4	**FR:** **AR:**	Bubbling fluidized bed Freeboard: no Riser	HCD	125 kW_{th}
	Mahalatkar et al. [351]	OC: Fuel:	40 wt% Mn_3O_4 on Mg-ZrO_2 CH_4	**FR:**	Bubbling fluidized bed Freeboard: no	HCD	0.3 kW_{th} (v)
	Mahalatkar et al. [352,353]	OC: Fuel:	Fe–Ni on bentonite CH_4	**FR:**	Bubbling fluidized bed Freeboard: no	HCD	1 kW_{th} (v)
	Mahalatkar et al. [354]	OC: Fuel:	60 wt% Fe_2O_3 on $MgAl_2O_4$ Coal	**FR:**	Bubbling fluidized bed Freeboard: no	HCD	batch mode (v)

[1] AR: air–reactor; FR: fuel–reactor; CFD: computing fluid dynamic; PSR: perfectly stirred reactor; RTD: residence time distribution; PB: population balance; HCD: homogenous conversion distribution

[2] v: validated against experimental results

Table 10. Algebraic expressions for different reactions models in the particle. L_p and L_g: characteristic length of the particle and grain, respectively; F_p and F_g: shape factor for particle and grain, respectively (F_i = 1 for plates, F_i = 2 for cylinders, and F_i = 3 for spheres).

External diffusion to the particle	
$f_{F_p}(X) = X$	$\tau_{film,p} = \dfrac{\rho_m L_p}{F_p b k_g C_g}$
Internal diffusion in the particle	
Spherical particles with constant size $p_{F_p}(X) = 1 - 3(1-X)^{2/3} + 2(1-X)$	
Spherical particles changing its size during reaction $p_{F_p}(X) = 3\left[1 - (1-X)^{2/3} + \dfrac{1 - \left[Z + (1-Z)(1-X)^{2/3}\right]}{Z-1}\right]$	$\tau_{pl,p} = \dfrac{\rho_m L_p^2}{2F_p b D_g C_g}$
Diffusion in the product layer around a grain	
Spherical grains with constant size $p_{Fg}(X) = 1 - 3(1-X)^{2/3} + 2(1-X)$	
Spherical grains changing its size during reaction $p_{F_g}(X) = 3\left[1 - (1-X)^{2/3} + \dfrac{1 - \left[Z + (1-Z)(1-X)^{2/3}\right]}{Z-1}\right]$	$\tau_{pl,g} = \dfrac{\rho_m L_g^2}{2F_g b D_s C_g}$
Chemical reaction in the grain	
$g_{Fg}(X) = 1 - (1-X)^{1/F_g}$	$\tau_{reac,g} = \dfrac{\rho_m L_g}{b k_s C_g}$

Table 11. Summary of kinetic data determined for oxygen-carriers

Oxygen–Carrier		Experimental conditions	Kinetic Model	Reference
60 wt% NiO on YSZ	d_p = 1.0–3.0 mm	TGA T = 800–1000 ºC	SCM(reacc+pl) with F_g = 3	[221]
R_{OC} = 12.9%	ε = 35.2%	100 vol% H_2	n = 1.0 E_r = 82 kJ/mol	
		21 vol% O_2	n = 1.0 E_r = 17 kJ/mol	
58 wt% NiO on bentonite	d_p = 80 μm	TGA T = 600–750 ºC	SCM(reacc) with F_g = 3	[222]
R_{OC} = 12.2%	ε = 64.5%	5 vol% CH_4	n = n.a. E_r = 37 kJ/mol	
78 wt% NiO on bentonite	d_p = 80 μm	TGA T = 600–750 ºC	SCM(pl) with F_g = 3	[222]
R_{OC} = 16.4%	ε = 79.5%	21 vol% O_2	n = n.a. E_{pl} = 131 kJ/mol	
60 wt% NiO on bentonite	d_p = 106–150 μm	TGA T = 700–1000 ºC	Red.: MVM Ox.: SCM	[108]
R_o = 12.9%	ε = n.a.	10 vol% CH_4	n = n/a E_r = 57 kJ/mol	
		10 vol% O_2	n = n/a E_r = 2.4 kJ/mol	
60 wt% NiO on $NiAl_2O_4$	d_p = 90–210 μm	TGA T = 750 ºC	ChRSM	[377]
R_{OC} = 12.9%	ε = n.a.	3–15 vol% CH_4	n = 0.75 E_r = n.a.	
		3–15 vol% H_2	n = 1.0 E_r = n.a.	
		5–15 vol% O_2	n = 1.0 E_r = n.a.	
60 wt% NiO on Al_2O_3	d_p = 90–250 μm	TGA T = 600–950 ºC	SCMg(reacc) with F_g = 3	[124,232]
R_{OC} = 8.6%	ε = 36%	5–70 vol% CH_4	n = 0.8 E_r = 78 kJ/mol	
		5–70 vol% H_2	n = 0.5 E_r = 26 kJ/mol	
		5–70 vol% CO	n = 0.8 E_r = 25 kJ/mol	
		5–21 vol% O_2	n = 0.2 E_r = 7 kJ/mol	
60 wt% NiO on $MgAl_2O_4$	d_p = 125–180 μm	TGA T = 800–1000 ºC	SCMg(reacc) with F_g = 3	[376]
R_{OC} = 10.7%	ε = 36%	5–20 vol% CH_4	n = 0.4 E_r = 114 kJ/mol	
		3–15 vol% O_2	n = 1.0 E_r = 40 kJ/mol	
NiO on Al_2O_3	d_p = 70 μm	TPR-TPO T = 200–700 ºC	RNM	[217]
R_{OC} = n.a.	ε = n.a.	5 vol% H_2	n = n.a. E_r = 53 kJ/mol	
		5 vol% O_2	n = n.a. E_r = 45 kJ/mol	
NiO on Co–Al_2O_3	d_p = 70 μm	TPR-TPO T = 200–700 ºC	RNM	[217,218]
R_{OC} = n.a.	ε = n.a.	CH_4	n = n.a. E_r = 49 kJ/mol	
		5 vol% H_2	n = n.a. E_r = 45 kJ/mol	
		5 vol% O_2	n = n.a. E_r = 44 kJ/mol	
20 wt% NiO on Al_2O_3	d_p = 10–110 μm	CREC–RS T = 600–680 ºC	RNM	[214]
R_{OC} = 4.2%	ε = n.a.	CH_4	n = 1.0 E_r = 44 kJ/mol	
40 wt% NiO on $NiAl_2O_4$	d_p = 125–425 μm	TPR T = 300–600 ºC	DRM	[374]
R_{OC} = 8.4%	ε = n.a.	20 vol% H_2	n = n.a. E_r = 96 kJ/mol	
65 wt% NiOon Al_2O_3	d_p = 90–106 μm	TGA T = 800–950 ºC	SCMg(reacc) with F_g = 3	[379]
R_{OC} = 13.6%	ε = 34%	20–70 vol% CH_4	n = 0.4 E_r = 55 kJ/mol	
		20–70 vol% H_2	n = 0.6 E_r = 28 kJ/mol	
		20–70 vol% CO	n = 0.8 E_r = 28 kJ/mol	
15 wt% NiO on Al_2O_3	d_p = 140 μm	Fixed Bed T = 600–900 ºC	MVM	[164]
R_{OC} = 3.2%	ε = n.a.	100 vol% CH_4	n = 1.0 E_r = 77 kJ/mol	
		H_2 appearing during reaction	n = 1.0 E_r = 26 kJ/mol	
		CO appearing during reaction	n = 1.0 E_r = 27 kJ/mol	
40 wt% NiO on $NiAl_2O_4$	d_p = 90–212 μm	TGA T = 750–1000 ºC	SCMg(reacc) with F_g = 3	[341]
R_{OC} = 8.4%	ε = n.a.	5–50 vol% CH_4	n = 0.6 E_r = 70 kJ/mol	
		5–50 vol% H_2	n = 0.8 E_r = 35 kJ/mol	
		5–50 vol% CO	n = 0.8 E_r = 34 kJ/mol	
18 wt% NiO on α-Al_2O_3	d_p = 100–300 μm	TGA T = 700–950 ºC		[94]
R_{OC} = 3.8%	ε = 42%	NiO reduction:	ChRSM	
		5–20 vol% CH_4	n = 0.8 E_r = 137 kJ/mol	
		5–50 vol% H_2	n = 0.8 E_r = 20 kJ/mol	
		5–50 vol% CO	n = 0.8 E_r = 18 kJ/mol	
		$NiAl_2O_4$ reduction:	SCMg(reacc) with F_g = 3:	
		5–20 vol% CH_4	n = 1.7 E_r = 137 kJ/mol	
		5–50 vol% H_2	n = 0.6 E_r = 235 kJ/mol	
		5–50 vol% CO	n = 0.7 E_r = 82 kJ/mol	
		Ni oxidation:	ChRSM	
		5–21 vol% O_2	n = 0.8 E_r = 24 kJ/mol	
21 wt% NiO on γ-Al_2O_3	d_p = 100–300 μm	TGA T = 700–950 ºC		[96]
R_{OC} = 4.4%	ε = 50%	NiO reduction:	ChRSM	
		5–20 vol% CH_4	n = 0.8 E_r = 137 kJ/mol	
		5–50 vol% H_2	n = 0.8 E_r = 20 kJ/mol	
		5–50 vol% CO	n = 0.8 E_r = 18 kJ/mol	
		$NiAl_2O_4$ reduction:	SCMg(reacc) with F_g = 3	
		5–20 vol% CH_4	n = 1.0 E_r = 373 kJ/mol	
		5–50 vol% H_2	n = 0.6 E_r = 237 kJ/mol	
		5–50 vol% CO	n = 1.0 E_r = 89 kJ/mol	
		Ni oxidation:	ChRSM	
		5–21 vol% O_2	n = 1.0 E_r = 22 kJ/mol	

Oxygen–Carrier		Experimental conditions	Kinetic Model	Reference
60 wt% CuO on SiO_2 R_{OC} = 12.0%	d_p = 0.8–1.2 mm ε = 40%	TGA T = 700–850 ºC 100 vol% CH_4	SCMg(reacc) with F_g = 3 n = 1.0 E_r = 41 kJ/mol	[337]
10 wt% CuO on Al_2O_3 R_{OC} = 2.0%	d_p = 100–300 µm ε = 57%	TGA T = 600–800 ºC 5–70 vol% CH_4 5–70 vol% H_2 5–70 vol% CO 5–21 vol% O_2	SCMg(reacc) with F_g = 1 n = 0.4 E_r = 60 kJ/mol n = 0.6 E_r = 33 kJ/mol n = 0.8 E_r = 14 kJ/mol n = 1.0 E_r = 15 kJ/mol	[126]
82 wt% CuO on Al_2O_3 R_{OC} = 16%	d_p = 355–500 µm ε = 75%	Fluid. bed T = 250–900 ºC 2–10 vol% H_2 ($CuO \rightarrow Cu_2O$) 2–10 vol% H_2 ($Cu_2O \rightarrow Cu$) 2–10 vol% CO 2–10 vol% O_2 ($Cu \rightarrow Cu_2O$) 2–10 vol% O_2($Cu_2O \rightarrow CuO$)	DRM n = 1.0 E_r = 58 kJ/mol n = 1.0 E_r = 44 kJ/mol n = 1.0 E_r = 52 kJ/mol n = 1.0 E_r = 40 kJ/mol n = 1.0 E_r = 60 kJ/mol	[180,380,381]
62 wt% CuO on Al_2O_3 R_{OC} = 12.4%	d_p = 90–106 µm ε = 60%	TGA T = 600–800 ºC 20–70 vol% H_2 20–70 vol% CO	SCMg(reacc) with F_g = 1 n = 0.55 E_r = 30 kJ/mol n = 0.8 E_r = 16 kJ/mol	[379]
14 wt% CuO on Al_2O_3 R_{OC} = 2.8%	d_p = 100–500 µm ε = 53%	TGA T = 600–800 ºC 5–70 vol% CH_4 5–70 vol% H_2 5–70 vol% CO	SCMg(reacc) with F_g = 1 n = 0.5 E_r = 106 kJ/mol n = 0.5 E_r = 20 kJ/mol n = 0.8 E_r = 11 kJ/mol	[200]
60 wt% Fe_2O_3 on bentonite R_{OC} = 2.0%	d_p = 106–150 µm ε = n.a.	TGA T = 700–1000 ºC 10 vol% CH_4 10 vol% O_2	Red.: MVM Ox.: SCM n = n.a. E_r = 29 kJ/mol n = n.a. E_r = 6.0 kJ/mol	[108]
60 wt% Fe_2O_3 on Al_2O_3 R_{OC} = 4.1%	d_p = 90–250 µm ε = 30%	TGA T = 600–950 ºC 5–70 vol% CH_4 5–70 vol% H_2 5–70 vol% CO 5–21 vol% O_2	SCMg(reacc) with F_g = 3 n = 1.3 E_r = 49 kJ/mol n = 0.5 E_r = 24 kJ/mol n = 1.0 E_r = 20 kJ/mol n = 1.0 E_r = 14 kJ/mol	[124,232]
58 wt% Fe_2O_3on Al_2O_3 R_{OC} = 4.0%	d_p = 90–106 µm ε = 32%	TGA T = 800–850 ºC 20–70 vol% CH_4 20–70 vol% H_2 20–70 vol% CO	SCMg(reacc) with F_g = 3 n = 0.2 E_r = 25 kJ/mol n = 0.85 E_r = 22 kJ/mol n = 1.0 E_r = 19 kJ/mol	[379]
Fe_2O_3 R_{OC} = 3.3%	d_p = 300–425 µm ε = 60%	Fluid. bed T = 250–900 ºC 1–9 vol% CO	DRM n = 1.0 E_r = 75 kJ/mol	[382]
40 wt% Mn_3O_4 on Mg–ZrO_2 R_{OC} = 2.8%	d_p = 125–180 µm ε = 39%	TGA T = 800–1000 ºC 5–25 vol% CH_4 3–15 vol% O_2	ChRSM n = 1.0 E_r = 119 kJ/mol n = 0.65 E_r = 20 kJ/mol	[376]
Calcined Ilmenite (Fe_2TiO_5) R_{OC} = 4.0%	d_p = 150–300 µm ε = 1.2%	TGA T = 800–850 ºC 5–50 vol% CH_4 5–50 vol% H_2 5–50 vol% CO 5–21 vol% O_2	SCMg(reacc) with F_g = 3 n = 1.0 E_r = 165 kJ/mol n = 1.0 E_r = 109 kJ/mol n = 1.0 E_r = 113 kJ/mol n = 1.0 E_r = 12 kJ/mol	[296]
Activated Ilmenite (Fe_2TiO_5) R_{OC} = 3.3%	d_p = 150–300 µm ε = 35%	TGA T = 800–850 ºC 5–50 vol% CH_4 5–50 vol% H_2 5–50 vol% CO 5–21 vol% O_2	SCMg(reacc) with F_g = 3 n = 1.0 E_r = 136 kJ/mol n = 1.0 E_r = 65 kJ/mol n = 0.8 E_r = 80 kJ/mol n = 1.0 E_r = 25 kJ/mol	[296]
$CaSO_4$ R_{OC} = 47%	d_p = 8.9 µm ε = n.a.	TPR T = 850–1200 ºC 20 vol% CO	AEM with ν = 2 n = n.a. E_r = 280 kJ/mol	[273]
$CaSO_4$ R_{OC} = 44%	d_p = 150–200 µm ε = n.a.	Fixed bed T = 880–950 ºC 20–70 vol% CO	SCM(reacc+pl) with F_g = 2 n = n.a. E_r = 145 kJ/mol E_{pl} = 162 kJ/mol	[274]

Table 12. Algebraic equations for the characteristic reactivity for different time dependent conversion of the reaction *i*, X_i, i.e. reduction or oxidation.

Type of kinetic equation	Characteristic reactivity	δ in Eq. (67)
$\frac{t}{\tau} = X_s$	$\Phi_j = 1 - \exp\left(-\frac{\left(1 - \bar{X}_{s,in}\right)}{\Delta X_s} \Phi_j \right)$	1
$\frac{t}{\tau} = 1 - \left(1 - X_s\right)^{1/3}$	$\Phi_j = 3\left[1 - \bar{X}_{s,in}^{2/3} \exp\left(-\frac{\left(1 - \bar{X}_{s,in}^{1/3}\right)}{\Delta X_s} \Phi_j \right) \right] - \frac{6\Delta X_s}{\Phi_j} \left[1 - \bar{X}_{s,in}^{1/3} \exp\left(-\frac{\left(1 - \bar{X}_{s,in}^{1/3}\right)}{\Delta X_s} \Phi_j \right) \right] + \frac{6\Delta X_s^2}{\Phi_j^2} \left[1 - \exp\left(-\frac{\left(1 - \bar{X}_{s,in}^{1/3}\right)}{\Delta X_s} \Phi_j \right) \right]$	3
$\frac{t}{\tau} = -\ln\left(1 - X_s\right)$	$\Phi_j = \frac{\Phi_j}{\Phi_j + \Delta X_s} \left[1 - \exp\left(\frac{\Delta X_s + \Phi_j}{\Delta X_s} \ln\left(\bar{X}_{s,in} \right) \right) \right]$	1

Captions of Figures

Fig. 1. General scheme of a Chemical-Looping Combustion system for gaseous fuels.

Fig. 2. Possible reactor concepts for Chemical-Looping Combustion: a) interconnected fluidized-bed reactors; b) alternating fixed bed reactors; and c) rotating reactor, taken from Hakonsem et al. [121].

Fig. 3. Equilibrium constant, K_{eq}, for the reduction reaction with H_2 and CO with different redox systems.

Fig. 4. Oxygen transport capability, R_O, of different redox systems.

Fig. 5. Circulation rates of the oxygen-carrier necessary to fulfill the oxygen mass balance as a function of the variation in solids conversion, ΔX_s, oxygen transport capacity, R_{OC}, and fuel gas. Upper limit in the circulation flow rate determined by riser transport capacity: − − - (adapted from [124]).

Fig. 6. Temperature variation in the fuel-reactor as a function of the mass conversion, ω, for redox systems usually considered in CLC when CH_4 or syngas (45 % CO, 30 % H_2, 10 % CO_2, 15 % H_2O) is used as fuel. Data collected from [122,124,127,128].

Fig. 7. SEM photographs of oxygen-carriers prepared by large-scale methods: (a) impregnation, taken from [40]; and (b) spray drying, taken from [43].

Fig. 8. Average annual cost of materials used for oxygen-carriers preparation. SfC: spot for cathodes; LME: London Metal Exchange. Data taken from [135]

Fig. 9. Effect of sulfur on the CO_2 concentration from the fuel-reactor of a 500 W_{th} CLC unit. Fuel gas: 30 vol% CH_4 with different amounts of H_2S. Oxygen-carrier: 18 wt% NiO on Al_2O_3 prepared by impregnation. T_{FR} = 870 ºC, T_{AR} = 950 ºC. (Data taken from [45]).

Fig. 10. Schematic layout of different alternatives to process solid fuels in a CLC system: (a) previous gasification of the solid fuel (syngas–CLC); and (b) feeding of solid fuel to the fuel-reactor (solid fuelled–CLC).

Fig. 11. Main processes involved in fuel-reactor for the three different options proposed for solid fuel processing in a CLC system.

Fig. 12. Reactor scheme of the iG-CLC process for solid fuel using two interconnected fluidized bed reactors.

Fig. 13. Equilibrium partial pressure of gas-phase O_2 over the metal oxide systems CuO/Cu_2O, Mn_2O_3/Mn_3O_4 and Co_3O_4/CoO as a function of temperature.

Fig. 14. Schemes of the reactor system for the (a) Steam Reforming integrated with Chemical-Looping Combustion (SR-CLC); and (b) Autothermal Chemical Looping Reforming (a-CLR). (1) air reactor, (2) fuel reactor, (3) cyclone for particle separation, (4) and (5) loop seals fluidized with steam. (Adapted from [51])

Fig. 15. Effect of $NiO_{reacted}/CH_4$ molar ratio on the gas product composition for both oxygen-carriers. Filled dots: NiO18-αAl_2O_3. Empty dots: NiO21-γAl_2O_3. Lines: thermodynamic equilibrium data. (□, ■, ·····): H_2O/CH_4 = 0, (○, ●, -----): H_2O/CH_4 = 0.3, (Δ, ▲, ——): H_2O/CH_4 = 0.5. T = 900 ºC. (Data taken from [170])

Fig. 16. Main Chemical-Looping Combustion pilot plants for gas and solid fuels with power higher than $10kW_{th}$.

Fig. 17. Predictions of solids distribution by CFD model in two interconnected fluidized beds, as proposed for CLC. (Taken from [363])

Fig. 18. Scheme of different reaction models in the particle: a) Changing grain size model (CGSM); b) Shrinking core model (SCM); and c) nucleation and nuclei growth model, as described in [218].

Fig. 19. Effect of particle size on the maximum particle temperature reached during the CLC reactions with Ni-, Co-, Cu-, Fe-, and Mn-based oxygen-carriers. Data taken from [373].

Fig. 20. Effect of total pressure on the decrease of the pre-exponential factor for several oxygen-carriers and reducing gases, k_P being the kinetic constant at pressure P and k at atmospheric pressure. Continuous line: fitting of data for reduction of NiO with CO. Data taken from [236].

Fig. 21. Triangular diagram to calculate the characteristic reactivity, Φ_j, as a function of $\overline{X}_{o,inFR}$ and ΔX_s. Spherical geometry of particles or grains.

Fig. 22. Concentration of solids, C_s, and gases in the fuel-reactor by using a) macroscopic model (showing also the combustion efficiency, η_C), taken from [200]; and b) CFD model, taken from [352].

Fig. 23. Minimum solids inventory in the fuel-reactor, m_{FR}, air-reactor, m_{AR}, and total, m_{tot}, as a function of a) the solid conversion at the inlet of the fuel-reactor ($X_{o,inFR}$), (data taken from [376] and b) the variation of the solid conversion between the fuel- and air-reactor, ΔX_s (data taken from [124]). The solids inventories are calculated without considering the gas exchange resistance processes in the reactors. Figure b) also shows the corresponding solids circulation flow rate.

Fig. 24. Total solids inventory in the fuel- and air-reactors for the combustion of 1 MW_{th} of CH_4. Oxygen-carrier: Ni40Al-FG (data taken from [124]). Discontinuous line: minimum solids inventory at a certain ΔX_s value. The solids inventory is calculated without considering the gas exchange resistance processes in the reactors.

Fig. 25. Prediction from a macroscopic model of the solids inventory in the fuel-reactor (bubbling fluidized-bed) to reach a combustion efficiency of 99.9% CH_4 as a function of the solids circulation flow rate and the reactor temperature. Oxygen-carrier: Cu14Al-I. (Data taken from [200])

Fig. 26. Comparison net plant efficiency using a CLC combined cycle composed by 1 set of reactors (CLCCC), two sets of reactors (SR-CLCCC), or three sets of reactors (DR-CLCCC) of cycles as a function of the corresponding turbine inlet temperature (TIT). (Data taken from [402])

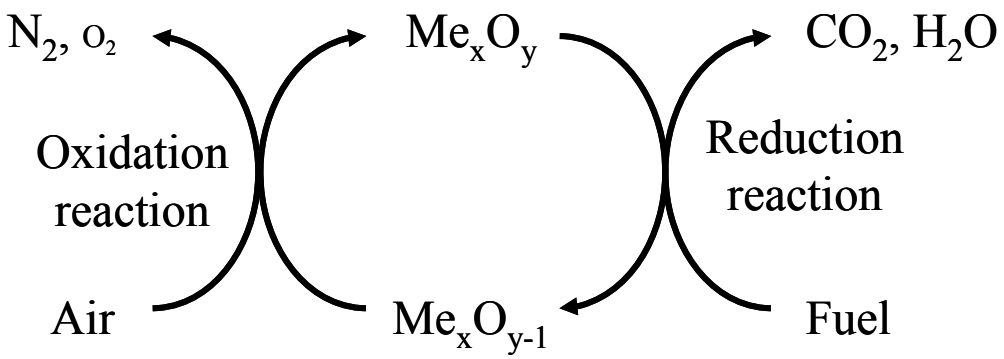

Fig. 1. General scheme of a Chemical-Looping Combustion system for gaseous fuels.

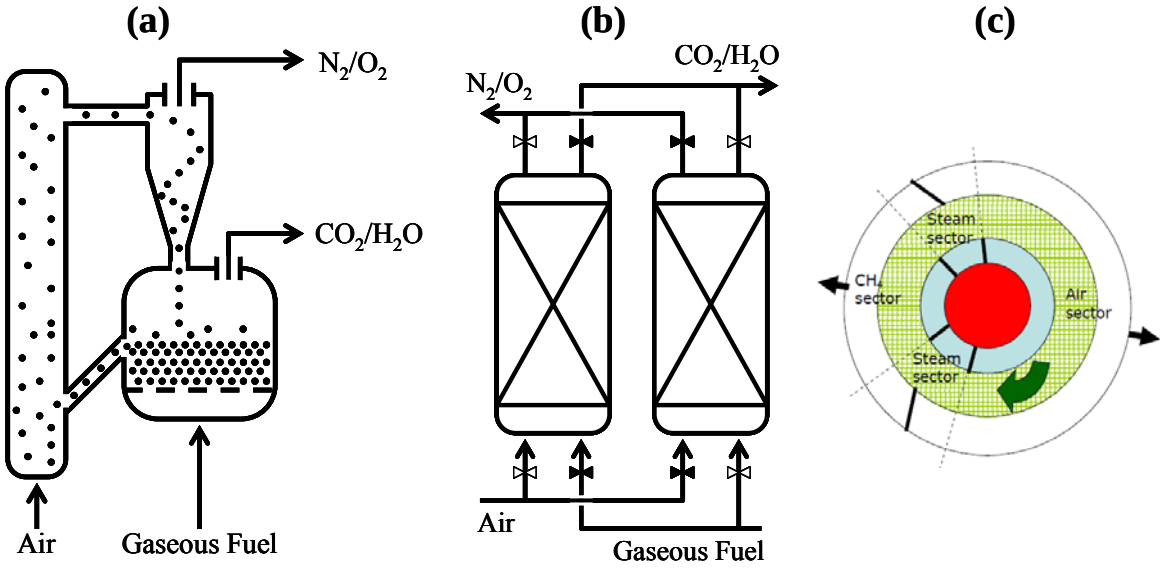

Fig. 2. Possible reactor concepts for Chemical-Looping Combustion: a) interconnected fluidized-bed reactors; b) alternating fixed bed reactors; and c) rotating reactor, taken from Hakonsem et al. [121].

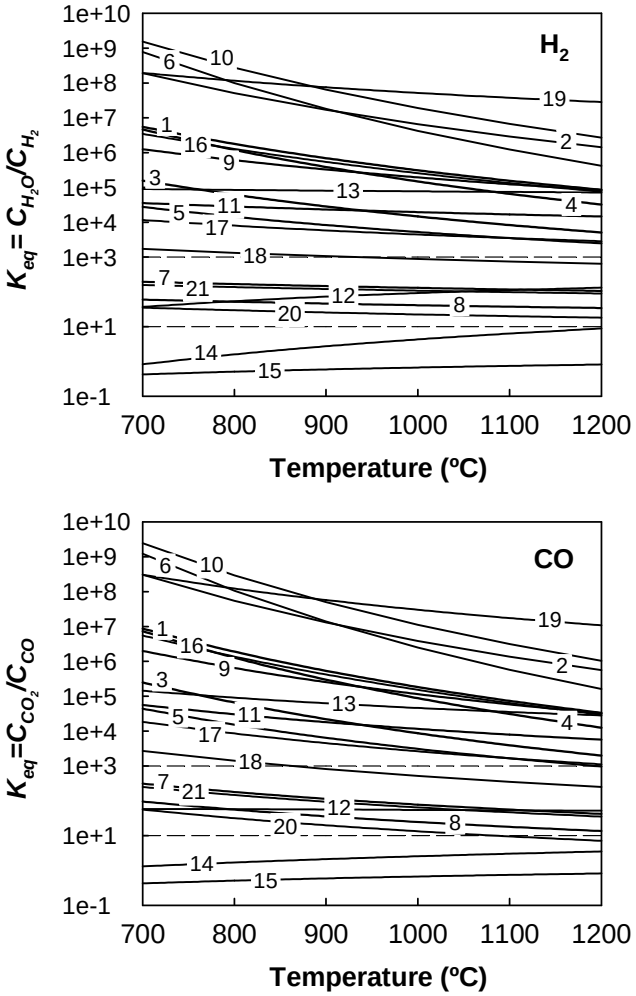

1. $CuO – Cu$
2. $CuO – Cu_2O$
3. $Cu_2O – Cu$
4. $CuAl_2O_4 – Cu{\cdot}Al_2O_3$
5. $CuAlO_2 – Cu{\cdot}Al_2O_3$
6. $CuAl_2O_4 – CuAlO_2$
7. $NiO – Ni$
8. $NiAl_2O_4 – Ni{\cdot}Al_2O_3$
9. $Mn_2O_3 – MnO$
10. $Mn_2O_3 – Mn_3O_4$
11. $Mn_3O_4 – MnO$
12. $Fe_2O_3 – FeO$
13. $Fe_2O_3 – Fe_3O_4$
14. $Fe_3O_4 – FeO$
15. $FeO – Fe$
16. $Fe_2O_3{\cdot}Al_2O_3 – FeAl_2O_4$
17. $Fe_2TiO_5 – FeTiO_3$
18. $Co_3O_4 – Co$
19. $Co_3O_4 – CoO$
20. $CoO – Co$
21. $CaSO_4$ - CaS

Fig. 3. Equilibrium constant, K_{eq}, for the reduction reaction with H_2 and CO with different redox systems.

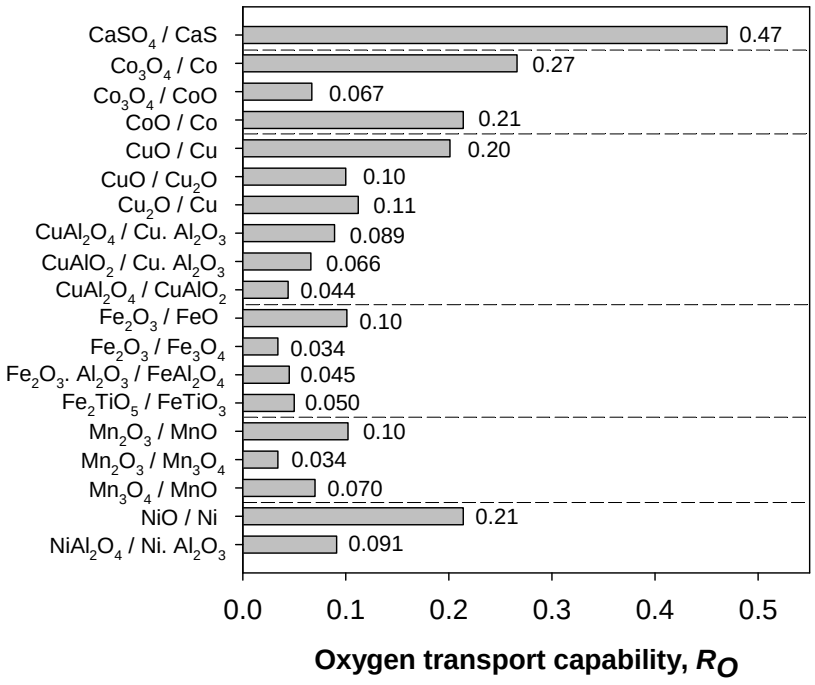

Fig. 4. Oxygen transport capability, R_O, of different redox systems.

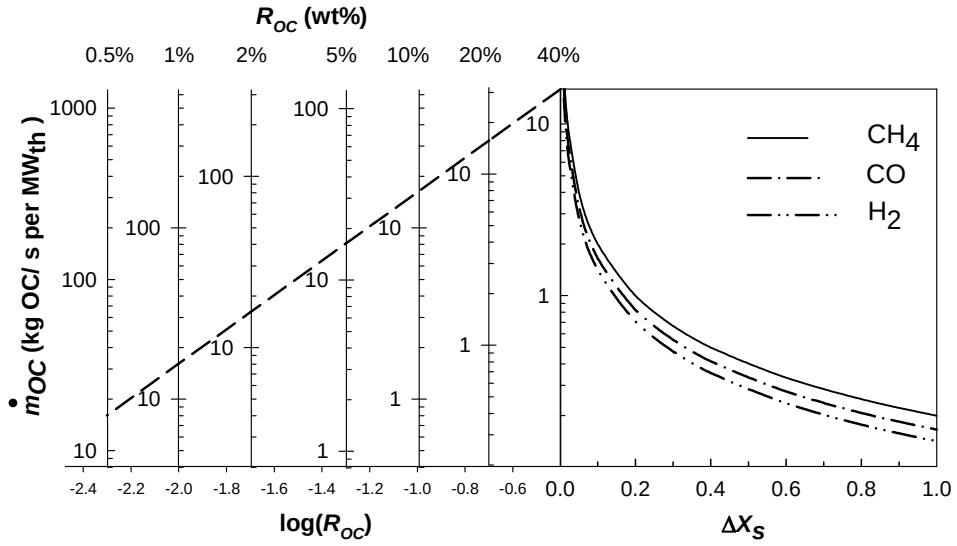

Fig. 5. Circulation rates of the oxygen-carrier necessary to fulfill the oxygen mass balance as a function of the variation in solids conversion, ΔX_s, oxygen transport capacity, R_{OC}, and fuel gas. Upper limit in the circulation flow rate determined by riser transport capacity: – – – (adapted from [124]).

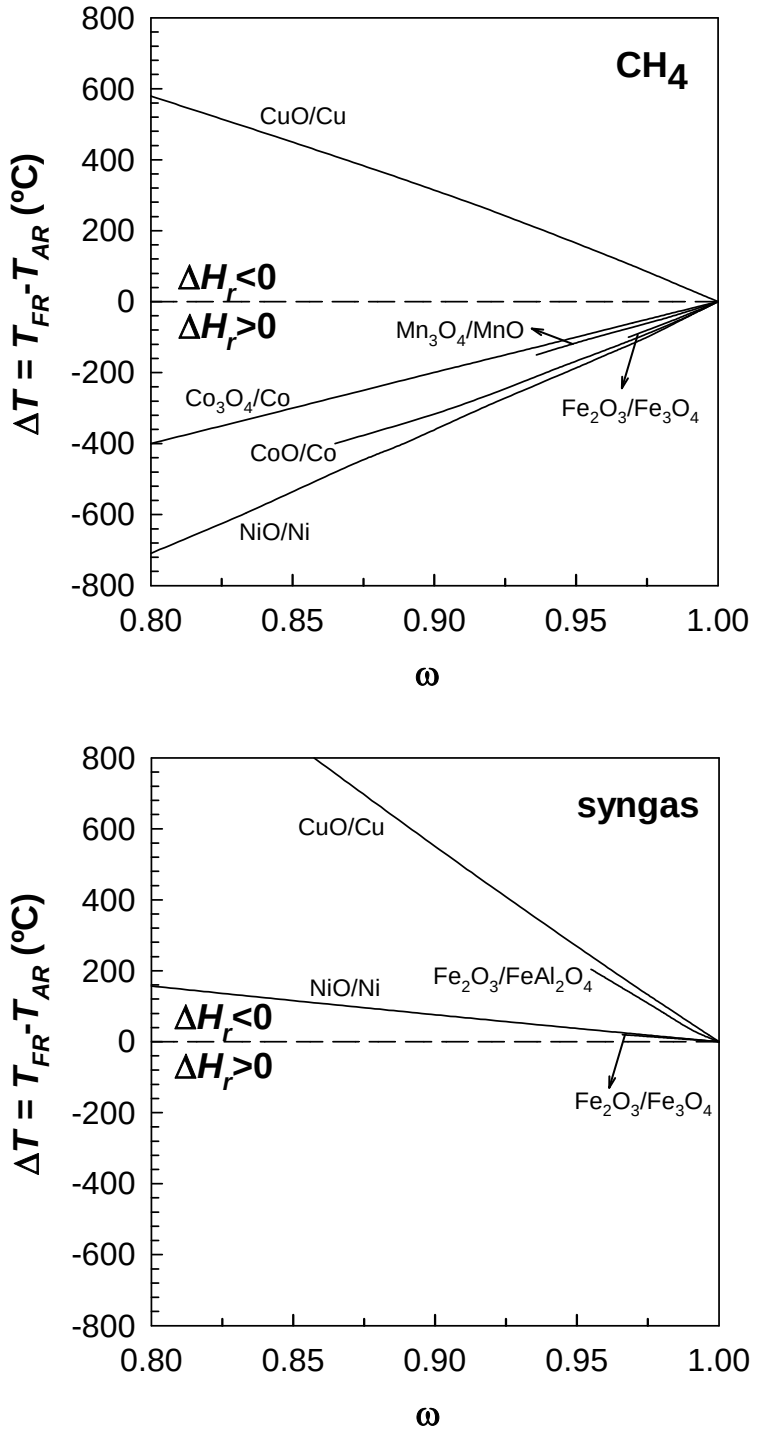

Fig. 6. Temperature variation in the fuel-reactor as a function of the mass conversion, ω, for redox systems usually considered in CLC when CH_4 or syngas (45 % CO, 30 % H_2, 10 % CO_2, 15 % H_2O) is used as fuel. Data collected from [122,124,127,128].

(a) Cu-based impregnated particles

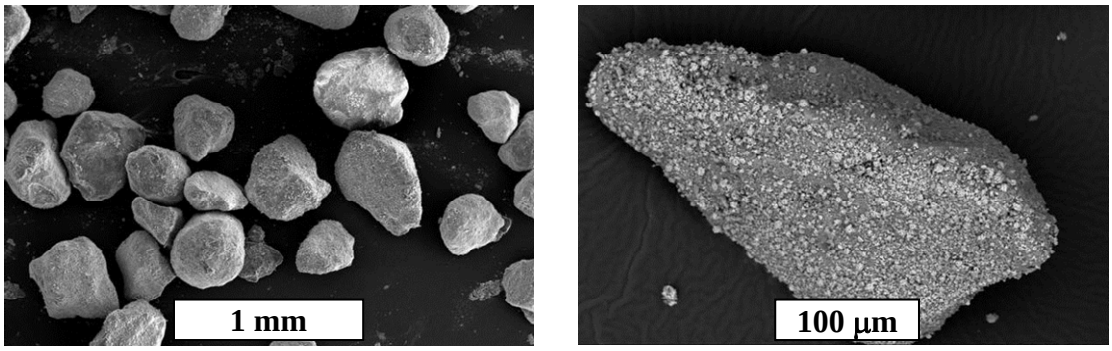

(b) Ni-based spray dryed particles

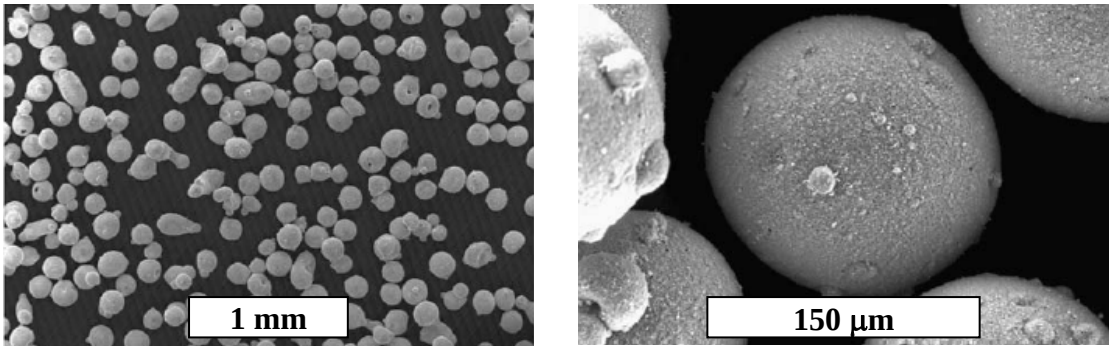

Fig. 7. SEM photographs of oxygen-carriers prepared by large-scale methods: (a) impregnation, taken from [40]; and (b) spray drying, taken from [43].

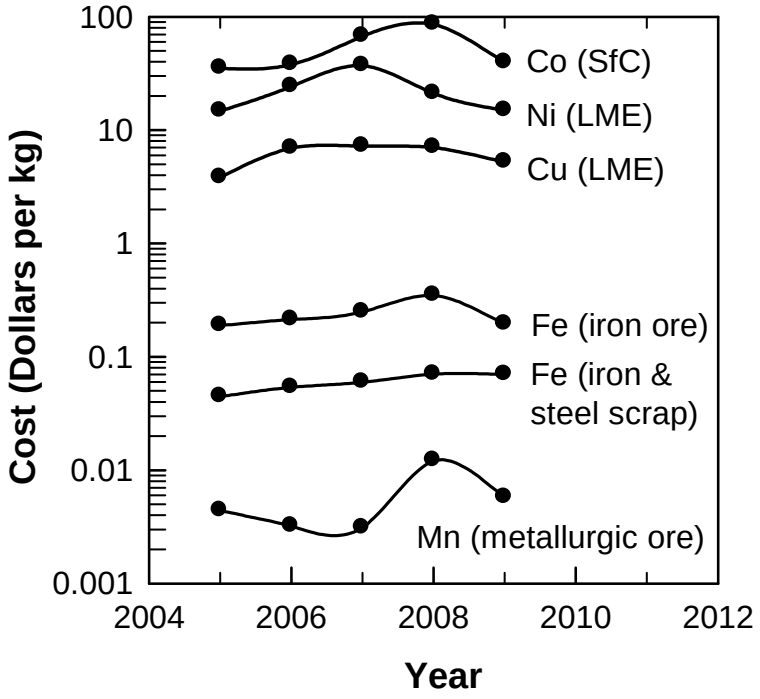

Fig. 8. Average annual cost of materials used for oxygen-carriers preparation. SfC: spot for cathodes; LME: London Metal Exchange. Data taken from [135]

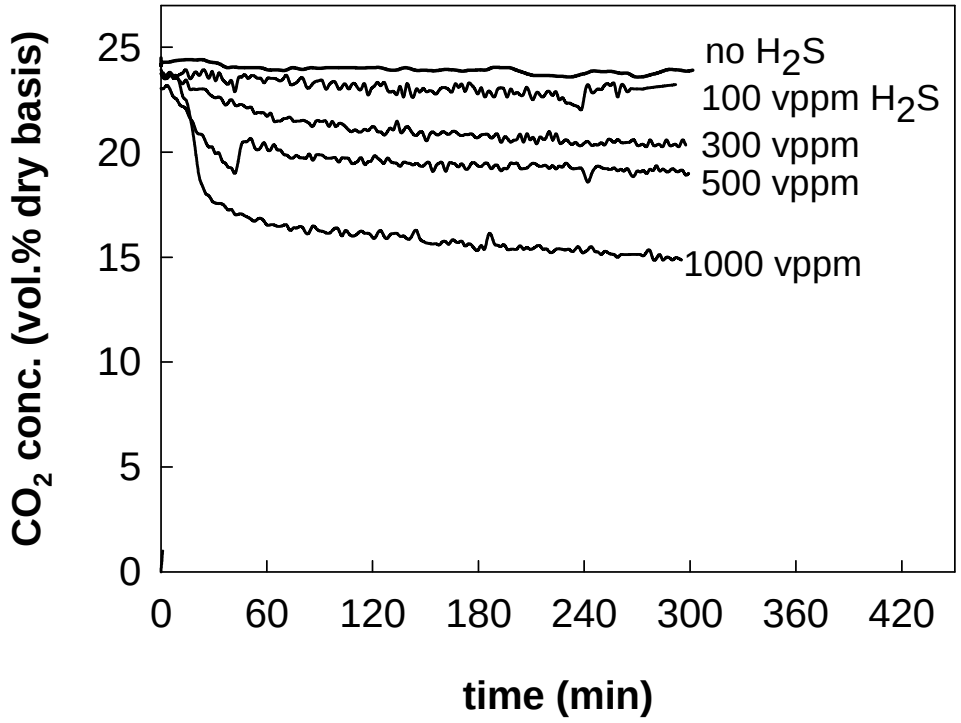

Fig. 9. Effect of sulfur on the CO_2 concentration from the fuel-reactor of a 500 W_{th} CLC unit. Fuel gas: 30 vol% CH_4 with different amounts of H_2S. Oxygen-carrier: 18 wt% NiO on Al_2O_3 prepared by impregnation. T_{FR} = 870 ºC, T_{AR} = 950 ºC. (Data taken from [45]).

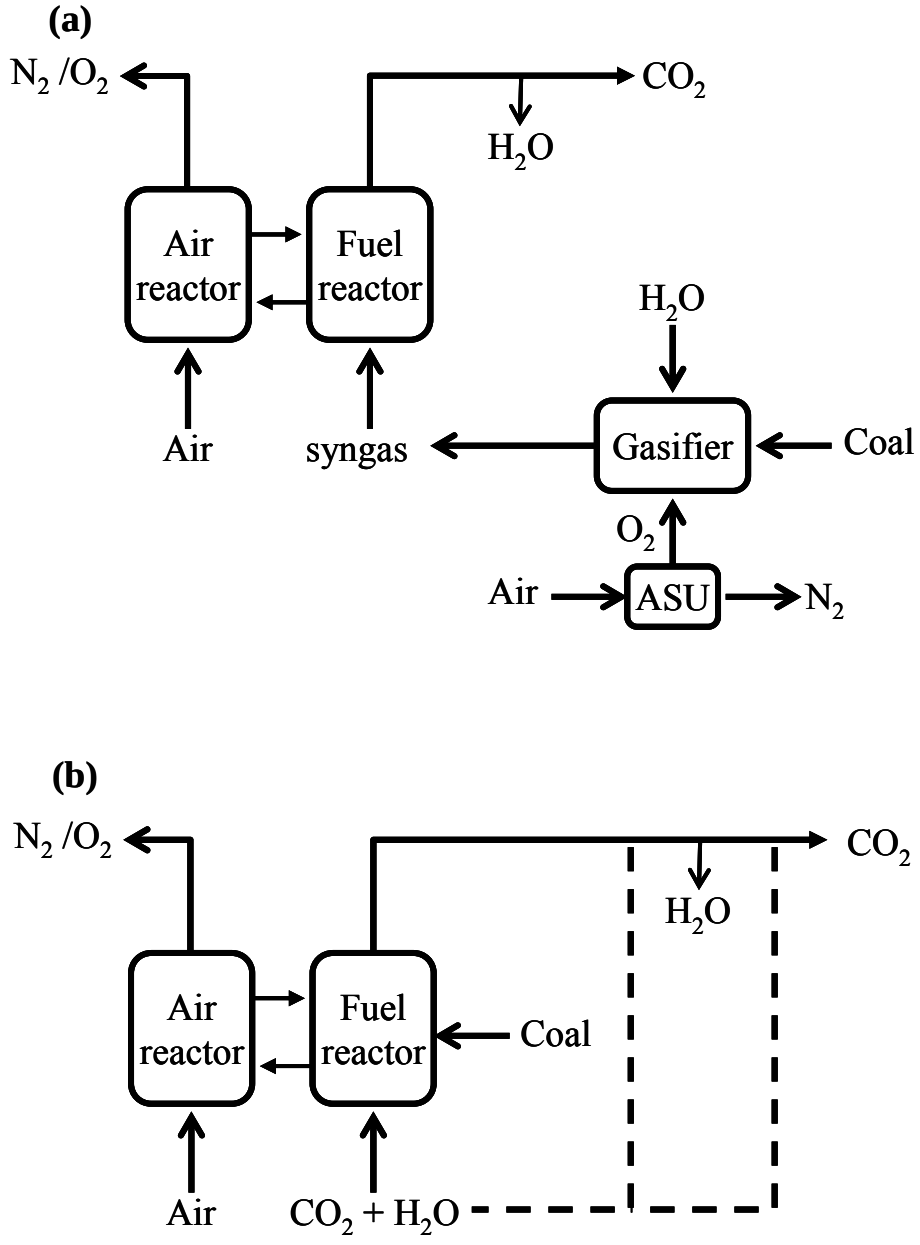

Fig. 10. Schematic layout of different alternatives to process solid fuels in a CLC system: (a) previous gasification of the solid fuel (syngas–CLC); and (b) feeding of solid fuel to the fuel-reactor (solid fuelled–CLC).

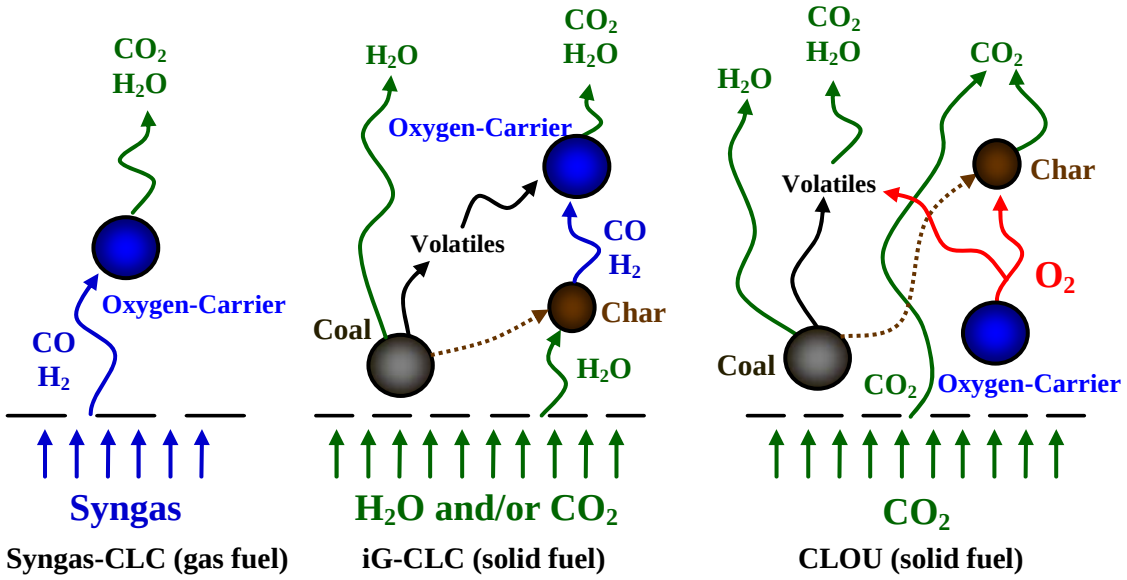

Fig. 11. Main processes involved in fuel-reactor for the three different options proposed for solid fuel processing in a CLC system.

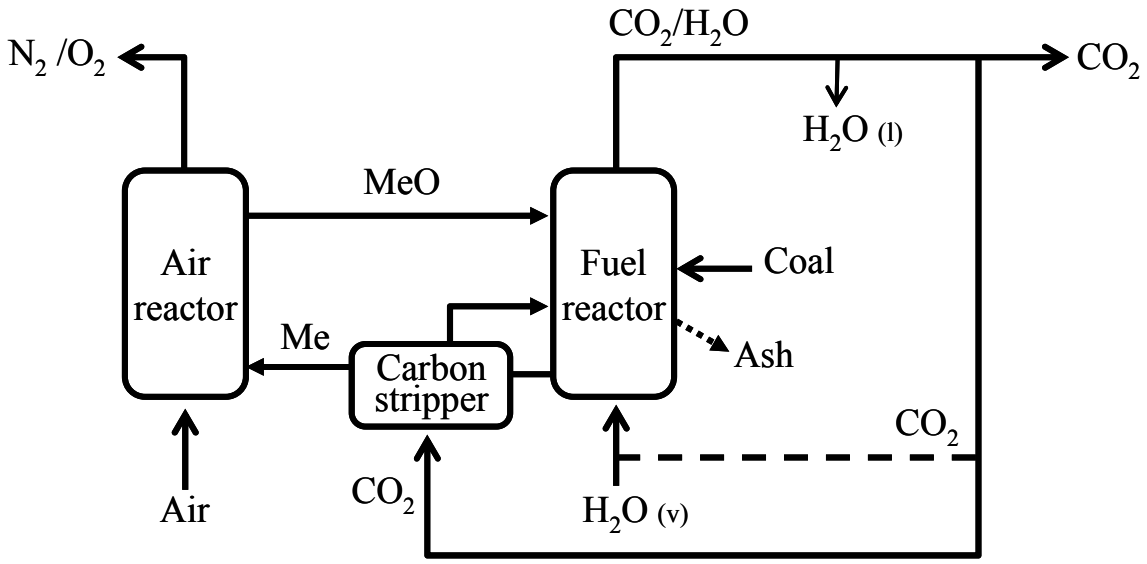

Fig. 12. Reactor scheme of the iG-CLC process for solid fuel using two interconnected fluidized bed reactors.

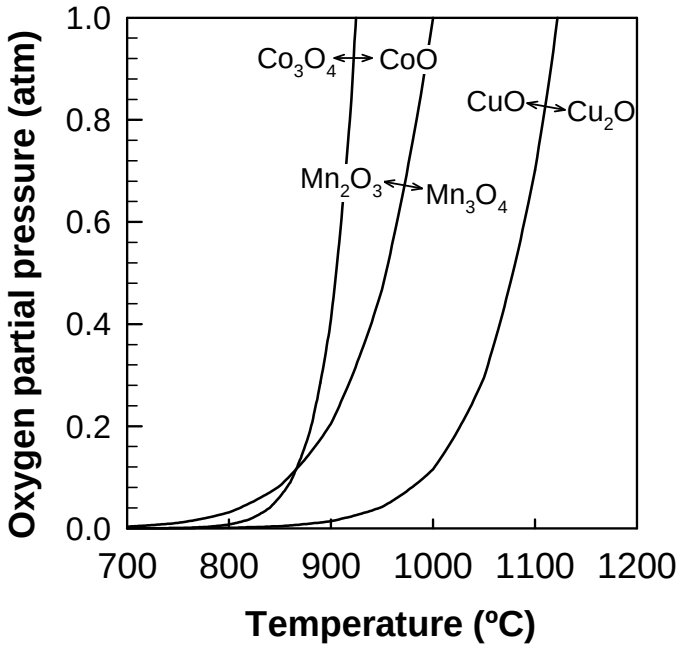

Fig. 13. Equilibrium partial pressure of gas-phase O_2 over the metal oxide systems CuO/Cu_2O, Mn_2O_3/Mn_3O_4 and Co_3O_4/CoO as a function of temperature.

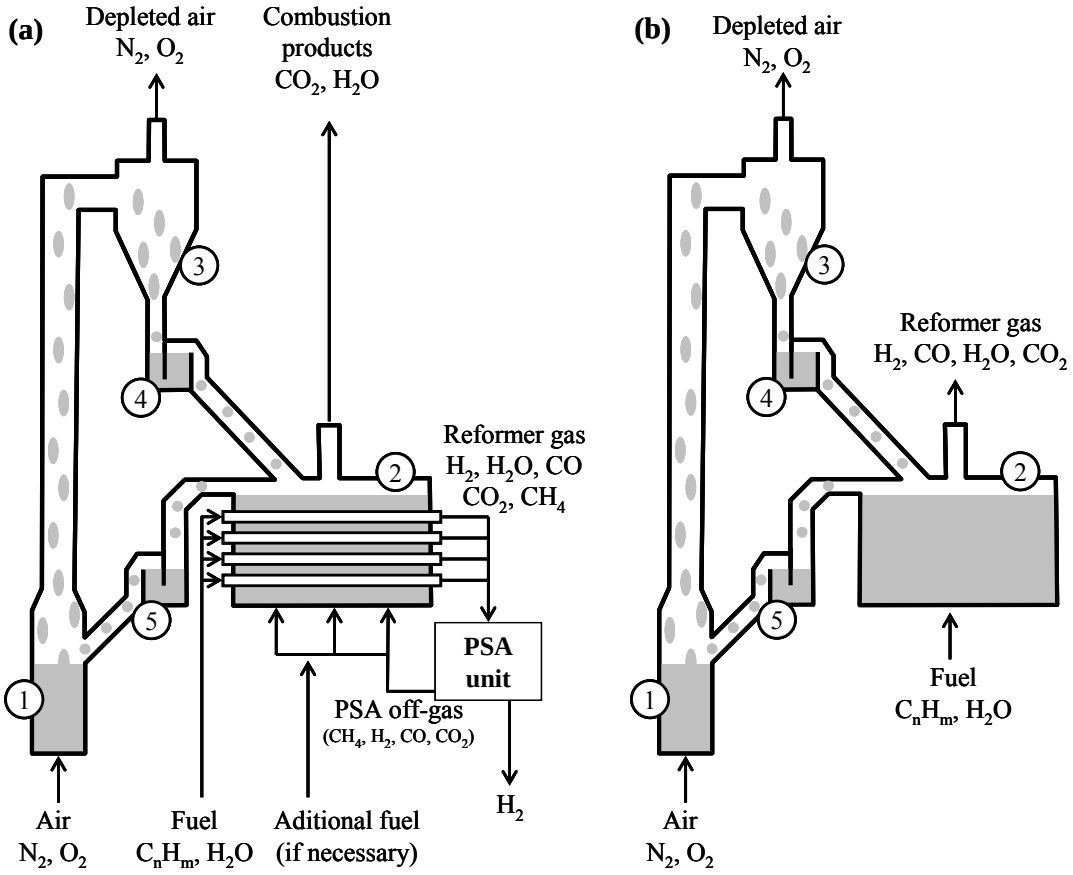

Fig. 14. Schemes of the reactor system for the (a) Steam Reforming integrated with Chemical-Looping Combustion (SR-CLC); and (b) Autothermal Chemical Looping Reforming (a-CLR). (1) air reactor, (2) fuel reactor, (3) cyclone for particle separation, (4) and (5) loop seals fluidized with steam. (Adapted from [51])

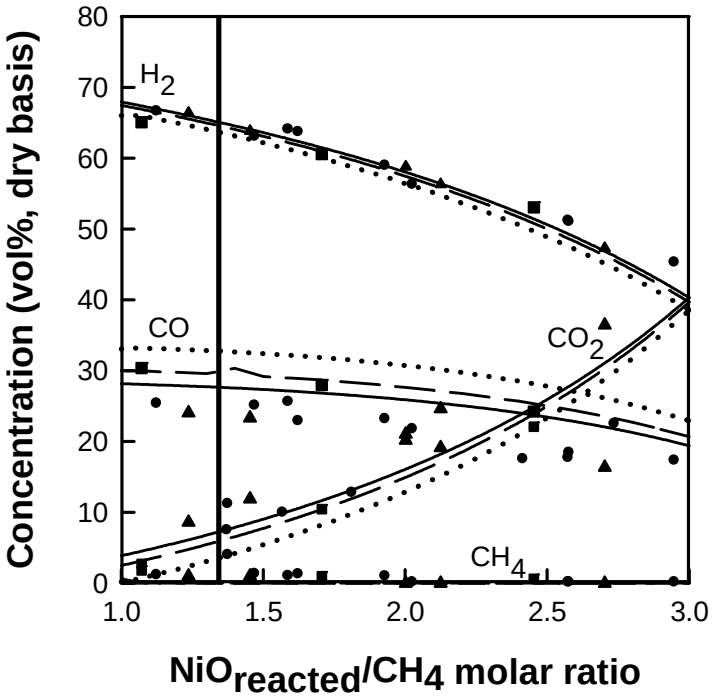

Fig. 15. Effect of $NiO_{reacted}/CH_4$ molar ratio on the gas product composition for both oxygen-carriers. Filled dots: NiO18-αAl_2O_3. Empty dots: NiO21-γAl_2O_3. Lines: thermodynamic equilibrium data. (□, ■, ·····): H_2O/CH_4 = 0, (○, ●, -----): H_2O/CH_4 = 0.3, (Δ, ▲, ──): H_2O/CH_4 = 0.5. T = 900 ºC. (Data taken from [170])

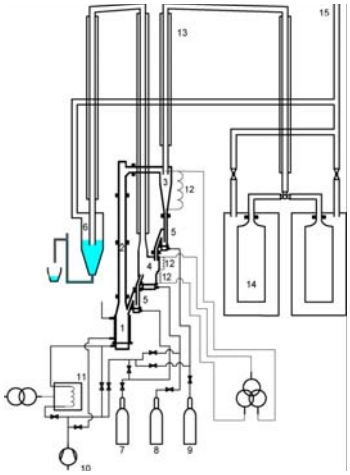

10 kW_{th} CLC for gaseous fuels
CHALMERS, Sweden [33]

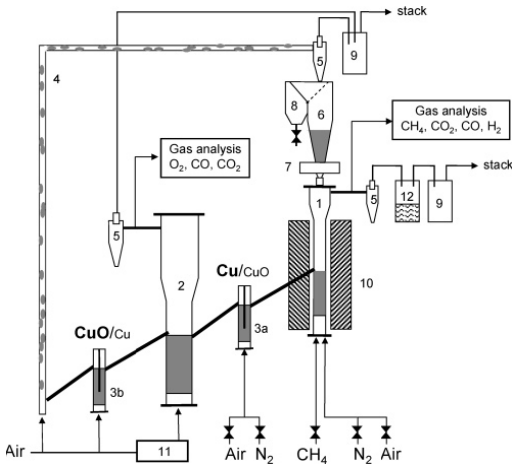

10 kW_{th} CLC for gaseous fuels
ICB-CSIC, Spain [39]

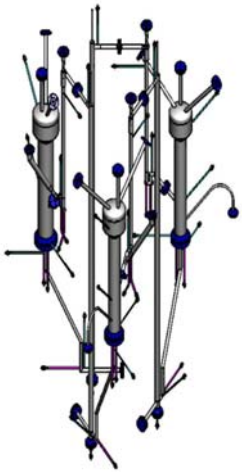

10 kW_{th} CLC for gaseous fuels
IFP-TOTAL, France [110]

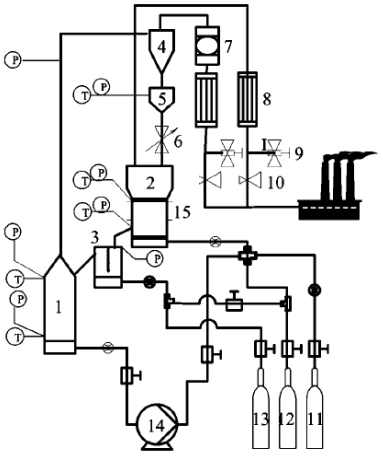

10 kW_{th} pressurized CLC for gas fuel
Xi'an Jiaotong University, China [205]

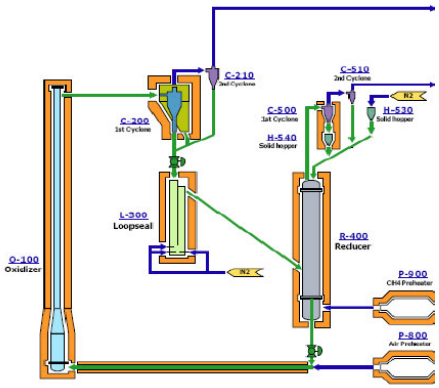

50 kW_{th} KIER-1 CLC for gaseous fuels
KIER, Korea [37]

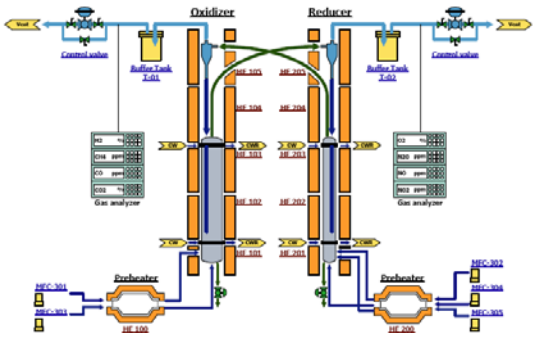

50 kW_{th} KIER-2 CLC for gaseous fuels
KIER, Korea [107]

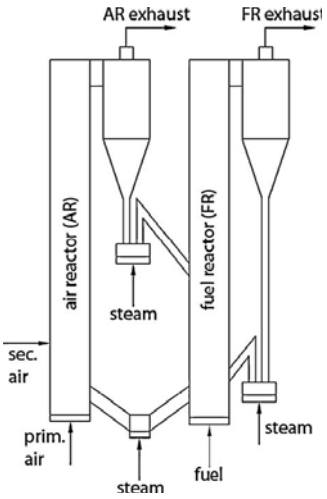

120 kW_{th} CLC for gaseous fuels
TUWIEN, Austria [167]

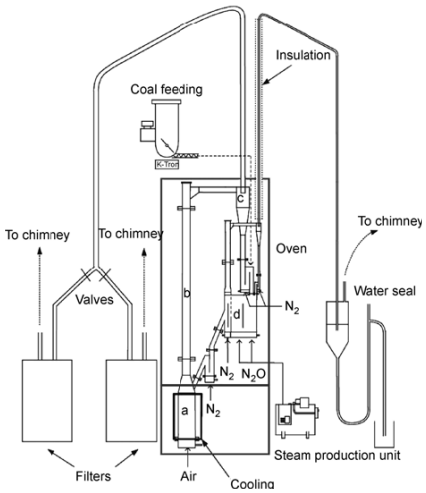

10 kW_{th} CLC for solid fuels
CHALMERS, Sweden [54]

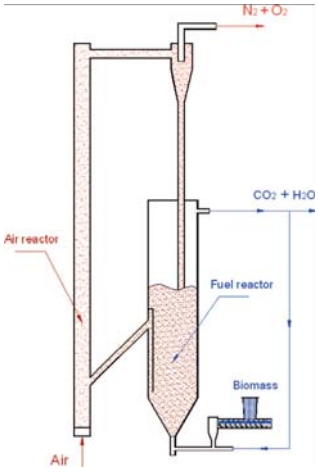

10 kW_{th} CLC for solid fuels
Southeast University, China [109]

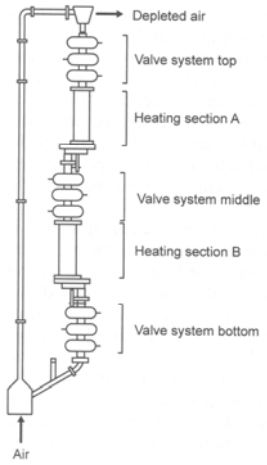

25 kWth CDCL process for solid fuels
Ohio State University, USA [20]

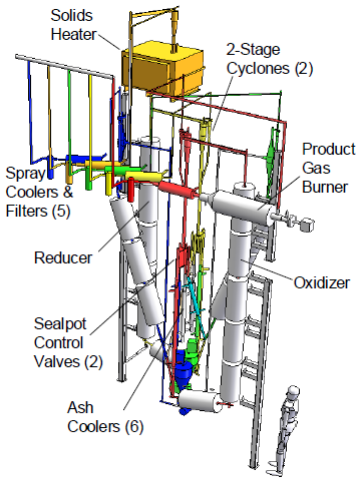

65 kW_{th} CLC for solid fuels
ALSTOM, USA [280]

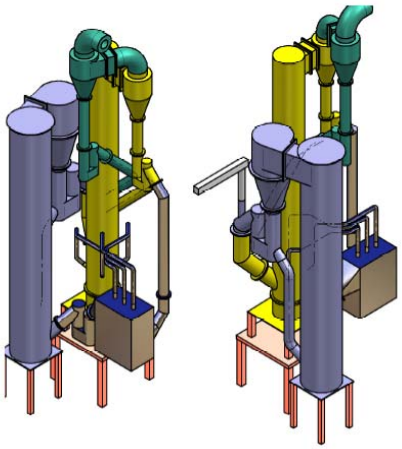

1 MW_{th} CLC for solid fuels
TUD, Germany [56]

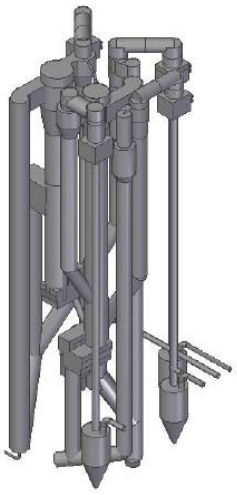

3 MW_{th} CLC for solid fuels
ALSTOM, USA [390]

Fig. 16. Main Chemical-Looping Combustion pilot plants for gas and solid fuels with power higher than 10kW_{th}.

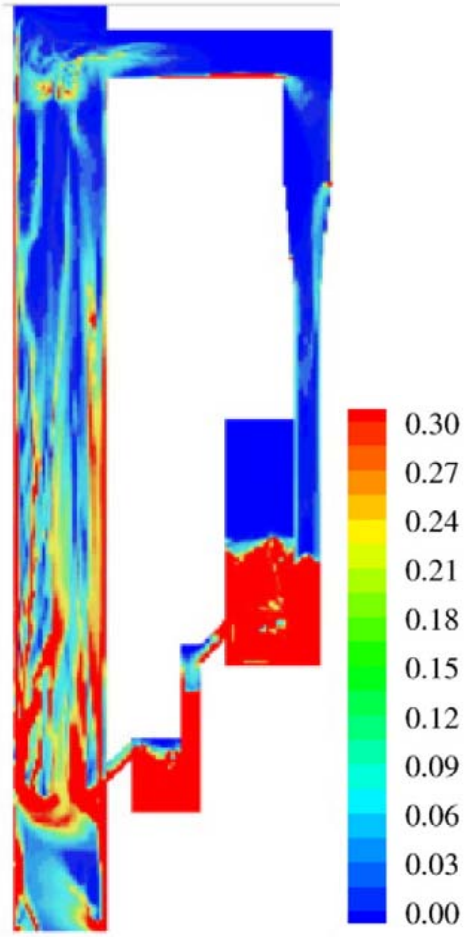

Fig. 17. Predictions of solids distribution by CFD model in two interconnected fluidized beds, as proposed for CLC. (Taken from [363])

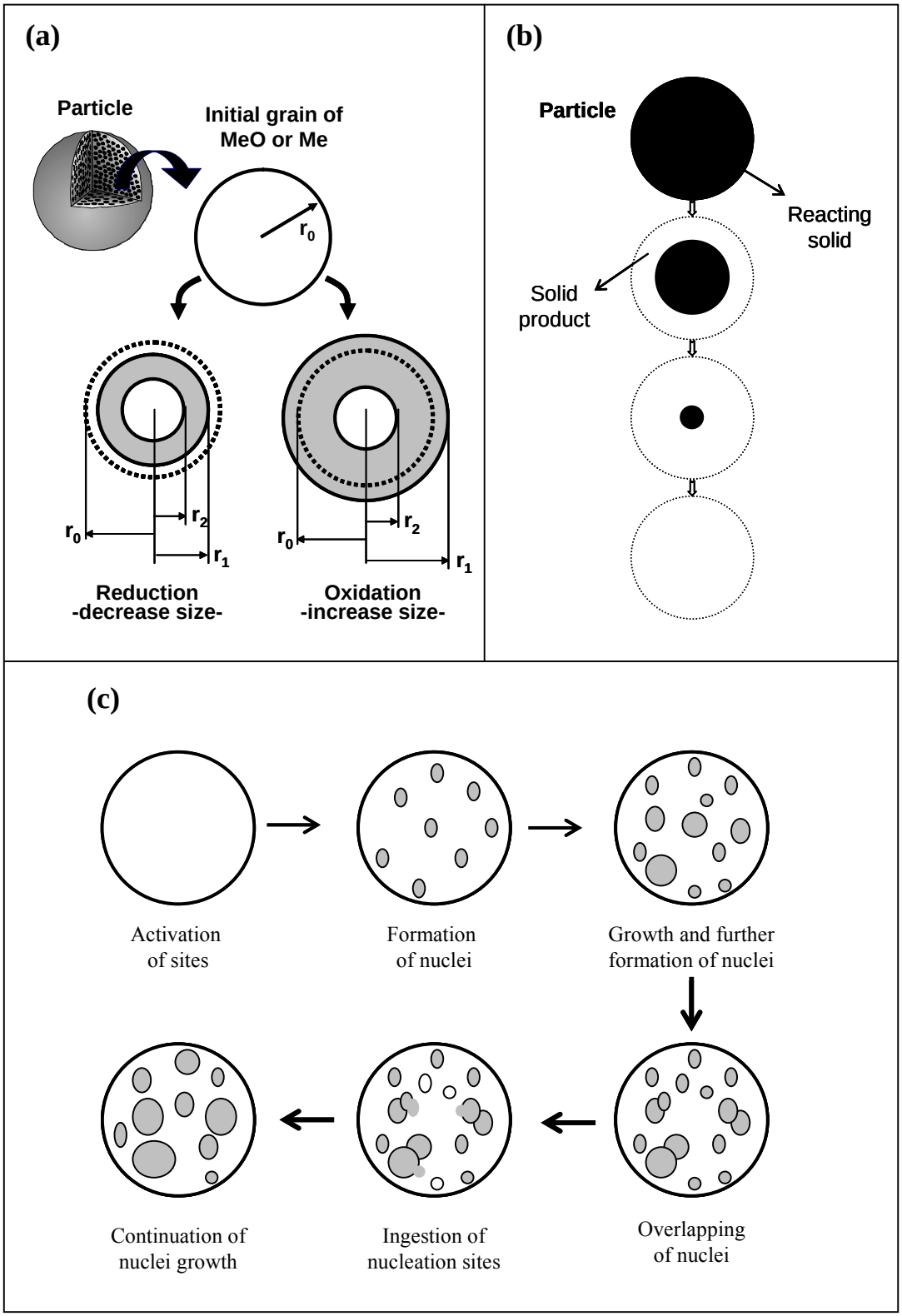

Fig. 18. Scheme of different reaction models in the particle: a) Changing grain size model (CGSM); b) Shrinking core model (SCM); and c) nucleation and nuclei growth model, as described in [218].

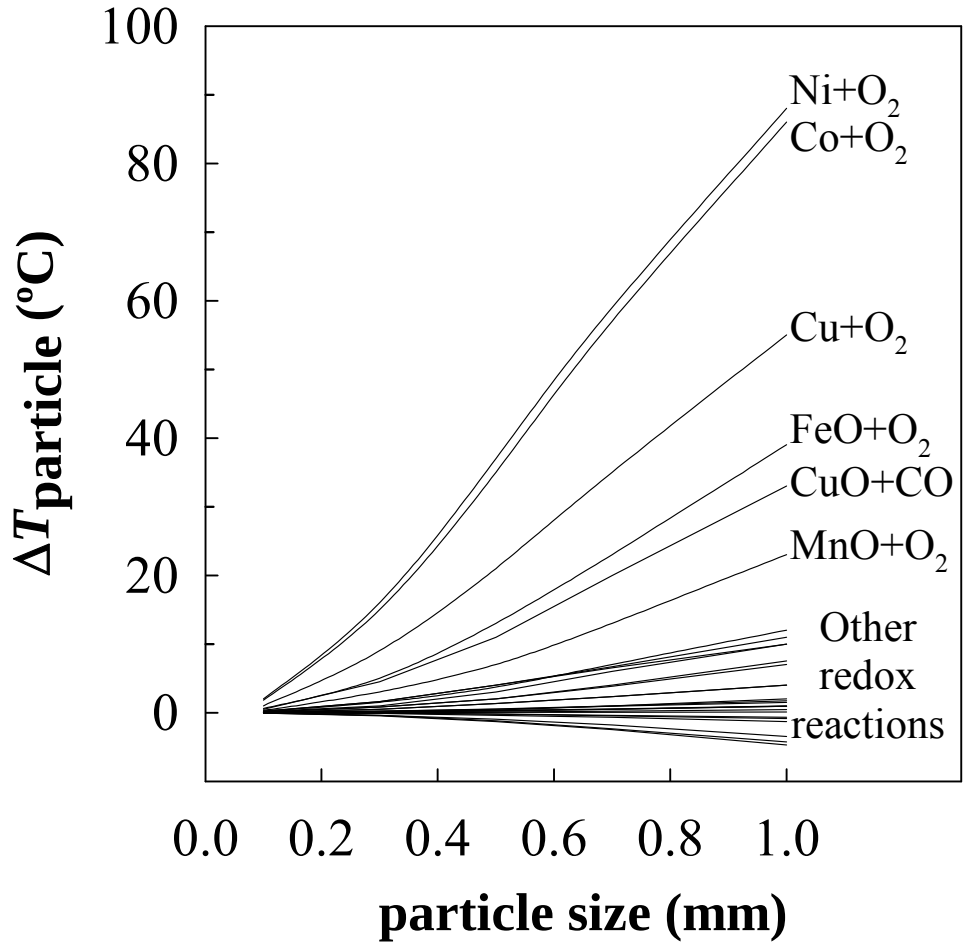

Fig. 19. Effect of particle size on the maximum particle temperature reached during CLC reactions with Ni-, Co-, Cu-, Fe-, and Mn-based oxygen-carriers. Data taken from [373].

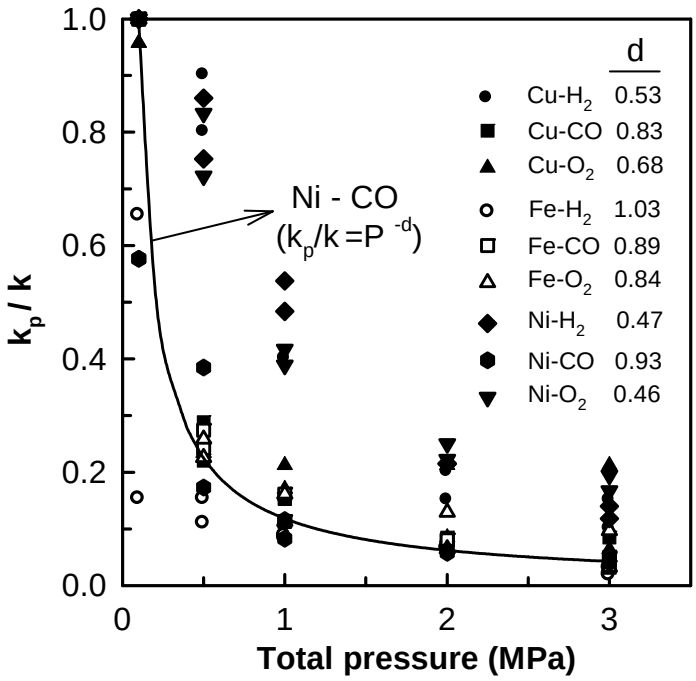

Fig. 20. Effect of total pressure on the decrease of the pre-exponential factor for several oxygen-carriers and reducing gases, k_P being the kinetic constant at pressure P and k at atmospheric pressure. Continuous line: fitting of data for reduction of NiO with CO. Data taken from [236].

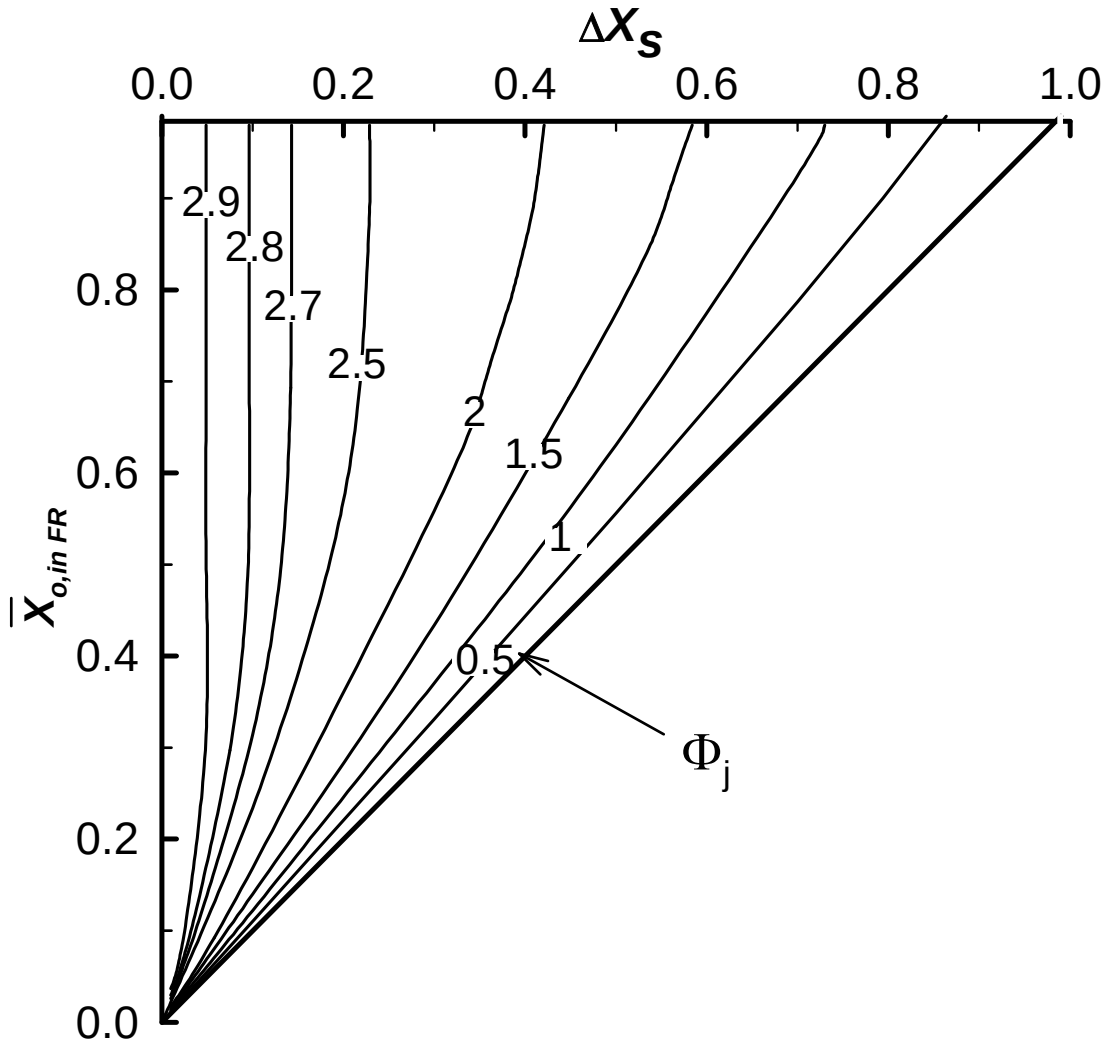

Fig. 21. Diagram to calculate the characteristic reactivity, Φ_j, as a function of $\overline{X}_{o,inFR}$ and ΔX_s. Spherical geometry of particles or grains.

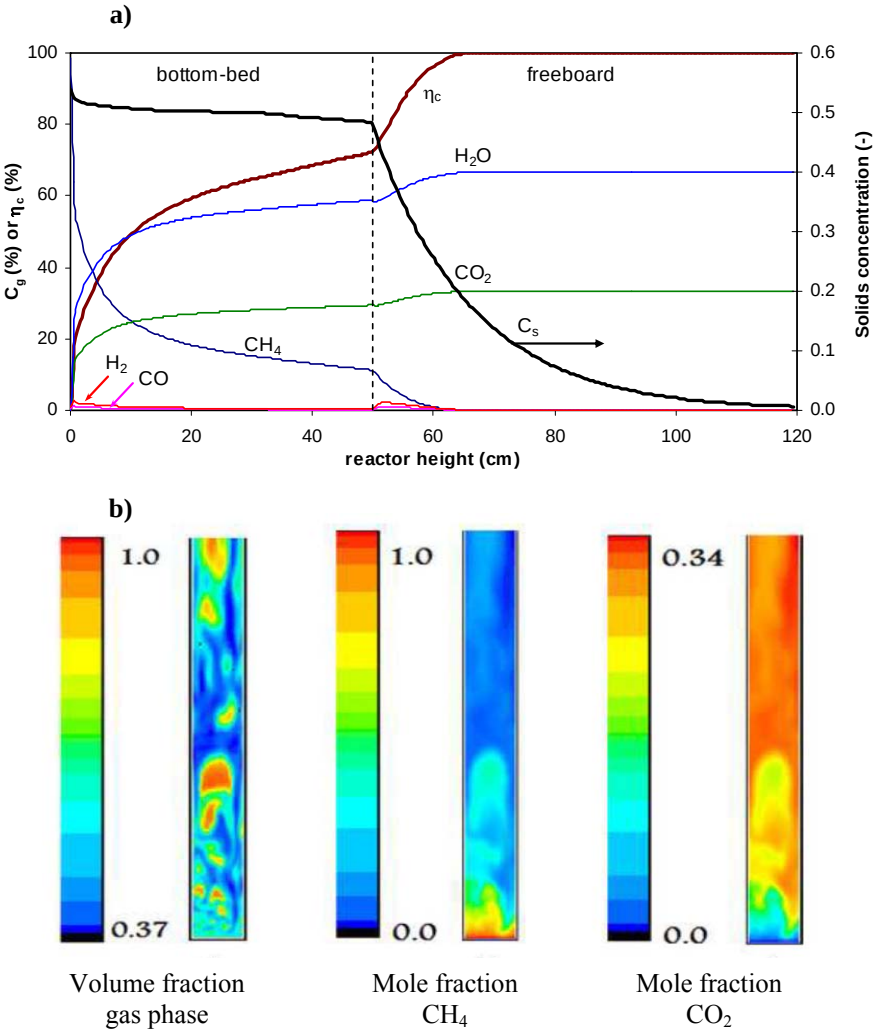

Fig. 22. Concentration of solids, C_s, and gases in the fuel-reactor by using a) macroscopic model (showing also the combustion efficiency, η_C), taken from [200]; and b) CFD model, taken from [352].

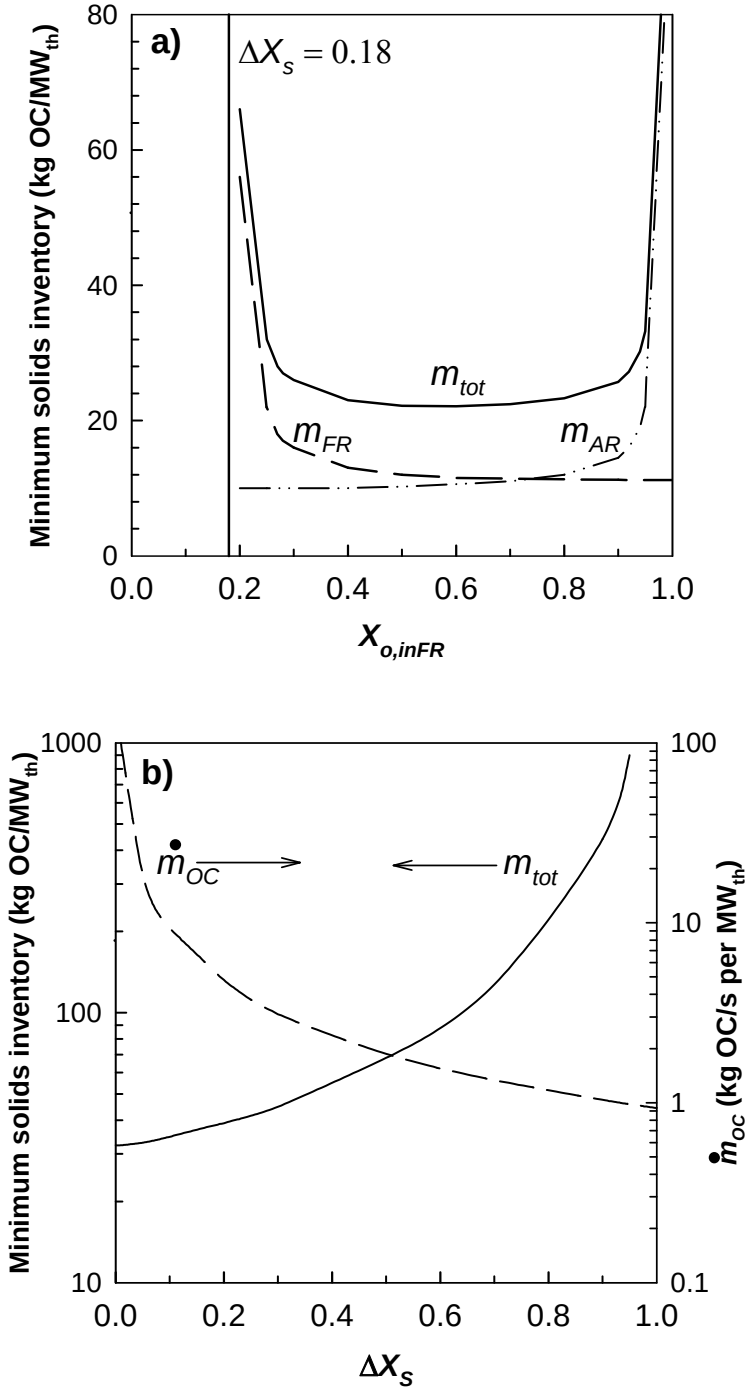

Fig. 23. Minimum solids inventory in the fuel-reactor, m_{FR}, air-reactor, m_{AR}, and total, m_{tot}, as a function of a) the solid conversion at the inlet of the fuel-reactor ($X_{o,inFR}$), (data taken from [376] and b) the variation of the solid conversion between the fuel- and air-reactor, ΔX_s (data taken from [124]). The solids inventories are calculated without considering the gas exchange resistance processes in the reactors. Figure b) also shows the corresponding solids circulation flow rate.

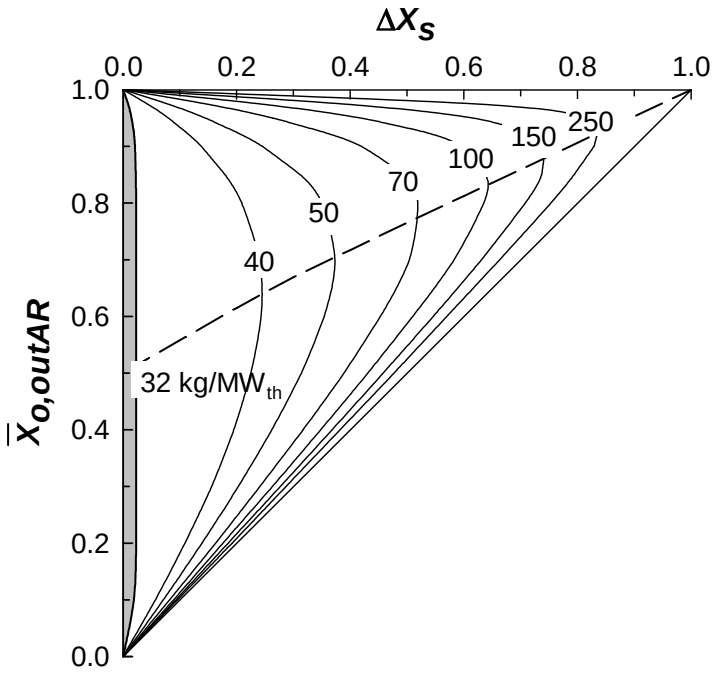

Fig. 24. Total solids inventory in the fuel- and air-reactors for the combustion of 1 MW_{th} of CH_4. Oxygen-carrier: Ni40Al-FG (data taken from [124]). Discontinuous line: minimum solids inventory at a certain ΔX_s value. The solids inventory is calculated without considering the gas exchange resistance processes in the reactors.

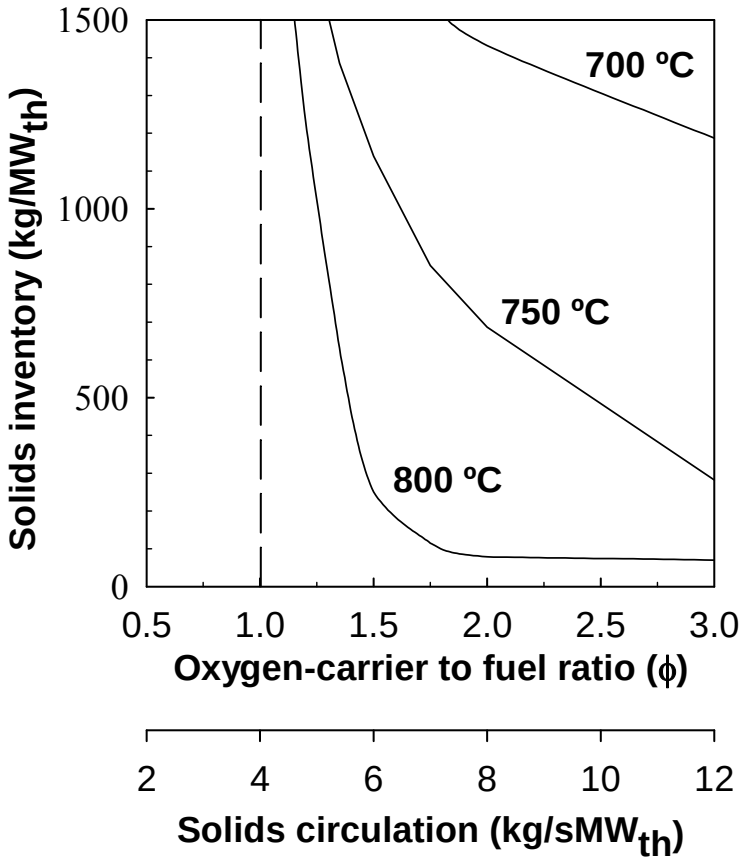

Fig. 25. Prediction from a macroscopic model of the solids inventory in the fuel-reactor (bubbling fluidized-bed) to reach a combustion efficiency of 99.9% CH_4 as a function of the solids circulation flow rate and the reactor temperature. Oxygen-carrier: Cu14Al-I. (Data taken from [200])

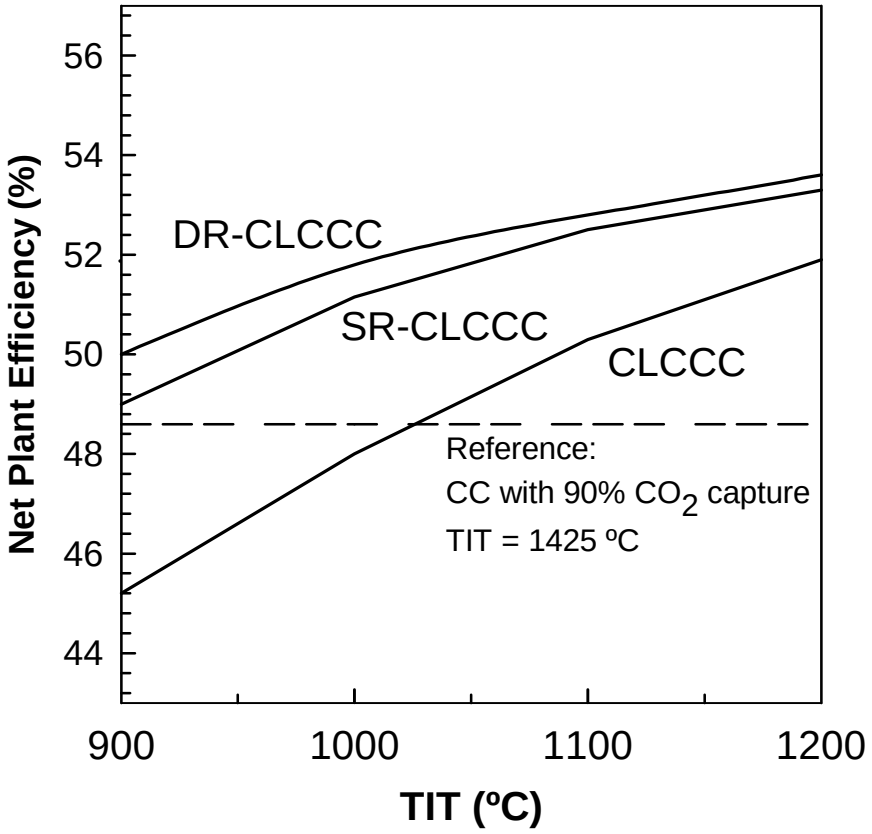

Fig. 26. Comparison net plant efficiency using a CLC combined cycle composed by 1 set of reactors (CLCCC), two sets of reactors (SR-CLCCC), or three sets of reactors (DR-CLCCC) of cycles as a function of the corresponding turbine inlet temperature (TIT). (Data taken from [402])

Annex.

Table A1. Summary of Ni-based oxygen-carriers.

Metal oxide content (%)	Support material	Preparation method[a]	Facility[b]	Reacting agent[c]	Application	Reference
100		MM+SD	TGA, FxB	CH_4, H_2, O_2	CLC	[27,386,404]
100			TGA	CH_4, O_2	CLC	[230]
100			TGA	coal	CLCs	[227]
100			TGA	syngas	CLCs	[229]
100		SC	TGA	H_2	CLC	[374]
33	Al_2O_3	IMP	TGA	CH_4, O_2	CLC	[176]
35	Al_2O_3	COP	TGA, CLC 10 kW, CLC 1 kW	coal, syngas + H_2S, CO, O_2	CLCs	[184-186]
36-40	Al_2O_3	SD	TGA	CH_4, O_2	CLC	[254]
40-80	Al_2O_3	MM+PE	TGA	CH_4, O_2	CLC	[32]
60	Al_2O_3	SG	TGA	H_2	CLC	[405]
60	Al_2O_3	MM	TGA	CH_4, O_2	CLC	[230]
60	Al_2O_3	DIS+SD	TGA	CH_4, CO, H_2, O_2	CLC	[152,159,404]
60	Al_2O_3	MM	TGA	CH_4, O_2	CLC	[406]
60	Al_2O_3	MM	TGA	CH_4, O_2	CLC	[108]
65	Al_2O_3	n.a.	TGA	CH_4, H_2, CO	CLC	[379]
2.5-20	α-Al_2O_3	IMP	TPR, TPO, CREC	CH_4, H_2, O_2	CLC	[213,214,216,217,219]
6-38	α-Al_2O_3	IMP	TGA, FxB, bFB	CH_4, H_2, CO, O_2	CLC	[146,151]
18	α-Al_2O_3	IMP	TGA, bFB, CLC 300 W, CLC 500 W, CLR 900 W	n.g., syngas, CH_4, H_2, CO, C_2H_6, C_3H_8, O_2	CLC, CLR	[45,46,141,151,169,170,182,183,215,330,331]
26	α- Al_2O_3	DP	TGA, bFB	CH_4 O_2	CLC	[151]
60-70	α-Al_2O_3	MM	TGA	H_2	CLC	[407]
12-30	γ-Al_2O_3	IMP	TGA, FxB, bFB	CH_4, H_2, CO, O_2	CLC	[146,150,151]
20	γ-Al_2O_3	IMP	CREC	CH_4	CLC	[219]
21	γ-Al_2O_3	IMP	TGA, bFB, CLC 300 W, CLR 900 W	n.g., CH_4, O_2	CLC, CLR	[150,170,182,330,331]
28-40	γ- Al_2O_3	DP	TGA, bFB	CH_4, O_2	CLC	[151]
60-70	γ-Al_2O_3	MM	TGA	H_2	CLC	[407]
70	γ-Al_2O_3	SD	TGA	CH_4, O_2	CLC	[408]

40	Al_2O_3-Bentonite	FG	bFB	CH_4, syngas	CLC	[172,409]
40	Al_2O_3-CaO	FG	bFB	CH_4, syngas	CLC	[149,172,409]
5	Al_2O_3-Co	IMP	CREC	CH_4, O_2	CLC	[216,217]
20	Al_2O_3-Co	IMP	TPR, TPO, CREC	CH_4, H_2, O_2	CLC	[218]
20	Al_2O_3-La	IMP	CREC	CH_4, biomass	CLC, CLCs	[219,302]
20	Al_2O_3-La-Co	IMP	TPR/TPO	H_2, O_2	CLC	[220]
60-70	γ-Al_2O_3-MgO	MM	TGA	H_2	CLC	[407]
70	γ-Al_2O_3-Pseudoboehmite	SD	TGA	CH_4, O_2	CLC	[408]
18	Al_2O_3-SiO_2	IMP	FxB, bFB	CH_4, O_2	CLC	[164]
60	$AlPO_4$	DIS	TGA	H_2	CLC	[405]
30	$BaAl_2O_4$	SG	TGA	syngas, H_2S	CLC	[410]
26-78	Bentonite	MM	TGA	CH_4, O_2	CLC	[222]
60	Bentonite	MM	TGA, CLC 1.5 kW	CH_4, O_2	CLC	[108]
60	Bentonite	MM	TGA, bFB, FxB, CLC 50 kW	CH_4, syngas, O_2	CLC	[37,107,153,165,199,411]
60	Bentonite	MM	TGA, FxB	syngas, H_2S	CLC	[223,226]
60-70	Boehmite	MM	TGA	H_2	CLC	[407]
20	$CaAl_2O_4$	IMP	TGA, bFB	CH_4, O_2	CLC	[150]
40	$CaAl_2O_4$	FG	bFB	CH_4, O_2	CLC	[147,172]
60	CaO	MM	TGA	CH_4	CLC	[230]
20-40	$LaAl_{11}O_{18}$	IMP	TGA	H_2, O_2	CLC	[412]
40	MgO	FG	bFB	CH_4, syngas	CLC	[409]
60	MgO	MM	TGA	CH_4	CLC	[230]
60	MgO	DIS+SD	TGA	CH_4, H_2, O_2	CLC	[152,404]
60	MgO	FG	bFB	CH_4, O_2	CLC	[172]
20	$MgAl_2O_4$	IMP	TGA, bFB	CH_4, O_2	CLC	[150]
20	$MgAl_2O_4$	FG	CLC 300 W	n.g.	CLC, CLR	[182]
30	$MgAl_2O_4$	SC+MM	TGA	CH_4, syngas	CLC	[413]
35	$MgAl_2O_4$	FG+IMP	TGA	CH_4, O_2	CLC, CLR	[224]
35	$MgAl_2O_4$	COP	TPR	CH_4, H_2, O_2	CLC	[212]
40	$MgAl_2O_4$	SD	bFB	CH_4, O_2	CLC	[129,225]
60	$MgAl_2O_4$	FG	TGA, bFB, CLC 300 W	n.g., syngas, CH_4, O_2	CLC, CLR	[36,147,157,172,188,196,197,238,376,409]
14-60	$NiAl_2O_4$	COP	TPR	CH_4, H_2, O_2	CLC	[212]
20-40	$NiAl_2O_4$	SC+MM	TGA	CH_4, H_2, syngas	CLC	[374,413]
23	$NiAl_2O_4$	IMP	bFB	coal-H_2O	CLCs	[314]

32.7	$NiAl_2O_4$	IMP	CLC 10 kW	Coal	CLCs	[187]
40	$NiAl_2O_4$	SC+MM	TGA	CH_4, H_2	CLC	[374,414]
40	$NiAl_2O_4$	SD	TGA, bFB, CLC 120 kW	CH_4, CO, H_2, O_2	CLC, CLR	[129,191,181,225,415,416]
40-60	$NiAl_2O_4$	FG	TGA, bFB, CLC 300 W, CLC 10 kW	n.g., CH_4, CO, H_2, O_2	CLC	[33,36,124,147-149,157,172,188,189,409]
40-60	$NiAl_2O_4$	SD	TGA, bFB, CLC 300 W, CLC 10 kW	n.g., CH_4, H_2	CLC, CLR	[139,167,168,183,192-195,225]
40-60	$NiAl_2O_4$	SG	TGA	CH_4, H_2, coal	CLC, CLCs	[306,417]
60	$NiAl_2O_4$	DIS+SD	TGA, pFxB, CLC	CH_4, H_2, syngas	CLC	[152,190,294,386,404]
60	$NiAl_2O_4$	DIS+PE	FxB	CH_4	CLC	[160]
60	$NiAl_2O_4$	DIS	TGA	CH_4, H_2, O_2	CLC	[377]
60	$NiAl_2O_4$	FG	TGA, pTGA, bFB, CLC 300 W	n.g. CH_4, H_2, CO, O_2	CLC	[154,171,178,188,232,236]
60	$NiAl_2O_4$	SF	bFB, CLC 10 kW	n.g., CH_4, syngas, coal	CLC, CLCs	[140,315]
60	$NiAl_2O_4$	CP	TGA, bFB	CH_4, O_2	CLC	[161,162,418]
60-90	$NiAl_2O_4$	DIS	bFB	H_2	CLC	[419]
70	$NiAl_2O_4$	DIS	bFB	syngas, O_2	CLC	[411]
40	$NiAl_2O_4$- CaO	FG	bFB	CH_4, O_2	CLC	[149,225]
40	$NiAl_2O_4$- CaO	SD	bFB	CH_4	CLC	[225]
32	$Ni_{0.62}Mg_{0.38}Al_2O_4$	SC+MM	TGA	CH_4	CLC	[414]
40	$NiAl_2O_4$- MgO	FG	bFB	CH_4, O_2	CLC	[149]
40	$NiAl_2O_4$-MgO	SD	TGA, bFB, CLC 300 W, CLC 120 kW, CLR 140 kW	n.g., CH_4, O_2	CLC, CLR	[139,167,183,194,195,225,227]
40-80	Sepiolite	MM+PE	TGA	CH_4, O_2	CLC	[32]
35	SiO_2	IMP	TGA, bFB	CH_4, O_2	CLC,CLR	[224,237]
40-80	SiO_2	MM+PE	TGA	CH_4, O_2	CLC	[32]
4-30	TiO_2	IMP	FxB	CH_4	CLC	[155]
40-44	TiO_2	IMP	FxB	CH_4	CLC	[156]
40-80	TiO_2	MM+PE	TGA	CH_4, O_2	CLC	[32]
40-80	TiO_2	FG	bFB	CH_4, O_2	CLC	[147]
60	TiO_2	MM	TGA	CH_4, O_2	CLC	[108]
60	TiO_2	MM	TGA	CH_4	CLC	[230]
60	TiO_2	MM+SD	TGA	CH_4, H_2, CO, O_2	CLC	[152,159,404]
20-80	YSZ	MM+SD	TGA, FxB	CH_4, H_2, CO, O_2	CLC	[27,134,144,152,159,221,386,404,406]
60	YSZ	DIS	TGA	H_2	CLC	[405]
40	ZrO_2	FG	bFB	CH_4, O_2	CLC	[147]

40-80	ZrO_2	MM+PE	TGA	CH_4, O_2	CLC	[32]
60	ZrO_2	DIS	TGA	H_2	CLC	[405]
40	ZrO_2-MgO	FG	bFB, CLC 300 W	CH_4, n.g.	CLR	[198]
$NiAl_2O_4$		CP	TGA	CH_4, O_2	CLC	[418]
$NiAl_{0.44}O_{1.67}$		P	bFB	biogas	CLC	[249]
Ni-SETS			Pressurised bFB	CH_4	CLC	[211]
OCN-650	n.a.	SD	bFB	syngas, O_2	CLC	[411]
OCN601-650	n.a.	n.a.	TGA	CH_4	CLC	[199]
OCN702-1100	n.a.	n.a.	TGA, CLC 50 kW	CH_4	CLC	[199]
OCN702-125	n.a.	n.a.	TGA	CH_4	CLC	[199]
OCN703-1100 (70)	n.a.	SD	CLC 50 kW	n.g., syngas	CLC	[107]
--	CaAlum7825		TGA	syngas	CLCs	[229]
--	CaAlum7817		TGA	syngas	CLCs	[229]

Table A2. Summary of Cu-based oxygen-carriers.

Metal oxide content (%)	Support material	Preparation method[a]	Facility[b]	Reacting agent[c]	Application	Reference
100			TGA	CH_4	CLC	[133]
100			TGA	coal, wood, polyethene	CLCs	[228,420]
100			TGA	CH_4, O_2	CLC	[230]
100			TGA	H_2	CLC	[231]
100			TGA	syngas, O_2	CLC	[229]
100			TGA, FxB	Coal, O_2	CLCs	[227]
4.5	Al_2O_3		TGA	H_2	CLC	[29]
10	Al_2O_3	Com. Cat.	TGA, pTGA	CH_4, H_2, CO, syngas, O_2	CLC	[126,232,236]
13	Al_2O_3	Com. Cat.	FxB	CH_4, H2, O_2	CLC-FxB	[117,421]
21	Al_2O_3	IMP	bFB	coal	CLCs	[303,305]
30-100	Al_2O_3	MM	bFB	CO, O_2	CLC	[179]
20-100	Al_2O_3	COP	bFB	CO, O_2	CLC	[179]
40-80	Al_2O_3	MM+PE	TGA	CH_4, H_2, syngas, O_2	CLC	[32,133]
60	Al_2O_3	MM	TGA	CH_4, O_2	CLC	[230]
62	Al_2O_3		TGA	CH_4, H_2, CO	CLC	[379]
82.5	Al_2O_3	COP	bFB	H_2, CO, O_2	CLC, CLCs	[180,380,381]
15	α-Al_2O_3	IMP	TGA, CLC 500 W	CH_4, H_2, O_2	CLC	[138]
10-26	γ-Al_2O_3	IMP	TGA, bFB	CH_4, H_2, O_2	CLC	[166]
14	γ-Al_2O_3	IMP	TGA, bFB, CLC 500 W, CLC 10 kW	CH_4, H_2, CO, syngas, HC, H_2S, O_2	CLC	[39,40,136,138,142,200-203,422]
21-78	γ-Al_2O_3	IMP	bFB	CO, O_2	CLC	[179]
33	γ-Al_2O_3	IMP	TGA	CH_4, O_2	CLC	[176]
21	θ-Al_2O_3	IMP	scFB	coal, O_2	CLCs	[303,305]
60	Bentonite	MM	TGA	syngas, H_2S, O_2	CLC	[231,226]
30	BHA	SG	TGA	syngas, H_2S, O_2	CLC	[410]
45	BHA	SG	TGA	syngas, O_2	CLC	[231]
60	$CuAl_2O_4$	FG	bFB	CH_4, O_2	CLC	[178]
60	MgO	MM	TGA	CH_4, O_2	CLC	[230]

12	$MgAl_2O_4$	IMP	CLC 500 W	CH_4, O_2	CLC	[138]
43	$MgAl_2O_4$	FG	TGA	CH_4, O_2	CLC, CLR	[224]
40-80	Sepiolite	MM+PE	TGA	CH_4, H_2, syngas, O_2	CLC	[32,133]
10-45	SiO_2	IMP	TGA, bFB, FxB	CH_4, H_2, O_2	CLC	[133,145,423]
40	SiO_2	COP	TGA	CH_4, H_2, syngas, O_2	CLC	[133]
40	SiO_2	IMP	bFB	CH_4, O_2	CLR	[237,329]
41.3	SiO_2	IMP	TGA	CH_4, O_2	CLC, CLR	[224]
40-80	SiO_2	MM+PE	TGA, bFB	CH_4, H_2, syngas, O_2	CLC	[32,133,145,337]
60	SiO_2	FG	bFB	CH_4, O_2	CLC	[244]
5-31	TiO_2	IMP	TGA, bFB, FxB	CH_4, H_2, syngas, O_2	CLC	[133,145,424]
40	TiO_2	FG	bFB	CH_4, O_2	CLC	[244]
40-80	TiO_2	MM+PE	TGA	CH_4, H_2, syngas, O_2	CLC	[32,133]
60	TiO_2	MM	TGA	CH_4, O_2	CLC	[230]
40	ZrO_2	FG	bFB	CH_4, O_2	CLC	[244]
40-80	ZrO_2	MM+PE	TGA	CH_4, H_2, syngas, O_2	CLC	[32,133]

Table A3. Summary of Fe-based oxygen-carriers.

Metal oxide content (%)	Support material	Preparation method[a]	Facility[b]	Reacting agent[c]	Application	Reference
100		MM	bFB	coal, O_2	CLCs	[118,241]
100			TGA	CH_4, O_2	CLC	[230]
100			FxB	coal	CLCs	[299]
100		COP	TGA	CH_4, O_2	CLC	[251]
100			TGA-DSC-MS	syngas, char, O_2	CLCs	[229]
100			CLC 10 kW	biomass, O_2	CLCs	[109]
100			TGA	coal	CLCs	[227]
100		FG	bFB	syngas, O_2	CLC	[263]
100		SD	bFB	CO, O_2	CLC	[425]
100		MM	TGA	CH_4, O_2	CLC	[254]
100 (Fused Iron)			TGA	char, O_2	CLCs	[229,318]
100 (Wustite)			TGA	char, O_2	CLCs	[229,318]
70 (Fe_2O_3)	30 (Fe_3O_4)	MM	bFB	coal, O_2	CLCs	[240]
20	Al_2O_3	IMP	CLC 500W	PSA-off gas	CLC	[204]
22	Al_2O_3	IMP	bFB	CH_4, O_2	CLC	[173,244]
25	Al_2O_3	SD	FxB	H_2	CLC	[426]
40-80	Al_2O_3	MM+PE	TGA, bFB	CH_4, O_2	CLC	[31,32,145]
40–80	Al_2O_3	FG	FxB, bFB	CH_4, O_2	CLC	[427,428]
58	Al_2O_3		TGA	CH_4, H_2, CO	CLC	[379]
60	Al_2O_3	MM	TGA	CH_4, O_2	CLC	[230]
60	Al_2O_3	MM	TGA	CH_4, O_2	CLC	[108]
60	Al_2O_3	MM	TGA	CH_4, O_2	CLC	[254]
60	Al_2O_3	FG	TGA, pTGA, bFB, CLC 300 W	n.g., CH_4, CO, H_2, syngas, O_2	CLC	[31,36,124,131,154,171,173,178,232,236,244,246]
60	Al_2O_3	DIS	TGA	H_2, CO, O_2	CLC	[152,159,404]
80	Al_2O_3	IMP	TGA,FxB	CH_4, O_2	CLC	[364]
n.a.	Al_2O_3		TGA, bFB	CH_4, H_2, O_2, syngas	CLC	[29,177]
60	Al_2O_3 + Bentonite	FG	bFB	CH_4, O_2	CLC	[172,409]
60	Al_2O_3 + Kaolin	FG	bFB	CH_4, O_2	CLC	[173,244]

40	Bentonite	MM	TGA	syngas, syngas+H_2S, O_2	CLC	[226]
60	Bentonite	MM	TGA, CLC 1 kW	CH_4, O_2	CLC	[108]
60	CaO	MM	TGA	CH_4, O_2	CLC	[230]
60	Kaolin	FG	bFB	CH_4, O_2	CLC	[178]
60	MgO	MM	TGA	CH_4, O_2	CLC	[230]
60	MgO	DIS	TGA	H_2, O_2	CLC	[152,404]
60	MgO	FG	bFB	CH_4	CLC	[428]
32	$MgAl_2O_4$	FG	TGA	CH_4, O_2	CLR	[224]
40-80	$MgAl_2O_4$	FG	bFB	CH_4, O_2	CLC	[172,173,235,409]
40	$MgAl_2O_4$	FG	FxB	CH_4, O_2	CLC, CLR	[158]
60	$MgAl_2O_4$	FG	bFB	CH_4, syngas, coal, O_2, petcoke, petcoke+SO_2	CLC, CLCs	[123,238,239,244,267]
40-80	Sepiolite	MM+PE	TGA, bFB	CH_4, O_2	CLC	[31,32]
39	SiO_2	IMP	TGA, bFB	CH_4, O_2	CLC, CLR	[224,237]
40	SiO_2	FG	bFB	CH_4, O_2	CLC	[172,409]
40-80	SiO_2	MM+PE	TGA, bFB	CH_4, O_2	CLC	[31,32,145]
4-29	TiO_2	IMP	FxB	CH_4	CLC	[233]
40	TiO_2	FG	bFB	CH_4, O_2	CLC	[244]
40-80	TiO_2	MM+PE	TGA, bFB	CH_4, O_2	CLC	[31,32,145]
60	TiO_2	FG	bFB	CH_4, O_2	CLC	[173]
60	TiO_2,	DIS	TGA	H_2, CO, O_2	CLC	[152,159,404]
60	TiO_2	MM	TGA	CH_4, O_2	CLC	[230]
60	TiO_2	MM	TGA	CH_4, O_2	CLC	[108]
Fe_2TiO_5 (Fe/Ti: 0.33-1.22)	TiO_2	FG	bFB	syngas, O_2	CLC	[263]
Fe_2TiO_5/Fe_2O_3 (Fe/Ti=3)		FG	bFB	syngas, O_2	CLC	[263]
60	YSZ	MM	TGA	CH_4,H_2, O_2	CLC	[27,406]
60	YSZ	DIS	TGA	H_2, CO, O_2	CLC	[144,159]
60	YSZ	DIS	TGA	H_2, O_2	CLC	[405]
40-80	ZrO_2	MM+PE	TGA, bFB	CH_4, O_2	CLC	[31,32,145]
40-80	ZrO_2	FG	bFB	CH_4, O_2	CLC	[172,173,244,409]
60	ZrO_2-Ca	FG	bFB	CH_4	CLC	[234]
60	ZrO_2-Ce	FG	bFB	CH_4	CLC	[234]
60	ZrO_2-Mg	FG	bFB	CH_4	CLC	[234]
n.a.	n.a.	n.a.	TGA, CLC 10 kW	Natural gas	CLC	[33]

Table A4. Summary of Mn-based oxygen-carriers.

Metal oxide content (%)	Support material	Preparation method[a]	Facility[b]	Reacting agent[c]	Application	Reference
100 (MnO_2)			TGA	CH_4, O_2	CLC	[230]
100 (Mn_2O_3)			TGA	coal	CLCs	[227]
wt% as MnO_2						
26	MgO	FG	bFB	CH_4, O_2	CLC	[244]
wt% as Mn_2O_3						
29.4	Al_2O_3	IMP	TGA	CH_4, O_2	CLC	[176]
40	Bentonite	MM	TGA	syngas, syngas+H_2S, O_2	CLC	[226]
46	$MgAl_2O_4$	IMP	TGA	CH_4, O_2	CLC	[224]
47	SiO_2	IMP	TGA, bFB	CH_4, O_2	CLC, CLR	[224,237]
wt% as Mn_3O_4						
37-78	Al_2O_3	MM+PE	TGA, bFB	CH_4, O_2	CLC	[32,145]
40	Mg-ZrO_2	FG	TGA, bFB, FxB, CLC 300 W	n.g., syngas, CH_4, CO, H_2, O_2	CLC,	[130,158,171,172,243,246]
60	$MnAl_2O_4$	FG	bFB	CH_4, O_2	CLC	[178]
37-78	Sepiolite	MM+PE	TGA, bFB	CH_4, O_2	CLC	[32,145]
37	SiO_2	FG	bFB	CH_4, O_2	CLC	[172,245]
37-78	SiO_2	MM+PE	TGA, bFB	CH_4, O_2	CLC	[32,145]
37-78	TiO_2	MM+PE	TGA, bFB	CH_4, O_2	CLC	[32,145]
37	ZrO_2	FG	bFB	CH_4, O_2	CLC	[172,245]
37-78	ZrO_2	MM+PE	TGA, bFB	CH_4, O_2	CLC	[32,145]
37-78	ZrO_2	FG	bFB	CH_4, O_2	CLC	[244]
40	ZrO_2-Ca	FG	bFB	CH_4, O_2	CLC	[172,245]
40	ZrO_2-Ce	FG	bFB	CH_4, O_2	CLC	[172,245]

Table A5. Summary of Co-based oxygen-carriers.

Metal oxide content (%)	Support material	Preparation method[a]	Facility[b]	Reacting agent[c]	Application	Reference
wt% as Co_3O_4						
100			TGA	coal	CLCs	[227]
34.5	Al_2O_3	IMP	TGA	CH_4, O_2	CLC	[176]
wt% as CoO						
100			TGA	syngas, O_2	CLC	[229]
60	Al_2O_3	DIS	TGA	H_2, O_2	CLC	[152]
60	MgO	DIS	TGA	H_2, O_2	CLC	[152]
60	TiO_2	MM	TGA	H_2, O_2	CLC	[152]
60	YSZ	DIS	TGA	CH_4, H_2, O_2	CLC	[144]
60	YSZ	DIS	TGA	H_2, O_2	CLC	[405]
wt% as Co_xO_y						
70	$CoAl_2O_4$	COP+IMP	CLC 50 kW	n.g.	CLC	[38]

Table A6. Summary of mixed oxides used as oxygen-carriers.

Metal oxide 1 (%)	Metal oxide 2 (%)	Support material	Preparation method[a]	Facility[b]	Reacting agent[c]	Application	Reference
CuO	NiO	γ-Al_2O_3	IMP	TGA, bFB, FxB, CLC 500 W	CH_4, CO, H_2, O_2	CLC	[138,146]
CuO	NiO	α-Al_2O_3	IMP	TGA, bFB, FxB	CH_4, CO, H_2, O_2	CLC	[146]
CuO	NiO	α-Al_2O_3-K	IMP	TGA, bFB, FxB	CH_4, CO, H_2, O_2	CLC	[146]
CuO	NiO	α-Al_2O_3-La	IMP	TGA, bFB, FxB	CH_4, CO, H_2, O_2	CLC	[146]
NiO	$Cu_{0.95}Fe_{1.05}AlO_4$		IMP	TGA	CH_4, O_2	CLC	[248,418]
NiO (15)	$Ce_{0.5}Zr_{0.5}O_2$ (85)		COP	TGA	CH_4, O_2	CLC	[418]
NiO (15-40)	$Ce_{0.25}Zr_{0.75}O_2$ (85-60)		COP	TGA	CH_4, O_2	CLC	[418]
NiO (27-40)	$Ce_{0.75}Zr_{0.25}O_2$ (73-60)		COP	TGA	CH_4, O_2	CLC	[418]
CoO	NiO	α-Al_2O_3	IMP	CREC simulator	CH_4, O_2	CLC	[216,217]
CoO	NiO	YSZ	DIS	TGA, pFxB	CH_4, H_2, syngas, O_2	CLC	[144,160,294]
Mn_3O_4	Fe_2O_3		FG	bFB	CH_4	CLOU	[253]
Mn_3O_4	NiO		FG	bFB	CH_4	CLOU	[253]
Fe_2O_3	MnO_2	Sepiolite	MM	TGA	syngas+H_2S, O_2	CLC	[252]
Fe_2O_3	MnO_2	ZrO_2	MM	TGA, FxB	syngas+H_2S, O_2	CLC	[252]
Fe_2O_3	NiO	Al_2O_3	MM	TGA	CH_4, O_2	CLC	[254]
Fe_2O_3	NiO	Bentonite	MM	TGA, CLC 1 kW	CH_4, O_2	CLC	[108]
Fe_2O_3	CuO	$MgAl_2O_4$	MM	TGA, CLCp 10 kW	coke oven gas	CLC P	[205]
CuO	$Cu_{0.95}Fe_{1.05}AlO_4$		COP	bFB	CH_4, O_2	CLC	[162,248,250]
$Cu_{0.95}Fe_{1.05}AlO_4$			COP	TGA, bFB	CH_4, biogas, O_2	CLC	[161,162,248-250]
$Cu_{0.5}Ni_{0.5}FeAlO_4$			COP	TGA	CH_4, O_2	CLC	[248,418]
$Co_{0.5}Ni_{0.5}FeAlO_4$			COP	TGA	CH_4, O_2	CLC	[248]
$CoFeAlO_4$			COP	TGA	CH_4, O_2	CLC	[248]
$CoFeGaO_4$			COP	TGA	CH_4, O_2	CLC	[248]
$NiFeAlO_4$			COP	TGA	CH_4, O_2	CLC	[248]
$CoFe_2O_4$		Al_2O_3	COP	TGA	CH_4, O_2	CLC	[250]
$CuFe_2O_4$		YSZ	COP	TGA, bFB	CH_4, O_2	CLC	[250]
$Mn_{1.415}Fe_{0.585}O_3$			COP	TGA, bFB	CH_4, O_2	CLC	[250]
Fe oxide	Mn oxide		COP, HS	TGA	CH_4, O_2	CLC	[251]

Table A7. Summary of perovskites used as oxygen-carriers.

Solid material	Preparation method[a]	Facility[b]	Reacting agent[c]	Application	Reference
$La_{0.8}Sr_{0.2}CoO_{3-\delta}$	CAM	insitu XRD	H_2	CLC	[257]
$La_{0.8}Sr_{0.2}Co_{0.8}Fe_{0.2}O_{3-\delta}$	CAM	insitu XRD	H_2	CLC	[257]
$La_{0.9}Sr_{0.1}Co_{0.8}Fe_{0.2}O_{3-\delta}$	CAM	insitu XRD	H_2	CLC	[257]
$La_{0.8}Sr_{0.2}Co_{0.5}Fe_{0.5}O_{3-\delta}$	CAM	insitu XRD, FxB	CH_4, H_2	CLC	[257]
$La_{0.8}Sr_{0.2}Co_{0.2}Fe_{0.8}O_{3-\delta}$	CAM	insitu XRD, TGA	H_2, O_2	CLC	[257]
$La_{0.5}Sr_{0.5}Co_{0.5}Fe_{0.5}O_{3-\delta}$	SD	FxB	CH_4	CLC	[158]
$LaFeO_{3-\delta}$	SD	FxB	CH_4	CLR	[158]
$La_{0.8}Sr_{0.2}FeO_{3-\delta}$	SD	FxB	CH_4	CLR	[158]
$La_{0.5}Sr_{0.5}FeO_{3-\delta}$	SD	FxB	CH_4	CLR	[158]
$La_{0.7}Sr_{0.3}Cu_{0.05}Fe_{0.95}O_{3-\delta}$	CAM	FxB	CH_4, O_2	CLR	[258]
$La_{0.7}Sr_{0.3}Cr_{0.05}Fe_{0.95}O_{3-\delta}$	CAM	FxB	CH_4, O_2	CLR	[258]
$La_{0.7}Sr_{0.3}Co_{0.05}Fe_{0.95}O_{3-\delta}$	CAM	FxB	CH_4, O_2	CLR	[258]
$La_{0.7}Sr_{0.3}Ni_{0.05}Fe_{0.95}O_{3-\delta}$	CAM	FxB	CH_4, O_2	CLR	[258]
$La_{0.7}Sr_{0.3}FeO_{3-\delta}$	CAM	FxB	CH_4, O_2	CLR	[258]
$CaMn_{0.875}Ti_{0.125}O_3$	SP+FG	bFB, CLC 300 W	CH_4, O_2, pet-coke	CLOU	[259,260]

Table A8. Summary of low cost materials used as oxygen-carriers for solid fuels.

Material, ore	Active specie for oxygen transport	Facility[b]	Reacting agent[c]	Application	Reference
Ilmenite mineral Norway, Titania A/S	Fe_2TiO_5, Fe_2O_3,	TGA, bFB, CLC 500W, CLC 10 kW, CLC 120 kW	CH_4, H_2, CO, syngas, petcoke, coal, biomass, O_2	CLC, CLCs	[54,55,123,174,175,191,206-208,263,265-267,296,304,309,310,311,316,317,429]
Ilmenite mineral South Africa IFP	Fe_2TiO_5, Fe_2O_3	bFB	syngas, O_2	CLC, CLCs	[263]
Ilmenite mineral Australia	Fe_2TiO_5, Fe_2O_3	CLC 1.3 kW	syngas	CLC	[209]
Ilmenite mineral Arcelor Mittal	Fe_2TiO_5, Fe_2O_3	FxB	CH_4, H_2, CO, O_2	CLC, CLCs	[113,264]
Iron ore-LKAB	Fe_2O_3	bFB	syngas	CLC, CLCs	[317]
Iron ore-Carajas	Fe_2O_3	FxB, bFB	CH_4, syngas, O_2	CLC	[123,268,427]
Iron ore-Malmberget	Fe_2O_3	bFB	CH_4, syngas, O_2	CLC	[123]
Iron ore-Mt. Wright	Fe_2O_3	bFB	CH_4, syngas, petcoke, coal, biomass, O_2	CLC, CLCs	[123,265,310]
Iron ore-Pea Ridge	Fe_2O_3	bFB	CH_4, syngas, O_2	CLC	[123]
Iron ore-QCM	Fe_2O_3	bFB	CH_4, syngas, O_2	CLC	[123]
Iron ore	Fe_2O_3	FxB	CH_4, H_2, CO, O_2	CLC, CLCs	[113]
Iron ore-CVRD	Fe_2O_3	pFxB	Coal	CLCs	[269-271]
Iron ore-Australia	Fe_2O_3	CLC 1 kW	Coal, O_2	CLCs	[143]
Oxide scale-Glödskal A	Fe_2O_3	bFB	CH_4, syngas, pet coke, coal, biomass O_2	CLC, CLCs	[123,265,310]
Oxide scale-Glödskal B	Fe_2O_3	bFB	CH_4, syngas, O_2	CLC	[123]
Steel by-product-SSAB Brun	Fe_2O_3	bFB	CH_4, syngas, O_2	CLC	[123,256]
Steel by-product-SSAB Röd	Fe_2O_3	bFB	CH_4, syngas, O_2	CLC	[123,256]
Steel by-product-Scana1	Fe_2O_3	bFB	syngas	CLC, CLCs	[317]
Steel by-product-Scana2	Fe_2O_3	bFB	syngas	CLC, CLCs	[317]
Steel by-product-Scana3	Fe_2O_3	bFB	syngas	CLC, CLCs	[317]
Steel by-product-Scana8	Fe_2O_3	bFB	syngas	CLC, CLCs	[317]

Steel by-product-Sandvik 1	Fe_2O_3	bFB	syngas	CLC, CLCs	[317]
Steel by-product-Sandvik 2	Fe_2O_3	bFB	syngas	CLC, CLCs	[317]
Vehicle recycling-Stena Metall	Fe_2O_3	bFB	syngas	CLC, CLCs	[317]
Iron ore concentrate	Fe_2O_3	TGA	CH_4, H_2, O_2	CLC	[262]
Redmud	Fe_2O_3	TGA, bFB, CLC 500 W	CH_4, H_2, CO, O_2, PSA-off gas, coal	CLC	[210,430]
Olivine	Mgsilicates, someFe_2O_3	TGA	CH_4, H_2, O_2	CLC	[262]
Biotite	$K(Mg,Fe)_3(AlSi_3O_{10})(OH)_2$	TGA	CH_4, H_2, O_2	CLC	[262]
Fe-Mn slag	$CaFeSiO_4$, $(Mn,Fe)SiO_3$ and Fe	TGA	CH_4, H_2, O_2	CLC	[262]
Fe-Mn slag	Mn/Fe carbonates, some (Fe,Mn)O	TGA	CH_4, H_2, O_2	CLC	[262]
Si-Mn	silicates, some Mn_2O_3	TGA	CH_4, H_2, O_2	CLC	[262]
Mn ore	MnO_2. some SiO_2	TGA	CH_4, H_2, O_2	CLC	[262]
Iron hydroxide	$Fe(OH)_3$	TGA	CH_4, H_2, O_2	CLC	[262]
Mn ore-Tinfoss	Mn_3O_4, Fe_2O_3	bFB	CH_4, syngas, O_2	CLC	[123]
Mn ore- Elkem	Mn_3O_4, Fe_2O_3	bFB	CH_4, syngas, O_2	CLC	[123]
Mn ore- Eramet	Mn_3O_4, Fe_2O_3	bFB	CH_4, syngas, O_2	CLC	[123]
up-concentration-Colormax P	Mn_3O_4	bFB	CH_4, syngas, O_2	CLC	[123]
up-concentration-Colormax R	Mn_3O_4	bFB	CH_4, syngas, O_2	CLC	[123]
up-concentration-Colormax S	Mn_3O_4, Fe_2O_3	bFB	CH_4, syngas, O_2	CLC	[123]
$CaSO_4$ pure	$CaSO_4$	TGA	H_2, CO, O_2	CLC, CLCs	[273,278,282]
$CaSO_4$ pure	$CaSO_4$	TGA	H_2, CO, O_2	CLC, CLCs	[283]
Natural anhidryte ore (Nanjing)	$CaSO_4$	FxB, bFB	CH_4, CO, syngas, coal, O_2	CLC, CLCs	[272,274-277,281]

[a] Key for preparation method: C&S: crush and sieve Com. Cat.: commercial catalyst CAM: citric acid method COP: coprecipitation DP: deposition-precipitation DIS: dissolution FG: freeze granulation HIMP: hot impregnation HS: hydrothermal synthesis IMP: impregnation MM: mechanical mixing P: precipitation PE: pelletizing by extrusion SC: solution combustion SD: spray drying SF: spin flash SG: sol-gel SP: spray pyrolysis	[b] Key for facility: bFB: batch fluidized bed CLC: CLC system for gaseous fuels CLCp: pressurized CLC system CLCs: CLC system for solid fuels CREC: chemical reactor engineering centre DSC: differential scanning calorimeter FxB: fixed bed MS: mass spectrometer pFxB: pressurized fixed bed pTGA: pressurized thermogravimetric analyzer scFB: semi-continuous fluidized bed TGA: thermogravimetric analyzer TPO: temperature programmed oxidation TPR: temperature programmed reduction XRD: X-ray diffraction [c] Key for reacting gas: n.g.: natural gas [d] n.a.: not available